Flood probability analysis of the Huangpu barrier in Shanghai

M.Sc. thesis

J.Y. Nai

August 2003

Thesis committee:

Prof. dr. ir. M.J.F. Stive	(Delft University of Technology)
Prof. ir. E. van Beek	(Delft University of Technology)
dr. ir. P.H.A.J.M. van Gelder	(Delft University of Technology)
dr. ir. Z.B. Wang	(Delft University of Technology)
ir. P.J.M. Kerssens	(WL | Delft Hydraulics)

TU Delft
Delft University of Technology

WL | delft hydraulics

Preface

This thesis forms the completion of my study Civil Engineering (M.Sc.) at the Faculty of Civil Engineering and Geosciences of Delft University of Technology. This thesis contributes to the ongoing feasibility study of the Shanghai Municipal Government to protect Shanghai City against future floods of the Huangpu River by building a storm surge barrier in the mouth of the river.

Hereby I would like to express my gratitude for the many people and organizations that have contributed to this thesis in one way or another. I would like to thank WL | Delft Hydraulics for providing me an excellent environment to complete this thesis and for making the $2^{1/2}$ months internship at the Shanghai Water Authority possible. I also would like to thank WL | Delft Hydraulics and the Lamminga Fonds for their financial support.

Much gratitude is owed to Mr. Chen Meifa and Mr. Huang Sili of the Shanghai Water Authority for their help on my quest for relevant data during my stay in Shanghai. In addition, I would like to thanks Mrs. Qiao Ying of the Shanghai Hydrology Administration for her help in Shanghai and for replying my many emails on the water regime in the Tai Lake Basin. Also, I would like to thank my mother for her assistance in my translation works of the vast collection of Chinese documents required for this study.

I would like to thank Mr. Suryadi of WL | Delft Hydraulics for sharing his knowledge on modelling with SOBEK-RIVER, Bert Jagers for explaining me the principles of programming in MATLAB, Simon Groot for helping me out with various useful maps and reports on the Tai Lake Basin. I also thank Ferdinand Diermanse for his always useful advices on the probabilistic used in this study.

Finally, I would like to thank my supervisors Professor dr. ir. M.J.F. Stive, Professor ir. E.van Beek, dr. ir. P.H.A.J.M. van Gelder, dr. ir. Z.B. Wang and last but not least ir. P.J.M. Kerssens for guiding me in the course of this thesis with valuable advices and recommendations.

Delft, August 2003

J.Y. Nai

Summary

The Huangpu River meanders through downtown Shanghai City and links China's third largest Lake with the Yangtze River estuary. Typhoons passing Shanghai from June to October annually are the main trigger for flooding of the Huangpu River. When storm surges due to a tropical cyclone meet the local astronomical tide, the water levels in the river can easily exceed the warning water levels and cause flooding of the downtown area of Shanghai City. Moreover, during the typhoon season the water levels in the region are sustained higher because of the rain season earlier. As a result flooding of the urban area occurs frequently during the typhoon season. A storm surge barrier in the mouth of the river will effectively keep out high water levels caused by passing tropical cyclones. However, typhoons also bring heavy downpour to the area, which is able to temporarily increase the upstream discharge into the river substantially. The increased upstream discharge because of torrential rainfall triggered by passing tropical cyclones can be a cause for flooding of the river even though the barrier is closed.

This study is aimed to determine the flood probability of the Huangpu River during *closure* of the storm surge barrier as a result of the upstream discharge for the three proposed barrier locations in the mouth of the river. This upstream discharge includes the base discharge of the Huangpu River and the torrential rainfall runoff triggered by the passage of a tropical cyclone. These discharges are investigated as well as their probabilities of exceedance. The situation in which the river is on the verge of flooding is termed the limit state condition. Hence, the flood probability of the river can be expressed as the probability that the upstream discharged water volume during barrier closure exceeds the storage capacity of the river.
The storage capacity of the Huangpu River is considered to be deterministic, in contrast with the upstream discharge. The storage capacity is investigated with one-dimensional flow simulations of an enhanced model of the Huangpu River in SOBEK RIVER. The allowed upstream discharges per closure duration, i.e. critical discharge, per barrier location are computed to represent the storage capacity. Subsequently, the probabilities of occurrence of the critical discharges are studied with analyses of the probabilities of the components that build up the upstream discharge.

Because of the limited availability of appropriate discharge records, the torrential rainfall runoff distribution is derived from the joint distribution of storm surge and torrential rainfall in the Shanghai area given storm tide levels in the mouth of the river equal to the barrier closure water level. The torrential rainfall probability is related to the storm surge level probability in the mouth of the river; since both are caused by passing typhoons. Therefore, the joint distribution of storm surge and torrential rainfall in the area is investigated with the known distribution of storm surge and torrential rainfall. These individual distribution functions are linked into their joint distribution with a copula. Copulas separate the dependence structure of multivariate distributions with the individual marginal distribution functions. The study of copulas and its applications is rather new but a rapid growing field in the literature of statistics. Eventually the runoff distribution is derived from the torrential rainfall probabilities with empirical runoff relations found from analysis of historical major rainfall events in the area.

Prior to the analysis of the torrential rainfall probabilities, the required surge levels for barrier closure are computed by random combination of the tide and storm surge distribution in the mouth of the river. The present warning water level in the mouth of the river is regarded as the future barrier closure level. Subsequently, the required surge level for barrier closure is found by the conditional probability of the surge levels given the barrier closure water level.

The analysis of the flood probability is characterized by the format of the base discharge records of the Huangpu River available. Therefore, at first, the flood probability is determined for given barrier closure, month and type of hydrological year. These results are analysed and subsequently, the flood probability for given the month in the typhoon season only is determined, taken into account the variability of the type of hydrological year. Finally, the flood frequency of the Huangpu River during barrier closure is investigated in the typhoon season in general taken into the monthly barrier closure frequency.

From the results it appears that flooding of the Huangpu River during barrier closure is a real threat. The flood frequency is 1:1.88 to 1:0.93 with reference to the warning water level at Mishidu station with a barrier respectively at Wusongkou and Fishery Yard. For the Huangpu Park station, in the city centre, the flood frequency is 1:135 to 1:7.70 respectively. The flood frequency of the Huangpu River is much higher than the desired 1:1000 years regardless of the storm surge barrier location in the mouth of the river. To acquire a lower flood frequency, the barrier may not be closed for longer than 8 and 16 hours with reference to Mishidu and Huangpu Park respectively. These results form a strong indication that accurate data and precise knowledge on the study area is vital to analyse the exact flood probability because flooding of the Huangpu River concerns the loss of property and even human lives.

Contents

List of Figures

List of Tables

1 Introduction

1.1 Background of the study

Floods are the main natural threat to the densely populated coastal regions and cities along a number of major rivers in China. Like many other cities along the country's eastern and southern coastline, Shanghai is vulnerable for floods brought by typhoons from the Pacific Ocean. At present, the city is the most important economic, trade and shipping centre in China. The city's main river, the Huangpu River, is the main waterway of the region as well as the main flood diversion route to the westward-located Tai Lake, China's third largest fresh water lake. The river meanders through urban Shanghai and links the Tai Lake with the mouth of the Yangtze River in the north. Each year, typhoons in the East China Sea bring heavy rainfall and wind gusts to the area stressing the urban drainage system and infrastructures. Moreover, the storm surges accompanying the typhoons can easily swell the tide in the Huangpu River to unparalleled levels overflowing and breaching the flood defenses along the river with inundation of large parts of urban Shanghai as a result.

From the 1950's onwards a system of floodwalls and gates is constructed along the Huangpu River and along the downtown sections of its main tributaries to protect the city against flooding of the river. However, rapid land subsidence of the urban area as a result of extensive ground water extraction associated with the economic development of Shanghai caused the floodwalls to subside as well. And moreover, the water storage capacity of the vast network of rivers and lakes in the area has been reduced in time mainly due to land reclamation. In time, these events resulted in a rise of the water levels in the Huangpu River stressing the floodwalls as flooding of the river occurred more frequently. To keep the city protected against floods, the Shanghai Municipal Government already initiated programs to upgrade the flood defenses in 1953, 1965, 1968, 1974 and 1988.

However, Shanghai is still vulnerable for flooding of the Huangpu River today and the water levels in the river still show an upward trend. Moreover, the protection level of the flood defenses along the Huangpu River is diminished from floods with a return period of 1:1000 years to 1:200 years. This is certainly not reflecting the present and expected economic and social importance of Shanghai to China.

In 1984, the state Ministry of Water Resources and Electric Power announced that by the year 2010 urban Shanghai has to be protected against floods with a return period of at least 1:1000 years. Since heightening and reinforcements of the existing floodwalls has proven not to be a sustainable solution, the Shanghai Municipal Government (SMG) intends to protect the city by building a storm surge barrier in the mouth of the Huangpu River. The Shanghai Water Authority (SWA) is entrusted with the feasibility study of this plan. This study contributes to it by investigating the probability that the Huangpu River will be flooded by an increased upstream discharge during barrier closure in a typhoon storm. Typhoons moving towards Shanghai not only bring higher tide levels but also torrential rainfall to the area. These intense rains temporarily increase the runoff into the Huangpu River substantially and may cause flooding of the Huangpu River when this occurs during barrier closure.

1.2 Problem definition

The Huangpu River is the main waterway and flood diversion route in Shanghai. The river flows through the downtown area and diverse flood water from the westward located Tai Lake to the Yangtze River estuary in the north. Flooding of the Huangpu River is caused when the following three factors combine in a typhoon storm (Hohai University, 1999) (Chen and Zong, 1999):

- Storm surge,
- High astronomical tide level,
- Increased upstream discharge into the Huangpu River due to heavy rainfall.

To protect the city against future floods the Shanghai Water Authority is investigating the feasibility to construct a storm surge barrier in the mouth of the Huangpu River. With it, the city will be protected against floods with a return period of at least 1:1000 years. However, the discharge volume that has to be stored in the river during barrier closure may impose a flood risk as well considering the heavy rainfall to the area brought by the passage of a typhoon.
Hence the study problem is defined as:

Will the Huangpu River be flooded because of an increased upstream runoff into the river during closure of the storm surge barrier in a typhoon storm?

1.3 Objectives

The main objective of this study is stated as follows:

Determine, for each of the proposed barrier locations, the flood probability of the Huangpu River during closure of the storm surge barrier in the river mouth as a result of the river's discharge.

The following analyses are carried out to satisfy this main objective:

1. Analyze the factors that determine the storage capacity as well as the discharge of the Huangpu River,
2. Analyze the probability distributions of these factors,
3. Analyse the joint probability distribution of upstream discharge and barrier closure.

1.4 Approach

The overall problem approach of this study is structured in this section. During barrier closure, flooding of the Huangpu River occurs in either of the following two situations (figure 1-1). The barrier collapses and storm tides that subsequently enter the river from the Yangtze River estuary flood the downtown area of Shanghai. Alternatively, discharge into the river during barrier closure can cause the inside water levels to breach or overtop the floodwalls alongside the river flooding the downtown area.

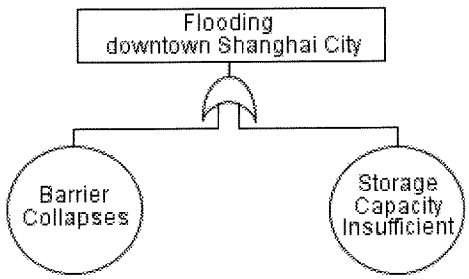

Figure 1-1 Fault tree for flooding of the downtown area of Shanghai City during barrier closure, the focus of this study is on flooding as a result of insufficient storage capacity of the Huangpu River during barrier closure.

This study focuses on the flood probability of the Huangpu River as a result of an insufficient storage capacity during barrier closure. This event is expressed in terms of a limit state function

$$Z = R - S \tag{1.1}$$

in which

R = storage capacity Huangpu River [m^3]
S = upstream discharge volume during barrier closure [m^3]

When $Z = 0$ the river is on the verge of flooding and this is defined as the limit state condition. In contrast, when $Z < 0$, the Huangpu River floods, with inundation of downtown Shanghai City as a result. This relation is depicted in the figure below.

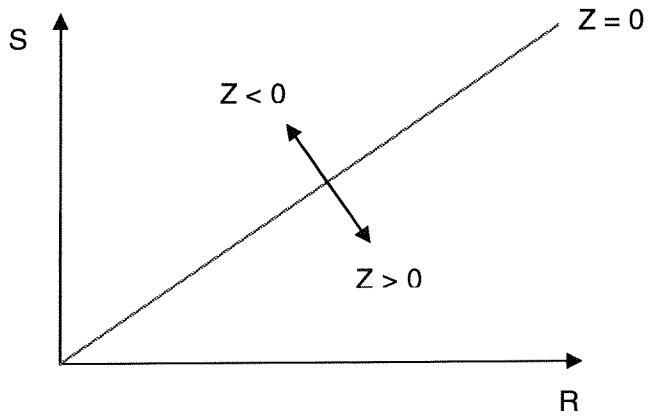

Figure 1-2: Linear reliability function in *RS*-space

The storage capacity is the Huangpu River's ability to store the upstream discharge during barrier closure. The storage capacity is determined by the geometry of the river, which is considered deterministic within the time frame of barrier closure. The upstream discharge consists of the base discharge in the Huangpu River and the tropical cyclone induced torrential rainfall runoff, which is denoted as

$$Q_{upstream} = Q_{base} + Q_{torrential} \tag{1.2}$$

in which

$Q_{upstream}$ = Upstream discharge [m^3/s]

Q_{base} = Base discharge [m^3/s]

$Q_{torrential}$ = Torrential rainfall runoff triggered by a tropical cyclone [m^3/s]

The upstream discharge volume is now expressed as the product of upstream discharge and the barrier closure duration $t_{closure}$, hence

$$S = Q_{upstream} t_{closure} \tag{1.3}$$

The closure duration depends on the movements of the tropical cyclone, which is very difficult to predict despite the developments of satellite monitoring possibilities. Therefore, we neglect the variation in closure duration. The flood probability during barrier closure is now expressed as the probability that the upstream discharge volume exceeds the storage capacity during barrier closure, which is denoted as

$$P(Z < 0) = P(R < S) \tag{1.4}$$

This is the general expression for flooding of the Huangpu River during barrier closure. This expression will be further sophisticated in the continuation of the study, especially in chapter 3 and 5.

The probability of flooding during barrier closure as a result of collapse of the barrier (figure 1-1) can be determined by analyzing the possible causes for barrier collapse and their corresponding probabilities. Since the probability of barrier collapse is related to the probability of insufficient storage capacity during barrier closure, the overall flood probability can be determined by means of the Ditlevsen upper and lower bounds. Detailed information on Ditlevsen bounds can be found in ©CUR-publikatie 190 (1997). Some examples on flooding as a result of barrier collapse is enclosed in appendix V.

In figure 1-3 we present the factors that are important to the flood probability of the Huangpu River during barrier closure. The factors will be discussed briefly hereafter. The storage capacity will be treated in detail in chapter 3 whereas the torrential rainfall in chapter 4.

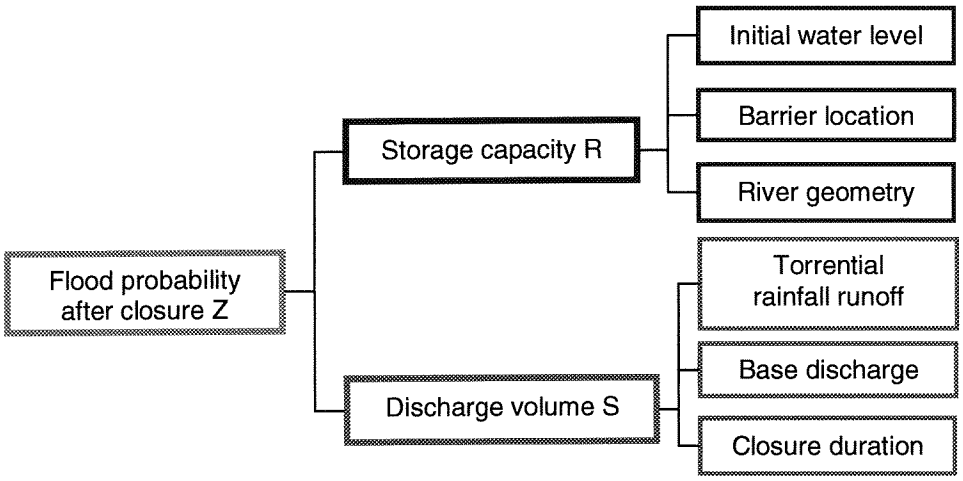

Figure 1-3: Relation diagram flood probability after barrier closure

Storage capacity

The factors that determine the available storage capacity are a associated the following factors:

- Initial water level

This is the water level in the river direct after closure of the storm surge barrier. The initial water level determines the amount of available storage volume in the river during barrier closure. The initial water level is determined by the tide situations at the moment the barrier is about to close.

- Barrier location

The location of the barrier determines the overall length of the river. In this study the Huangpu River ends at Mishidu station, the more upstream the barrier is located from the river mouth the less volume is available during barrier closure.

- Geometry of the river

The river dimension is simply determined by its length, width and depth. The margin that water level in the Huangpu River has to rise is determined by the height of the floodwalls along the river. In this study the current flood warning water levels in the river is used. Land subsidence and sea level rise, however, will lower the floodwalls with consequences to the storage capacity.

Discharge volume

The water volume to be stored in the Huangpu River during barrier closure, S, is composed of the following factors:

- Torrential rainfall runoff

Storm surges caused by tropical cyclones in the vicinity of Shanghai are the reason for flooding of the Huangpu River (section 2.3). In addition, these tropical cyclones bring torrential rainfall to the area as well, and their intensity is such that it can increase the base discharge in the Huangpu River substantially. As the typhoon season follows the rain season it is presumed that the soil and the rivers and lakes in the area are saturated and runoff of the torrential rainfall occurs through surface runoff. Furthermore, a distinction between runoff inside and outside urban Shanghai into the Huangpu River is applied:

  - Runoff outside urban Shanghai

    This is the runoff into the Huangpu River through the upstream connections with the Tai Lake Basin.

  - Runoff in urban Shanghai

    The urban area is located around Shanghai lowest points, therefore drainage pump are required to prevent water logging during heavy rainfall. As a consequence, the urban

torrential rainfall runoff into the Huangpu River is limited by the capacity of the pumps and water logging occurs whenever the rainfall intensity exceeds the pump capacity.

- Base discharge

The base discharged water volume must be stored in the river during barrier closure even when torrential rainfall might not occur. The Tai Lake is the main contributor to the base discharge of the Huangpu River. The magnitude of the base discharge depends on the hydrological year and month.

- Closure duration

The closure duration is related to the closure strategy determined by duration of the passage of the storm and the barrier operation time. Naturally, the longer the river is closed, the more storage capacity is needed. Long closure durations can cause the storage capacity of the river too collapse or even collapse of the barrier as the water level behind the barrier becomes too high. Since no records are available of the duration of typhoon storms in Shanghai, we assume that a barrier closure of 24 hours is representative.

1.5 Report outline

The structure of this thesis corresponds to the main steps of the analyses carried out in this study. General information on the study area and the main cause for flooding of the Huangpu River are treated in chapter 2. The insights in this chapter on tropical cyclones and the study area will be used throughout in the chapters hereafter. In chapter 3, the storage capacity of the Huangpu River for each of the barrier locations is analysed. Moreover, the causes for the progressive rise of the flood frequency of the river are investigated and taken into account in the analysis of the storage capacity. Subsequently in chapter 4, the torrential rainfall runoff distribution is derived from the conceptual joint probability of storm surge and torrential rainfall in the region. Then in chapter 5, the findings of the previous chapters will come together and used to derive the flood probability of the Huangpu River for given barrier closure and month. Subsequently, with this result, the flood frequency of the Huangpu River in the typhoon season is derived and the results are analysed. The main conclusions of this study can be found in the final chapter of this report.

2 Huangpu River water system

2.1 Introduction

In this chapter the Huangpu water system will be introduced. The Huangpu River is part of the complex water system of the Tai Lake Basin (or Taihu Basin) and in terms of hydrology; the Huangpu River is the main drainage route to the basin. Annually from June to October, tropical cyclones passing the region can cause flooding of the Huangpu River with inundation of Shanghai City as a result. We start this chapter with general information about the study area. In addition, the main water bodies, which the Huangpu River is dependent on, are discussed. In section 2.3, the phenomenon of tropical cyclones is treated. We explain the mechanism of tropical cyclones, and moreover why Shanghai is affected by these severe storms. These insights are used in the continuation of this study. Finally, in section 2.4 the actual flooding of the river by tropical cyclones is described.

2.2 Description of the study area

2.2.1 Setting of the Huangpu River

The study area is bound by the course of the Huangpu River which flows within the borders of the Shanghai Municipality. More specifically, the course of the Huangpu River from the river mouth at Wusongkou till the most upstream located station at Mishidu. The Shanghai Municipality is roughly triangular shaped and bounded to the north by the Yangtze River, to the south by the Hangzhou Bay of the East China Sea. The region has an administrative status of a province. Shanghai borders the provinces Jiangsu and Zhejiang in the west. Shanghai covers an area of 6340km^2, of which 3249km^2 are urban. Its population is nearly 14 million permanent and 3 to 4 million transient inhabitants. Chongming Island, located in the Yangtze River estuary, covers an area of 1041km^2 and is the third largest Island in China. Shanghai is divided into 16 districts and 4 counties. Shanghai is the most important financial, trade, industrial and shipping centre in China. By the year 2010, the city intends to achieve the status of an anchor city to the Pacific region.

The Huangpu River is part of the complex water system of the Tai Lake Basin. The Tai Lake Basin covers an area of 36900km^2, about 0.4 percent of China's territory but it accounts for 21% of China's GDP (by the end of the year 2000). It is one of the fastest developing regions in China. The population

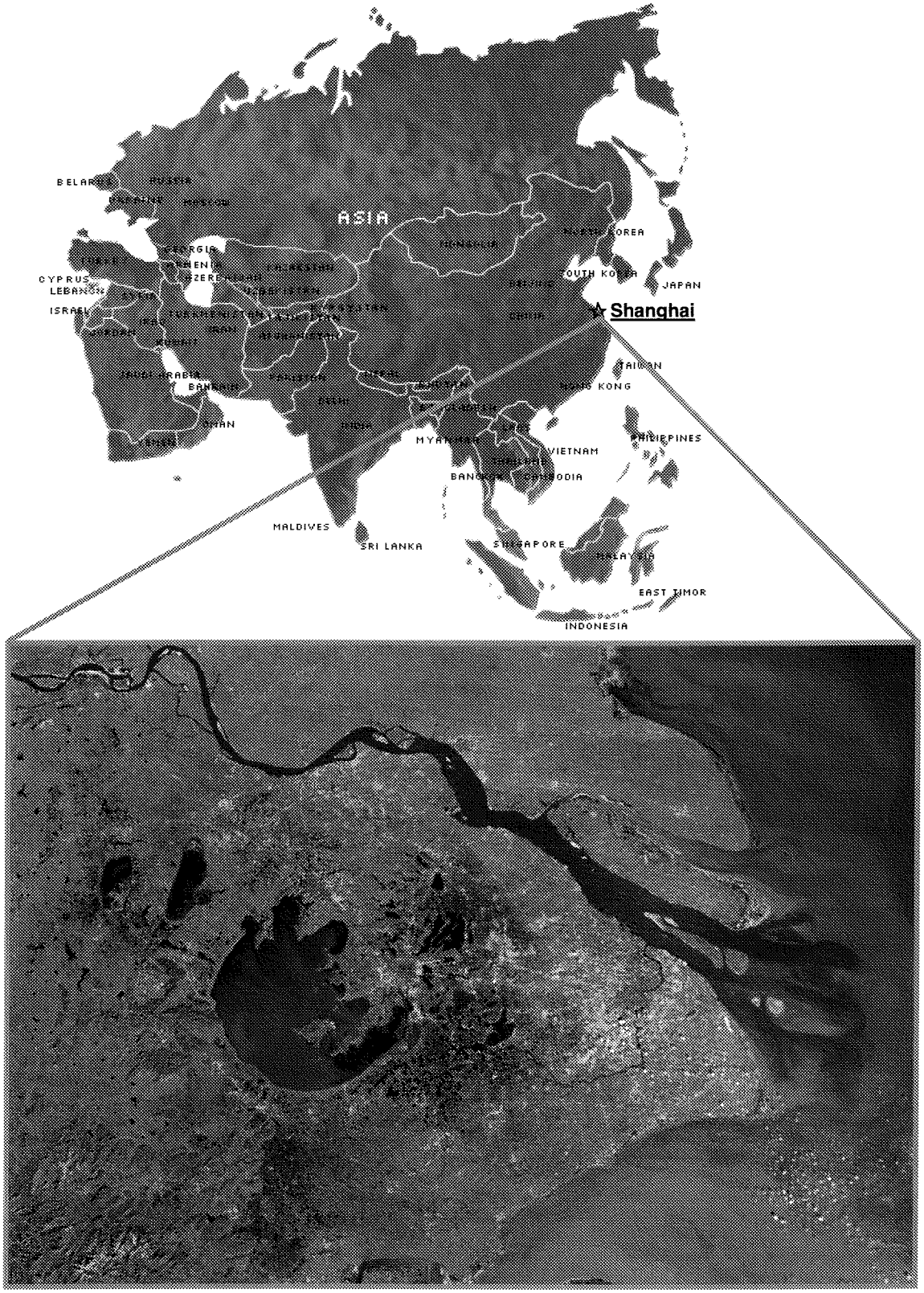

Figure 2-1: Orientation of the Tai Lake Basin. The Tai Lake is in the middle of the satellite image, to the right just below the mouth of the dominating Yangtze River, lies urban Shanghai through which the Huangpu River meanders (source: www.visibleearth.nasa.gov and www.kilroytravels.com)

density in the Tai Lake Basin is also the highest in China, about 8 times the country's average density corresponding to 946 persons per square kilometre. Shanghai Municipality accounts only 15% of the Basin's area. The Tai Lake, about 120km to the west of urban Shanghai, as the largest lake at the centre of the Basin, plays a critical role in the region with its vast network of smaller rivers and lakes. The water surface of the Tai Lake totals 2338km^2, it is the third largest freshwater lake in China and the key source of water supply to the region. The Huangpu River originates from the Dianshan Lake, links the Tai Lake via the Taipu River and winds through the downtown area of Shanghai before it converges with the Yangtze River. The Huangpu River is the main water way as well as the main flood diversion route in the Tai Lake Basin. The river drains 70% to 80% of the Tai Lake Basin (Hohai, 2001).

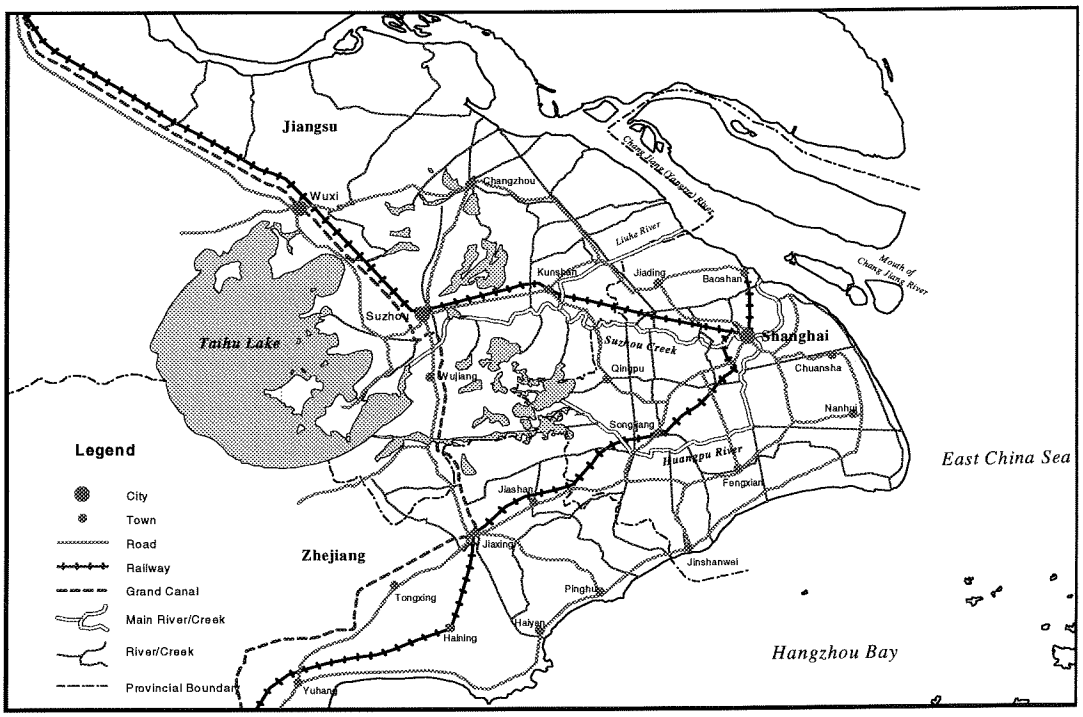

Figure 2-2: Tai Lake Basin topographical map (source: WL | Delft Hydraulics)

2.2.2 Climate

The Shanghai area has a monsoon climate with warm wet weather from April through September and cool relatively dry weather from October to March. Temperatures exceed 30° Celsius in the summer and seldom drop below freezing in the winter. The average annual temperature is around 15.6° Celsius. August is the warmest month of the year with an average temperature of around 27.6° Celsius. Considering the Tai Lake Basin as a whole, the average annual rainfall varies from 1100mm in the north to more than 1700mm in the south along Hangzhou Bay. Annual rainfall in Shanghai is average 1146mm with 132 rain days. However, different hydrological years can result in vast deviations of this figure. In 1985, the annual average rainfall soared to a record of 1673mm. In contrast, the rainfall can be as low as 709mm in 1892 (Yuan, 1999). About 60% of the annual rain falls in the rain season from May to September. The total rainfall in the area varies annually. For instance, in 1991 the rain season brought averagely 1011mm of rain in 4 months, nearly the total amount of rain in a normal year. This excessive rainfall caused severe flooding of the Tai Lake. The rain season starts with the so-called *plum rains* from May to early July followed by torrential rains brought by typhoons

Plum rains

The term plum rains refer to the time of the year that plums are ripening, according to an old Chinese saying, the plum rains will last for 40 days as rainfall occur at the day the first plums are ripe. These plum rains are monsoon induced wide spread prolonged rains and can cause severe flooding of the inland areas as they can fall for a period of three months continuously and swell the water levels in the lakes and rivers of the Tai Lake basin and raise the groundwater table in the deltaic area. Typical rain depths range from 300mm to 800mm per month. In general, the discharges into the Huangpu River are highest in this period.

Longest period	1954:	the rainy season lasted two months from June 1 to August 2.
Shortest period	1958 and 1978:	the season lasted for just three days.
Most rain	1999:	the plum rain season was about 800 mm, which accounted for 75% of the normal annual precipitation.
Least rain	1958 and 1978:	the precipitation was less than 40 mm.
Most desastrous	1991 and 1999:	the unbroken heavy rain caused serious flooding.

Table 2-1: Historical extreme rain seasons Source Shanghai Star 2001/6/28

Torrential rains

In Shanghai, rainfall with intensity of at least 100mm/24hrs is termed torrential rain. Moreover, a distinction is made in three categories of torrential rain:

1. Torrential rain, intensity 100 - 150mm/24 hours
2. Heavy torrential rain, intensity 150 - 200mm/24 hours
3. Extreme torrential rain, intensity ≥200 mm/24 hours

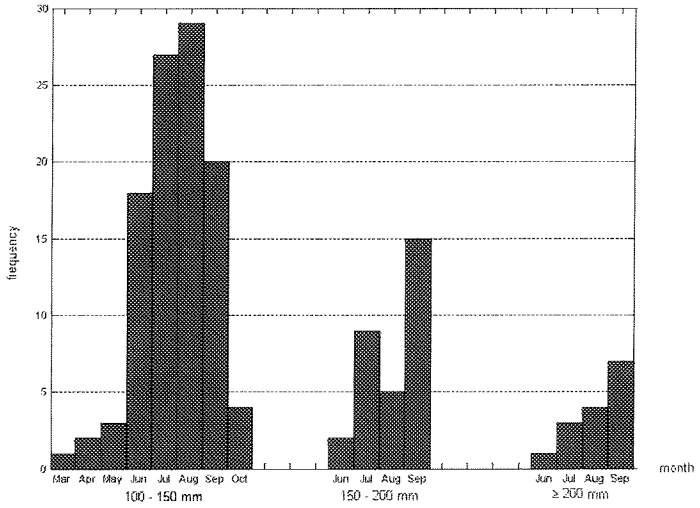

Figure 2-3: Monthly torrential rainfall distribution in Shanghai from 1959- 1991 (with data from Yuan, 1999)

Torrential rainfall of category 2 and 3 are the most frequently occurred in Shanghai; these intensities typically cause water logging hazards in the urban area. Theoretically the occurrence of torrential rainfall is throughout the year, depending on the actual meteorological conditions. However, the main trigger for this type of rain is the tropical cyclones in the vicinity of Shanghai from June to October. According to historical records (Yuan, 1999) from the period 1959 to 1991 about 80% of the 150 torrential rain events with intensities over 100mm per 24 hours

occurred in the typhoon season. Typically, the torrential rains in this period are distinguished by the accompanying strong wind gusts of the tropical cyclone.

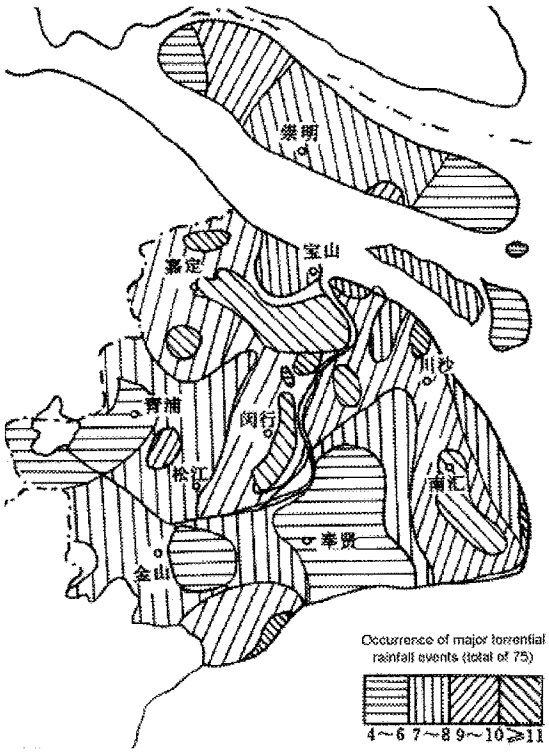

Figure 2-4: Spatial distribution of the 75 major torrential rainfall events in Shanghai from 1954–1991 (adapted from Yuan 1999)

2.2.3 Hydraulic features of the Huangpu River

River dimensions

The Huangpu River is the main river in the Tai Lake basin. The Huangpu River is about 113.4km long and around 770m wide at the mouth at Wusongkou and average 360m elsewhere. The depth of the river ranges from -15m to -8m with reference to Wusong Datum (WD). The river depth is well maintained for navigation.

Tide

The water levels in the Huangpu River and its tributaries are governed by the semi diurnal tide in the East China Sea. At Wusongkou station, in the river mouth, the mean low and high water level are respectively 3.24m and 1.03m WD. The flood period is shorter than the ebb period in the Huangpu River. At Wusongkou station in the river mouth the flood tide rises averagely in 4 hours and 33 minutes, while the ebb tide period last nearly 8 hours. See also table 2-2 and figure 2-5 for the locations of the three main stations. The average tidal range at Wusongkou station is 2.21m. The tidal range at the upstream-located Huangpu Park and Mishidu station are 1.83m WD and 1.04m WD respectively.

		Wusongkou	Huangpu Park	Mishidu
Average high tide	[m] WD	3.24	3.12	2.71
Ebb period	[hrs:mn]	7:52	8:08	8:00
Flood period	[hrs:mn]	4:33	4:18	4:26
Average low tide	[m] WD	1.03	1.29	1.67
Average tidal range	[m]	2.21	1.83	1.04
Highest water level (9711)	[m] WD	5.99	5.72	4.27
Average tide level	[m] WD	2.34	2.21	2.19

Table 2-2: Characteristic water levels at Wusongkou station in the Huangpu River (source: Shanghai Water Authority)

Discharge

The tide conditions determine the actual discharge of the river. In addition, drainage is slow in general because of the river's flat course of about 1:110000. The discharge is during the typhoon season lowest because of the higher tides caused by storm surges. The long term annual average discharge is 304m^3/s measured at Mishidu station in the rain season from May to September and 328m^3/s for the remaining months (Yuan, 1999). The upstream water inflow into the Huangpu River varies with the hydrological year. In 1954, the rain season brought more rain than expected and flood water from the Tai Lake needed to be diverted into the river (see next section) increasing the annual average discharge to 755m^3/s. In contrast, the annual average discharge can be as low as 153m^3/s in a dry year as in 1979.

		Wusongkou	Huangpu Park	Mishidu
Distance	[km]	0	25.6	79.8

Table 2-3: Distances of the hydrological stations relative to Wusongkou station in kilometres

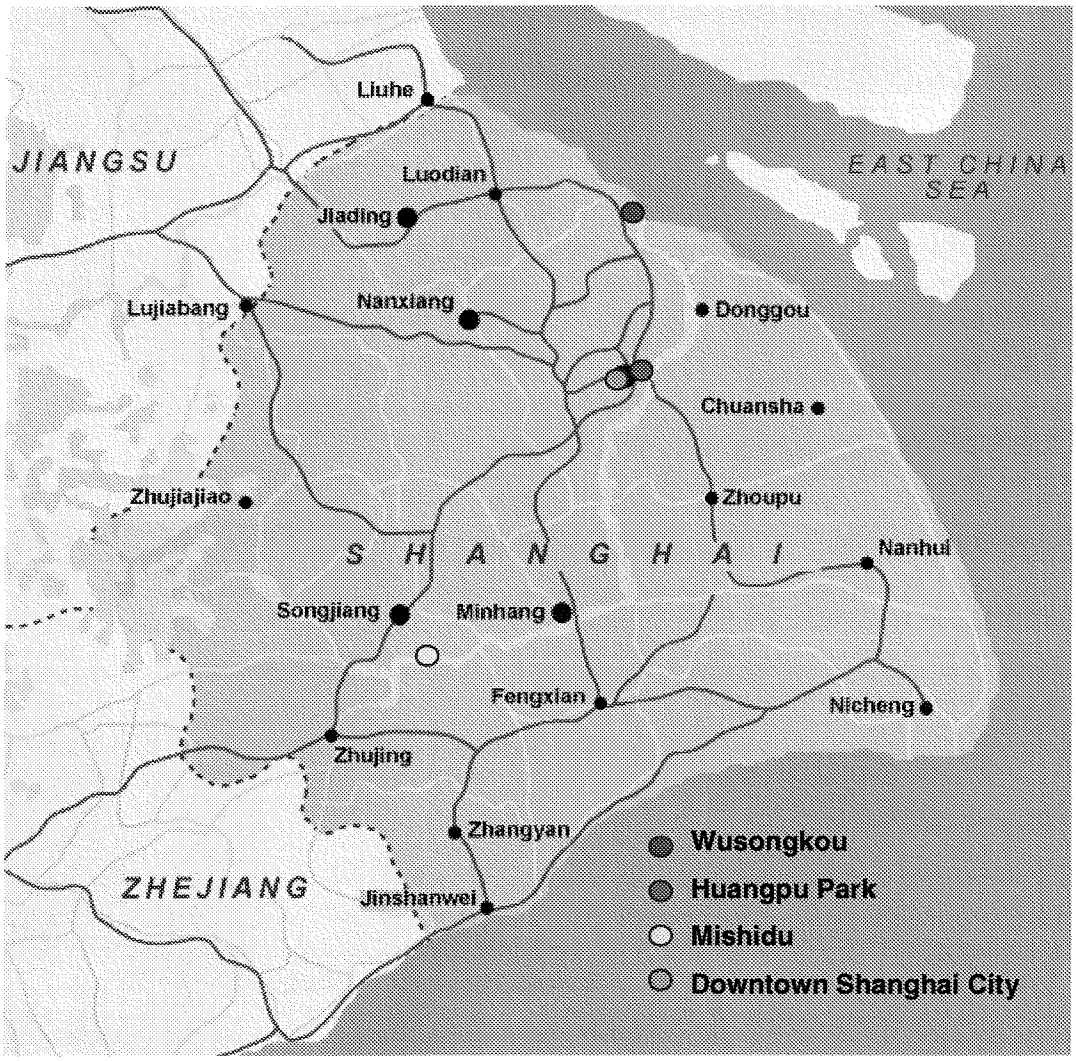

Figure 2-5: Overview hydrological observation stations along the Huangpu River in Shanghai

2.2.4 Hydraulic features of the surrounding water bodies

Yangtze River estuary

The Yangtze River, the world's third largest river, originates from the Himalayas and meanders westwards to the central east coast of China where it discharges in the East China Sea. The Huangpu River converges in the mouth of the Yangtze River; it is the last tributary of the river. The annual average discharge of the Yangtze River is around 29000m^3/s. About 70% of the discharge takes place during the rain season from May to October; the average discharge then is 41100m^3/s.

Months rain season	May	Jun	Jul	Aug	Sep	Oct	Annual average
Volume [m^3]·10^8	903	1049	1351	1223	1076	936	9142
Discharge [m^3/s]	33700	40500	50400	45700	41500	34900	29000

Table 2-4: Monthly average Yangtze River discharge at Datung station during typhoon season (adapted from Wang *et al.*, 2001)

Tai Lake

The Huangpu River is the main water outlet to the Tai Lake Basin. The Basin is scattered with lakes and rivers of which the Huangpu River is the largest river. The Tai Lake is the largest lake in the basin with a water surface of 2338km^2; it is the third largest fresh water lake in China and the main water supplier to Shanghai. The lake is mainly supplied by rivers and steams draining the higher grounds to the west. The Basin has an annual water deficit of 2.0 billion m^3 for normal years and 10 to 12 billion m^3 for dry years. Therefore, water diversion from the Yangtze River is necessarily through the Wangyu River as well as via 14 other river inlets along the Yangtze River equipped with pumping stations.

Dikes with a total length of 270km surround the Tai Lake's entire perimeter as prolonged and heavy rainfall can cause flooding of the lake. The maximum crest height of the dikes is 7.08m WD and is designed for a flood frequency of 1:50 years. Historic flood disasters of the Tai Lake occurred in 1921, 1931, 1949, 1954, 1962, 1963, 1980, 1983, 1991 and 1999. The most disastrous flood event of the Tai Lake occurred in 1991. Early monsoon rains in May filled the lake and subsequent wide spread rainstorms in June eventually collapsed the Tai Lake and a large area surrounding the lake was flooded. The losses are estimated at 2 billion USD. It was during this event that the Taipu River gate had to be opened for the first time in 33 years to release floodwater. Since this disastrous flood, large-scale reinforcements of the flood control works in the Tai Lake has been carried out and when the severest rain season occurred in 1999, the damages caused were substantial less than in 1991. As a result of continuous rainfall from May to the end of August the water levels in the lake raised to a record breaking level of average 5.08m WD (Zhang, 1999) about 1.58m higher than the warning water level (3.5m WD) in the lake and 0.29m higher than the previous record in 1991. The 30 days average rain depth in the Tai Lake reached 714.4mm.

At present, there are 4 main outlets in the Tai Lake to divert flood water to the Yangtze River (World Bank, 1993):

1. Taipu River, starts at the southeast corner of the Tai Lake and flows over in the Huangpu River before discharging in the Yangtze River estuary at Wusongkou. This discharge capacity of this 57km long river is recently improved. The outlet at the Tai Lake is provisioned with a control structures and a pumping station with a capacity of 300m^3/s.

2. Wangyu River is the second outlet. This river is extends 61km from the northern end of the Tai Lake to the Yangtze River. The river is widened and deepened recently to increase both its capacity of releasing floodwaters into the Yangtze River during floods as well as its capacity for replenishing the lake in the dry season. Control structures and pumping stations exists at the head of the river on the Yangtze River. The discharge capacity of the river is 450m3/s.

3. The Dushangkou River, the third outlet flows northward into the Yangtze River as well.

4. The fourth outlet is the Dongtai Lake flowing eastward into the Wusong River, and eventually flows into the Huangpu River.

The main outlet is the Taipu River. In 1958 a gate was build in the river to regulate the inflow to the Taipu River, it was not open until the Tai Lake flood in 1991. After this disaster, the Taipu River is widened and deepened to increase its discharge capacity. At present it drains about 70 to 80% of Tai Lake's waters (Yuan, 1999). The outlet at the Tai Lake is controlled with a gate, as soon as the water levels in the Tai Lake reach the warning water levels of 3.5m WD the gate will open to divert floodwater if the water level in the Taipu River is lower. The operation rules of the gate are shown in table 2-5. The Taipu River has a bottom width of 150m and a depth of 6m at the gate, and a width of 137m and a depth of 9m at the downstream end. With use of equation 2.1, the maximum discharge of the Taipu River is estimated at around 854m^3/s. This magnitude seems to be correct, as during the Tai Lake flood in 1999, the maximum discharge at the gate was 729m 3/s (Zhu, 2002).

$$Q = BhC\sqrt{hi} \tag{2.1}$$

in which

h = 7.5m
B = 143.5m
C = 40$m^{-1/2}$/s
i = 5.25·10^{-5}

These additional discharges into the Huangpu River has resulted in higher mean water levels in the river, which put the flood defences along the river under stress during storm tides. However, it also helped to clean the Huangpu River and reduced the water shortage of Shanghai.

Main tributaries of the Huangpu River

The Shanghai area has a vast river network covering almost 11% of the municipality's territory. Most of the rivers in this area are tributaries of the Huangpu River. The two tributaries of interest are the Suzhou Creek and the Wencao Bang.

The Suzhou Creek is the largest tributary of the Huangpu River. The 125km long Suzhou Creek originates east from the Tai Lake and runs through Jiangsu Province (where it is named Wusong River) to the Huangpu River in Shanghai, passing through the city Suzhou. The Suzhou Creek is

a narrow (40 to 60m) and shallow (5 to 10m depth) tidal river with an annual average discharge of 10 to 25m^3/s. Due to the mild slopes of the ground and the water shortage during most of the year, the discharge of the Suzhou Creek is not significant and depends on the downstream tide levels. The Suzhou Creek runs for 17km through the downtown of Shanghai and converges with the Huangpu River near Huangpu Park hydrological station in city centre. A control gate at the convergence of the Suzhou Creek with the Huangpu River prevents storm tides entering the Suzhou Creek (section 3.3.3).

The Wencao Bang is located in the mouth of the Huangpu River. This small river flows westwards and flows over into the Suzhou Creek. The discharge of the Wencao Bang is not significant and the water levels are totally governed by the tide. This river is important with regard to the protection area of the storm surge barrier as two out of three of the by the Shanghai Water Authority suggested barrier locations would not protect the Wencao Bang (section 4.4) from storm tides.

2.2.5 Hydrology

Rainfall runoff from the higher grounds to the west is the main water source to the Tai Lake. The actual annual discharge volume that reaches the Huangpu River is sensitive to the annual precipitation variations in the area. In a hydrological wet year the annual discharge is $132.10 \cdot 10^8 m^3$ with a peak in July of $22.31 \cdot 10^8 m^3$. In contrast, in a dry year the annual average discharge volume of only $58.70 \cdot 10^8$ m^3 is 2.25 times lower. In an average year the annual discharge volume is $106.6 \cdot 10^8$ m^3, with a low in August ($7.30 \cdot 10^8$ m^3) and a peak in December ($10.11 \cdot 10^8$ m^3). In general the discharge volume from July to October is $34.84 \cdot 10^8$ m^3, about 33% of the annual total. Apart from that, the upstream annual average discharge volume of $106.6 \cdot 10^8$ m^3 is composed as follows: $100.6 \cdot 10^8$ m^3 is contributed by the Tai Lake, measured at Mishidu station. In addition, an annual average of $10.1 \cdot 10^8$ m^3 reaches the Huangpu River through its tributaries, of which $1.92 \cdot 10^8$ m^3 accounts to the Suzhou Creek. It also appears that at Mishidu station a water volume of $4.1 \cdot 10^8$ m^3 is extracted permanently. In conclusion, the total annual average discharge volume into the Huangpu River is $106.6 \cdot 10^8$ m^3.

The average monthly upstream discharge volumes into the Huangpu River for different hydrological years with data from 1956 to 1999 are presented in figure 2-9 (Wang *et a.l*, 2001) Subsequently, these water volumes are translated into net discharges into the Huangpu River, presented in the figures below. These discharges are used throughout this study, as these are the only discharges figures available. When later on in chapter 3, the storage capacity of the Huangpu River is analysed it is assumed that no further water extraction takes place downstream of Mishidu.

Two conclusions are drawn from figure 2-9. First, in an average year the monthly variations of the discharged volumes is little and during flood season from July to September, the discharge volume is even lower than in the other months. Clearly, the higher tides in the Huangpu River caused by typhoons obstruct the discharges into the Yangtze River estuary. Consequently, the sustained higher water levels in the Huangpu River will easily cause floods when storm tides enter the river. Second, the extreme high discharge volumes during flood season in a hydrological wet year falls in the same period as the extreme low discharges in a very dry hydrological year, namely between June and September.

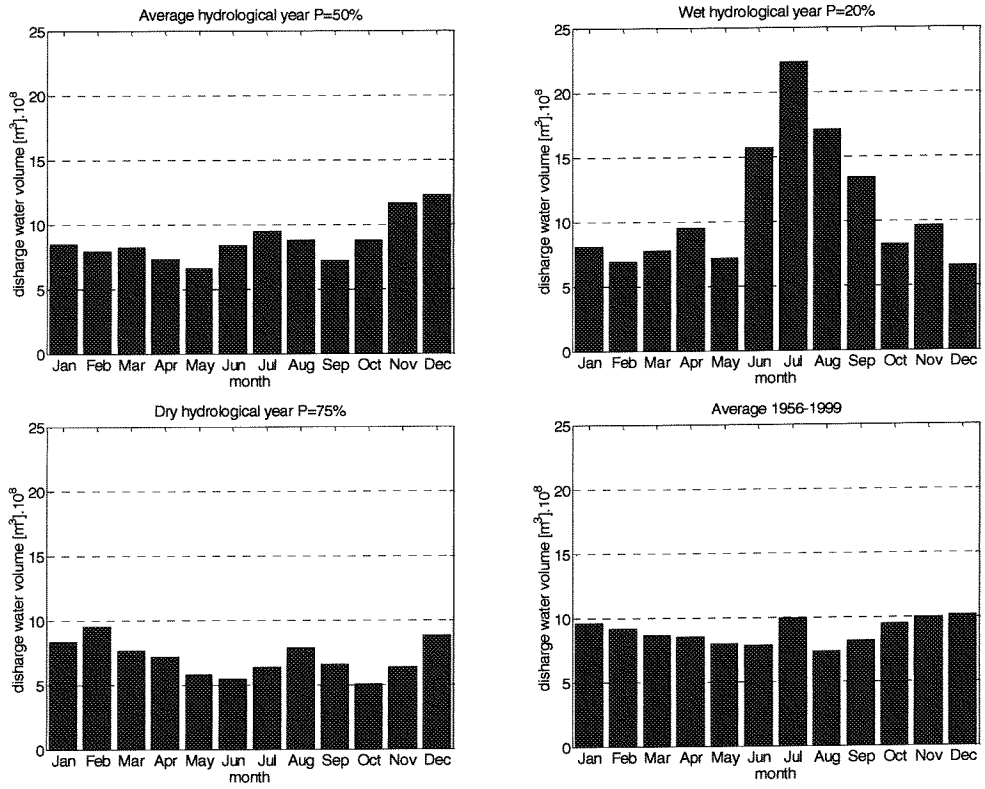

Figure 2-6: Tai Lake basin average monthly discharge volumes into the Huangpu River for different hydrological years from 1956-1999 (with data from Wang *et al.*, 2001)

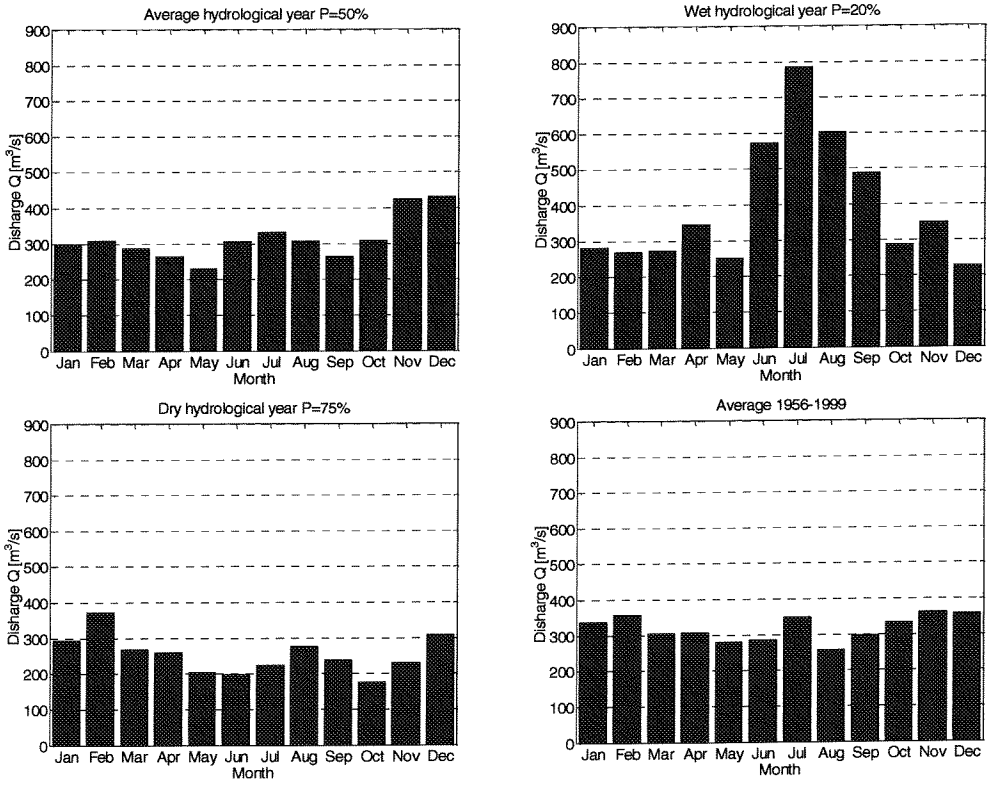

Figure 2-7: Derived average monthly base discharges of the Huangpu River for different hydrological years

2.3 Typhoons in the Shanghai region

2.3.1 Introduction

Typhoons from the Northwest Pacific Ocean are the main trigger for flooding of the Huangpu River. According to Chen *et al.* (1999), flooding of the Huangpu River occurs when torrential rainfall, astronomical high tide and high storm surge combines in a typhoon storm.
Typhoon is a regional specific name for the severest category of a tropical cyclone occurring the Northwest Pacific or Indian Oceans. According to Holland (1993), a tropical cyclone is the generic term for a non-frontal synoptic scale low-pressure system over tropical or sub-tropical waters with organized convection (i.e. thunderstorm activity) and definite cyclonic surface wind circulation. This section discusses more in detail the nature of tropical cyclones and their occurrence in the Shanghai area.

2.3.2 Genesis of tropical cyclones

Tropical cyclones evolve through a life cycle of stages from birth to death. The atmospheric and oceanic conditions play an important role in the process in which a tropical cyclone evolves into typhoon strength. The most important conditions are:

- Surface water temperature has to reach or exceed 26.5 degrees of Celsius
- Pre-existing weather disturbances
- Moistly atmosphere
- Relative low wind shear

Growth

These conditions are constantly met in the Northwest Pacific Ocean (see figure 2-8), where average 30 tropical storms arise annually from which 20 will grow into typhoons. Tropical cyclones are mostly formed from simple clusters of thunderstorms. The heat and moisture from the warm ocean waters are the key energy source for typhoons. The tropical cyclone extracts latent and sensible heat from the warm ocean waters. Moreover, inside the clouds of a tropical cyclone, as water vapours condense, the latent heat is released into the higher troposphere as sensible heat that drives the circulation in the storm. The concentration of latent heat is critical to driving the system.

A tropical disturbance in time can grow to a more intense stage by attaining a specified sustained surface wind speed. Tropical cyclones with maximum sustained surface winds of less than 62km/hr are called *tropical depressions (TD)*. Once the tropical cyclone reaches winds of at least 63km/hr (10 minutes average), they are called a *tropical storm (TS)* and assigned a name. When the wind speed of tropical storm subsequently reaches 119km/hr it is called a typhoon in this region. Figure 2-9 depicts the typhoon Sinlaku in its tropical storm stage in the Northwest Pacific. If the atmospheric and oceanic conditions persist long enough a tropical storm may grow into each subsequent stage in just a half a day to a couple of days. When a tropical cyclone has evolved into a typhoon, it can remain for up to three weeks and travel thousands of miles during its existence. According to historical records of typhoon hazards in Shanghai, typhoons last averagely three days in the Shanghai area.

Intensity of tropical cyclones

The intensity of tropical cyclones is categorized according to their sustained wind speed in the Saffir-Simpson scale from category 1 to 5, presented in table 2-5. To cause flooding of the

Huangpu River, the tropical cyclone has to reach typhoon strength. However, the lower category typhoons can create large damages to Shanghai as well. Almost any typhoon that approaches Shanghai will cause water logging to the urban area. In general, a tropical cyclone that stalls over an area causes the severest damages. The rainfall caused by a tropical cyclone is related to the following factors:

- Forward speed tropical cyclone,
- Landfall location,
- Distance location to the tropical cyclone,
- Interactions with local weather.

	Category	Central pressure [hPa]	Winds [km/hr]
Tropical depression	TD	-----	< 62
Tropical storm	TS	-----	63-118
Typhoon	1	> 980	119-153
Typhoon	2	965-980	154-177
Typhoon	3	945-965	178-209
Typhoon	4	920-945	210-249
Typhoon	5	< 920	>249

Table 2-5: The Saffir-Simpson scale for classification of tropical cyclones

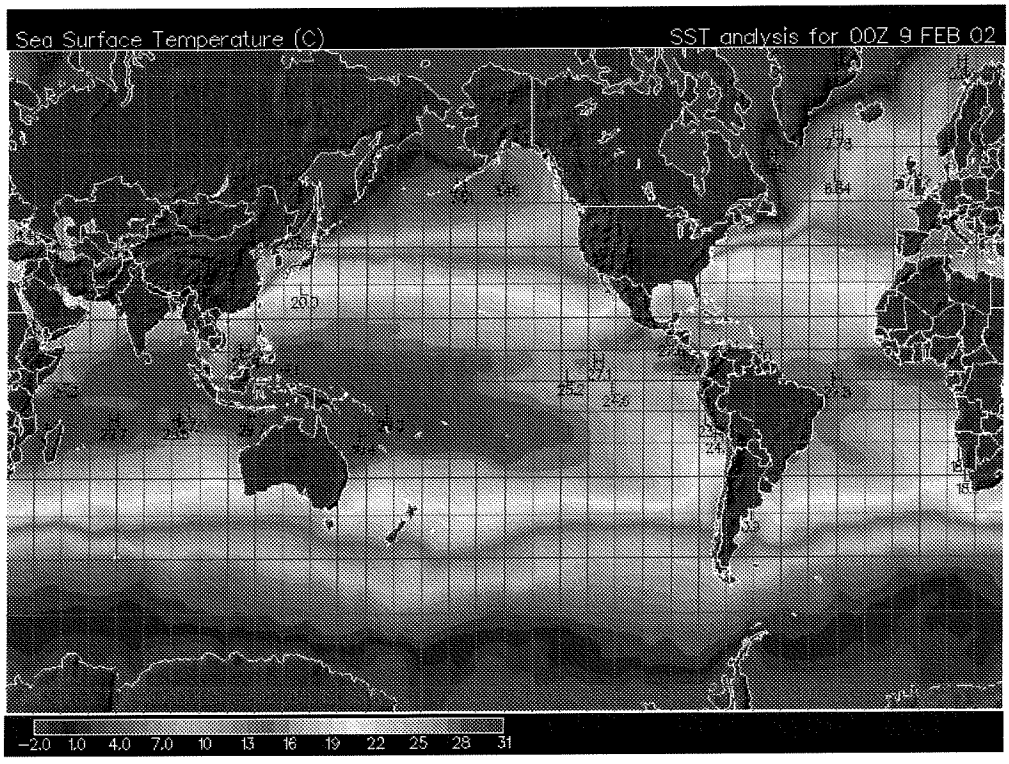

Figure 2-8: Sea surface temperature (sst) map of February 2002. The water temperatures in red are warm enough to develop and sustain tropical cyclones (t > 26.5°C) (source: Unisys Weather Server)

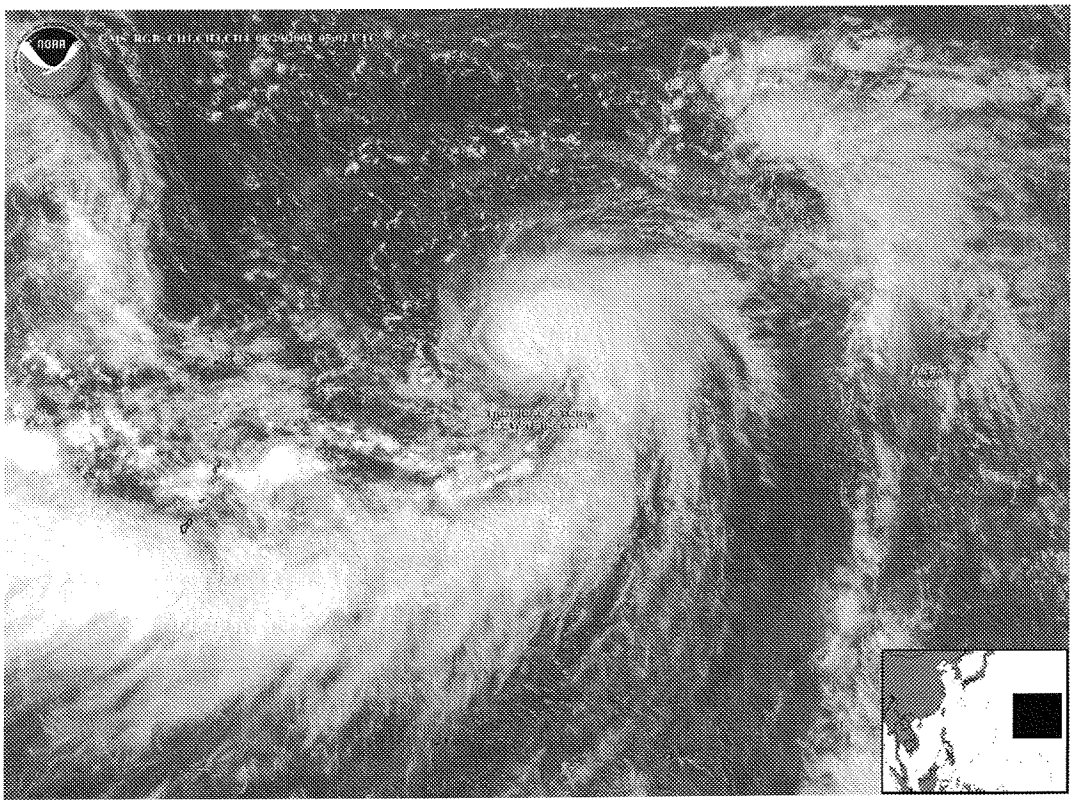

Figure 2-9: Tropical Storm Sinlaku. Located over the Western Pacific Ocean near 18.3N 155.5E on 29 August 2002 at 06:00 UTC. Sinlaku has been moving northward with 3 knots with maximum sustained winds at 35 knots, gusts to 45 knots. (source: NOAA)

Decay

Just as many factors contribute to the genesis and development of a tropical cyclone, there are many reasons why a tropical cyclone begins to decay. The most important factor is the lack of moisture and heat, when it moves into cooler waters. Second, shear winds can tear a typhoon apart. Landfall of a typhoon shuts off the cyclones moisture source and surface friction can reduce the circulation as well. In general, a weakening typhoon can regain its strength when it moves into a more favourable region or when it interacts with mid-latitude frontal systems.

2.3.3 Structure of tropical cyclones

The area that is affected by the typhoon is larger than they appear on weather maps, and their tracks are more than a line. The width of a typhoon can vary considerably, but in general typhoons are about 400 to 500km in width. The size of the typhoon does not necessarily indicate the typhoon's intensity. A distinctive feature of typhoons is the clear centre of the typhoon, called the eye, caused by sinking air. The pressure at this location is the lowest of the tropical cyclone. Surrounding the eye is the region with the most intense winds and rainfall within the storm, and is called the eye wall. Large bands of clouds and precipitation spiral slowly from the eye wall and are called spiral rain bands. These rain bands are 80 to 800km long from the eye, and range in width from a few miles to tens of miles. Higher clouds sometimes obscure these rain bands making satellite monitoring of the storm difficult. Typhoons circulate counter-clockwise about their eyes, in the Northern Hemisphere and clockwise in the Southern Hemisphere. These features can be clearly seen in figure 2-10, which depicts the typhoon Sinlaku (category 4) in the East China Sea just before it makes landfall at the east coast of China.

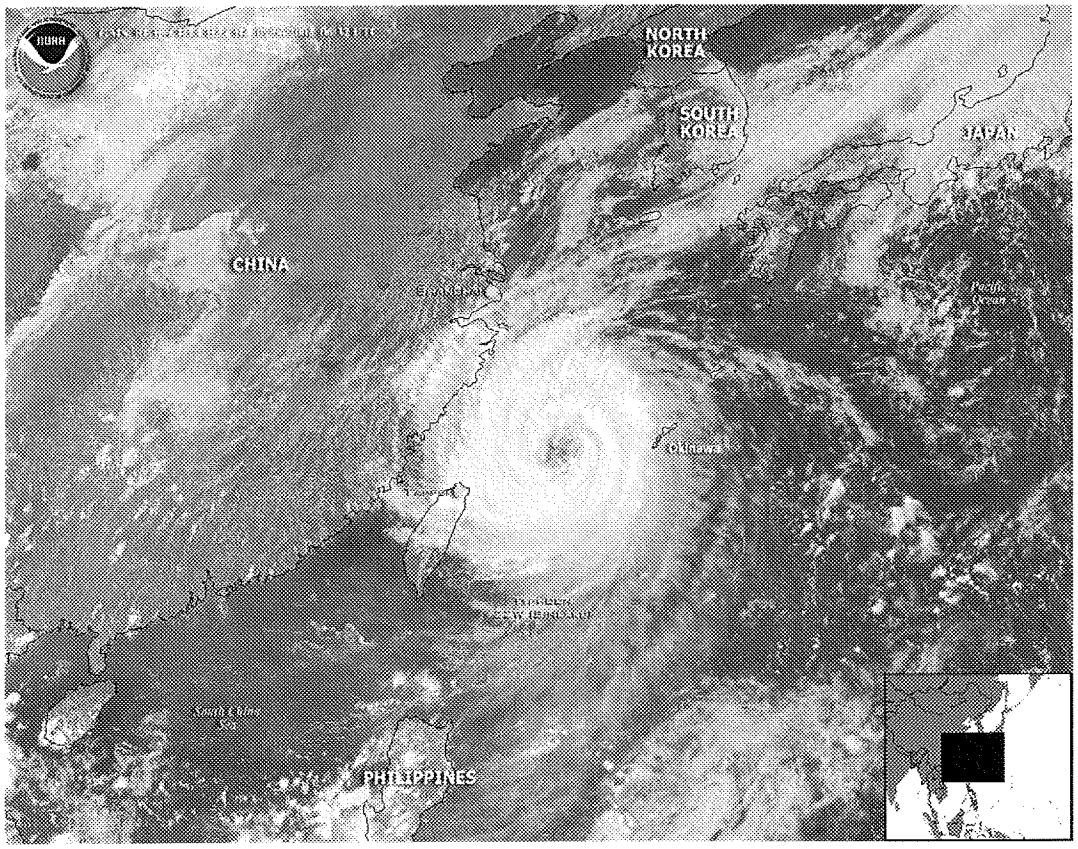

Figure 2-10: Typhoon Sinlaku. Located over the East China Sea near on 6 September 2002 at 06 :32 UTC. Typhoon Sinlaku has been moving west-southwestward at 3 knots with maximum sustained winds estimated at 85 knots, gusts to 105 knots. The powerful storm swept over the Okinawan island chain injuring 29 people and caused major power outages. (source: NOAA)

2.3.4 Tropical cyclone landfall in the Shanghai region

As long as the tropical cyclones stay offshore, the damages caused are overseen. The severest damages are associated with the *landfall* of a tropical cyclone. At present the landfall location of a tropical cyclone can be forecasted quite accurate by means of satellite monitoring of the tropical cyclone's movements, however, some storms can show sudden erratic changes in their moving direction, intensity and speed. These sudden changes in the cyclones path are difficult to forecast and can cause severe disasters to an area as evacuation and other measures cannot be taken in time. Unlike an earthquake for example, a natural disaster as a tropical cyclone is not confined to a local region. A tropical cyclone is a moving system, and its accompanying torrential rain, storm surges and strong winds move along with the storm. Therefore, the development and movement of these storms are closely watched by meteorological observation stations from various countries in the Northwest Pacific.

Landfall distribution

Chen (2000) investigated the frequency distributions of tropical cyclones from the northern West Pacific that makes landfall in China. It appeared that during 1947-1997, there were 341 out of 1382 tropical cyclones making landfall in the east coast of China. Some tropical cyclones make landfall twice. For example, a storm first made landfall over Taiwan, then over Fujian successively. The 341 tropical cyclones resulted in 434 landfalls, distributed along the coast of

China; this is an average of 9 landfalls each year which is the global highest tropical landfall rate for a country. This is not strange when considered that about 18.000km of China's coastline is exposed to the Pacific ocean. The landfall distribution peaks along the southern regions of China's coastal line. The Shanghai area, including Jiangsu Province, has one of the lowest landfall frequencies along the coast, during the observed 50 years period only 7 landfalls occurred. The distribution of tropical cyclone landfalls along the coast are shown in figure 2-11. Some tropical cyclones does not make landfall, they just approach and pass the offshore region. The majority of the floods in Shanghai are caused by these kinds of tropical cyclones.

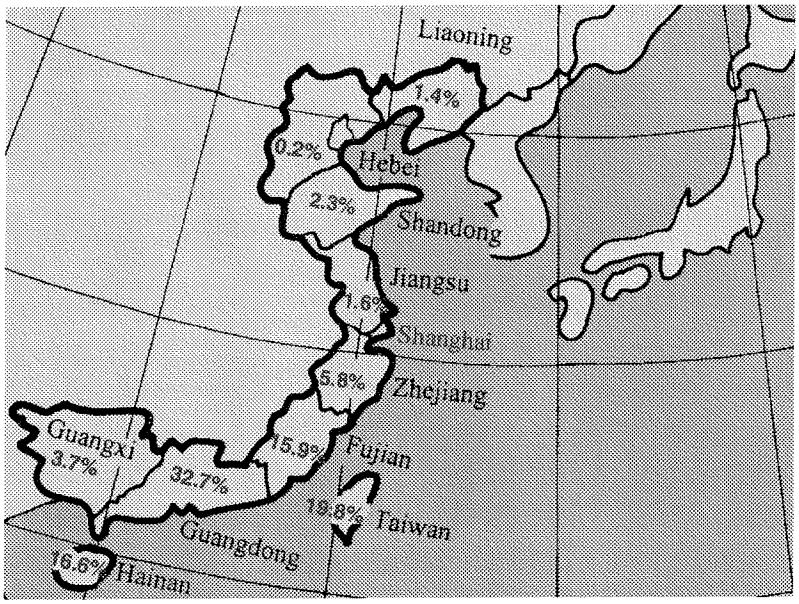

Figure 2-11: Tropical cyclone landfall distribution along the coastal line of China during 1949-1997 (with data from Chen, 2000)

Moving direction of tropical cyclones

Tropical cyclones from the Northwest Pacific tend to landfall somewhere along the east coast of China. This is because the geographic orientation of China's east coast is along the natural track of tropical cyclones. The track of a tropical cyclone is the result of complex interactions between the storm's own internal circulation and the earth's atmosphere. The *wind belt* in which the tropical cyclone is located determines a large part of the track. In general, tropical cyclones from the Northwest Pacific (including the South China Sea) are driven westward by easterly trade winds in the tropics towards China's coast. Eventually, these storms mostly turn north-westward around the subtropical high and migrate into higher latitudes. This can be seen in figure 2-12, where the tracks of the occurred tropical cyclones in the Northwest Pacific in 2002 are presented. From figure 2-9, it can also be noticed that the Northwest Pacific tropical cyclones can be further categorized in:

- Category 1: Tropical cyclones from the South China Sea,
- Category 2: Tropical cyclones from the Northwest Pacific and enter South China Sea,
- Category 3: Tropical cyclones from the Northwest Pacific and do not enter South China Sea.

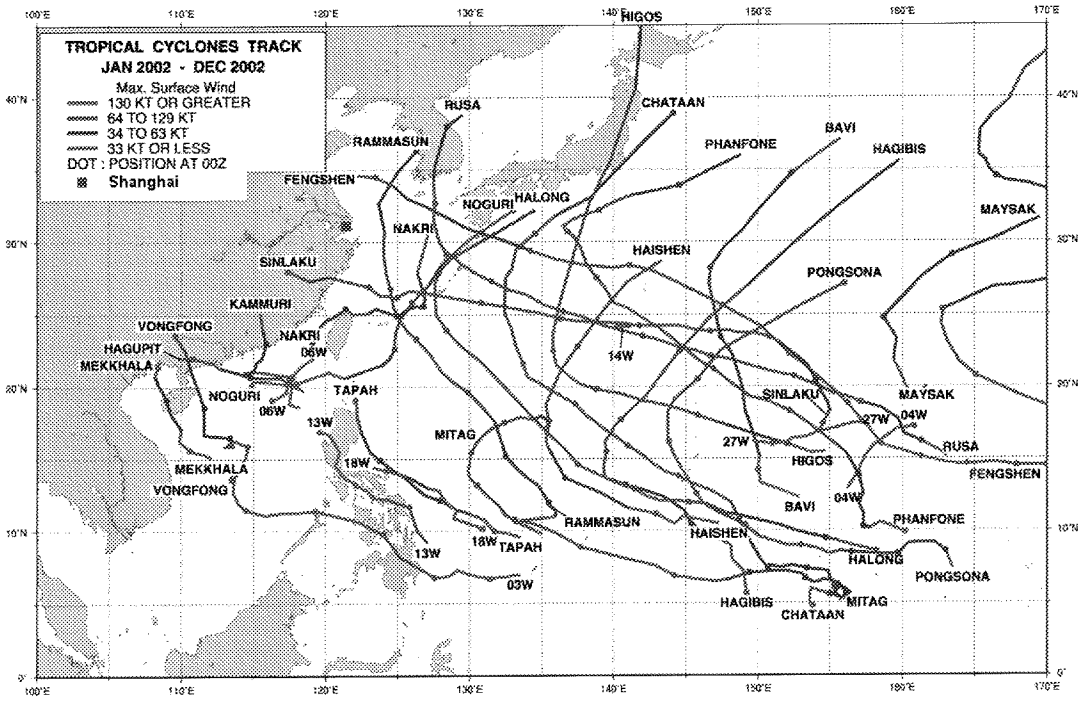

Figure 2-12: Tropical cyclone tracks in the Northwest Pacific Ocean in 2002 (adapted from TRMM Tropical cyclone database)

Most disastrous tropical cyclone track to Shanghai

Most of the tropical cyclones, that cause Huangpu River to flood, have reached typhoon strength and belong to category two and three on the Saffir-Simpson scale. In the northern hemisphere the winds of a tropical cyclone rotates counter clockwise and the strongest winds and surges can be expected on the upper right quadrant of the storm relative to the typhoon's moving direction as the motion of the typhoon also contributes to its swirling winds.

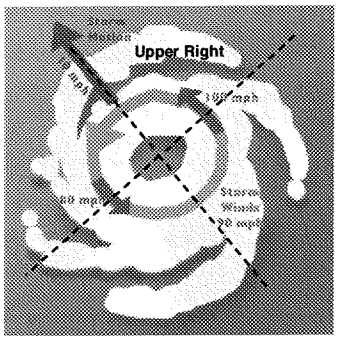

Figure 2-13: Upper right quadrant of a tropical cyclone

The most disastrous floods of the Huangpu River is believed to occur when typhoons move towards Shanghai *perpendicular* to the coast and *stalls* in front of the city driving storm surges into the Yangtze River estuary and the strong winds over the area. In addition, the heaviest downpour, in turn rainfall runoff, can be expected when a tropical cyclone slows down. This typhoon track is confirmed by Chu (2002) in his study on the extreme hydrodynamic conditions in the Yangtze Estuary.

Typhoon season in the Shanghai area

In general, the conditions in the Northwest Pacific are such that tropical cyclone can develop all year round. However, the tropical cyclones that can cause flooding of the Huangpu River are concentrated in the months June to October, this period is the typhoon season for the Shanghai region. Average two typhoons annually can actually cause flooding of the Huangpu River. Figure 2-14 shows the monthly variation of tropical cyclone genesis in the Northwest Pacific with the number of tropical cyclones that successively make landfall somewhere along the coast of China. The overall peak landfall month is August.

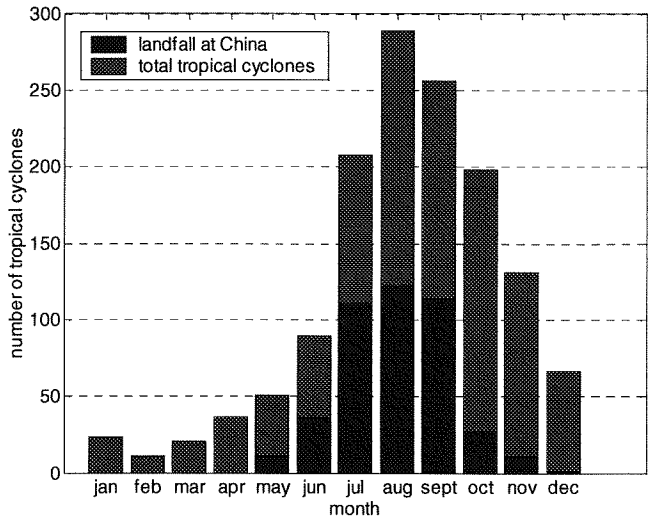

Figure 2-14: Monthly variation of tropical cyclone genesis in the Northwest Pacific including the South China Sea in red and the monthly landfall variation along the coast line of China in blue during 1949-1997 (with data from Chen, 2000)

With data from Chen (2000), the distribution of landfall in Shanghai and the area of the area above Shanghai along the coast of China is computed (figure 2-15). Tropical cyclones, we know now, turn to the north when they are at the height of Shanghai; therefore, these tropical cyclones moving to the north which do not necessarily landfall at Shanghai still affect Shanghai by passing the city.

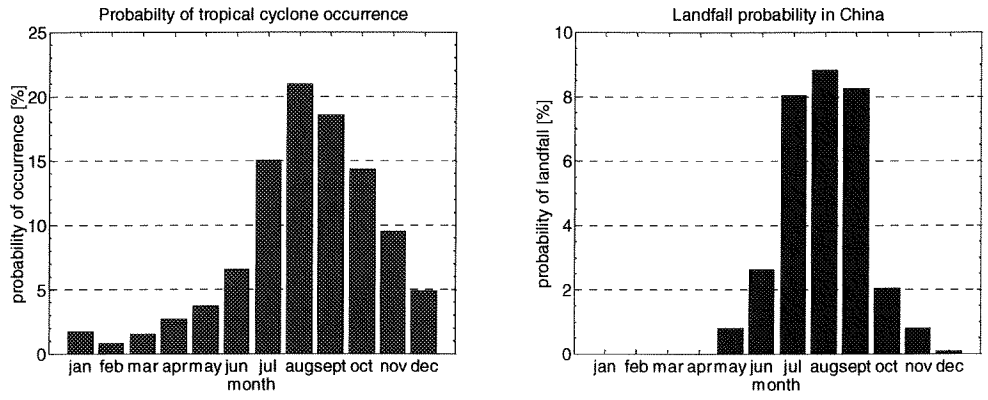

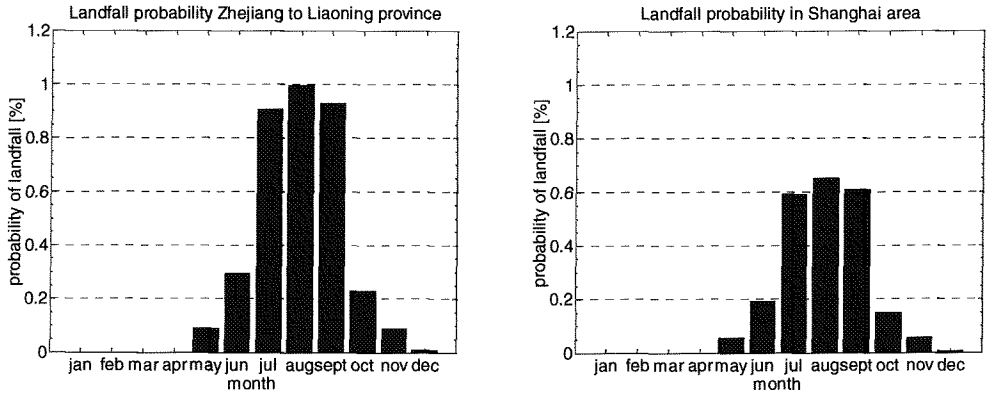

Figure 2-15: Landfall probability of tropical cyclones along the coast of China

2.3.5 Climate change and tropical cyclones

The predicted climate change in this century (Houghton *et al.*, 1990, 1992, 1996) may result in increased sea surface temperatures and increased tropical rainfall. Since warm ocean water is one of the prerequisite conditions for tropical cyclones genesis and development it is among scientists (Henderson-Sellers *et al*, 1998), however, not clear whether this will lead to an increase of tropical cyclone occurrence frequency and intensity. A changing climate will result in a change in the remaining typhoon growth requirements as well and it is still unclear how these conditions will develop in a changing climate. Regionally there may be areas that have small increases or small decreases in frequency, but globally seen it is not certain how the frequencies will be affected by climate change. For the Northwest Pacific basin, Chan and Shi (1996) found that both the frequency of typhoons and the total number of tropical storms and typhoons have been increasing since about 1980. However, the increase was preceded by a nearly identical magnitude of decrease from about 1960 to 1980. Results that are more confident are obtained recently about the typhoon strength with regard to climate change. Studies based upon thermodynamic cyclonic models (Henderson-Sellers *et al*, 1998) (Holland, 1997) suggest that the typhoon wind strength may increase 10% to 20% in a doubled CO^2 climate. However, more research is needed to validate the assumptions made in these studies.

2.4 Flooding of the downtown area of Shanghai City

2.4.1 Introduction

Typhoons are the main trigger for flooding of the Huangpu River. This chapter discusses the three factors that cause the flooding: storm surge, high tide level and the sustained higher water levels in the river as a result of the higher tide in the mouth of the river and the rain season earlier. The first paragraph treats the storm tides created by the simultaneous occurrence of storm surge and high tide levels, followed by a discussion on the torrential rainfall caused by the typhoon. The final paragraph treats the upstream discharge in the Huangpu River during the typhoon season.

2.4.2 Storm surges at Wusongkou

Typhoons bring along storm surge, torrential rainfall and strong winds. These hazards move along with the typhoon and affect the areas the typhoon passes. When a typhoon passes Shanghai, the storm surges caused will be driven into the Yangtze River estuary causing the storm tide levels to increase additionally because of the shallow waters and confined dimensions within the estuary. When this occurs simultaneously with high tide, the storm tide travelling into the Huangpu River can easily cause the water levels in the river rise to unparalleled levels with inundation of urban Shanghai as a result.

The storm tide is defined as the total water level elevation, including the astronomical tide above or below a standard datum resulting from the passage of a typhoon. The magnitude of the eventual storm tide level involves some non-meteorological factors including the topography of the seabed and the funnelling effects in bays and other inlets along the coast.

Storm surge can be imagined as a dome of water moving with the typhoon, created by the low atmospheric pressure in centre of the typhoon and the local wind stress on the water surface. The strength of a typhoon determines a large part of the storm surge's magnitude.
The magnitude of the storm surge depends on:

- Moving direction of the typhoon,
- Atmospheric pressure,
- Distance and angle of landfall,
- Wind strength

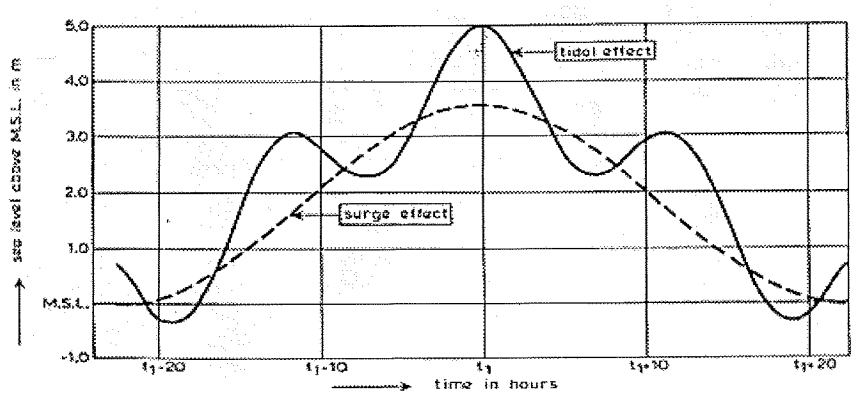

Figure 2-16: Storm tide

Days before the tropical cyclone passage, the water levels will be affected by the swells of the tropical cyclone. Waves caused by the strong winds of the tropical cyclone tend to pass through the cyclone wind system into regions with weaker wind or calm conditions. When those waves reach the shore they are known as swells. Swells can be noticed days before the arrival of the storm itself as a slow rise of the water levels, therefore swells are also termed forerunners. In contrast, storm surges of a tropical cyclone cause a much quicker and severe rise in the water levels. In general, the atmospheric reduction caused by the typhoon surges the water tide between 0.5 to 1.5m. The strong winds additionally increase the tide 0.5 to 3m in the Shanghai area. The eventual storm tide at Wusongkou, in the mouth of the river, depends on the actual tide level and the local bathymetry.

The highest storm tides recorded in the river are caused by the typhoon 9711; this is the 11th typhoon in 1997 (also named Winnie). At Huangpu Park observation station in the city centre the water level reached the historical height of 5.72m WD, about 1.32m above the flood warning level and 0.5m higher than the last historical record. Moreover the water level was only 0.14m lower than the design 1:1000 year's water level at this location. Table 2-7 shows the water levels as a result of this typhoon and the accompanying flood warning levels for the three main observation stations in the river. Recall figure 2-5 for the locations of the stations.

Barrier location		Wusongkou	Huangpu Park	Mishidu
Water level typhoon 9711	[m] WD	5.99	5.72	4.27
Water level typhoon 8114	[m] WD	5.72	5.22	3.70
Flood warning levels	[m] WD	4.70	4.40	3.30

Table 2-6: Historical highest water levels in the Huangpu River, caused by typhoon 9711

The highest storm surge level recorded at Wusongkou is 1.81m during typhoon 5612 (this is the 12th typhoon in 1956), it caused a storm tide of 4.64m WD. If this had occurred simultaneously with spring tide, the flood damages caused would be tremendous.

Decade		1950 - 1959	1960 - 1969	1970 - 1979	1980 - 1989	1990 - 1999	2000 - 2002
Wusongkou	[m] WD	4.98	5.31	5.29	5.74	5.99	5.87
Huangpu Park	[m] WD	4.65	4.76	4.98	5.22	5.72	5.70
Mishidu	[m] WD	3.80	3.60	3.59	3.86	4.27	4.15

Table 2-7: Maximum water levels per decade in the Huangpu River from 1950 to 2002

Decade		1950 - 1959	1960 - 1969	1970 - 1979	1980 - 1989	1990 - 1999	2000 - 2002
h_{WS} >5	[m] WD	10	7	16	12	20	11
h_{surge} >0.5	[m]	0	1	1	2	4	13

Table 2-8: The number of typhoons causing high water levels at Wusongkou increased tremendous from 1950 onwards (Hohai University, 1999)

2.4.3 Torrential rainfall

The torrential rainfall associated with typhoons brings water logging hazards and the extensive runoff can cause flooding of the inland areas. The heaviest rains are concentrated in the eye wall. The key driving mechanism of the typhoon is the conversion of latent and sensible heat from the ocean into wind. The latent heat is provided by condensation of water, these masses of water are collected in this eye wall. In fact, heavy rainfall is an inevitable exhaust product of a typhoon. The closer this eye wall nears a location, the heavier and more frequent the rainsqualls are expected to the area. The rains in the spiral bands in the outer parts storms are lighter and more spread out. In effect, some of the greatest rainfall amounts associated with tropical systems occurs from weaker tropical storms that have a slow forward speed (1.6 to 16km/hr) or stall over an area. Due to the amount of rainfall a tropical storm can produce, they are capable of causing as much damage as a category 2 hurricane. Hence, we summarize that the magnitude of the torrential rainfall depends on the following characteristics of the typhoon:

- Typhoon strength
- Distance of location to the tropical cyclone
- Forward speed

2.4.4 Sustained higher water levels in the rivers and lakes

Plum rains sustain the water levels in the lakes and rivers and the raises the ground water table in the Tai Lake basin. Runoff into the main water way of the area, the Huangpu River increases. When the typhoon season then follows, the heavy downpour to the area will temporarily increase the already higher discharges into the Huangpu River. When the water levels in the Yangtze River estuary are raised by the storm surge and high tide, it will be amplified further as it moves into the Huangpu River where it meets the high discharge. Consequently, defences are breached and the urban area is flooded.

This is especially true during a hydrological wet year where the upstream discharges are much higher. The average discharge volume from the Tai Lake and the main tributaries into Huangpu River in the typhoon season for different hydrological years are summarized in table below.

Year type	Long average	Wet	Average	Dry	Very dry
Discharged volume $[m^3]\cdot 10^8$	34.84	60.99	34.15	25.79	7.44
Annual percentage [%]	33	46	32	30	13
Annual $[m^3]\cdot 10^8$	106.60	132.10	104.90	84.80	58.70

Table 2-9: Average Tai Lake basin discharge volume into the Huangpu River during the typhoon season from July to October 1956-1999 (Wang *et al.*, 2001)

3 Storage capacity of the Huangpu River

3.1 Introduction

Flooding of the Huangpu River occurs when the storage capacity of the river is insufficient to store the upstream discharge during barrier closure. Several factors determine the storage capacity of the Huangpu River, like the dimension of the river, the location of the barrier and the water regime in region generally. We treat these factors in the first three sections of this chapter. This chapter starts with a discussion on the progressive rise of the water levels and in turn the flood frequency of the Huangpu River. It appears the rapid industrial development of Shanghai is the cause for the rising trend of the water levels in the river and, in turn, increased the flood frequency. Subsequently, in section 3.3 the conditions of the present flood control works along the river is treated. Particularly, the floodwalls that at present surround the entire course of the river is important to the storage capacity of the river after barrier closure. The present condition of the flood control works as well as its role *after* barrier completion is investigated in this section. We also sophisticate our definition of flooding of the Huangpu River during barrier closure in this section. The proposed barrier locations will be treated in section 3.4. In the final section, we compute the storage capacity with an improved one-dimensional flow model of the Huangpu River in SOBEK RIVER. An existing model of the river based on the actual geometry of the Huangpu River is further schematized to improve the results at Mishidu station. The new model is calibrated and verified with different water level time series from the typhoon season.

3.2 Progressive rise in flood frequency

3.2.1 Introduction

The first records of flooding of Shanghai City by the Huangpu River date back to early 13th century. However, since 1920 the flooding of the Huangpu River occurred with increased frequency. According to the Shanghai Water Authority (2000), most of the possible causes are consequences of the rapid economic development of Shanghai. The three main causes are treated in this subsection. We start with the ground level subsidence in Shanghai City and the sea level rise in this region. Then in subsection 3.2.2 the changes in the upstream water regime in the past are treated. It appears that the storage capacity has been reduced substantially. In subsection 3.2.3 the increased urban drainage into the Huangpu River is treated. These factors are considered the main cause for the increased flood frequency of the river. Insight in these factors is vital in the study on flooding of the Huangpu River during barrier closure.

3.2.2 Sea level rise and ground level subsidence

The flood protection of Shanghai is sensitive to sea level rise and land subsidence. Relative sea level rise reduces the protection height floodwalls provide. The ground level in the urban areas of Shanghai is generally lower than 4m with reference to Wusong Datum. For instance, at Jing'An district and some parts of Putuo Districts the ground level is even less than 3m WD. The lowest point is 2.3m WD (UNESCAP, 2003).

At Huangpu Park station, in the city centre, the average high tidal level is 3.12m WD (see table 2-2) while the storm tides at this location ranges from 4.00m to 5.72m WD (typhoon 9711). That is all urban ground level is lower than the storm tides in the typhoon season. Large parts of the urban area inundates when the Huangpu River floods because of its dish shaped ground level profile.

Excessive ground water exploitation by industry is the main cause of land subsidence in urban Shanghai. The first signs of land subsidence dates back to 1921 during the industrial development of the area. The accumulated mean subsidence from 1949 to 1956, is 1.67m with a maximum of 2.63m covering a downtown area of 130km^2 (Hohai University, 1999). Since 1966 the subsidence rate has been basically under control by reducing the ground water extraction, artificial replenishments and adjustment of the pumping layers. However, the expansion of the urban infrastructure and construction of high rise buildings from the 1960's onwards accelerated the ground level subsidence again. The accumulative settlement from 1966 to 1996 was 124.5 mm. At present the annual groundwater extraction is controlled at $1.42 \cdot 10^8 m^3$ annually (Wang *et al.*, 2001).

The severe ground level subsidence of the urban area had serious consequences to the flood control works along the Huangpu River (next subsection), as a result the floodwalls had been heightened continously to keep the city protected. The overall future ground surface settlement, including the geological structure of Shanghai, is forecasted at 3.5mm annually from 2010 to 2030 and 2.5mm from 2030 to 2050 (see table 3-1). For Wusongkou this figure is estimated at 5mm annually from 2010 to 2030 and 3.5mm annually from 2030 to 2050.

Year	Item	Wusongkou [mm]	Huangpu Park [mm]	Mishidu [mm]	Shanghai average [mm]
2010	ESL	5	4	4	4
	Bedrock	2	2	2	2
	Ground surface	12	7	8	10
	RSL	**19**	**13**	**14**	**16**
2030	ESL	11	10	9	10
	Bedrock	4	4	4	4
	Ground surface	20	10	12	15
	RSL	**35**	**24**	**25**	**29**
2050	ESL	21	19	17	20
	Bedrock	6	6	6	6
	Ground surface	25	12	15	18
	RSL	**52**	**37**	**38**	**44**

Table 3-1: Relative sea level rise in Shanghai (Shanghai Water Authority, 2000)

3.2.3 Increasing reduction of the storage capacity in the area

The economic development of Shanghai goes hand in hand with the need for more land which in turn reduced the storage capacity in the rivers and lakes in the Tai Lake basin. As a result, the water levels in the Huangpu River rose progressively in time. Storm tides in the typhoon season, easily over topped the floodwalls alongside the river with flooding of Shanghai City as a result. In this subsection, we summarize the most important events that have reduced the storage capacity of the Tai Lake Basin causing higher average water levels in the river.

- The water surface of the Tai Lake area is reduced with 13.6% since 1985 with dike constructions and reclamation of surrounding smaller lakes. About 165 of these smaller lakes have been reclaimed. The tidal boundary has increased with 5km to 20km in the upper reaches of the river.

- The opening of the Taipu River has increased the runoff from the Tai Lake into the Huangpu River.

- The Huangpu River has been narrowed during the industrial boom of Shanghai. In the 1960's the total number of wharfs along the river was 109, in the 1990's this is raised to more than 1000. Not only did these wharfs reduce the water surface but they also increased the roughness coefficient, thus sustaining the water level in the river. Moreover, the floodwall construction along the Bund, in the city centre has narrowed the river 20m additionally.

The tables below show the upward trend of the mean high water levels at Mishidu station, the station most close to the Tai Lake in the Huangpu River. In average, the mean water level raised in average 1cm per year at this location.

Decade	1950 - 1959	1960 - 1969	1970 - 1979	1980 - 1989	1990 - 1999
Mean high water level [m] WD	3.49	3.39	3.41	3.70	3.90

Table 3-2: Progressive rise annual mean high water levels at Mishidu station (Shanghai Water Authority, 2000)

Year	1984	1988	1992	1996	2000
Annual maximum [m] WD	3.62	3.61	3.87	3.97	4.21

Table 3-3: Annual maximum water levels at Mishidu station of some years in the past two decades (Hohai University, 2000)

The water surface area in the Yangtze River estuary has been reduced as well since 1960 onwards. In total the area is reduced with 18% and, moreover, the transition zone between the Yangtze River and its estuary is narrowed with 9km to 5km. Plans exists to reduce estuary even more in the future. However, it is not presumable that they will raise the average water levels in the Huangpu River.

In the near future, Shanghai wishes to become a major anchor city to the Asia-Pacific region. The economic development required for this purpose might indirectly feed the already upward trend in the Huangpu River water levels as proved in the past decades.

3.2.4 Increased urban rainfall runoff into the Huangpu River

The flat and dish shaped topography of the urban area (subsection 3.2.2) makes natural drainage of rainwater difficult. During storm tides situations in the Huangpu River, discharge of excessive rainwater into the Huangpu River via the tributaries is even impossible. As a result, inundation of large parts of the urban area, including the city's subway system occurs frequently as a result of heavy downpour. A network of underground drainage pipes and drainage pumps along side the Huangpu is constructed to discharge excessive rainwater into the Huangpu River. An increased ground level subsidence of the urban area has lead to the increase of the discharge capacity. At present, 165 drainage pumps alongside with a total capacity of 1720m^3/s is available

of which an estimated 930m3/s ends up in the Huangpu River. This capacity is based on the design rainfall of 36mm/hr with recurrence interval of one year (UNESCAP, 2003).
Plans exists to increase the drainage capacity up to 2200m^3/s (Shanghai Water Authority, 2000), of which more than 1000m^3/s will be diverted into the Huangpu River. Simple calculations show that the water level in the river then will rise with about 0.09m per hour.

However, in practice it is difficult to utilize the drainage capacity fully because of poor management of the drainage system and the high ground level subsidence rate.
Consequently, waterlog hazards are common in Shanghai and almost any typhoon that brings torrential rainfall in the area will cause water logging of the downtown area. For instance, in 1998 the drainage system is improved, and the rainfall is two third of that in 1985, therefore less houses were inundated (table 3-4). Subsequently in the event of 1990 the rainfall intensity is similar to that of 1988. However, more roads and more number of houses have been damaged by water logging, because many drainage pumps were blocked by litter refuse released from factories and mud from construction sites. According to statistics last year, 7000 construction sites were scattered around the city. In the first five months of this year, drainage administers inspected 47 construction sites on 84 occasions, and 40 were fined, totalling 657.000 Yuan (76.000 Euro[1]), up 179 per cent over the same period last year.

	Rainfall [mm/24hrs]	Roads water logged [%]	Water depth [cm]	Number of house inundated
31 August 1990	162	91	10–40	11.700
31 September 1988	175	34	5–30	2.000
31 Augustus 1985	281	44	10–20	17.350

Table 3-4: Comparison of three water logging events recorded in Jing'An District (after Chen and Zong, 1999)

Water logging hazards in urban Shanghai is a serious problem, as it occurs for almost every typhoon that passes the region. The low ground level profile of the urban area requires pumps for drainage. During barrier closure, when presumed that the Huangpu River is closed off from its tributaries as at present, the discharge from the urban area into the river is limited by the discharge capacity of the pumps that is around 1000m3/s. The increased urban discharge into the Huangpu River has to be taken into account for the flood probability during barrier closure. In the continuation of this study, we assume no difference between available and theoretical pump capacity. Moreover, the torrential rainfall runoff into the river is limited by theoretical pump capacity of 1000m3/s. The remaining water volume as a result of torrential rainfall is logged in the urban area.

[1] *Exchange rate of 28 February 2003 (ABN AMRO).*

3.3 Present flood control works

3.3.1 Introduction

This subsection treats the flood control works alongside the Huangpu River and its influence to the storage capacity. To combat floods, the city has reinforced and extended its four defence lines from seaboard to downtown areas several times last decades. The 508km sea dike, which is considered to be the first defence, now, can stand the severest tropical cyclones. The second line is the urban floodwall with its sluices and gates along the Huangpu River. This floodwall is 208km long and is recently extended with almost 107km through the new urban areas and some of the river's tributaries. The third line of defence forms the smaller floodwalls along the remaining rivers in the city. A network of underground drainage pipes and drainage pumps along side the Huangpu are required to prevent water logging of the urban area during heavy rainfall. This is the fourth defence line and since this can be considered as a load to the storage capacity this aspect is treated in subsection 3.2.4.

3.3.2 Floodwalls

The first floodwall originates from the 1950's. During that time many administrative units involved in the management of the floodwall. As a consequence, the structure and the quality of the floodwall are different along the course of the floodwall. Moreover, the geological conditions vary along the floodwall but and proper soil research was only possible in recent years. As a result the shortcomings in the older floodwall affected the new one. As a result, during numerous typhoon storms, the water levels in the Huangpu River overflowed and burst the floodwall at different locations.
To keep Shanghai City protected against progressive rising water levels of the Huangpu River, the floodwalls have been reinforced, heightened and extended continuously in the course of this century. Despite, recently the typhoon 9711 caused the Huangpu River to overflow a 13.7km long urban section of the floodwall with an average head of 30cm. Subsequently, this section was immediate heightened after this event, but nonetheless it was overflowed again in 2000.

Five major flood protection reinforcement programs have been carried out in this century. The latest floodwall reinforcement program started in 1988. The 208km urban floodwall is reinforced and heightened with averagely 50cm since 1988 to withstand water levels with a return period of once in thousand years set in 1984 by the state Ministry of Water Resources (table 4-10).

P [%]	Wusongkou [m] WD	Huangpu Park [m] WD	Mishidu [m] WD
0.01	6.81	6.29	4.26
0.1	6.27	6.56	4.10
1	5.74	5.40	4.33

Table 3-5: Design water levels and their probabilities of exceedance in the Huangpu River as from 1984

Lately, the floodwall is extended with 107km to protect new urban areas. However, the lack of construction space in the dense urban area and construction problems related to the stability of the present floodwall, still 30km of floodwall is unfinished at present. The top elevation of the current floodwall is 7.30m WD at Wusongkou and lowers to 6.90m WD in the downtown area to

4.70m WD at Mishidu (table 3-6). A detailed map of the flood control works in Shanghai City is presented in figure 3-2.

	Wusongkou	Huangpu Park	Mishidu
Top elevation floodwall [m] WD	7.30	6.90	4.70

Table 3-6: Floodwall top elevation at different locations along the Huangpu River (Shanghai Flood Control Administration, 1994)

The probability of flooding of the Huangpu River is substantial whenever the water levels in the river exceed the so-called warning water levels in the river. The warning water levels differ per location in the river. At Huangpu Park station this water level is set at 4.55m WD whereas at the upstream Mishidu the warning water level is set at 3.50m WD. This tidal dominance of the water levels in the river is the cause for this difference.

	Wusongkou	Huangpu Park	Mishidu
Warning water level [m] WD	4.8	4.55	3.50

Table 3-7: Warning water levels Huangpu River (Shanghai Water Authority, 2000)

At present, the floodwall along the Huangpu River faces the following problems, which have to be kept in mind in the continuation of this study:

- Wrong assumptions on the geological conditions applied to the floodwall in the past caused instability of the current floodwall,
- Structure and quality of the floodwall varies per river section,
- Poor floodwall management permitted unauthorized construction and or dredging works close to the floodwall causing structure instability.

Decade	1950 - 1959	1960 - 1969	1970 - 1979	1980 - 1989	1990 - 1999	2000 - present
Wusongkou [m] WD	4.98	5.31	5.29	5.74	5.99	5.87
Year of occurrence	1954	1962	1974	1981	1997	2000
Huangpu Park [m] WD	4.65	4.76	4.98	5.22	5.72	5.7
Year of occurrence	1954	1962	1974	1981	1997	2000
Mishidu [m] WD	3.8	3.6	3.59	3.86	4.27	4.15
Year of occurrence	1954	1962	1979	1981	1997	2000

Table 3-8: Maximum water levels along the Huangpu River per decade (source: Shanghai Water Authority, 2000)

Finally, within the urban area of the floodwall 5 bridges and 6 roads cross the Huangpu River. The intersections of these crossings are the locations where the floodwall breaches most of the time during high water levels in the river. At present, these locations are supported temporary during typhoon storms. The flood protection level at these locations is certainly not for once in thousand year water levels.

3.3.3 Tide Gates

The many tributaries of the Huangpu River in Shanghai are controlled with tide gates. When the warning water level in the river is expected to be reached, these tide gates will be closed to prevent flooding. As much as 1300 tide gates along the Huangpu River exits to prevent storm

tides in the river moving into the tributaries and channels. The width of these gates varies from 1.5m to 20m, these gates in total represent a width of 7km, and all of them are operated manually. Furthermore, most of the gates are lower than the top elevation of the floodwalls and poorly maintained as well. These gates are weak spots in the flood defence of the tributaries. Figure 3-2 presents an overview of the flood control works in the urban sections of the Huangpu River. The two main tributaries of interest the Wencao Bang and the Suzhou Creek can be closed off from the Huangpu River as well.

The Suzhou Creek Barrier is the largest tide gate along the Huangpu River. This barrier is build to safeguard the downtown area along the Suzhou Creek after the 1984-flood. This barrier closes whenever the water level in front of the barrier is predicted exceed 4.55m WD. During the typhoon season, the barrier will be closed once or twice monthly for maintenance and to flush silt depositions from the sill. During typhoon 9711, the water levels at Huangpu Park station near the Suzhou Creek Barrier reached the historical high of 5.72m WD and the barrier successfully prevented storm tides entering the Suzhou Creek. In 2003, the construction of a new barrier in the Suzhou Creek will start. The new barrier is located not far from the existing barrier

3.3.4 Urban flood control works and storage capacity of the Huangpu River

The floodwall is originally designed to withstand storm tides entering the river from Wusongkou with a return period of 1:1000 years. After completion of the barrier in the mouth of the river, the floodwall will become the second flood defence line with regard to storm tides.

Considering the present condition of the floodwall, it might be interesting to lower the floodwall to improve the stability of the wall after barrier completion. In addition, for scenic reasons, the Shanghai Municipal Government already indicated their wish to lower the floodwall along the sightseeing boulevard the Bund (Huangpu Park station's location). At present the floodwall elevates at 6.90m WD at this location, this is about 3m above street level diminishing the appeal of the Shanghai skyline.

Figure 3-1: Impression of the floodwall at the Bund of the Huangpu River in the city centre.

However, with regard to the flood probability after barrier closure, the current floodwall is the first defence line for the upstream discharge. The floodwall elevation determines the storage height of the river, i.e. the difference between the warning water level and the initial water level in the river immediately after barrier closure.
The future floodwall elevation should be determined based on:

- Discharges into the Huangpu River during closure,
- Predicted ground level subsidence of the area,
- Acceptable probability of failure of the floodwall after completion of the barrier.

Flooding of the Huangpu River occurs when the storage capacity of the river is insufficient to store the upstream discharge during barrier closure. In reality, this means that flooding occurs when the floodwalls alongside the river breaches or when the water levels in the river exceeds the top elevation of the floodwalls. The urban flood control works consisting of the floodwalls and the tide gates along the course of the river determine largely the available storage capacity of the river. Because of the uncertainty of the elevation of the eventual floodwall after completion of the storm surge barrier, we use the warning water level at Mishidu and Huangpu Park as reference for flooding. Hence, in the continuation of this study, flooding of the Huangpu River during barrier closure is defined as the exceedance of the warning water level in the river.

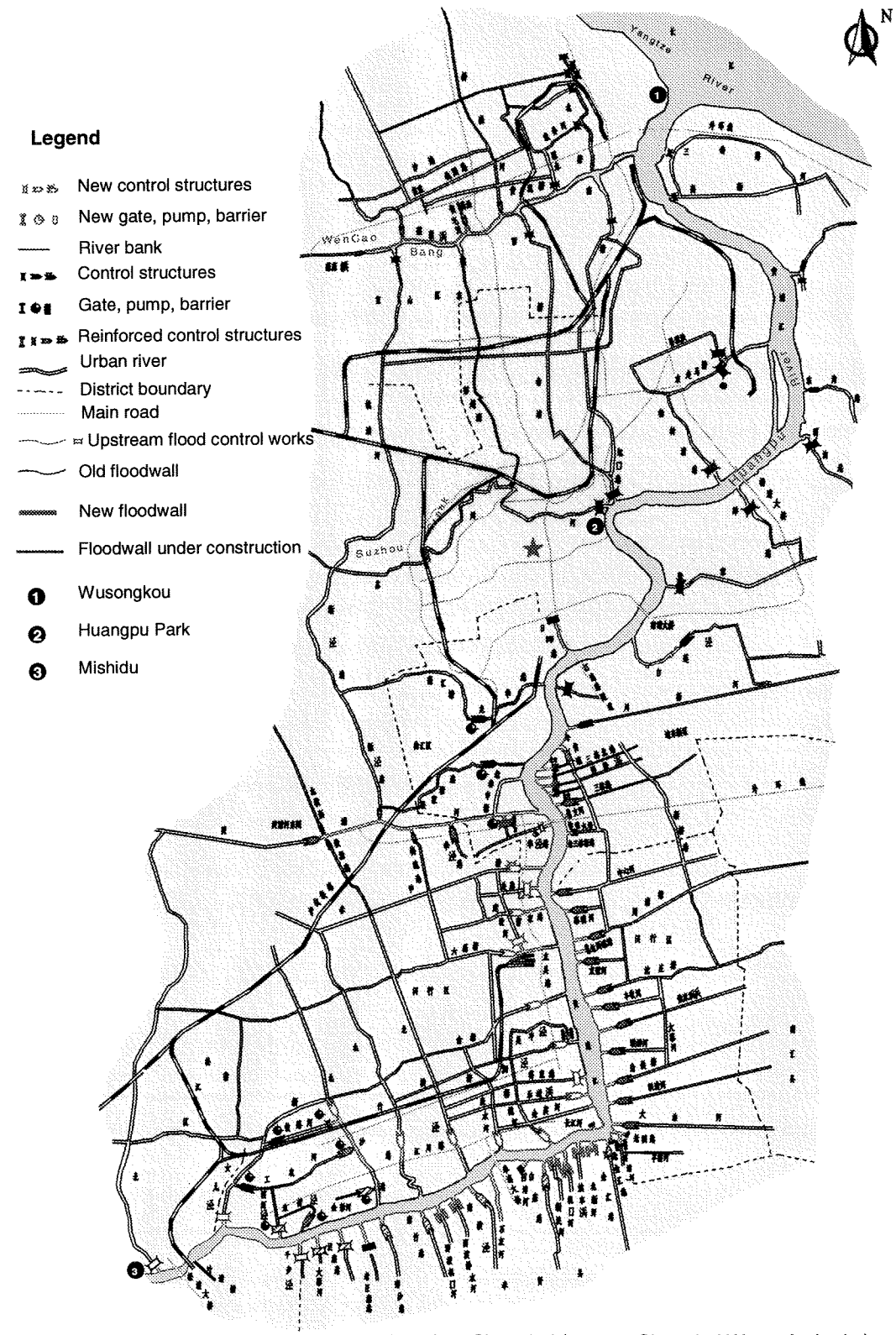

Figure 3-2: Overview flood control works urban Shanghai (source: Shanghai Water Authority)

3.4 Proposed storm surge barrier

3.4.1 Introduction

This section presents the proposed barrier locations and the influence of the barrier location to the storage capacity of the Huangpu River. The Shanghai Water Authority has appointed three potential locations in the mouth of the river. The exact location of the barrier is still under investigation by the Shanghai Water Authority. The barrier eventual location and barrier type depends on factors like the feasibility of construction, costs and the location's influence to the flood probability after barrier closure.

3.4.2 Barrier locations in the mouth of the river

The ultimate feasibility of the barrier location is determined on the bases of various factors and the flood probability after closure is just one of them. The prohibitive factors with regard to the navigation, construction, economic aspects that these locations introduce are beyond the scope of this study. The locations are presented below with a short description. In general, two problems will arise when the barrier site is located more upstream of Wusongkou. First the area protected by the barrier will be reduced. Secondly, less space is available for the barrier construction site upstream of the mouth of the river as the population density increases. Especially the west banks of the Huangpu River (Puxi) is scattered with ports and related industries. Three locations in and near the mouth of the Huangpu River are put forward by the Shanghai Water Authority, see also figure 3-3.

Wusongkou

The first location is at the Wusongkou in the mouth of the river. The storm surge barrier at this location will protect all the tributaries of the Huangpu River, including the Wencao Bang Moreover, the barrier might make use of the existing construction yard for the cross Huangpu River tunnel already ongoing. Furthermore, a barrier at this location will create the largest storage capacity of the river, thus reducing the flood probability during barrier closure in comparison with the locations more upstream. Only the naval base on the left riverbank at Wusongkou might be a prohibitive factor for a barrier at this location.

Zhanghua Bang

This location is in a straight section upstream in the river. A storm surge barrier at this location is favourable to shipping as little manoeuvring is needed to pass the barrier. However, the area protected by the barrier is reduced and the downstream section of the tributary Wencao Bang is not protected at all. A tide gate exists upstream of Wencao Bang. Furthermore, this site is densely populated with industry already, for instance the terminal of the Shanghai Container Terminals Ltd. Relocation of this terminal to create space for the barrier will introduce high costs.

Fishery Yard

This is the most upstream barrier location at about 10km from the river mouth. It is located just in front of a bend. As the name already reveals, a fishery yard is closed to this location. This location is the most unfavourable location for a storm surge barrier in terms of storage capacity and the protection provided by the barrier.

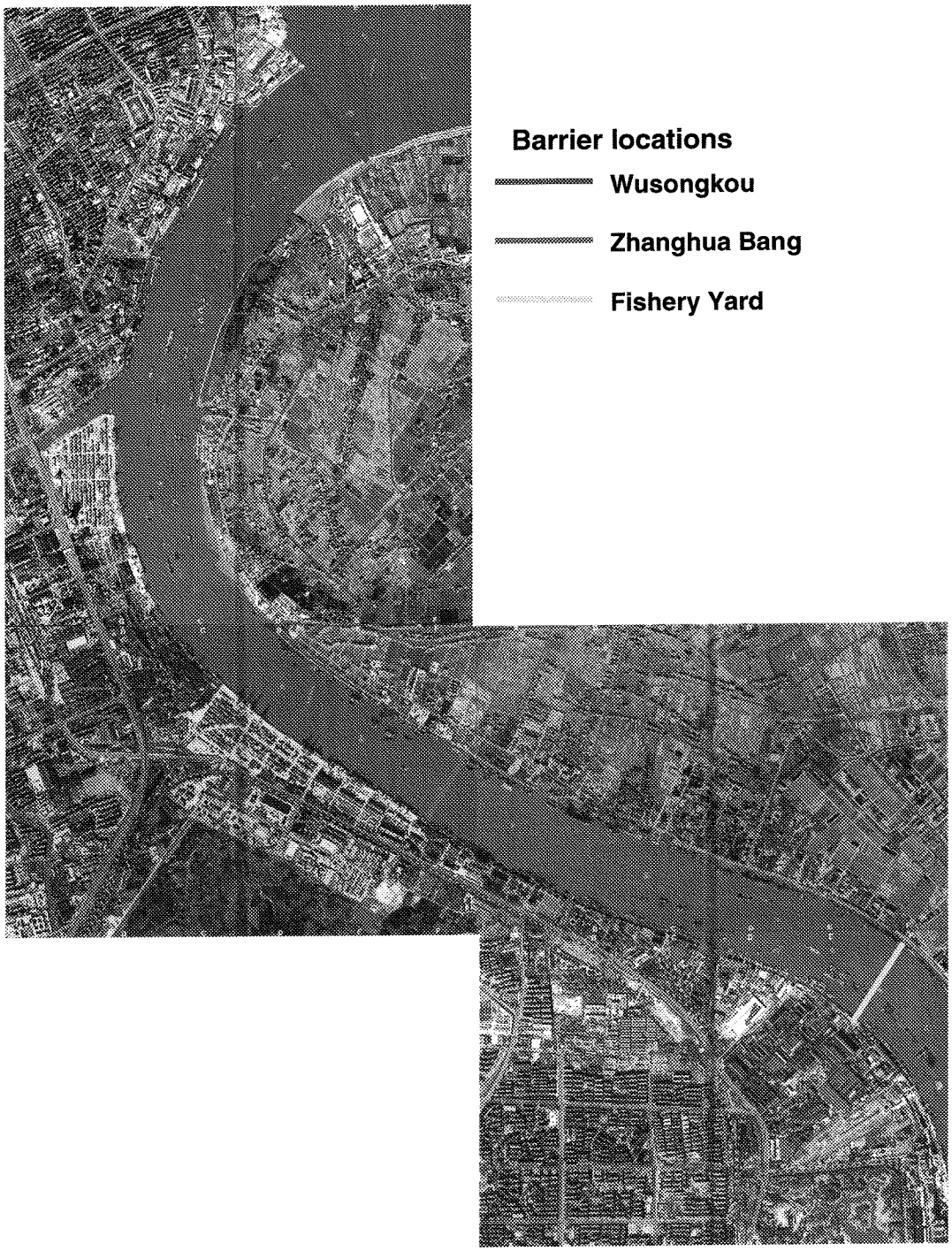

Figure 3-3: Storm surge barrier locations in the mouth of the Huangpu River

3.4.3 Closure strategy and frequency

The decision to close the storm surge barrier is based on several strategies. The storm surge barrier control authority can decide to close the barrier on the basis of the exceedance of the warning levels at Wusongkou and Huangpu Park station and for locations in the Yangtze River estuary. The Huangpu Park station in the city centre is believed to be the most important reference location with regard to flooding of Shanghai City. However, with this strategy the barrier will close after the storm tide already entered the Huangpu River. Therefore, a better philosophy is to close the barrier based on the *predicted* water levels at the reference locations. When the water levels at the reference locations are predicted to exceed the warning levels then the barrier closure procedure should proceed.

Closing a barrier is an important operation with catastrophic consequences when procedures are taken inaccurately. In a typhoon storm, the situation is stressful to many people and human faults are easily made when closure procedures are too complex, therefore simplicity of the procedures are necessarily and human intervention should be minimized. In choosing the type of the storm surge barrier the following important aspects should be taken into account:

- Simplicity of the closure procedure,
- No hinder of sediment accumulation,
- Flexibility to changes of operation of the barrier,
- No human interference at all during operations

To optimise the storage capacity of the river the inside water level should be as low as possible. In reality, this is not always possible because of the already higher water levels days before the typhoon passes. The time needed to close the barrier varies with the barrier type. The Maeslant barrier in the New Waterway in Rotterdam needs 2.5 hrs to close (BMK, 1997).
After barrier closure, the water levels inside the Huangpu River will rise as discharge into the Yangtze River estuary is not possible. The outside water levels will lower in time because of the tidal movement and the reduction of the storm surge when the tropical cyclone passes. As soon as the water levels at both sides of the barrier are similar, the barrier can be opened only if no storm tides are expected. Flooding of the Huangpu River might occur when the storage capacity is insufficient to store upstream discharge during closure. The closure duration is an important parameter in the flood probability. To prevent flooding during barrier closure the upstream discharge volume has to be either reduced or released. The first measure can be implemented simply with the existing control gate at the Taipu River. Also, during barrier closure the Huangpu River can be relieved from the stored water volume when hatches are facilitated in the barrier doors. During low tide, the river can discharge the stored water volume into the Yangtze River estuary through the hatches. The barrier itself remains closed, ready to protect Shanghai City against the next storm.

When the existing warning water level in the Huangpu River, with reference to Huangpu Park station, is persisted a closure rate of average 8 times annually can be expected. Water level records at Huangpu Park station (Shanghai Water Authority, 2000) show that since 1980, the warning water level at this location of 4.55m WD is exceeded average 8 times annually. The frequency of exceedance of the warning water level at Wusongkou, which is set at 4.80m WD, is average 4 times annually. Moreover, average two tropical cyclones a year can cause flooding of the Huangpu River. A high barrier closure rate is disadvantage to the port industry of Shanghai. Moreover, when the function of the barrier is also used for the planned drainage improvements purposes, an even higher closure rate can be expected. The sea level is predicted to rise with about 52cm at Wusongkou in the year 2050. Consequently, the warning water levels in the Huangpu River will be reached more frequently with even more barrier closures annually.

3.5 Storage capacity analysis with SOBEK-River

3.5.1 Introduction

In this final section of this chapter, we compute the storage capacity of the Huangpu River with one dimensional flow model of the river in the SOBEK RIVER. This chapter starts with the theoretical background of SOBEK RIVER and moves on with an explanation of the flow model of the Huangpu. In this study, an existing model of the Huangpu River with river cross sections after Hohai University is further schematized to improve the results at the upstream Mishidu station. The new model is calibrated and verified with different historical water level time series in the typhoon season of the three hydrological stations in the river. The calibration and verification of the model is treated in subsection 3.5.4. The limited information on the exact upstream connection of the Huangpu River gives rise to assumptions with regard to the storage capacity of the river. This is treated in the subsection 3.5.5. Subsequently, the storage capacity is computed in subsection 3.5.6 for each barrier location.

3.5.2 Theoretical background SOBEK-River

SOBEK RIVER is a one-dimensional open-channel dynamic numerical modeling system developed by WL | Delft Hydraulics. The topographic basis of each SOBEK model is a network of *branches* connected to each other with *nodes*. A node that is connected to only one branch represents a boundary. Real geographic data can be represented with a network of branches and nodes.

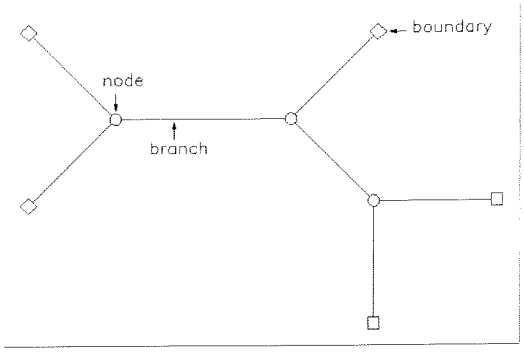

Figure 3-4: Network of branches and nodes

The water flow is described with the De Saint Venant equations for open channel flow. SOBEK solves these equations numerically using a finite difference method based on the implicit Preissman box scheme, which is unconditional stable.

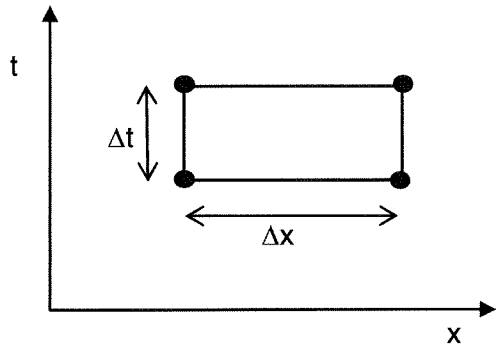

Figure 3-5: Preissman scheme

The expression for the continuity is:

$$\frac{\partial A_t}{\partial t} + \frac{\partial Q}{\partial x} = q_{lat} \tag{3.1}$$

in which

At	=	total cross-section area	[m^3]
q_{lat}	=	lateral discharge per unit length	[m^2/s]
Q	=	discharge	[m^3/s]

Moreover, the momentum reads:

$$\underset{1}{\frac{\partial Q}{\partial t}} + \underset{2}{\frac{\partial}{\partial x}\left(\alpha_B \frac{Q^2}{A_f}\right)} + \underset{3}{g A_f \frac{\partial h}{\partial x}} + \underset{4}{\frac{g Q|Q|}{C^2 R A_f}} - \underset{5}{W_f \frac{\tau_{wi}}{\rho_w}} + \underset{6}{+ g A_f(\eta + \xi Q|Q|)} + \underset{7}{\frac{g}{\rho_w}\frac{\partial \rho}{\partial x} A_{lm}} = 0 \tag{3.2}$$

in which

1	=	the acceleration term,
2	=	the convection term,
3	=	the water level gradient,
4	=	the bottom friction term,
5	=	the wind friction term and
6	=	the extra head loss term,
7	=	the density term.

and

Q	=	discharge	[m^3/s]
t	=	time	[s]
x	=	distance	[m]
B	=	Boussinesq constant	[-]
Af	=	cross-section flow area	[m^2]
g	=	gravity acceleration	[m^2/s]
h	=	water level (with respect to the reference level)	[m]

C	=	Chézy coefficient	[$m^{1/2}/s$]
R	=	hydraulic radius	[-]
Wf	=	flow width	[m]
τwi	=	wind shear stress	[$m^{1/2}/s$]
ρw	=	water density	[kg/m^3]
η	=	first additional resistance coefficient	[$m^{1/2}/s$]
ξ	=	second additional resistance coefficient	[$m^{1/2}/s$]
$A1m$	=	first order moment cross-section	[m^2]

Discretisation of the different terms is carried out with the Preismann Box scheme.

The resulting sets of equations are solved by means of a modified Newton method, whereby most of the terms are linearised. Only the hydraulic coefficients α_B, C and R, and the channel flow width W_f are not linearised, because of the complexity of their expressions. Instead, under relaxation is applied to ensure a stable and fast convergence method.

SOBEK uses a fully implicit numerical discretisation for the water flow, which is unconditionally stable provided that nonlinear phenomena are not predominant. Therefore, there is no stability limit on the Courant number, which is defined as

$$\sigma = c\frac{\Delta t}{\Delta x}$$

In which c is the propagation celerity of a small disturbance in the water-flow which at small Froude numbers is roughly equal to $\sqrt{g A_f / W_t}$, with A_f the flow area and W_t the storage width. Normally when the Courant number equals 1, a disturbance travels in one time step exactly from one grid point to the next. However, the Courant number is nonetheless important when looking at accuracy requirements

3.5.3 Network model of the Huangpu River

An existing model of the Huangpu River based on the data of the Hohai University is enhanced to improve the simulation results at Mishidu station. In the new model the Huangpu River is further schematized with topographical maps up to Dianshan Lake, the source of the river. The river cross section of the existing model are not changed because of the aim of this model is to determine the storage capacity of the Huangpu River after barrier closure. The river cross sections provided by the Hohai University are hence assumed to be representative. The layout of the final model is shown in figure 3.6.

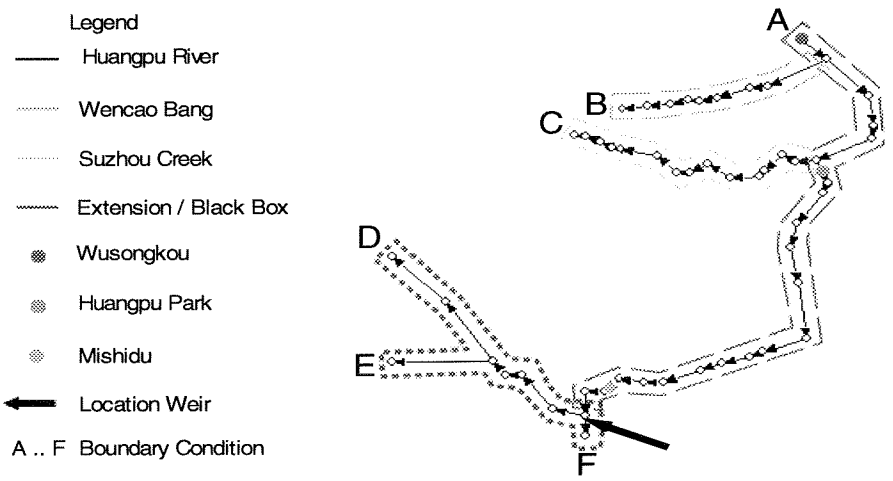

Figure 3-6: Layout Huangpu River SOBEK River model

Upstream connection of the Huangpu River

The water levels at Mishidu are affected by the tide as well as the upstream discharge and storage, whereas the water levels at Huangpu Park are solely governed by the tide. The Huangpu River drains the Tai Lake Basin through three main upstream tributaries. First, there is the Lanlugang in the north which links the Huangpu River with the Dianshan Lake. A tributary of the Lanlugang is the Taipu River is the flood route for the Tai Lake. The second and third upstream tributaries are the Yuanxiejin in the middle and the Damaogang in the south. Both are major drainage routes to Zhejiang Province. Because of the drainage function of the Huangpu River there are no gates to control the inflow of these three upstream tributaries. In contrast, all downstream tributaries have tide gates that will be closed whenever storm tides are expected. From topographical maps, it appears that Damaogang River ends in the Hangzhou Bay. The Shanghai Hydrology Administration confirms this as well, and probably the discharge of the Damaogang is controlled with a structure. The Damaogang River may form an outlet of the Huangpu River during barrier closure and hence reduces the flood risk of the Huangpu River during barrier closure substantially. In the continuation of this study it is assumed that the Damaogang can not discharge into the Hangzhou Bay during barrier closure.

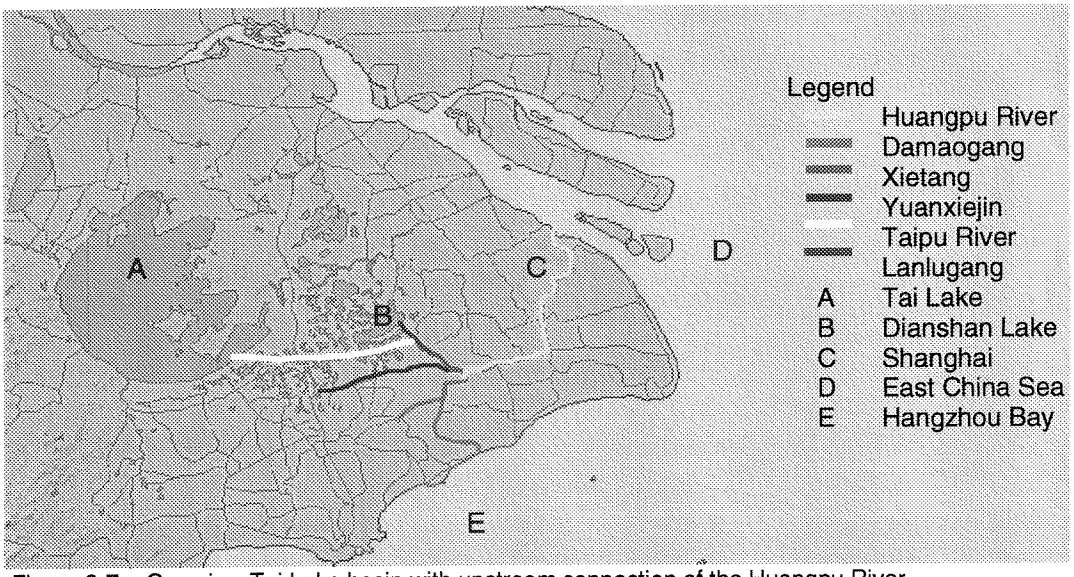

Figure 3-7: Overview Tai Lake basin with upstream connection of the Huangpu River

Boundary conditions and friction

The model requires 7 boundary conditions, of which 2 (A and E) are adjustable and the remaining conditions are fixed. The locations of the boundary conditions are numbered in alphabetical order in the model layout presented in figure 3-6. The specification of the two main boundary conditions is:

- Boundary condition A: water level time series is set at this location representing Wusongkou.
- Boundary condition E: the input discharge is set at this location.

The remaining boundary conditions are specified as follows:

- Boundary condition B and C: represents the discharge of Suzhou Creek and Wencao Bang, constant at $20m^3/s$.
- Boundary condition D: discharge boundary condition set at $0m^3/s$
- Boundary condition F: constant water level boundary condition set at 0.5m WD.

Model wide, the friction is set at Manning 0.025 for both flow directions. Modifications in the friction coefficient results in little change in the water level and therefore it is unchanged.

Blackbox

The best simulation results, in terms of water levels, are obtained with a weir upstream of Mishidu (see figure 3-6) This weir controls the water volume at Mishidu station and represents with the whole the extension the upstream connection of the Huangpu River. The crest height is constant at 1m WD, which is lower than the average water level in the river. Simulations with a higher crest level did not give satisfactory results.

The weir brings a linear relation between the input discharge boundary E and the average discharge at Mishidu; this is depicted in figure 6-2. It appears that this schematization of the Huangpu River needs an input boundary discharge over $-923m^3/s$ before the discharge at Mishidu is negative. In SOBEK RIVER, the discharge is negative when its direction is opposite to the direction of the river branch (see figure 3-8).

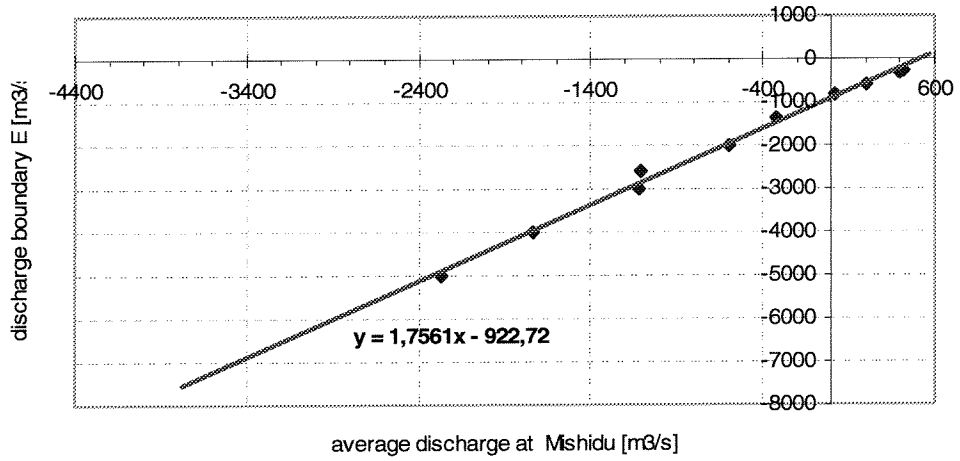

Figure 3-8: Relation between input discharge boundary condition and discharge at Mishidu

The direction of the discharge is determined with this relation (figure 3-9). An important consequence is that when the discharge at Mishidu is positive the Huangpu River will not have any flood risk during barrier closure.

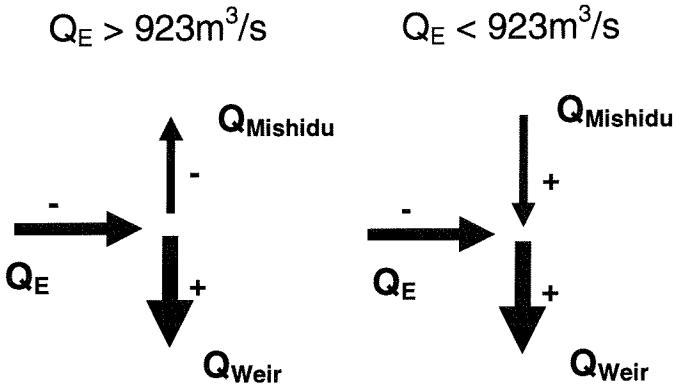

Figure 3-9: Discharge directions at Mishidu governed by discharge boundary E

An average positive discharge at Mishidu is not realistic during barrier closure. In contrast, when the average discharge is negative, the Huangpu River will be filled during barrier closure but the weir will cause the water levels to reach an equilibrium level. Consequently, flooding of the Huangpu River will not occur. A solution for this problem is treated in the subsection 3.5.5

The model gives good simulation results with regard to the water levels and average flow velocity. It is, however, not possible to judge the model's performance upstream of Mishidu with the current available information of the upstream water regime. The extension therefore acts as a *black box,* and only the simulation results of the Huangpu River are considered.

3.5.4 Calibration and verification of the model

The calibration is carried out with a water level time series record from 1-8 August 2000 provided by the Shanghai Flood Risk Information Centre. This period is chosen because it was within the typhoon season and no tropical cyclone occurred in the Shanghai area during that time. Furthermore, the year 2000 was a dry year (Ye *et al.*, 2002). The water level time series of Wusongkou station consist of maximum and minimum tide levels only and it is used in boundary condition A. The time series at Huangpu Park and Mishidu station are more accurate with an interval of 75 minutes and they are used to compare the simulation results. Unfortunately, no simultaneous discharge records are available to compare the results.
Two periods are used for model verification. The first period is from 2-13 August 2001 which is not a storm situation. The second period is from 25 August to 8 September 2000 which is during typhoon 0012 (Prapiroon). The maximum storm tide level at Wusongkou was 5.70m WD.

Water levels

The water levels at Huangpu Park and Mishidu show good resemblance with the observed water levels at these locations. The results are shown in figure 3-11.

Discharge

The long term average discharge at Mishidu station in August is 246m3/s. This discharge, however, could not be reached with any of the schematization used. The discharge at Mishidu appeared to be positive, most likely because of combination of low upstream discharge and high tide. The average discharge at the stations is calculated by averaging the discharge of whole tide cycles within the simulation period. In the calibration period it appears that the average discharge at Mishidu is +414m^3/s instead of -246m^3/s. At Wusongkou the average discharge is 228m^3/s.

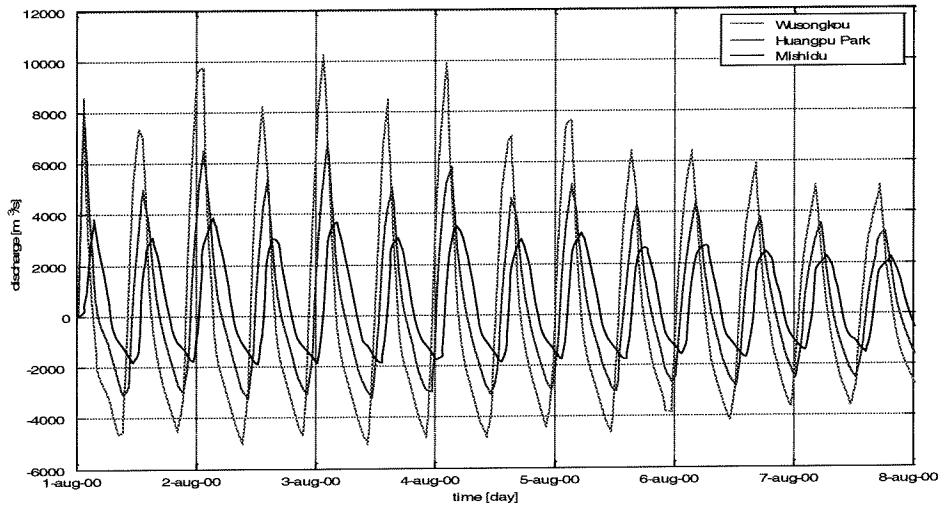

Figure 3-10: Simulated discharge in the Huangpu River during calibration period

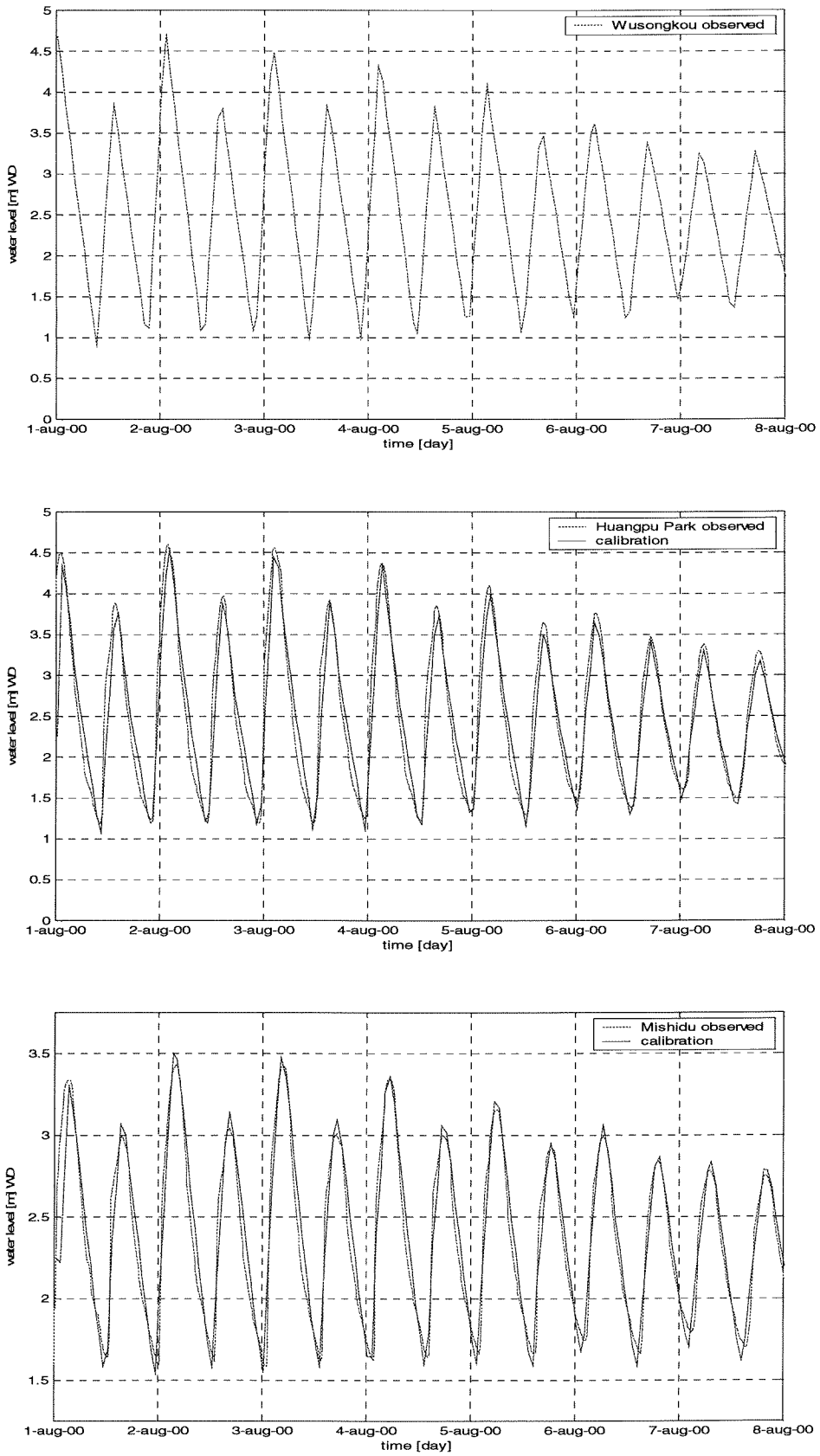

Figure 3-11: Simulated water levels in the Huangpu River during calibration period

Velocity

The average flow velocity at the three stations is the second parameter to review the performance of the model. The available velocity is restricted to Wusongkou and Mishidu station, presented in table 3-9. The ebb period average velocity is a little low compared with the actual figures, the results can be improved by decrease the friction level in the negative flow direction.

Velocity		Wusongkou	Mishidu
Flood period	[m/s]	+0.56	+0.48
Flood period calibration	[m/s]	+0.50	+0.50
Ebb period	[m/s]	-0.50	-0.49
Ebb period calibration	[m/s]	-0.39	-0.36

Table 3-9: Average flow velocity (source: Shanghai Hydrology Administration)

VERIFICATION 1: 2-13 August 2001

Water levels

The water levels showed good resemblance with the measured water levels. It appeared that the upstream discharge at Mishidu increased substantially during this period. Results are presented in figure 3-13.

Discharge

In the verification period the average discharge at Mishidu is -552m^3/s and -635m^3/s at Wusongkou. The discharge boundary condition E, was -800m^3/s from 2 – 4 August and increased subsequently to -2000m^3/s. The year 2001 was a wet hydrological year.

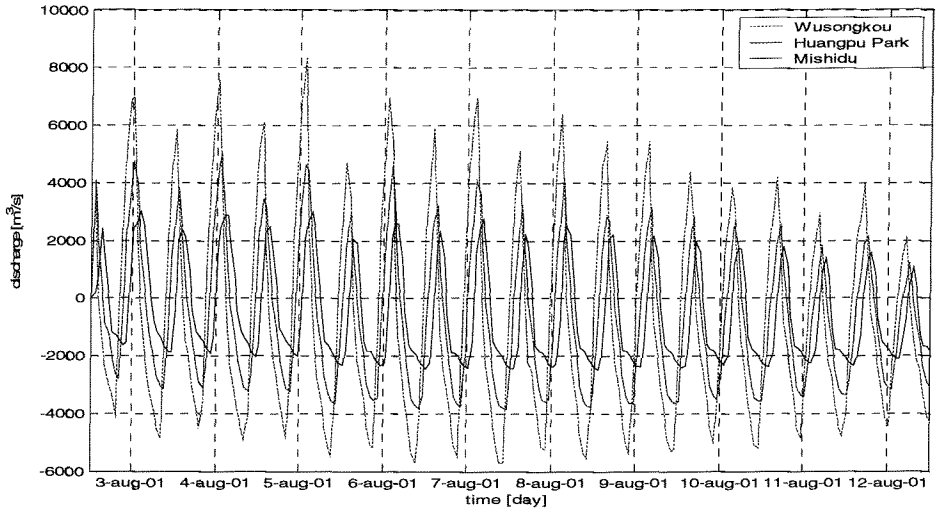

Figure 3-12: Discharge at the three station during verification period

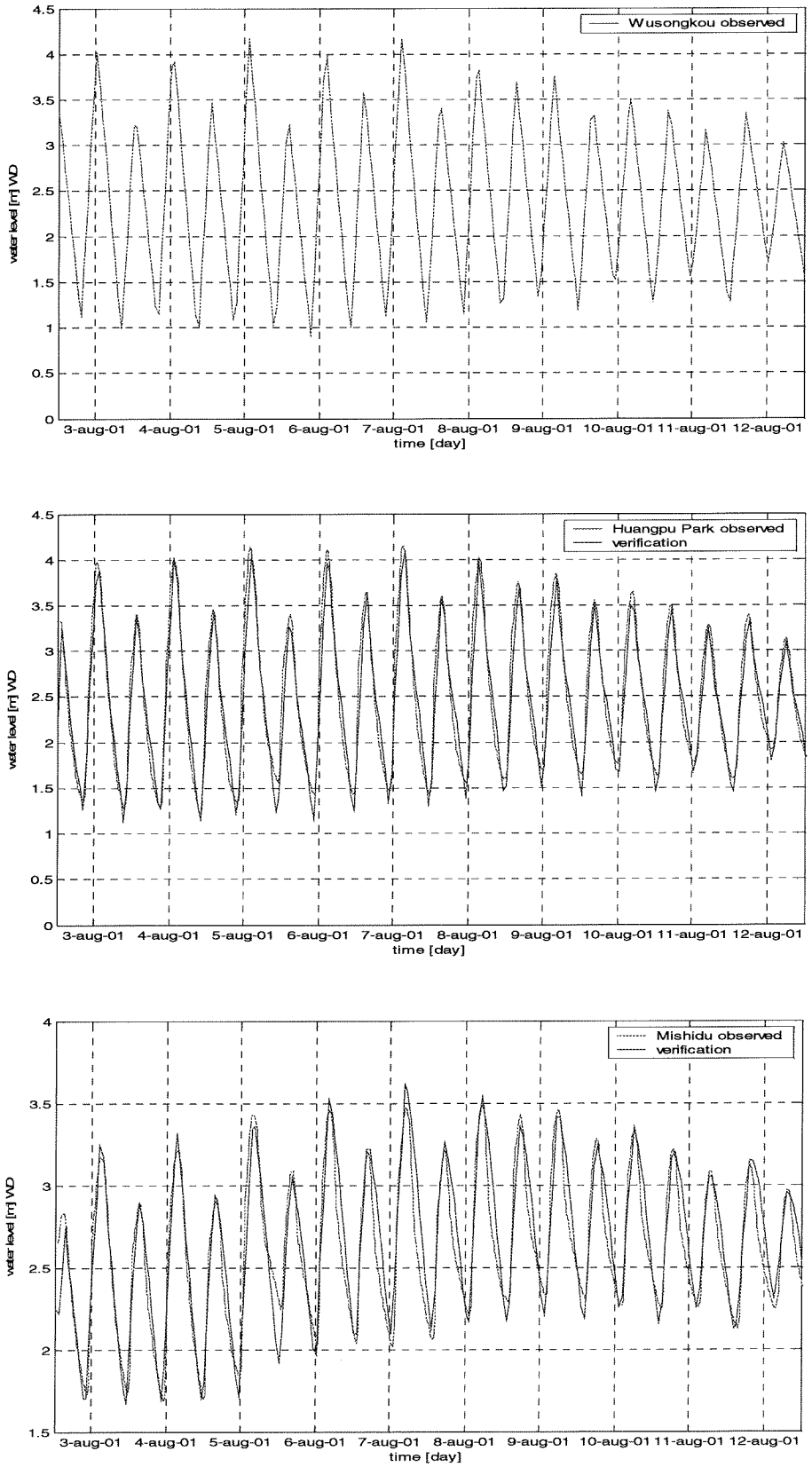

Figure 3-13: Simulated water levels in the Huangpu River during verification period

Velocity

The average flow velocity from the simulations is presented in table below:

Period	Wusongkou	Mishidu
Flood period simulated [m/s]	+0.56	+0.47
Ebb period simulated [m/s]	-0.57	-0.47

Table 3-10: Average flow velocity during verification period

VERIFICATION 2: Typhoon Prapiroon from 25 August –8 September 2000

Water levels

The ebb levels at Huangpu Park station appeared to lower with the simulations. When a lower discharge is chosen location F, the ebb levels will increase. The results are presented in figure 3-15.

Discharge

The discharge chosen for this simulation is -800m3/s. This gives an average discharge at Mishidu of +124m3/s, and at Wusongkou +23m3/s. The water levels at Mishidu showed good resemblance with the measured water levels.

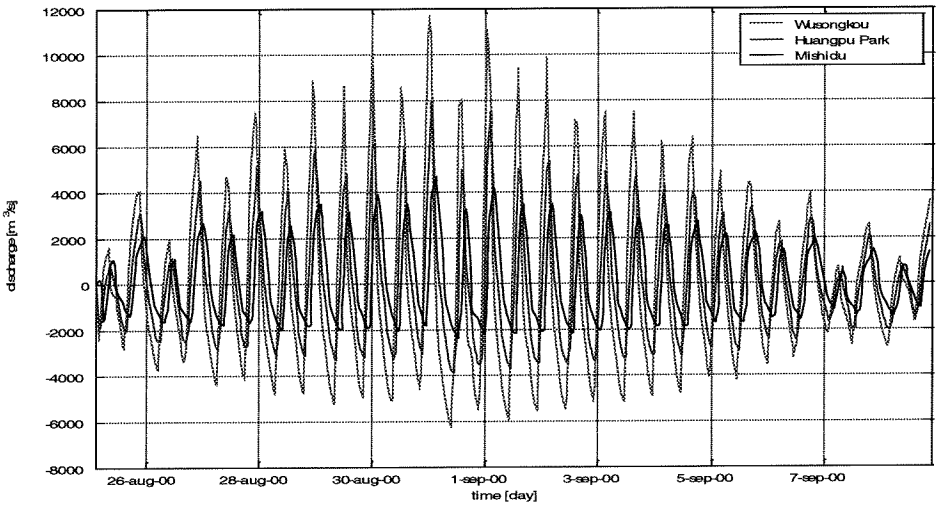

Figure 3-14: Simulated discharge in the Huangpu River during verification period 2

Velocity

Average flow velocity at Wusongkou and Mishidu are a bit higher and lower during respectively the flood and ebb period. Again this can be improved by adjusting the friction coefficient.

Period	Wusongkou	Mishidu
Flood period simulated [m/s]	+0.61	+0.50
Ebb period simulated [m/s]	-0.47	-0.37

Table 3-11: Average flow velocity during verification period 2

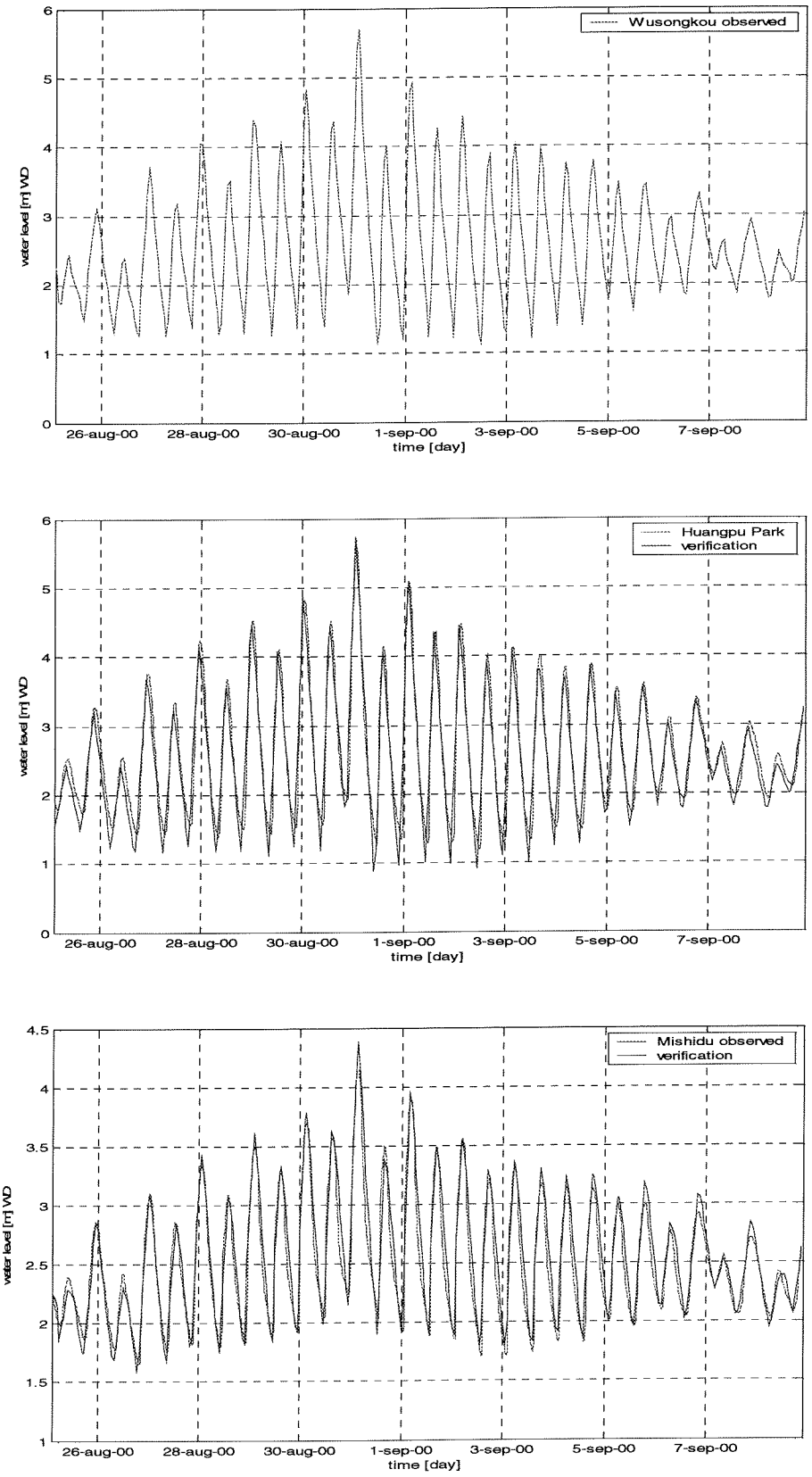

Figure 3-15: Simulated water levels in the Huangpu River during verification period 2 compared with observed levels

3.5.5 Model adjustments for barrier closure

The extension of the Huangpu River gives good simulations results as long as there is no barrier closure in the mouth of the river. After all, when the discharge at Mishidu is positive, i.e. in the upstream direction, the downstream sections of Mishidu will decrease to the weir height at location F during barrier closure. In contrary when the discharge at Mishidu is negative, the water levels downstream will rise and eventually reach an equilibrium level.

Without knowledge of the real upstream situation at Mishidu it is not possible to judge the correctness of the upstream discharge distribution (boundary condition E) over the Huangpu River and the Tai Lake basin represented by the extension and the weir. Therefore simultaneous closure of the weir with the barrier, enforcing a negative discharge at Mishidu, is not a sufficient solution. Instead, simultaneous closure of the *extension* with the barrier and the activation of a substitute discharge boundary condition downstream at Mishidu as long as the barrier is closed seem to be more realistic. This substitute discharge is determined by the average monthly discharge and varies with the hydrological year, in effect, it can be considered as a stochastic variable determined by the hydrological year and month of interest. The monthly base discharges with their corresponding probabilities of occurrence are treated in subsection 2.2.5.

For the month August for example, the long term average discharge at Mishidu varies between 294m^3/s in dry year (P=95%) and 639m^3/s in a wet year (P=20%) (Wang *et al.*, 2001).
The model layout for barrier closure is presented in figure 3-17, the extension is blurred.

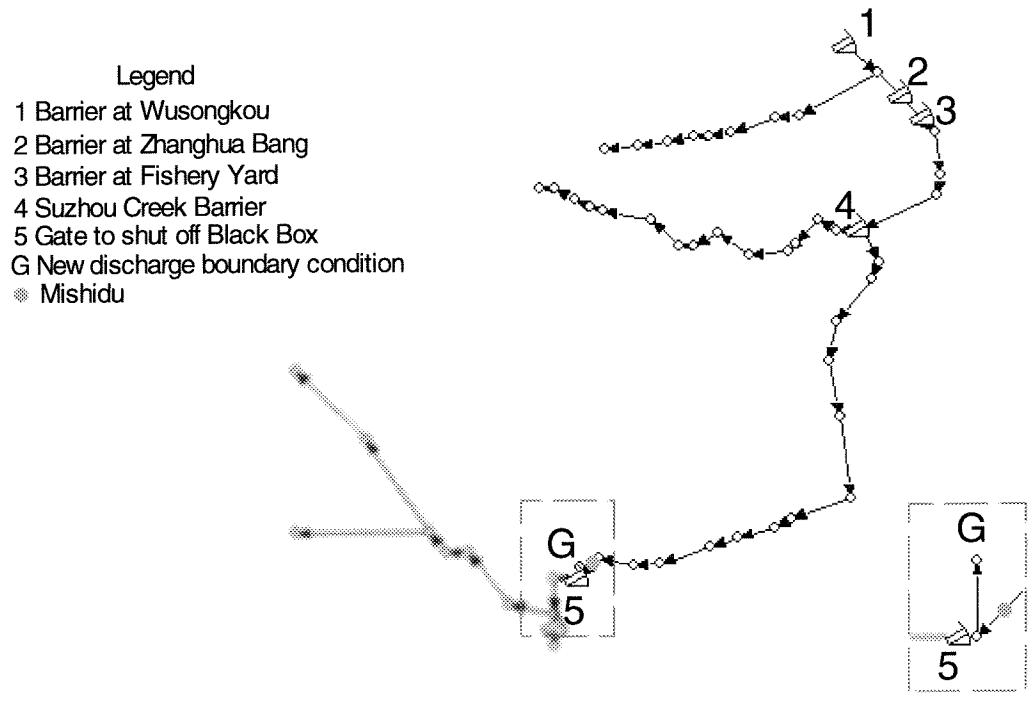

Figure 3-16: Model layout during barrier closure

Barrier closure performance

With this adjustment the storage of the upstream area will be completely neglected during barrier closure situations. To check the performance of the model for closure situations the water level records of typhoon 0111 are used. In order to represent the water levels at Mishidu correctly the

model input discharge at boundary E has to be set at -1270m^3/s, see figure 3-6 for this location. In the subsequent simulations a barrier is set at Wusongkou and simulations are carried out with different closure schematizations. Three schematizations are distinguished; the first schematization is in fact the base situation as no changes are applied to the model with regard to the weir and the extension. The weir is closed in the second schematization and the extension is closed in the third schematization. Figure 3-17 presents the water levels Mishidu with no barrier closure. The barrier closure simulations are subsequently shown in figure 3-18 to 3-21.

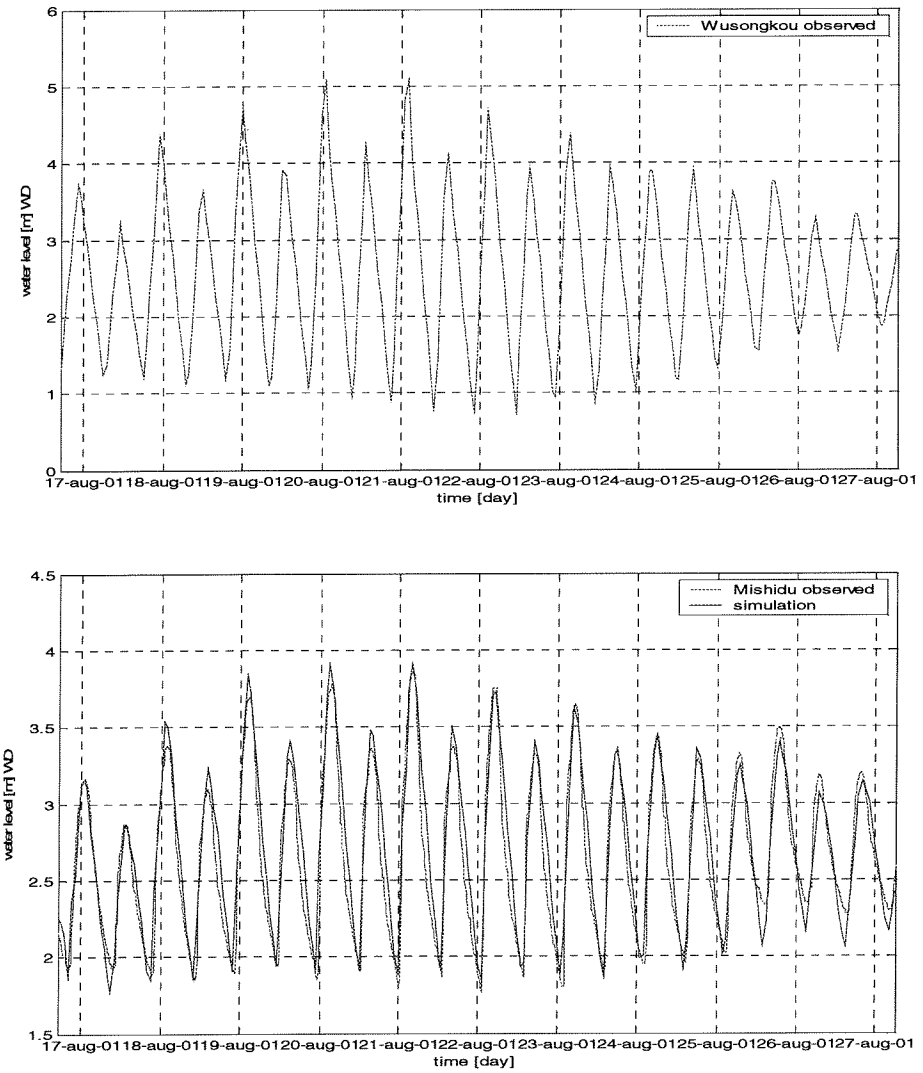

Figure 3-17: Observed water levels at Wusongkou and Mishidu and the corresponding simulated water levels at Mishidu during typhoon 0111 in August 2001

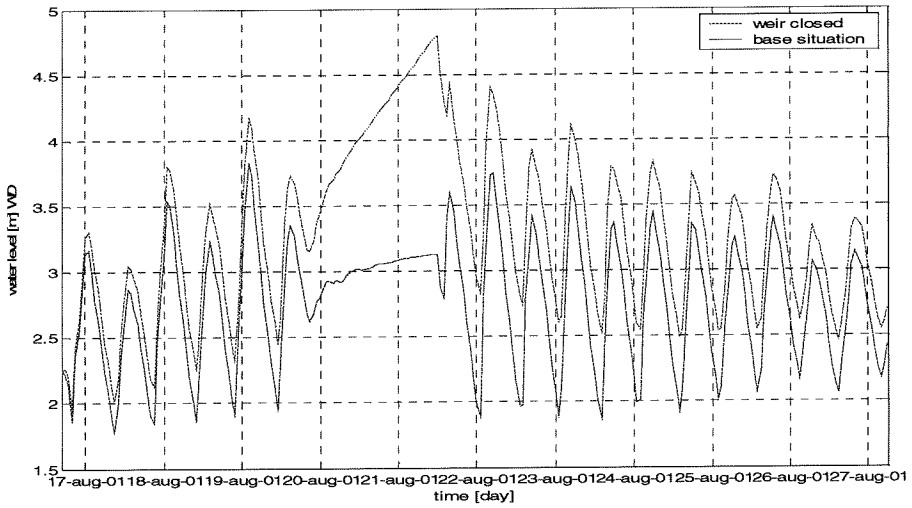

Figure 3-18: Simulated water levels at Mishidu during typhoon 0111 for the base and weir closed situation during barrier closure

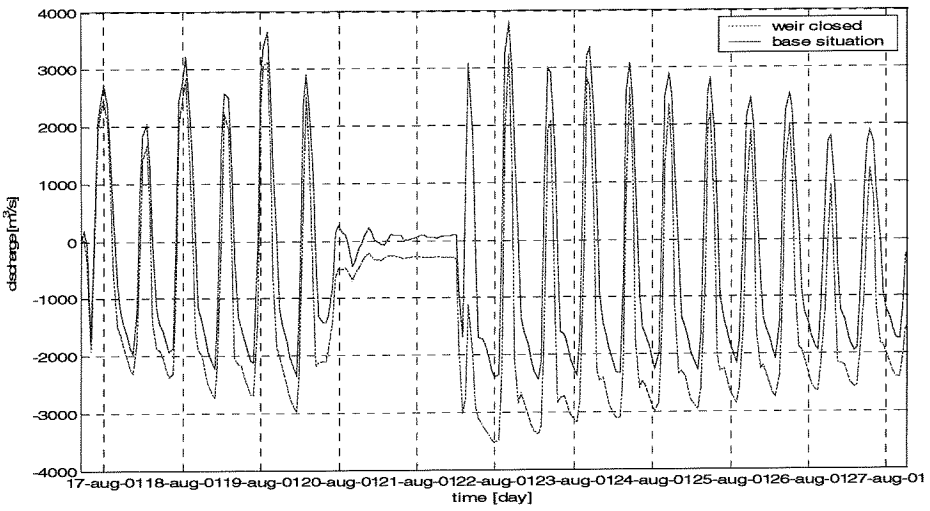

Figure 3-19: Simulated discharges at Mishidu during typhoon 0111 for the base and weir closed situation during barrier closure

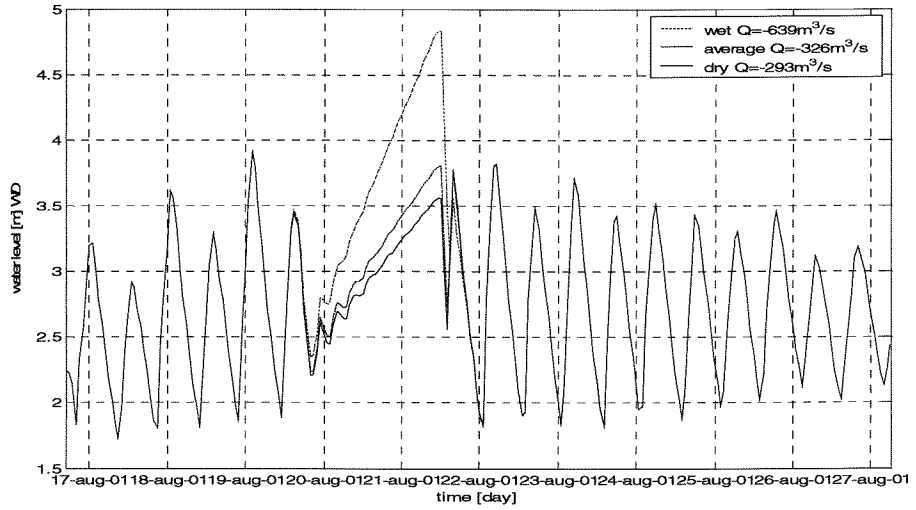

Figure 3-20: Simulated water levels at Mishidu during typhoon 0111 with substitute discharges during barrier closure. The substitute discharges are average discharges for August for three different hydrological years

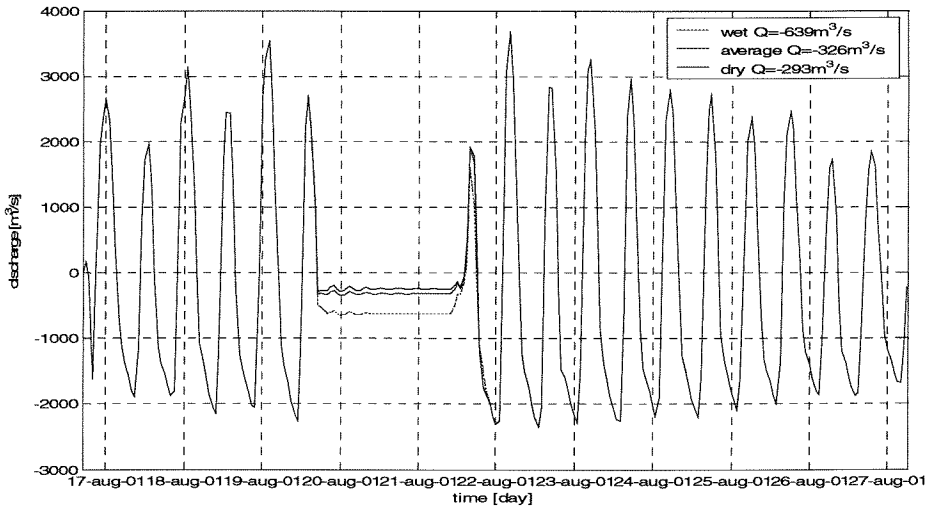

Figure 3-21: Simulated discharges at Mishidu during typhoon 0111 with substitute discharges during barrier closure. The substitute discharges are average discharges for August for different hydrological years

The discharges of the three simulations at Mishidu are presented below. As expected, when the only the weir is closed the discharge at Mishidu will increase significantly causing the water levels in the river to soar which is not realistic. In the base situation, the weir leads the water levels to an equilibrium level and the average discharge at Mishidu during closure is less than before closure.

		Base situation	Weir closed
Average discharge during closure	[m^3/s]	-86	-1114
Input discharge at boundary E	[m^3/s]	-1270	-1270

Table 3-12: Discharges at Mishidu during closure with and without closed weir

		Average P=50%	Wet P=20%	Dry P=75%
Average discharge during closure	[m^3/s]	-326	-639	-293
Probability of occurrence	[%]	50	20	95

Table 3-13: Discharges at Mishidu during closure with substitute discharges at Mishidu for different hydrological years

3.5.6 Critical discharges per barrier location

In this subsection, we use the previously found results to determine the so-called critical discharge of the Huangpu River per closure duration for each of the proposed barrier location. The critical discharge is defined as the uniform upstream discharge that can cause the limit state condition of the river during barrier closure. In fact, the critical discharge represents the storage capacity of the Huangpu River for a given closure duration. Recall the expression for the limit state condition of the Huangpu River during barrier closure, presented in section 1.4

$$Z = R - S \tag{3.3}$$

in which

R = storage capacity Huangpu River [m^3]
S = upstream discharge volume during barrier closure [m^3]

Moreover, we previously defined the upstream discharge volume is as

$$S = Q_{upstream} t_{closure} \tag{3.4}$$

in which

$Q_{upstream}$ = upstream discharge [m^3/s]
$t_{closure}$ = closure duration [s]

Hence, the flood probability of the Huangpu River is the probability of exceedance of the limit state condition

$$P(Z < 0) = P(R < S) \tag{3.5}$$

When we denote $V_{critical}$ as the deterministic critical storage capacity of the Huangpu River given the inside water level after barrier closure, then the flood probability during barrier closure can be expressed as

$$P(Z < 0) = P(S > V_{critical}) \tag{3.6}$$

which is equal to

$$P(Z < 0) = P(Q_{upstream} > \frac{V_{critical}}{t_{closure}}) \tag{3.7}$$

in which the critical discharge comes forward as

$$Q_{critical} = \frac{V_{critical}}{t_{closure}} \tag{3.8}$$

Hence, the critical discharge represents the storage capacity of the river during barrier closure given the closure duration.

In subsection 3.5.5, we concluded that the upstream water regime of the Huangpu River is essential in the storage capacity of the river. Because of the limited size of the data available to determine the exact upstream discharge distributions, we decided to consider only the storage capacity of the Huangpu River from Wusongkou to some extend beyond Mishidu. In effect, this is the course of the river in Shanghai. It should be remarked that the flood probability during barrier closure is not an issue when in reality one of the tributaries of the Huangpu River is connected with open water.

The storage capacity of the Huangpu River is furthermore, determined by the available storage height after barrier closure. The available storage height is defined as the difference between water level in the river just after barrier closure and the top elevation of the flood walls along side the river. From subsection 3.3.2, it appears that the floodwall along the river may be lowered for several reasons. Because of the uncertainty of the elevation of the eventual floodwall after completion of the storm surge barrier, we use the warning water level at Mishidu and Huangpu Park instead.

As a consequence, flooding of the Huangpu River during barrier closure is defined as the exceedance of the warning water level in the river.

The warning water level differs per location in the river, as treated in subsection 3.2.2. At Huangpu Park station this water level is set at 4.55m WD whereas at the upstream Mishidu the warning water level is set at 3.50m WD. This tidal dominance of the water levels in the river is the cause for this difference. We will compute the flood probability for both warning water levels. In effect, the top elevation of the embankments of the river is infinite height and the warning water level is a virtual line alongside the river. In reality, flooding occurs when the floodwalls alongside the river breaches or when the water levels in the river exceeds the top elevation of the floodwalls.

The critical discharge is now determined with SOBEK RIVER, since our model is assumed to reflect the actual dimension of the Huangpu River correctly. For each barrier location, simulations are carried out to fill the Huangpu River with different uniform upstream discharges. The water level in the river right after barrier closure is 2.5m WD.
For each barrier location, a dataset is hence collected consisting of the closure duration corresponding to the exceedance of the warning water level at Mishidu and Huangpu Park and the corresponding upstream discharge. In effect, this dataset is the critical discharge per barrier closure duration for each barrier location for Mishidu and Huangpu Park. The barrier locations are presented in figure 3-3.

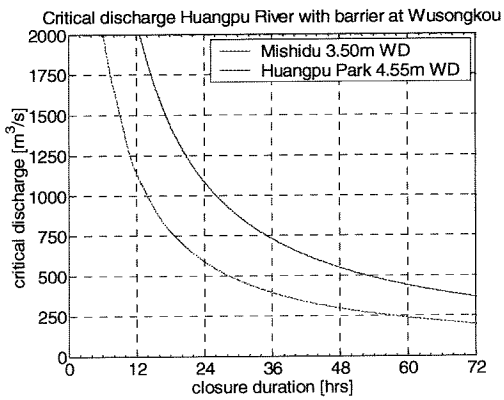

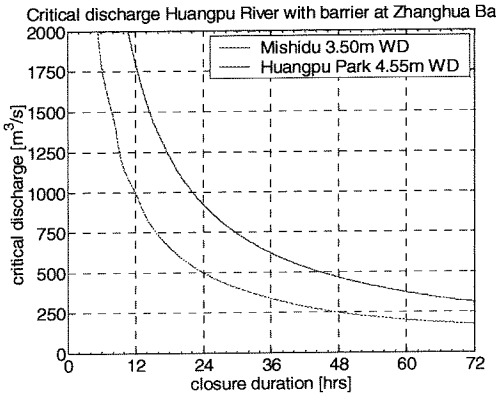

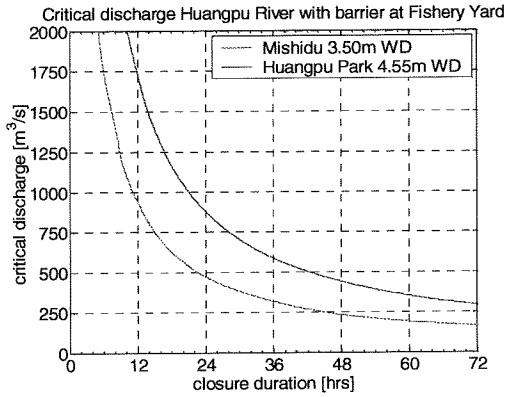

Table 3-14: Critical discharges per barrier location with reference to the warning water level at Mishidu (red) and Huangpu Park (blue)

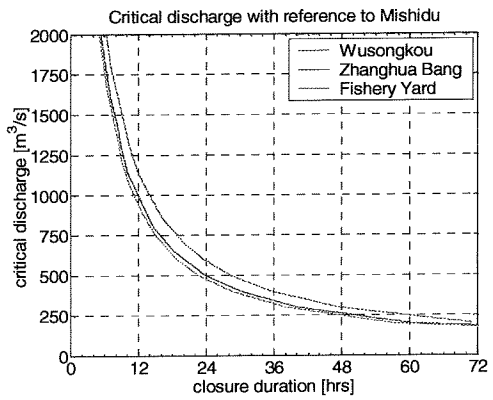

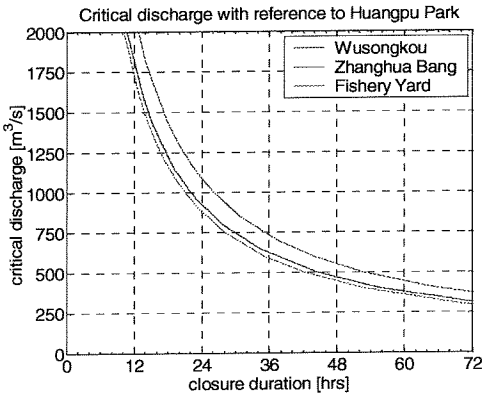

Table 3-15: Comparison of the critical discharges per barrier location with reference to the warning water level at Mishidu (left) and Huangpu Park (right)

In addition, in table 3-16 to 3-18 we summarize the closure durations before the limit state condition at Mishidu and Huangpu Park is reached for some typical critical discharges for each barrier location. As expected, the most upstream barrier location Fishery Yard has the smallest storage capacity. Furthermore, the storage capacities of Zhanghua Bang and Fishery Yard are close to each other.

	Mishidu [hrs]	Huangpu Park [hrs]
$Q_{critical}$=1200 [m^3/s]	11	22
$Q_{critical}$=800 [m^3/s]	18	33
$Q_{critical}$=300 [m^3/s]	47	88

Table 3-16: Closure durations before reaching the limit state condition at Mishidu and Huangpu Park for some typical critical discharges when the barrier is set at Wusongkou

	Mishidu [hrs]	Huangpu Park [hrs]
$Q_{critical}$=1200 [m^3/s]	10	18
$Q_{critical}$=800 [m^3/s]	15	28
$Q_{critical}$=300 [m^3/s]	40	74

Table 3-17: Closure durations before reaching the limit state condition at Mishidu and Huangpu Park for some typical critical discharges when the barrier is set at Zhanghua Bang

	Mishidu [hrs]	Huangpu Park [hrs]
$Q_{critical}$=1200 [m^3/s]	9	17
$Q_{critical}$=800 [m^3/s]	14	27
$Q_{critical}$=300 [m^3/s]	38	70

Table 3-18: Closure durations before reaching the limit state condition at Mishidu and Huangpu Park for some typical critical discharges when the barrier is set at Fishery Yard

3.6 Conclusions

In this section, the storage capacity of the Huangpu River is analyzed and subsequently quantified with an improved flow model of the river. The water levels in the river appeared to be rising progressively as a consequence of the changes in the water regime and soil structure related to the rapid economic development of Shanghai. Moreover, future development of Shanghai may sustain the reduction of the upstream storage capacity with consequences to the storage capacity of the river during barrier closure. A barrier in the mouth of the river will prevent storm tides entering the river, but the urban flood control works are the first line of defense for flooding of the Huangpu River during barrier closure.

Other conclusions are summarized below

- Although flooding of the Huangpu River during barrier closure may be a serious threat. It seems that at present flooding of the downtown area by torrential rainfall occurs more frequently in comparison with inundation because of flooding of the Huangpu River

- The existing SOBEK RIVER flow model of the Huangpu River is enhanced to improve the results at Mishidu station. The model gives very good results even for storm tides in the typhoon season.

- The upstream water regime of the Huangpu River is essential to the storage capacity of the river. However, no information on the upstream distribution of the Huangpu River is available. Consequently, the storage capacity is only determined for the Huangpu River from Wusongkou to some extend beyond Mishidu. In effect, this is the course of the river in Shanghai. This assumption can be regarded as the limitation of the model. The

flood probability during barrier closure is not an issue when in reality one of the tributaries of the Huangpu River is connected with open water.

- The floodwall along the river may be lowered for several reasons after barrier completion. Because of the uncertainty of the eventual elevation of the floodwall after completion of the storm surge barrier, we use the warning water level at Mishidu and Huangpu Park as reference for flooding of the river during barrier closure. As a consequence, flooding of the Huangpu River during barrier closure is defined as the exceedance of the warning water level in the river. In addition, the present floodwall alongside the Huangpu River is of great importance to flooding of the river during barrier closure. After barrier completion, this floodwall is the first line of defence against flooding of the river during barrier closure.

- The critical discharge is the upstream discharge that causes the limit state condition of the Huangpu River during barrier closure for given closure durations. The critical discharge for each of the proposed barrier locations is computed.

4 Torrential rainfall runoff in a typhoon storm

4.1 Introduction

The critical discharge of the Huangpu River during barrier closure consists of the torrential rainfall runoff together with the base discharge. The aim of this chapter is to determine the torrential rainfall runoff distribution into the Huangpu River in a typhoon storm. Torrential rainfall, like wind gust and storm surge are inevitable exhaust products of the mechanism of tropical cyclones, as a consequence the variables torrential rainfall storm surge are related to each other. Since no discharge records of the Huangpu River are available for analysis we derive the torrential rainfall runoff distribution from the conceptual joint distribution of storm surge at Wusongkou and torrential rainfall in the Tai Lake Basin. The structure of this chapter is analogously with the steps taken in the analyses. First, in section 4.2, the storm tide distribution at Wusongkou is analyzed with Monte Carlo simulation of the tide and storm surge distribution at this location. The aim is to determine the probabilities of occurrence of the presumed barrier closure water level and the corresponding required surge level. With this surge level we analyze the torrential rainfall probabilities in section 4.3 with the conceptual joint distribution of storm surge and torrential rainfall. The known individual distributions of surge and torrential rainfall are linked into their joint distribution with a copula. Copulas are functions that act as multivariate distributions. They allow us to study the dependence structure between variables separately from the individual margins. Finally, the runoff distribution is derived empirically with flow budgets of historical Tai Lake floods from the torrential rainfall probabilities.

4.2 Required surge levels at Wusongkou for barrier closure

4.2.1 Introduction

The storm surge barrier in the mouth of the Huangpu River closes whenever the water levels in front of the barrier are expected to exceed the closure water level due to a passing tropical cyclone. This water level is a result of the combination of storm surge and astronomical tide. In this section, the distribution of the storm tides at Wusongkou is analyzed by random combination of storm surge and tide levels at Wusongkou in the typhoon season. The aim is to determine the probability of exceedance of the presumed barrier closure water level and the required surge for this storm tide. This required surge level is used in the next section in the analysis of the torrential rainfall with the joint distribution of storm surge and torrential rainfall. This section starts with presenting the distributions of storm surge and tides in the typhoon season at Wusongkou. Then in subsection 4.2.4, random realization of these two variables leads to the distribution of storm tides at Wusongkou. From this distribution, the probability of the barrier closure water level is retrieved as well as some typical storm tide levels as the 1:1000 years storm tide level.

4.2.2 Surge level distribution at Wusongkou

The Hohai University (1999) has analysed the historical surge levels at Wusongkou of 71 typhoon induced floods of the Huangpu River from 1921 to 1997. Missing surge level records from 1937 to 1945, during the Second World War, are retrieved through interpolation of saved

records at Huangpu Park station. It appears that the Pearson type III distribution describes the surge levels at Wusongkou best. It should be noted that this data set did not include the highest water level at Wusongkou (typhoon 9711, 5.99m WD). However, it includes the highest surge level ever-recorded (typhoon 5612, 1.81m) and therefore it is representative for the analysis hereafter.

The mean surge level at Wusongkou is 0.61m; table 13 shows the typical surge levels from a Pearson type III distribution.

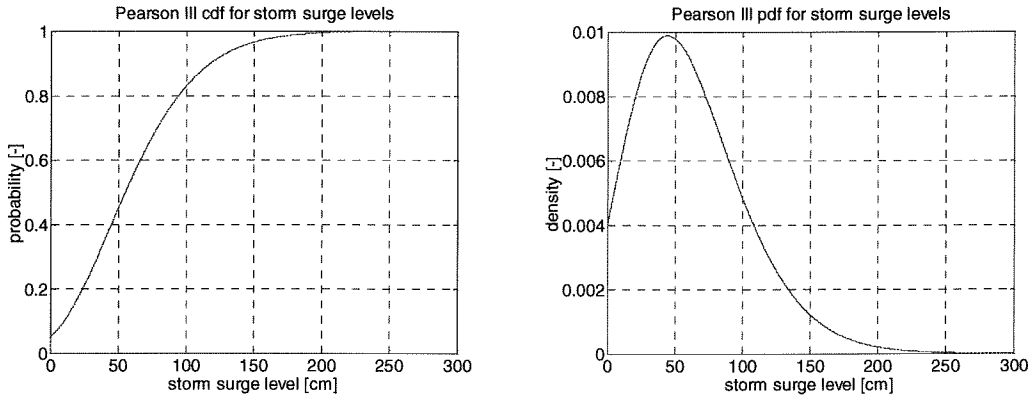

Figure 4-1: Pearson III distribution of the surge levels at Wusongkou

	E[H]=0.61m, σ=0.43m, C_s=0.7543, C_v=0.7105						
P [%]	0.01	0.1	1	2	5	10	20
H [m]	2.93	2.41	1.84	1.65	1.39	1.18	0.94

Table 4-1: Storm surge level probabilities at Wusongkou according to Hohai University (1999)

The Pearson type III has no closed form and the probability density function is given by:

$$f(x) = \frac{\beta^{\alpha}}{\Gamma(\alpha)}(x-b)^{\alpha-1}e^{-\beta(x-b)} \qquad b \le x \le \infty \tag{4.1}$$

in which

$$b = EX - \frac{2\sigma}{C_s} \tag{4.2}$$

$$\alpha = \frac{4}{C_s^{\,2}} \tag{4.3}$$

$$\beta = \frac{2}{\sigma C_s} \tag{4.4}$$

The $\Gamma(\alpha)$ is the gamma function, which is expressed as:

$$\Gamma(\alpha) = \int_0^\infty t^{\alpha-1} e^{-1} dt \tag{4.5}$$

4.2.3 Tide level distribution at Wusongkou in typhoon season

The gravity forces of the celestial bodies on the earth are responsible for the astronomical tide. In effect, it has no causal relation with the storm surge of caused by a tropical cyclone. In this study, the high tides in the typhoon season are modelled as periodical fluctuation described by the generalized beta distribution. The randomness embodies the daily inequalities. The average high tide is 3.63m WD and the minimum and maximum tide level is fixed at 2.22m WD and 4.45m WD.

Tidal prediction

The highest astronomical tide occurs in a cycle of 18.6 years. To include at least one cycle, the tide at Wusongkou is predicted for 50 years with the software package WL-Tide, developed by WL | Delft Hydraulics.

The tide at Wusongkou is predicted with the harmonics method (Schureman, 1988) and 28 constituents found in Hohai University (1999), see appendix U for the listing

The expression of the tide level reads

$$h = H + \sum_{n-1}^{N} f_n H_n \cos[a_n t + (V_0 + u)_n - \kappa_n] \tag{4.6}$$

with

$$H = H_0 + H_{season} \tag{4.7}$$

where

h	= Height of the tide at any time t	[m]
H_{season}	= Seasonal variation of the water level	[m]
H_0	= Mean water level above some defined datum such as mean sea level	[m]
N	= Total number of tidal constituents	[-]
f_n	= Node factor for reducing mean amplitude	[-]
H_n	= Mean amplitude of tidal constituents n	[m]
a_n	= Speed of constituent n	[s^{-1}]
t	= Time measured from some initial epoch	[s]
$(V_0 + u)_n$	= Equilibrium argument for constituent n at some location when $t = 0$	[-]
κ_n	= Local epoch of constituent n	[-]

According to WL-Tide the maximum tide level in the period of interest is 4.30m WD. The actual highest astronomical tide level at Wusongkou can be higher than this and deviation is possibly caused since the following factors are neglected by the calculations:

- The seasonal variation of the Yangtze River can increases the water level in the estuary.
- Set up of the tide level when it propagates from the East China Sea into the shallow waters of the Yangtze River estuary and subsequently into the Huangpu River.

These effects are can be considered as constants and can be accounted in H of equation (4.7).

Fitting distribution to tide data

In the next step, arbitrary distribution functions are fitted to the data with the maximum likelihood method in the software package Bestfit. Subsequently, the goodness of fit of the distribution functions is carried out with the Chi-Square method as well as the Anderson Darling method. From the results, it appears that the generalized beta distribution fits the data best. The most important characteristic of the generalized beta distribution is, like the astronomical tide, its fixed domain.

The generalized Beta probability density function is expressed as

$$f(x) = \frac{(x-\min)^{\alpha_1-1}(\max-x)^{\alpha_2-1}}{B(\alpha_1,\alpha_2)(\max-\min)^{\alpha_1+\alpha_2-1}} \tag{4.8}$$

In addition, the cumulative density function reads

$$F(x) = \frac{B_z(\alpha_1,\alpha_2)}{B(\alpha_1,\alpha_2)} = I_z(\alpha_1,\alpha_2) \tag{4.9}$$

in which

$$z = \frac{x-\min}{\max-\min} \tag{4.10}$$

Moreover, B is the beta function and B_z is the incomplete beta function.

The parameters of the Beta generalized distribution function, determined with Bestfit, are

α_1 = 2.7447

α_2 = 2.0722

The boundaries of the distribution correspond are

min = 222 cm

max = 445 cm

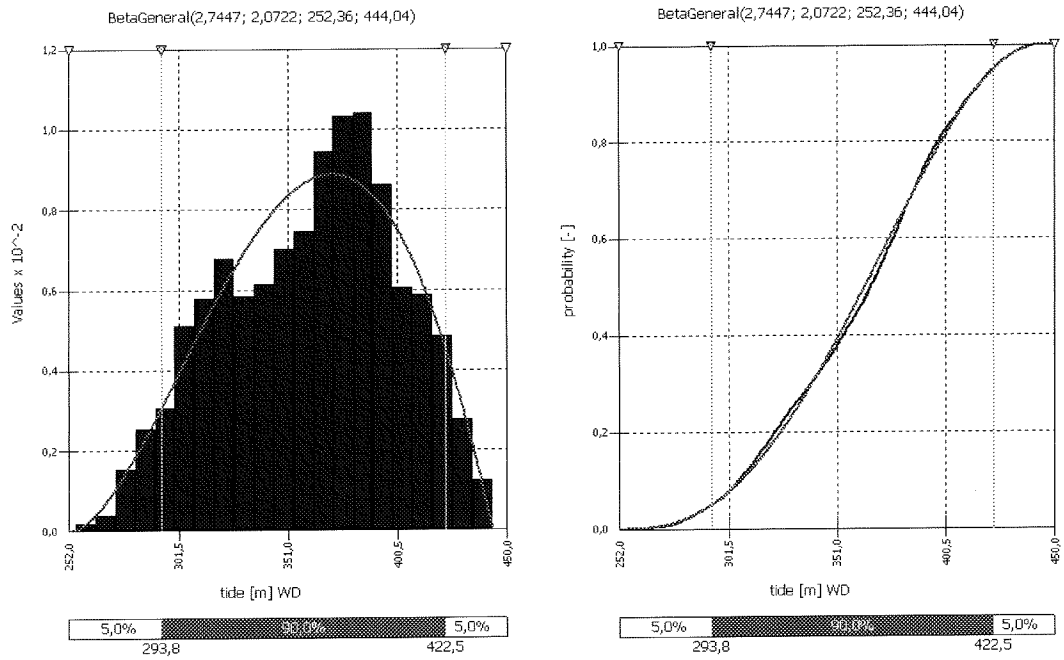

Figure 4-2: Generalized Beta distribution fitted to the tide data with Bestfit. The left image represents the probability density and the right image represents the cumulative probability distribution.

4.2.4 Monte Carlo simulations of the storm tide levels

The aim of this section is to determine the storm tide distribution by random combination of surge and tide levels. With this distribution we can determine the probability of exceedance of the barrier closure water level and the required surge level for barrier closure which are needed in the continuation of this study

The storm tides at Wusongkou is the result of the superposition of the tide and surge level, expressed as

$$h_{stormtide} = h_{tide} + h_{surge} \tag{4.11}$$

in which

$h_{stormtide}$ = storm tide [m] WD
h_{tide} = tide [m] WD
h_{surge} = storm surge [m]

Since the tide and the storm surge are mutually independent variables, the storm tide distribution can be expressed as

$$P(H_{st} > h) = \int f(H_{surge}) P(H_{surge} > H_{stormtide} - H_{tide}) dh$$

As we assume independency between the tide and the surge level it also means that the non-linear interaction between the two variables is not taken into account. The integration of both the distribution functions will result in storm tides with its probability of occurrence. In general, numerical integration and Monte Carlo simulations are the two methods widely used to integrate the joint density probability distribution function. Monte Carlo simulation makes use of the fact that the probability of not exceedance of an arbitrary stochastic variable is uniformly distributed from 0 to 1:

$$F_X(X) = X_u, \qquad \text{with } X_u \in [0,1] \tag{4.12}$$

The following formula is now valid for the variable X

$$X = F_X^{-1}(X_u) \tag{4.13}$$

in which $F_X^{-1}(X_u)$ is the inverse cumulative probability distribution of X.

With this theory random values of X can be generated for any distribution of $F_X(X)$ by random realization of $X_u \in [0,1]$. The number of simulations that have to be carried out depends on the desired reliability:

$$n > 400\left(\frac{1}{P_f} - 1\right) \tag{4.14}$$

The relative error with this method is:

$$\varepsilon = \frac{\frac{n_f}{n} - P_f}{P_f} \tag{4.15}$$

When the desired probability of exceedance is P=0.001. Accordingly, 400.000 simulations are carried out to achieve a 95% reliability of the results with a maximum relative error of 0.1. The relative error for the P(0.1%) water level is ε = 0.015 m with a deviation of 0.05 m.

The deviation is expressed as:

$$\delta_\varepsilon = \sqrt{\frac{1 - P_f}{nP_f}} \tag{4.16}$$

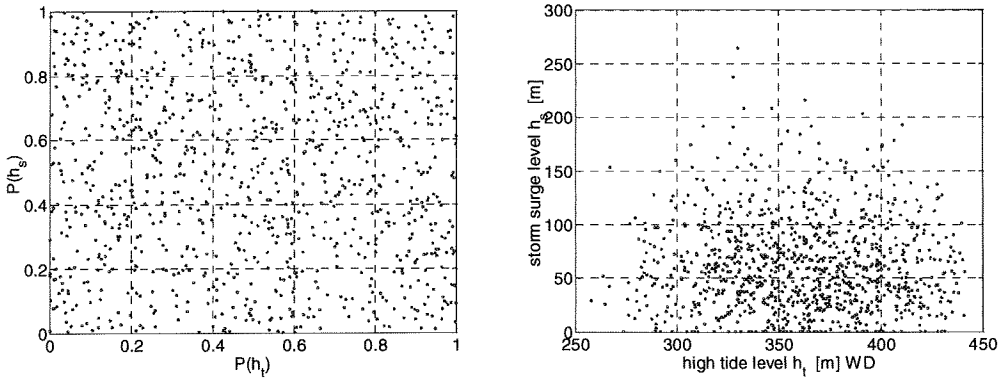

Figure 4-3: Scatter plot of n=1000 realizations of random independent surge and tide levels.

Results of the Monte Carlo simulations are presented in figure 4-4. The red curve is the retrieved storm tide distribution. When the storm tide level of 4.80m WD is given, which is the present warning water level at Wusongkou, we can clearly see the increase of the of the return periods for the tide and surge level distributions (yellow and blue curve).

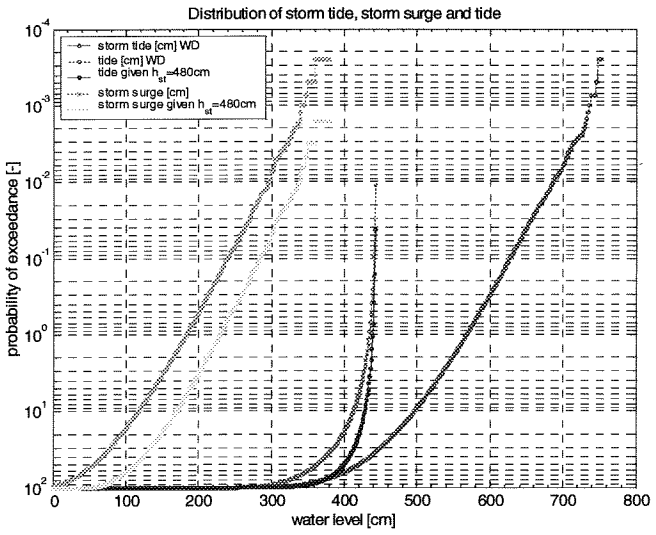

Figure 4-4: Return periods of storm tide, storm surge and tide at Wusongkou with n=400.000

From the figure above, we summarize some typical storm tide levels with their return periods in the table below

P	[%]	0.01	0.1	1	2	5	15.6
$h_{storm\ tide}$	[m] WD	6.81	6.27	5.68	5.48	5.21	4.80

Table 4-2: Simulated storm tide levels with return periods

When we compare these results with the design storm tide levels found by the Shanghai Water Authority, it appears that the for the 1:1000 years and 1:10000 years storm tide are identical with the design flood levels found by the Shanghai Water Authority with frequency analysis (table 3-5). This close resemblance in the results give confidence to believe that 6.27m WD is a good estimate for the 1:1000 years storm tide level at Wusongkou.

4.2.5 Barrier closure water level and required surge level

The barrier is assumed to close whenever the water level at Wusongkou is expected to exceed the barrier closure water level. In this study we assume that the future barrier closure water equals the present warning water level of 4.80m WD at Wusongkou.

When we compare the probability of exceedance of this water level found from the computations in the previous subsection with the actual frequency of exceedance a remarkable difference is found. The frequency of exceedance of a certain threshold is defined as the average annual frequency that this threshold is exceeded. The probability of the frequency is a value between 0 and 1, since this threshold is not exceeded every year. Shanghai Water Authority (2000) recorded the frequency of exceedance of warning water level at Wusongkou from 1981 to 2000 and it seems that this warning water level is exceeded annually 4.15 times, this is a return period of 1:0.24 year. This figure seems likely since we also know from section 1.3 that average 2 tropical cyclones annually can cause the water levels in the Huangpu River to exceed its warning water level and cause flooding of downtown area of Shanghai as a result. The return period is defined as the annually probability that an event will occur. Only for extreme events the difference between frequency of exceedance and probability of exceedance can be neglected as an extreme events is not likely to happen twice a year. Apparently, random combination of tide and storm surge at Wusongkou only gives representative results for the higher probabilities as these return periods are more reasonable compared with the results from the Shanghai Water Authority. Probably, the linear interaction between storm surge of a tropical cyclone and astronomical tide can not be neglected.

As a consequence, we use the more realistic frequency of exceedance for the 4.80m WD storm tide level found by the Shanghai Water Authority in the continuation of this study. The frequency of exceedance of the barrier closure water level in the typhoon season will be applied in chapter 5 in the computation of the flood probability.

With regard to the aim of this subsection, we use the mean surge level given the storm tide level of 4.80m WD derived from the results of the computations carried out in this section. We thus assume that this surge level is representative for the barrier closure water level, neglecting the fact that the return period corresponding is deviant. The results from this section to be used in the continuation of this study are summarized in the table below. The required surge level will be used in the next section in the analysis of the torrential rainfall probability given the barrier closure water level.

Barrier closure water level	[cm] WD	480
Frequency of exceedance	[per year]	4.15
Required surge level	[cm]	118.46
Probability of occurrence	[-]	0.10

Table 4-3: Barrier closure water level and the required surge level used in the continuation of this study

4.3 Copulas for joint distribution of storm surge and torrential rainfall

4.3.1 Introduction

This section aims to derive the torrential rainfall runoff distribution from the joint distribution of storm surge and torrential rainfall with the required surge level for barrier closure. This section starts with a discussion on the torrential rainfall distributions in the Tai Lake Basin. Torrential rainfall, like wind gust and storm surge are inevitable exhaust products of the mechanism of tropical cyclones. Therefore, the torrential rainfall and storm surge are related to each other. The different methods to measure relationships between variables and the correlation between torrential rainfall and storm surge are treated in subsection 4.3.2. Because of the already available distributions of storm surge at Wusongkou and torrential rainfall in the Tai Lake Basin, we use copulas to link these individual distributions into their conceptual joint distribution. The concept of copulas and the special class of Archimedean copulas used in this study are treated in subsection 4.3.3 onwards followed by a discussion on the results of the sampling of the joint distribution of storm surge and torrential rainfall. Then finally in the last two subsections, the torrential rainfall runoff into the Huangpu River is derived from the torrential probabilities given the surge level required for barrier closure.

4.3.2 Torrential rainfall distributions in the Tai Lake Basin

The Taihu Basin Authority conducted extensive studies on the torrential rainfall probabilities in the Tai Lake Basin. Studies on the rainfall probability distribution in the Basin are important to protect the Tai Lake from because of extensive rainfall with flooding of large surrounding areas as a result. This has happened on numerous occasions in the past (see subsection 2.2.4). In the latest study latest (Taihu Basin Authority, 2000), the rainfall probability distribution in the Basin is analysed with historical rainfall records from major rain events from 1954 to 1999. It appears that the rainfall probability distributions for different rainfall duration are well described with the Pearson III distribution, which is the same distribution as for the storm surge levels described in subsection 4.2.2. The parameters and some typical probabilities for these distributions are given in the table 4-4

The Taihu Basin Authority study made no distinction between torrential rainfall produced by tropical cyclones and torrential rainfall brought by the rain season. However from subsection 2.2.2, we learnt that the majority of the torrential rainfall in the Shanghai region, especially the rainfall with higher intensities (thus lower probabilities) is caused by tropical cyclones.
Given this fact we may assume that torrential rainfall distributions found by the Taihu Basin Authority can be used to represent the tropical cyclone induced torrential rainfall.

	EX [mm]	cv	cs/cv	P(2%) [mm]	P(1%) [mm]	P(0.33%) [mm]
1 day	70	0.51	4.0	174	199	238
3 days	109	0.45	4.0	249	282	332

Table 4-4: Rainfall probability distributions in the Tai Lake Basin for different rain days (Taihu Basin Authority, 2000)

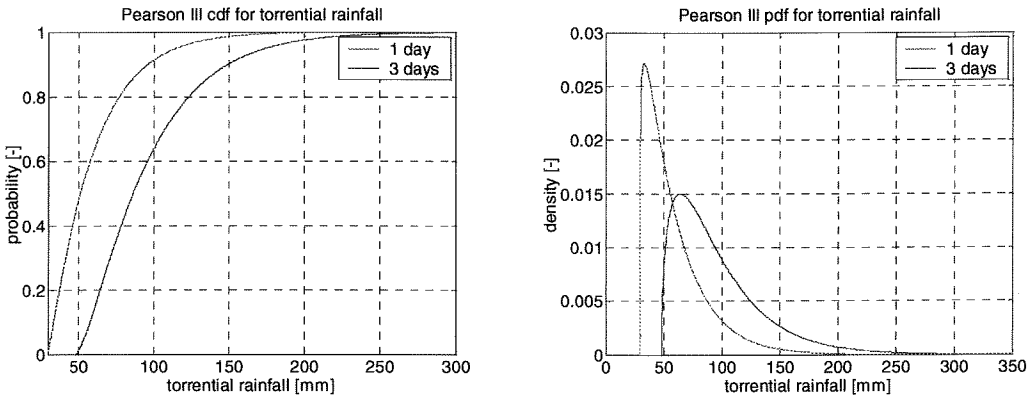

Figure 4-5: Pearson III probability distribution of 1 and 3 days of torrential rainfall in the Tai Lake Basin

The distributions for 1 and 3 days of torrential rainfall in the Tai Lake Basin are now used to create the joint probability distribution of storm surge at Wusongkou and torrential rainfall in the Tai Lake Basin. So, two joint probability distributions of storm surge and torrential rainfall are used distinguished by the rainfall duration. The 1 day rainfall distribution represents tropical cyclone passing Shanghai as normal mostly in a day. The distribution for 3 days of rainfall represents a slow passing typhoon, which therefore produces more rainfall.

4.3.3 Measures of association

Given the fact that torrential rainfall, like storm surge and wind gusts, is an inevitable exhaust product of the mechanism of tropical cyclones, a positive correlation between storm surge and torrential rainfall seems likely. Correlation is a measure for the *co-movement* of variables. The common mistake is to define correlation as the *cause and result* between variables. Correlation can be visualized in a scatter plot of the variables. Figure 4-6 show some examples of scatter plots of variables $X1$ and $X2$ with different correlations.

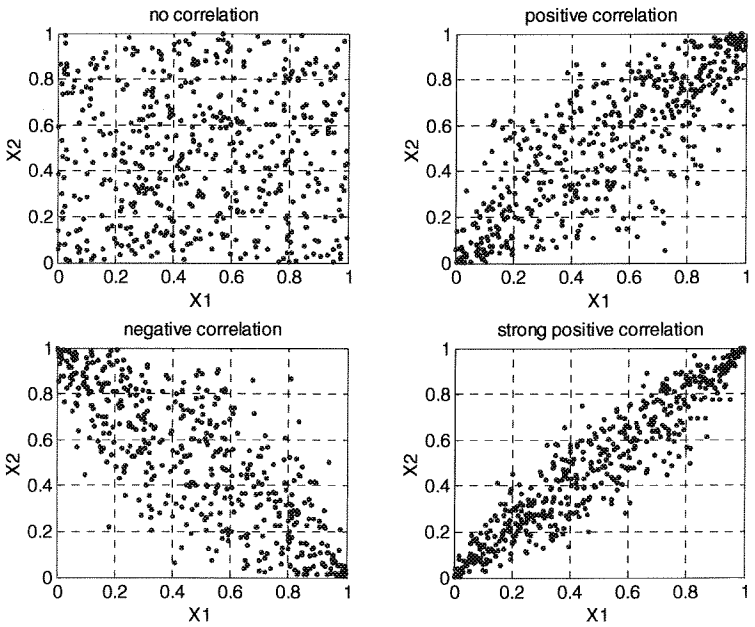

Figure 4-6: Random generated variables with different correlations

The Hohai University (2000) used historical records to investigate the correlation between high water levels in the Huangpu River and torrential rainfall in the Tai Lake Basin (table 4-5). From the results, it seems that torrential rainfall and the water levels in the Huangpu River are positively correlated. Thus, high water levels in the river are likely accompanied with high rainfall intensities in the Basin and vice versa.

However, before using these results we should regard the physical background of these correlations. The Huangpu River is a tidal river, and the only cause for storm tides in the river is tropical cyclones in the vicinity of Shanghai (section 2.3). This tidal dominance in the river is clearly reflected by the lower correlation for rainfall and water levels at Wusongkou and the correlation between the water levels at Wusongkou and Mishidu.

The water levels at the upstream located Mishidu are determined by both the tide at Wusongkou and the upstream discharge into the Huangpu River. Therefore, correlation between water levels and torrential rainfall at this station is believed to reflect the correlation more correctly than at Wusongkou. As a result, we assume that this correlation for the co-movement between storm tides, thus storm surges, and torrential rainfall is representative.

	Wusongkou water level ~ torrential rainfall	Mishidu water level ~ torrential rainfall	Mishidu water level ~ Wusongkou water level
correlation	0,15	0,30	0,76

Table 4-5: Correlation between water levels in the Huangpu River and torrential rainfall in the Tai Lake Basin (Hohai University, 2000)

Many methods are available to determine the correlation between variables. It is not clear which method the Hohai University has used for the correlation coefficients presented in the table above, therefore we assume that the correlation is according to Kendall's tau. More insight is needed in the concepts for association between variables; therefore the three main concepts are treated briefly hereafter including Kendall's tau.

Linear correlation

Traditionally, the measure of correlation is expressed in terms of linear correlation (or Pearson's r)

$$\rho(X,Y) = \frac{Cov[X,Y]}{\sqrt{\sigma^2[X]\sigma^2[Y]}} \quad , \rho \in [-1,1] \tag{4.17}$$

in which $Cov[X,Y]$ is the covariance between X and Y. Correlation ranges from $\rho = -1$ to $\rho = 1$. Independence between the variables is the case when $\rho = 0$. The linear correlation is a good measure for the co-movement for normal variables. For, in strongly non-normal distributions, linear correlation can conceal dependence between the variables contained in their joint distribution function. Furthermore, it is misleading that correlation is the only aspect that has to be known about a joint distribution next to its marginal distributions, for zero covariance does not mean independence. Besides, given the marginals, their joint distribution might not even exist in the full range of correlation $\rho = [-1,1]$. Another deficiency of linear correlation is that transformation of the variables will result in changes in the correlation between the variables.

Spearman's rho

A more sophisticated approach for correlation is Spearman's rho, which is closely linked with the concept of linear correlation. It is in fact, defined as the linear correlation coefficient of the variables transformed by their own marginal distribution functions. Spearman's rho can be expressed as

$$\rho_{rho} = 12 \int_0^1 \int_0^1 F_x(x) F_y(y) f_{xy}(x, y) dxy - 3 \tag{4.18}$$

in which F stands for the cumulative marginal distribution and f_{xy} stands for the joint distribution density. Since Spearman's rho is defined on the cumulative probability function of the individual variables, it is invariant to strictly increasing transformations of the variables.

Kendall's tau

Another measure of correlation is the Kendall's tau, which is based on the concept of concordance and discordance. Two separately drawn pairs (x, y) and (x', y') are considered concordant when both members of a pair are larger than the respective members of the other pair. In the situation that $x' > x \wedge y < y'$ or $x < x' \wedge y > y'$. Kendall's tau is now defined as the difference in probabilities of such discordant and concordant pairs

$$\rho_\tau = P((x - x')(y - y') > 0) - P((x - x')(y - y') < 0) \tag{4.19}$$

Naturally, this means that $\rho_\tau \in [-1,1]$. In addition, Kendall's tau can be expressed in terms of the joint distribution functions of the variables as

$$\rho_\tau = 4 \int_0^1 \int_0^1 F_{xy}(x, y) f_{xy}(x, y) dxdy - 1 \tag{4.20}$$

Kendall's tau is like the Spearman's rho 'scale-invariant' of the variables. However, the values of Kendall's tau and Spearman's rho can be quite different for the same correlation. More about the similarities and differences between these two correlation measures are referred to Nelson (1999).

Correlation alone is not enough

With regard to multivariate distribution functions, the correlation coefficient alone is not sufficient to specify the dependence between variables. Joint distributions with identical margins and identical correlation coefficient can have different *dependence structure* with consequences in the analysis. This is visualized figure 4-7.

The Gaussian distribution is symmetric and has no dependencies in the upper and lower probabilities whereas the Gumbel distribution has stronger dependence in the lower probabilities. The correlations given in table 4-5, hence, do not specify the dependence structure between storm surge and torrential rainfall. However, as both events are caused by tropical cyclones, it is confirmed by Dorst (2003) that the stronger the intensity of the typhoon the torrential rainfall intensity as well as the net storm surge level will increase as well. In reality, environmental factors heavily determine the eventual storm surge and torrential rainfall for the reference location as mentioned in section 2.3.

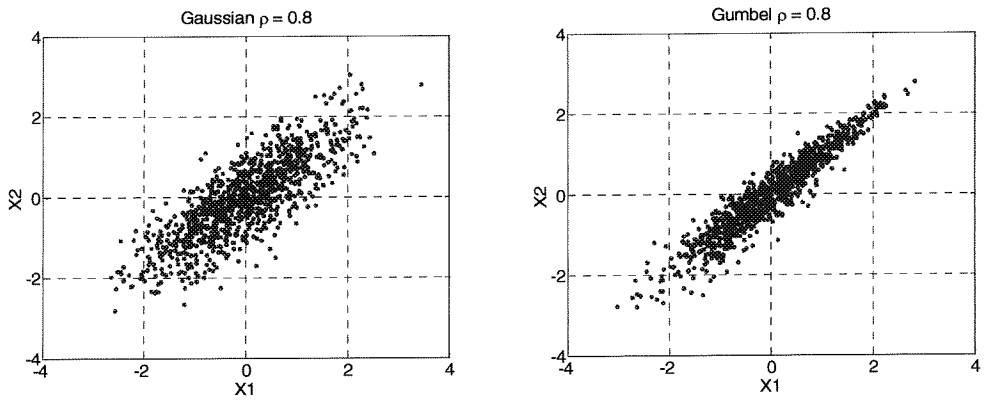

Figure 4-7: Scatter plot of 1000 random variables of two joint distributions with both identical standard normal margins and identical correlation $\rho_\tau = 0.8$, but with *different* dependence structure

Because of the strong physical relationship between storm surge and torrential rainfall of a tropical cyclone, the *Gumbel copula* is used to model their joint distribution. The dependence structure between the variables can be described with copulas, and the Gumbel copula has a stronger dependence in the lower probabilities. The next subsection introduces the theory of copulas.

4.3.4 Concept of copulas

Before we explain the Gumbel copula we first discuss the general concept of copulas. Copulas are functions that link arbitrary univariate distributions into their joint multivariate distribution. The study of copulas and its applications is rather new but a rapid growing field in the literature of statistics. Copulas originate from the study on probabilistic metric spaces. At present, copulas are particularly used in the field of financial mathematics and actuaries. Recent discussions on applications of copulas can be found in by Frees and Valdez (1997), De Michelle and Salvadori (2003) and Clemen *et al.*(1999).

The relation between copulas and multivariate distribution functions is stated in Sklar's theorem (1959). The version of this theorem for two-dimensional copula or 2-copula, which is of interest in this study, is as follows:

> Let H be joint distribution function with margins F and G, then there exists a copula C that, for all x,y in $[0,1]^2$,
>
> $$H(x, y) = C(F(x), G(y)) \tag{4.21}$$
>
> If F and G are continuous, then C is unique; otherwise C is uniquely determined on, Ran$F$ × Ran$G$, where Ran is the range of the margins. Conversely, if C is a copula and F and G are distribution functions then H, as in (4.21), is a joint distribution function with margins F and G.

From Sklar's theorem, we see that for continuous multivariate distribution functions, the univariate margins and the multivariate dependence structure can be separated, and the dependence structure is represented by the copula. Clearly, this provides a large freedom in choosing the margins once the desired dependence structure has been specified.

Properties

The elementary properties of a copula force it to act as a multivariate distribution function.
A 2-copula with random uniform distributed variables $u,v \in [0,1]^2$ satisfies the following properties:

(i) $C(0,v) = C(u,0) = 0$,

(ii) $C(1,v) = v$, $C(u,1) = u$

(iii) $C(u,v) = uv$

(iv) $\max(u+v-1,0) \leq C(u,v) \leq \min(u,v)$

Properties (i) and (ii) defines the uniformly distribution of the margins. Properties (iii) and (iv) captures the boundaries of 2-copulas, which are copulas themselves:

- the Fréchet lower bound $M = \max(u+v-1,0)$
- the independent or *product copula* $\Pi = C(u,v) = uv$
- the Fréchet upper bound $W = \min(u,v)$

The graph of a copula, i.e. the surface $z = C(u, v)$, is a continuous surface within the unit cube $[0,1]^3$, and z lies *within* the boundaries given in property (iv). Figure 4-6 presents the graphs and the corresponding contour diagrams of the boundaries of a 2-copula.

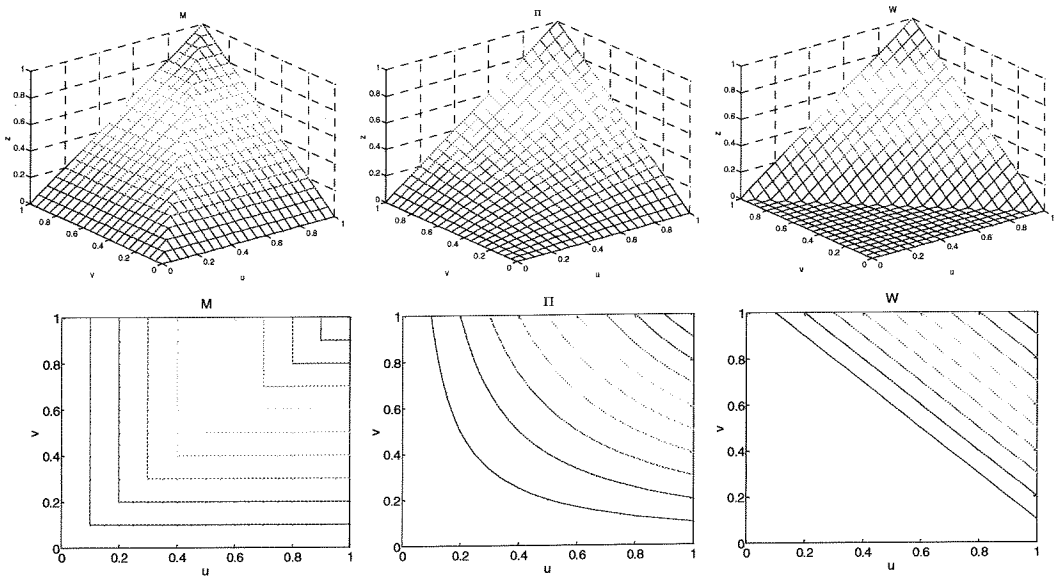

Figure 4-8: Graphs and corresponding contour diagrams of the copulas *M, Π, W*

Correlation with copulas

Much of the usefulness of copulas derives from the fact that copulas are invariant under strictly increasing transformations of the random variables. Since Spearman's rho and Kendall's tau share this characteristic as well, they can be expressed in terms of copulas in the following way

$$\rho_{rho}(X,Y) = 12 \int_0^1 \int_0^1 C(u,v)dudv - 3 = 12\mathrm{E}(C(U,V)) - 3 \qquad (4.22)$$

$$\rho_\tau(X,Y) = 4\int_0^1\int_0^1 C(u,v)dC(u,v) - 1 = 4\mathrm{E}(C(U,V) - 1 \tag{4.23}$$

in which E*(C(U,V)* is the expected value of the function *C(U,V)* of uniform (0,1) random variables with joint distribution function C. Correlation varies from perfect negative to perfect positive correlation $-1 \le \rho \le 1$. The boundaries of a copula are reflected in the correlation, if $C(u,v) = uv$ then $\rho = 0$. Moreover, $\rho = +1$ if and only if $C(u,v) = \min(u,v)$ which is the Fréchet lower bound and $\rho = -1$ if and only if $C(u,v) = \max(0, u+v-1)$ which is the Fréchet upper bound.

4.3.5 Archimedean copulas

The dependence structure between storm surge and torrential rainfall of a tropical cyclone is believed to be strong because of they are both related to the intensity of the tropical cyclone. Therefore, the Gumbel copula is used to link these two known distribution functions into their joint distribution. The Gumbel copula belongs to the important class of Archimedean copulas. The main characteristic of Archimedean copulas is that they allow us to reduce the study of multivariate copulas to a single univariate functions, the so-called generator of the copula. This nice property has made the Archimedean copula applied in a wide range of applications. The general expression of Archimedean copulas for variables *u, v* ∈ [0, 1]^2 is

$$C(u,v) = \varphi^{-1}(\varphi(u) + \varphi(v)) \tag{4.24}$$

in which φ is the generator of the copula. The generator φ is a strictly decreasing function, which maps the interval $(0,1]$ onto $[0,\infty)$. If $\varphi(u) = \infty$ than φ is termed *strict*, and the inverse function generator φ^{-1} exists. In this case, that φ is not strict, then the pseudo inverse is defined as $\varphi^{[-1]}$. When the generator is strict the copula is given as in (4-1), otherwise the Archimedean copula is expressed as

$$C(u,v) = \varphi^{[-1]}(\varphi(u) + \varphi(v)) \tag{4.25}$$

Different choices of generators yield several important families. And copulas with various dependence structures are developed. The focus of this study is on one-parameter Archimedean copulas. Hereafter we present the Gumbel copula which has stronger upper tail dependence and the Clayton which has a stronger dependence in the lower tail. A complete listing of the most common copulas can be found in Nelson (1999).

- Gumbel

The Gumbel copula, which is also referred as the Gumbel-Hougaard copula, gives rise to a strong dependence in the upper tail of the joint density distribution. This is shown in figure 4-9.

The generator of the Gumbel copula is given by

$$\varphi(t) = (-\ln t)^\theta \qquad \text{for } \theta \in [-1,\infty) \tag{4.26}$$

hence, the Gumbel copula is expressed as

$$C_\theta^{Gumbel} = (u,v) = \exp(-[(-\ln u)^\theta + (-\ln v)^\theta]^{-1/\theta}). \tag{4.27}$$

- Clayton

This copula is also known as the Pareto, Cook-Johnson or Oak copula. Contrary to the Gumbel copula, this copula gives a stronger dependence in the lower tail of the joint density distribution, as can be seen in figure 4-10.
The Clayton copula is determined by its generator expressed as

$$\varphi(t) = \frac{1}{\theta}(t^{-\theta} - 1) \qquad \text{for } \theta \in [-1,\infty) \setminus \{0\} \tag{4.28}$$

and reads

$$C_\theta^{Clayton}(u,v) = \max([u^{-\theta} + v^{-\theta} - 1]^{-1/\theta}, 0). \tag{4.29}$$

Elementary properties

Let C be an Archimedean copula with generator φ then:

(i) C is symmetric; i.e. $C(u,v) = C(v,u)$ for all $u,v \in [0,1]$,

(ii) C is associative; i.e. $C(C(u,v),w) = C(u,C(v,w))$ for all $u,v,w \in [0,1]$

(iii) If $c > 0$ is any constant then $c\varphi$ is also a generator of C,

(iv) The marginal distributions of U and V are uniform on the interval $(0,1)$, thus $C(u,1) = u$ for all $0 \le u \le 1$. Analogously $C(1,v) = v$ for all $0 \le v \le 1$.

Proof of these properties is given by Nelson (1999)

Correlation with Archimedean copulas

One of the reasons of the popularity of Archimedean copulas is the ease to express Kendall's tau directly in terms of the generator φ instead of the copula itself, which simplifies the computations significantly

$$\rho_\tau = 1 + 4\int_0^1 \frac{\varphi(t)}{\varphi'(t)}dt \tag{4.30}$$

For the Gumbel copula, the Kendall's tau is

$$\rho_\tau = 1 - \theta^{-1}, \qquad \text{for} \qquad \rho_\tau \in [0,1] \tag{4.31}$$

The Kendall's tau for the Clayton copula is

$$\rho_\tau = \frac{\theta}{\theta + 2} \qquad \text{for} \qquad \rho_\tau \in [-1,1] \setminus \{0\}. \tag{4.32}$$

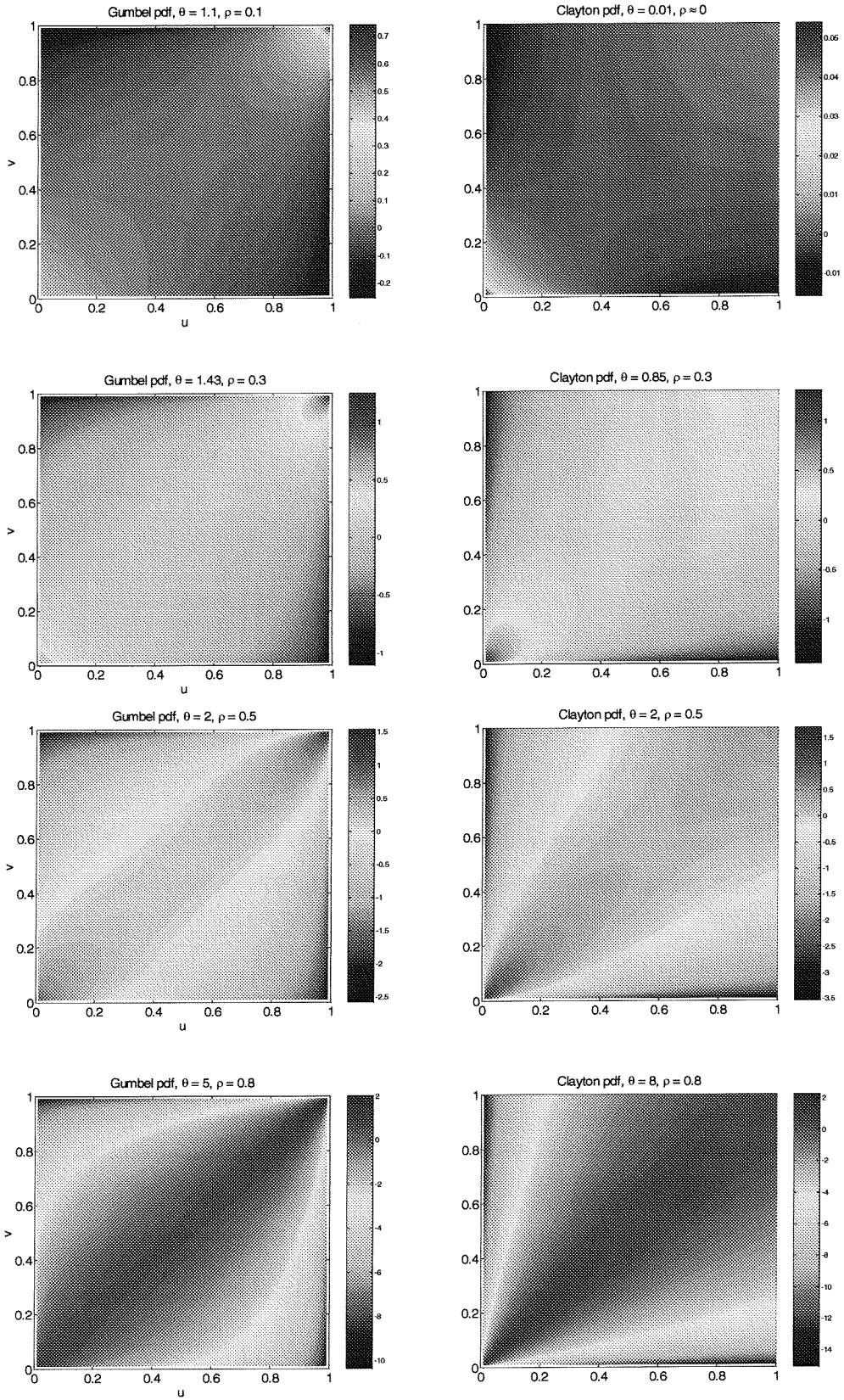

Figure 4-9: Density plots of the Gumbel copula and Clayton copula for variables $u,v \in [0,1]^2$ with different correlation coefficient ρ_τ

4.3.6 Sampling of storm surge and torrential rainfall with Gumbel copula

The next step in the analysis is to simulate the joint distribution of storm surge at Wusongkou and torrential rainfall in the Tai Lake Basin. The Gumbel copula used for the joint

Recall the expression of the Gumbel copula

$$C_\theta^{Gumbel} = (u,v) = \exp(-[(-\ln u)^\theta + (-\ln v)^\theta]^{-1/\theta}). \tag{4.27}$$

and its generator is denoted as

$$\varphi(t) = (-\ln t)^\theta \qquad \text{for } \theta \in [-1,\infty) \tag{4.26}$$

the Kendall's tau for the Gumbel copula is

$$\rho_\tau = 1-\theta^{-1}, \qquad \text{for } \rho_\tau \in [0,1] \tag{4.31}$$

The Archimedean copulas not only simplify the correlation expression with Kendall's tau but also the algorithm for simulation of the copulas. Simulation of the Archimedean copula can be carried out with just the generators of the copula. Many algorithms exist for random variable generation with copulas (Genest and Mackay, 1986) (Devroye, 1986) (Frees and Valdez, 1997).

Genest and Mackay (1986) proposed a universal algorithm for generation of random variables (u,v) from bivariate Archimedean copulas, the algorithm reads

1. Generate two independent uniform (0,1) variables u and t,
2. Set $w = \varphi^{'(-1)}(\varphi'(u)/t)$,
3. Set $v = \varphi^{[-1]}(\varphi(w)-\varphi(u))$,
4. The desired pair is (u,v).

The values for storm surge and torrential rainfall are now obtained by simply using the inverted margins of the individual variables. The sampling and the processing of the results is carried with a string of computer programmes in the MATLAB language especially written for this study. The eventual flood probability and runoff computations are incorporated within this program. See appendix W and X for the listing the programs can be found in the CD-ROM enclosed.

For any copula the input variables for sampling are the sample size and the Kendall's tau for correlation. The sample size used for analysis is n = 400000. The first series of simulations consisted in the joint probabilities of storm surge and 1 day of torrential rainfall in the Tai Lake Basin and the second series consisted in the combination of storm surge and 3 days of torrential rainfall. In figure 4-10, sample results for 1 rain day with the Gumbel as well as the Clayton and Gaussian copula are given for comparison. The sample size is n=1000 and the correlation ρ_τ = 0.3.

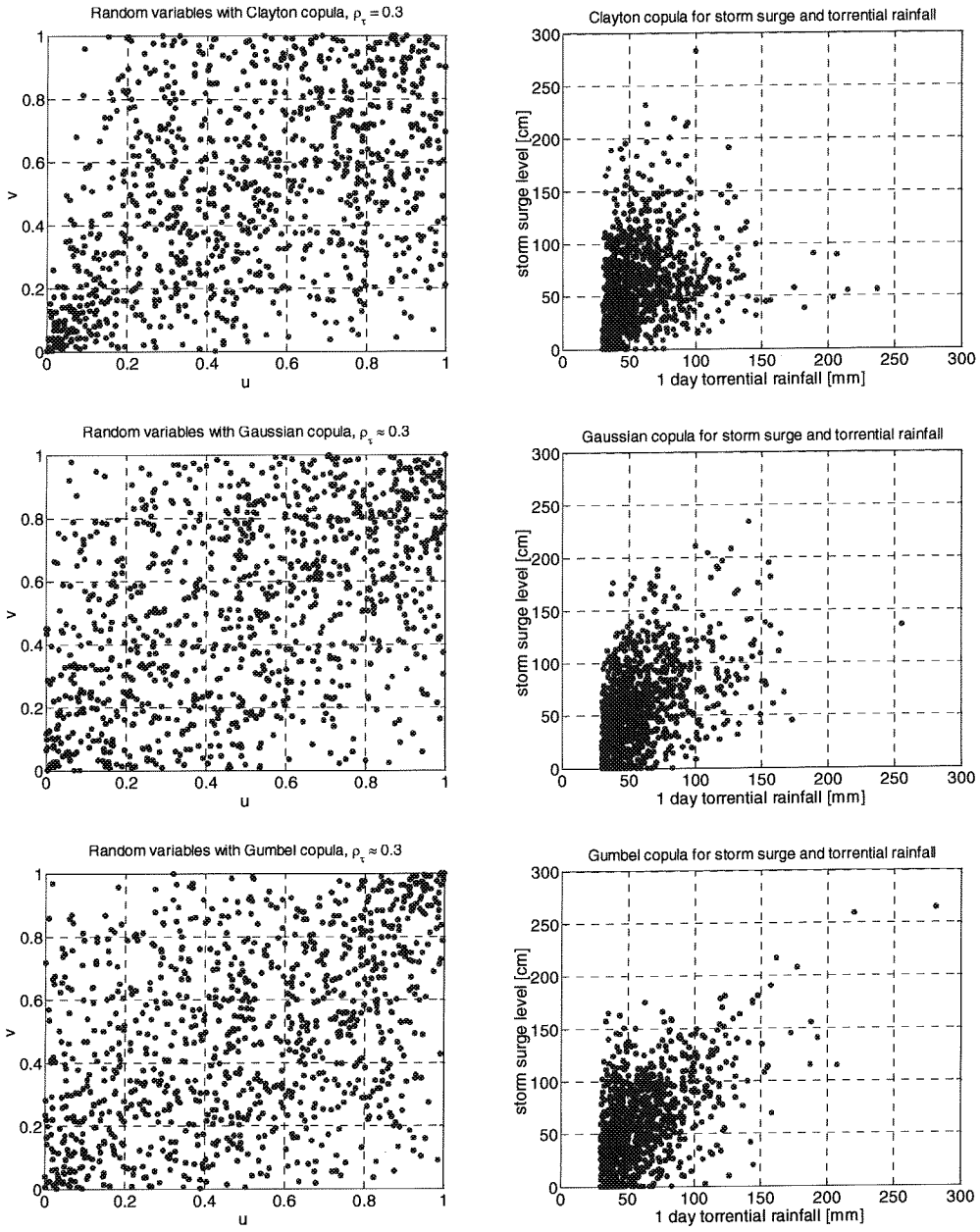

Figure 4-10: Scatter plot of the Clayton, Gaussian and Gumbel copula for joint storm surge at Wusongkou and torrential rainfall in the Tai Lake Basin with $\rho_\tau = 0.3$ and $n=1000$

The stronger dependence in the lower probabilities for the Gumbel copula is clearly visible. In contrast, the Clayton copula has a stronger dependence in the higher probabilities. Clearly, the Gaussian copula has no upper or lower tail dependence.

4.3.7 Torrential rainfall given the required surge levels

In this subsection we analyze the generated dataset of joint storm surge and torrential rainfall for 1 and 3 rain days. The aim is to determine the conditional probability of torrential rainfall given the surge level that, in combination with high tide, causes the barrier to close. Previously in subsection 4.2.5 we found that the required surge level for barrier closure is 118.46cm.

In figure 4-11, we show that the distribution of the generated samples of torrential rainfall is identical with its individual distribution. This is off course a straight forward consequence of the use of copulas.

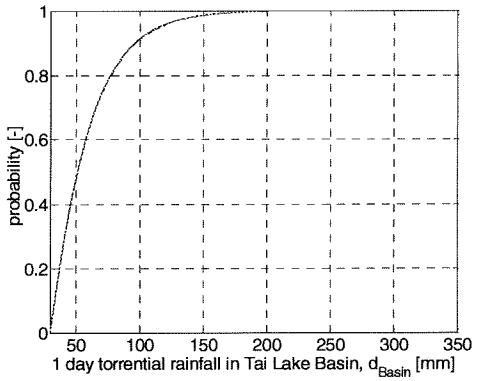

Figure 4-11: Marginal distribution function remains identical after copula simulation

After processing the samples, the conditional distribution of torrential rainfall given the required surge level of 118.46cm is computed and further analysed. The results for 1 and 3 days of torrential rainfall in the Tai Lake Basin are shown in the figures below. For comparison we also generated samples from the Clayton and Gaussian copula and computed their conditional torrential rainfall probabilities as well for comparison.

From the figures we can see that, logically, the conditional probabilities are shifted to the right in comparison with the margins. Furthermore, the Gumbel copula gives stronger upper tail dependence probabilities, which is visible in the conditional probabilities. The factor between the joint probabilities and the conditional probabilities is the probability for a storm surge level of at least 118.46cm (P=10%). Indeed, a lower surge level will cause the joint probability curve to lower since the probability of this surge level is higher. Moreover, the conditional probability curve will move towards the marginal distribution curve and it will become the marginal distribution curve when the given surge level is zero indeed (right panel figure 4-18). A higher correlation between storm surge and torrential rainfall will cause the conditional probability curve to shift more to the right from the marginal curve (left panel figure 4-18).

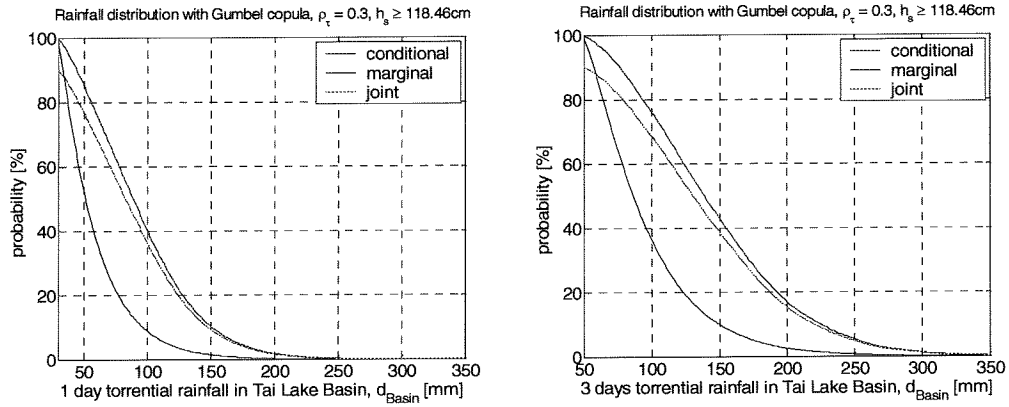

Figure 4-12: 1 and 3 days torrential rainfall distributions from Gumbel copula generated samples with $\rho_\tau = 0.3$ and a given surge level of at least 118cm P=10%

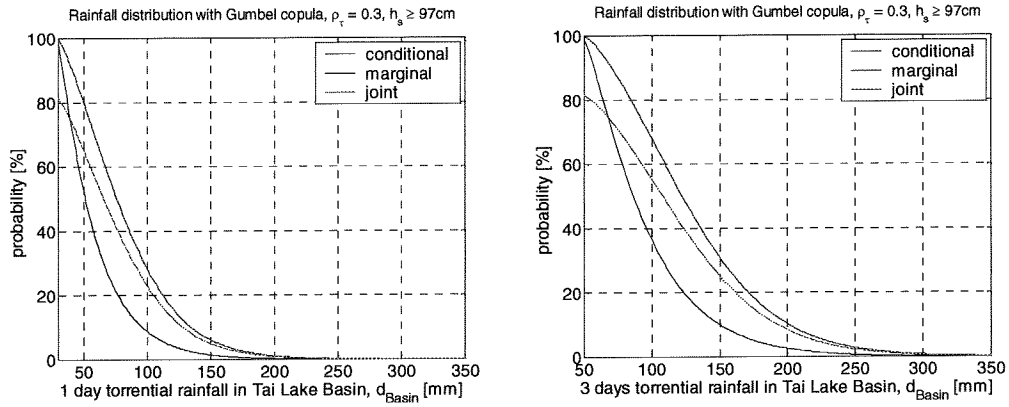

Figure 4-13: 1 and 3 days torrential rainfall distributions from Gumbel copula generated samples with $\rho_\tau = 0.3$ and a given surge level of at least 97cm P=20%

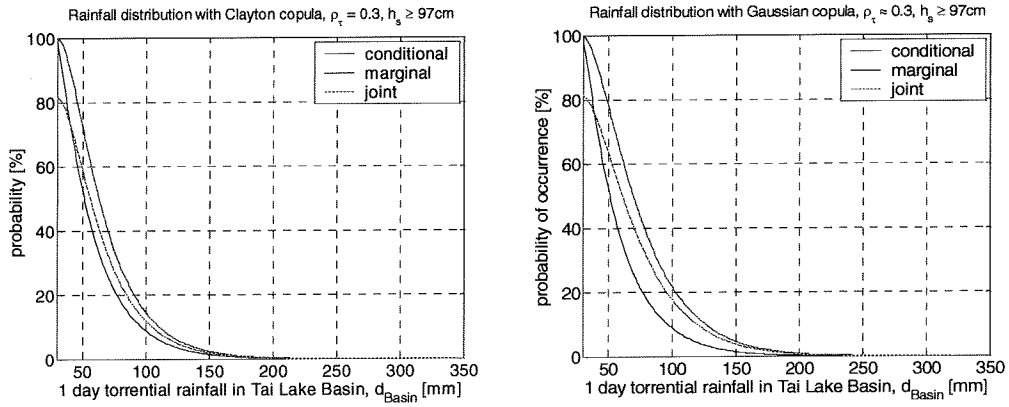

Figure 4-14: Torrential rainfall distributions after sampling with the Clayton and Gaussian copula with $\rho_\tau = 0.3$ and a given surge level of at least 97cm

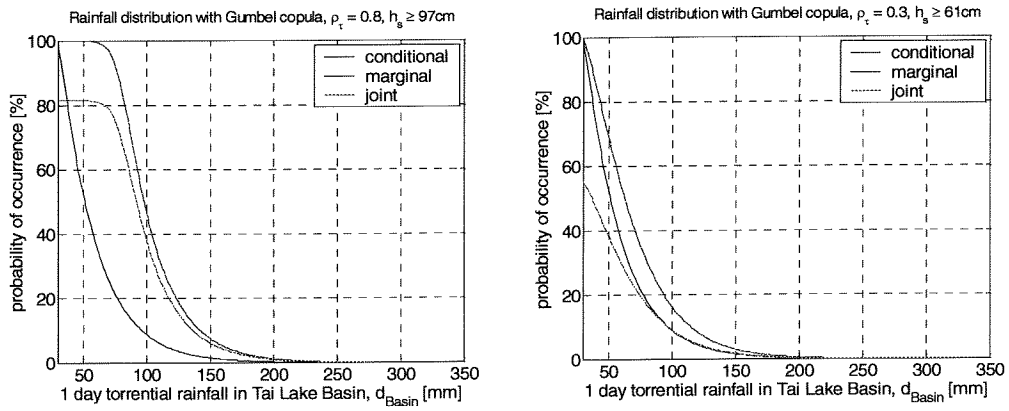

Figure 4-15: Torrential rainfall distributions after sampling with Gumbel copula for different ρ_τ and surge level.

4.3.8 Torrential rainfall runoff distribution

The final step in the analysis is to convert the torrential rainfall into the distribution of the runoff. Rainfall runoff is a complex process dependent on factors as

- Size of the catchment area
- Rainfall intensity in time
- Soil characteristics of the catchment area
- Altitude variations in the area

These factors determine the shape of the peak discharge, the eventual runoff depth and the time between rainfall and actual runoff. In this study we are interested in the distribution of torrential rainfall runoff into the Huangpu River during barrier closure. Unfortunately, only little information on the runoff characteristic of the Tai Lake Basin is available. We can only state that the Tai Lake and its network of rivers and lakes in the Basin are believed to have a large storage effect on the rainfall. Therefore, a model based on the few available records of rainfall events in the past is set up to determine the runoff.

The model assumes that rainfall in the Tai Lake Basin is first collected (runoff) in the Tai Lake, before it subsequently freely flows (discharge) into the Huangpu River via the Taipu River. This is believed to be a realistic approach, with regard to the storage effect of the Tai Lake. Moreover, with this approach the lag time between the rainfall and the actual runoff is separated.
The model is calibrated with the water budget of the 1991 flood of the Tai Lake described by the World Bank (1993) and verified with the few other publicly available records of major rainfall events in the Tai Lake Basin. A conservative surface runoff percentage of 18% is found for rainfall in the entire basin. The discharge of the Tai Lake into the Huangpu River is considered to be a uniform distributed free flow expressed as

$$Q = B\Delta h\sqrt{(2g\Delta h)} \tag{4.33}$$

in which

Q	= discharge into the Huangpu River	[m^3/s]
B	= width of the Taipu River at Tai Lake	[m]
Δh	= increment of the Tai Lake water level or runoff depth	[m]
g	= gravitational force	[m/s^2]

The width of the Taipu River at the Tai Lake end is 150m (see also section 2.2.4). The actual water level in the Tai Lake is not needed with this approach. And furthermore it is believed that the runoff depth will be discharged completely into the Huangpu River. In reality, the Taihu Basin Authority aims to keep the water level in the Tai Lake at a constant level, so discharge will occur certainly when warning water level in the Lake is about to be exceeded. Furthermore, since the typhoon season follows the rain season, it is reasonable to assume that the water level in the Tai Lake is already higher and therefore runoff into the Lake as a result of torrential rainfall has to be diverted completely.

Unfortunately, only little data is available to verify the results. However, the computed discharges are within the flood diversion capacity of 800m^3/s the Taipu River the main upstream connection with the Tai Lake, which is computed in section 2.2.4. It should be noted that this model simplifies the actual very complex rainfall runoff process and changes in the water regime of the basin in time will lead to different results. When detailed information on the rainfall runoff characteristic is available, the configuration of the torrential rainfall runoff into the Huangpu River can be determined more accurately. Figure 4-16 and 4-17 shows the distributions of the acquired runoff depth and corresponding uniform discharges for 1 and 3 days of torrential rainfall given a surge level of 118.46cm. The red curves represent a runoff of 18%, which is used in the continuation of this study. The pink and blue curves show the difference when a runoff of 13% and 23% respectively is used.

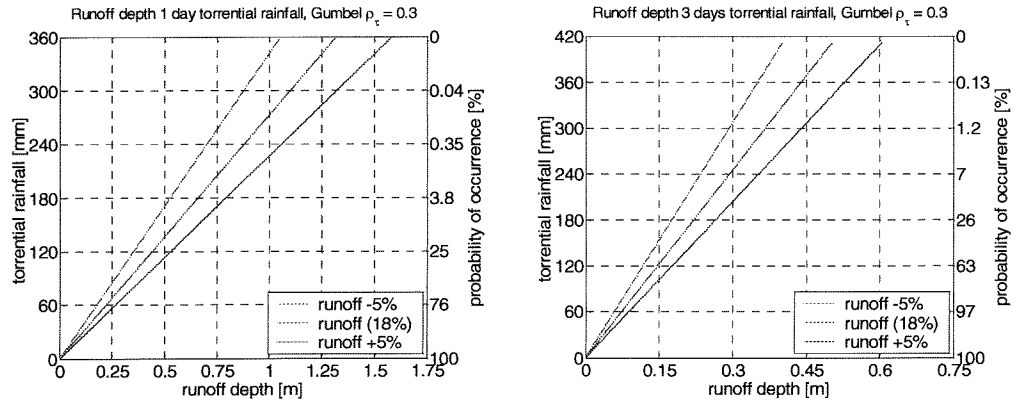

Figure 4-16 Runoff depth distribution for 1 and 3 days of torrential rainfall for given surge level of at least 118cm

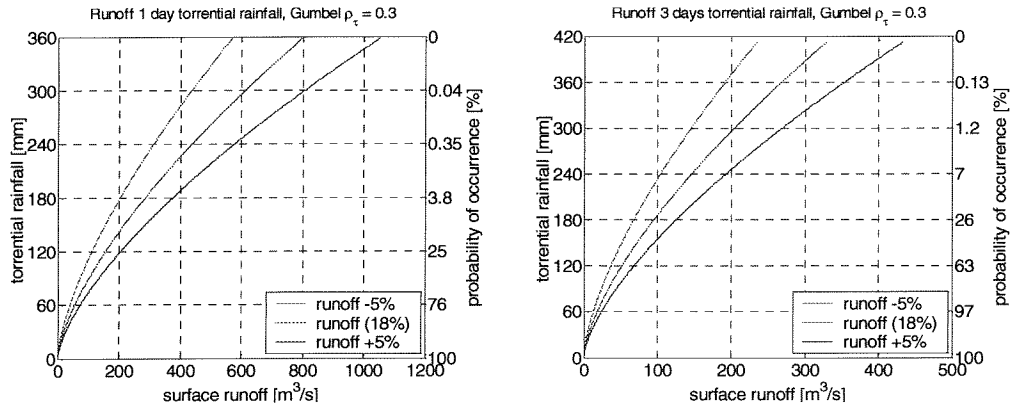

Figure 4-17 Torrential rainfall distribution for given surge level of at least 118cm

The probabilities of the 3 days torrential rainfall runoff distribution is lower in comparison. This is the result of the assumption that the rainfall intensity is uniformly distributed in time.

Because of the positive correlation between storm surge and torrential rainfall, a lower surge level will lead to lower conditional torrential rainfall probabilities. Moreover, since the discharge is one to one related with the torrential rainfall, the discharge probability decreases as well when the given surge level decreases. For comparison, this is visualized in figure 4-18 and 4-19 where the runoff depth and corresponding discharges (or surface runoff) for a given surge level of 97cm (P=19%).

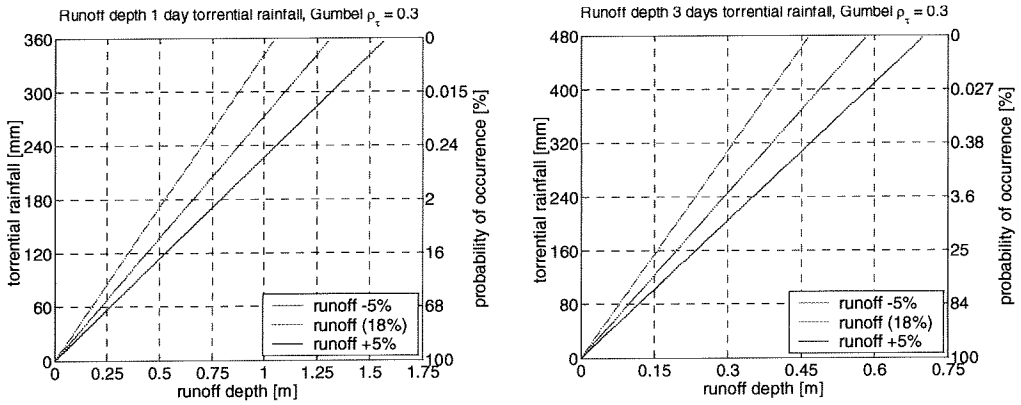

Figure 4-18 Runoff depth distribution for 1 and 3 days of torrential rainfall for given surge level of at least 97cm

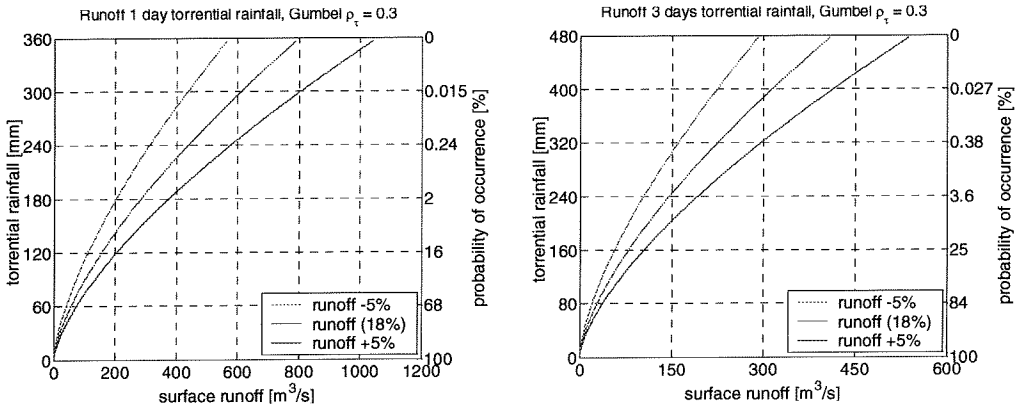

Figure 4-19 Torrential rainfall distribution for given surge level of at least 118cm

According to Neal (2003) the majority of the tropical cyclone induced rainfall occurs 6 hours before and after the cyclone passes the location of interest. In that case, torrential rainfall is likely to occur during the representative closure duration of 24 hours. When torrential rainfall runoff into the Huangpu River does occur during barrier closure, then the base discharge is the only factor that can cause flooding in the Huangpu River. However, because of the dish shaped ground level profile of Shanghai City, torrential rainfall in the downtown area has to be discharged into the Huangpu River immediately to prevent water logging. So, we may assume that torrential rainfall is likely to occur during barrier closure and even though the runoff from the Tai Lake does not start right after barrier closure the urban rainfall runoff into the Huangpu River is certain.

4.4 Conclusions

The torrential rainfall distribution into the Huangpu River during barrier closure in analysed in this chapter. The torrential rainfall runoff is together with the base discharge believed to be the main contributors to the so-called critical discharge of the river during barrier closure. In this chapter we derived the torrential rainfall distribution for 1 and 3 rain days from the joint distribution of storm surge at Wusongkou and torrential rainfall in the Tai Lake Basin.

The main results of this chapter are summarized chronologically below

- The storm tide distribution at Wusongkou is derived with Monte Carlo analysis of the tide and surge levels at this location. For this goal, the beta generalized distribution is found to describe the tide levels at Wusongkou best. The storm tide probability of exceedance appeared to resemble the design storm tide levels found by the Shanghai Water Authority only for the upper tail. As a consequence, the known historical frequency of exceedance of the barrier closure water level is used in the continuation of the study instead of the probability of exceedance. The present warning water level at Wusongkou is assumed to be the future barrier closure level. Furthermore, the computed mean surge level of 118.46cm from the Monte Carlo analysis is assumed to be still representative for the barrier closure water level. This level is used in the analysis of the torrential rainfall probabilities. The frequency of exceedance of the barrier closure level is essential in the next chapter when we analyse the flood probability during barrier closure.

- The Gumbel copula is used to create the conceptual joint distribution of storm surge at Wusongkou and torrential rainfall in the Tai Lake Basin. After analysis of the correlation between storm tides in the Huangpu Rive and rainfall in the Tai Lake Basin , the correlation between storm surge and torrential rainfall is set at $\rho_\tau = 0.3$. Datasets of storm surge and 1 and 3 days of torrential rainfall are generated with the Gumbel copula and compared with those created with the Clayton and Gaussian copula. These copulas have other dependence structures. The stronger upper tail dependence of the Gumbel copula is supposed to correctly reflect the dependence structure between storm surge and torrential rainfall of a tropical cyclone.

- After processing of the generated samples, the probabilities for 1 and 3 days of torrential rainfall are found for the required surge level for barrier closure. Furthermore, the effects of variations in the correlation and required surge level is analysed as well. In addition, the results are again compared with the conditional probabilities retrieved from the Clayton as well as from the Gaussian copula.

- The runoff distribution for 1 and 3 rain days is derived with empirical runoff relations of the Tai Lake Basin based on historical major rain events in the area. The model assumes a runoff percentage of 18% for rainfall in the Tai Lake Basin. Furthermore, variation of this percentage on is investigated. The storage capacity of the Tai Lake is taken into account by assuming a free discharge of the runoff depth into the Huangpu River. The computed runoff is within the limit of the flood diversion capacity of the Taipu River which is the main connection between the Tai Lake and the Huangpu River. Furthermore, we concluded that even though torrential rainfall runoff in the basin does not start immediately after barrier closure the urban area will discharge immediately to prevent water logging.

5 Flood probability during barrier closure

5.1 Introduction

In this chapter we determine the flood *probability* as well as the flood *frequency* of the Huangpu River during barrier closure with results from previous chapters. The analysis of the flood probability is characterized by the format of the base discharge records of the Huangpu River available. For each month in the typhoon season the flood probability given barrier closure is analysed. The main aim is to analyse the annual flood probability during barrier closure. For this purpose the probability of barrier closure is required. However, probability of exceedance of the barrier closure water level, which is computed in subsection 4.2.5, appears to be underestimated relatively to its historical frequency of exceedance. Therefore, we continue the analysis in section 5.3 with the flood frequency during barrier closure instead of the flood probability. The discussion on the limit state condition of the Huangpu River during barrier closure will be continued when we treat the maximum closure duration in section 5.2. Subsequently, the flood probabilities of the Huangpu River given barrier closure are presented in section 5.3. In section 5.4, we use the barrier closure frequency of exceedance and the flood probabilities computed in the previous sections to analyse the flood frequency of the river during barrier closure.

5.2 Maximum closure duration

During barrier closure, flooding of the Huangpu River occurs when the upstream discharge during barrier closure exceeds the storage capacity of the river. In reality, flooding will occur as soon the floodwalls along the river breaches during barrier closure or as the water levels overtop the elevation of the floodwalls. As mentioned in section 1.4, in this study we assume that flooding occurs when the warning water level in the river is exceeded. The warning water levels in the river are presented in table 3-7 of section 3.3.2.

Flooding of the Huangpu River as result of an insufficient storage capacity to store the upstream discharge during closure, can be expressed as

$$Z = R - S \tag{1.1}$$

in which

R = storage capacity Huangpu River [m^3]
S = upstream discharge volume during barrier closure [m^3]

The limit state condition $Z = 0$ is defined as the situation that the Huangpu River is on the verge of flooding during barrier closure. Recall the expression (1.2) of the upstream discharge into the river during barrier closure

$$Q_{upstream} = Q_{base} + Q_{torrential} \tag{1.2}$$

in which

$Q_{upstream}$ = upstream discharge [m^3/s]

Q_{base} = base discharge [m^3/s]

$Q_{torrential}$ = torrential rainfall runoff triggered by a tropical cyclone [m^3/s]

In chapter 3 we analysed the storage capacity of the Huangpu River and found the critical discharges $Q_{critical}$ per closure duration for each barrier location. The critical discharge is defined as the uniform total discharge needed to cause the limit state condition of the river during barrier closure.

We now define Q_r as the required torrential rainfall runoff, which is just the difference between the critical and base discharge as

$$Q_r = Q_{critical} - Q_{base} \tag{5.1}$$

The base discharges of the Huangpu River are already presented in section 2.2.5. In the table below we summarize the monthly base discharges in the typhoon season with their corresponding probabilities of occurrence. The base discharge depends on the prevailing type of hydrological year. In a wet hydrological year, the base discharges are significant higher, but their probability of occurrence is lower. As a consequence of the format of the base discharges, the flood probability of the Huangpu River is analysed accordingly in the next section.

Month	Wet year [m^3/s]	Average year [m^3/s]	Dry year [m^3/s]
Jun	607	323	211
Jul	833	352	237
Aug	639	326	293
Sep	517	279	253
Oct	305	327	188
Probability [%]	20%	50%	75%

Table 5-1 Average monthly base discharges of the Huangpu River in the typhoon season measured at Mishidu per type of hydrological year (with data from Wang *et al.*, 2001)

During barrier closure, the warning water level will be exceeded first at Mishidu because of its upstream position in the river and its lower warning water level. The critical discharges at Mishidu analyzed are therefore dominant in the flood probability analysis.
The flood probability at Huangpu Park is eventually analysed with the required torrential rainfall runoff corresponding the critical discharges at Mishidu.

For each month in the table above and for given type of hydrological year, the required torrential rainfall runoff Q_r per closure ration is computed with the critical discharges at Mishidu.
The required torrential rainfall runoff for the two critical months July and August are shown in figures 5-3 for each barrier location respectively. The figures for the remaining months can be found in appendix A. From the figures, the maximum closure duration for Mishidu is now clearly visible as the closure duration corresponding to a zero required torrential rainfall runoff. The maximum closure duration is defined as the closure duration of the Huangpu River after which the base discharge alone is capable to cause the limit state condition. Naturally, the maximum closure duration for Huangpu Park is relative higher because of its higher warning water level.

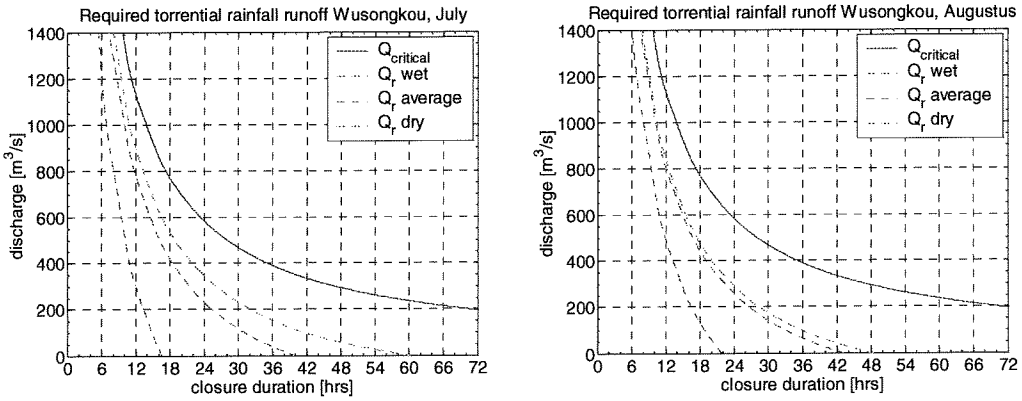

Figure 5-1: Required torrential rainfall runoff for the months July and August for a barrier at Wusongkou

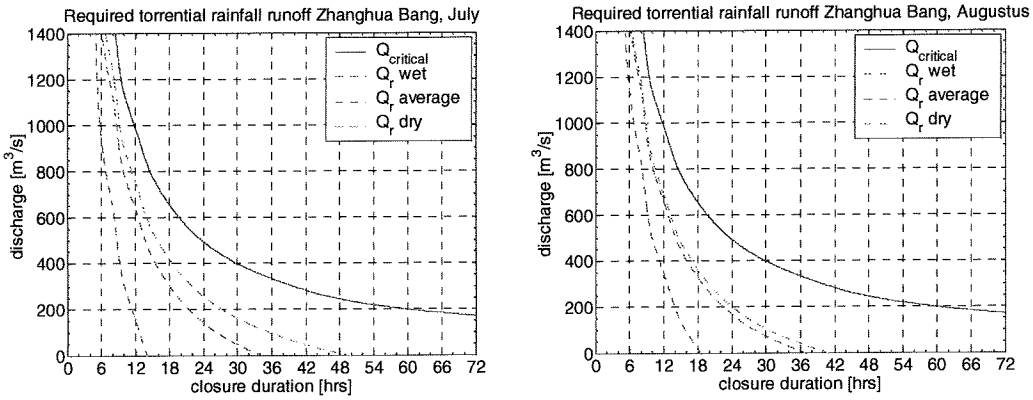

Figure 5-2: Required torrential rainfall runoff for the months July and August for a barrier at Zhanghua Bang

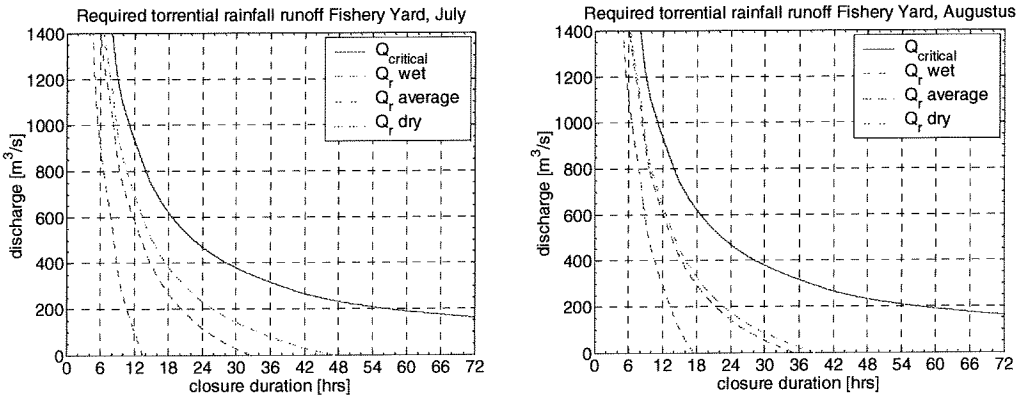

Figure 5-3: Required torrential rainfall runoff for the months July and August for a barrier at Fishery Yard with use of the critical discharges with reference to Mishidu

From the figures above the monthly maximum closure duration per barrier location given a wet year for Mishidu and Huangpu Park are summarized in the tables below.

Month		June	July	August	September	October
Wusongkou	[hrs]	23	17	22	27	47
Zhanghua Bang	[hrs]	20	14	19	23	39
Fishery Yard	[hrs]	19	14	18	22	37

Table 5-2: Maximum closure duration with reference to Mishidu in a wet year

		June	July	August	September	October
Wusongkou	[hrs]	43	31	41	51	87
Zhanghua Bang	[hrs]	37	27	35	43	73
Fishery Yard	[hrs]	35	25	33	41	69

Table 5-3: Maximum closure duration with reference to Huangpu Park in a wet year

The influences of the barrier location on the storage capacity of the Huangpu River and the magnitude of the base discharge are clearly visible from the tables above. The most upstream barrier location Fishery Yard has the shortest maximum closure duration. The same effect is caused by the higher base discharges in July. The longest maximum closure duration is found in October. Furthermore, the maximum closure duration at Huangpu Park is about twice as long as at Mishidu.

In the next section, the flood probability of the Huangpu River given barrier closure, month and type of hydrological year is analysed using these required torrential rainfall runoffs per closure duration.

5.3 Flood probability given barrier closure

5.3.1 Introduction

The flood probability of the Huangpu River given barrier closure is analysed in this section with reference to the locations Mishidu and Huangpu Park in the river. Because of the format of the discrete base discharge data used, the flood probability given barrier closure is first computed for a given month and hydrological year in the typhoon season. Subsequently, the flood probability given barrier closure for a given month alone is investigated. The flood probabilities are based on findings of the mean surge level required for the presumed barrier closure with the corresponding probabilities for 1 and 3 days of torrential rainfall.

5.3.2 Flood probability given month and hydrological year

The flood probability of the Huangpu River during barrier closure can be defined as the probability of exceedance of the limit state condition. Recall expression (1.4) for the flood probability presented in section 1.4

$$P(Z < 0) = P(R < S) \tag{1.4}$$

Moreover, since only the upstream discharges are stochastic variables, the flood probability is solely determined by the upstream discharge.

$$P(Z < 0) = P(Q_{upstream} > Q_{critical})$$

Or with use of expression (5.4) for the torrential rainfall required, the flood probability can be denoted as

$$P(Z < 0) = P(Q_{torrential} > Q_r) \tag{5.2}$$

Since the available upstream discharge is available for a given month and type of hydrological year the flood probability is computed accordingly. The expression for the flood probability given month and type of hydrological year is expressed as

$$P(Z < 0 \mid month, type\_year) = P(Q_{torrential} > Q_r) \tag{5.3}$$

The flood probability given barrier closure, month and type of hydrological year in the Huangpu River is computed for the locations Huangpu Park and Mishidu with the critical discharges of Mishidu as reference. Results for the critical month July with the conditional probabilities for 1 and 3 days of torrential rainfall are shown in figure 5-2 to 5-4 for each barrier location. The figures for the remaining months are enclosed in appendix A to G.

The figures in the left reflects the flood probability for 1 rain day whereas the figures in the right represent the flood probability caused by 3 days of torrential rainfall. The dotted lines represent the flood probabilities for Huangpu Park and the solid lines for Mishidu respectively. The flood probabilities at each location are derived from different warning water levels, i.e. different storage capacities. For example, for the situation of 1 day torrential rainfall in a wet year in July

with a barrier at Wusongkou, flooding at Mishidu at which the warning level is 3.50m WD occurs when the closure duration exceeds 16 hours. To cause flooding at Huangpu Park subsequently the barrier has to close for a total of 30 hours.

The contribution of the torrential rainfall runoff in the flood probability is represented in the slope of the flood probability curve. A larger slope reflects a higher torrential rainfall runoff required corresponding the closure duration. When we compare the flood probability caused by a 1 day rainfall with a 3 days rainfall, we conclude that the flood probability per closure duration is higher with a 1 day rainfall. The total rainfall is higher with a 3 days torrential rainfall. However since we assume the rainfall intensity in time to be uniformly distributed, the net discharge caused is therefore lower.

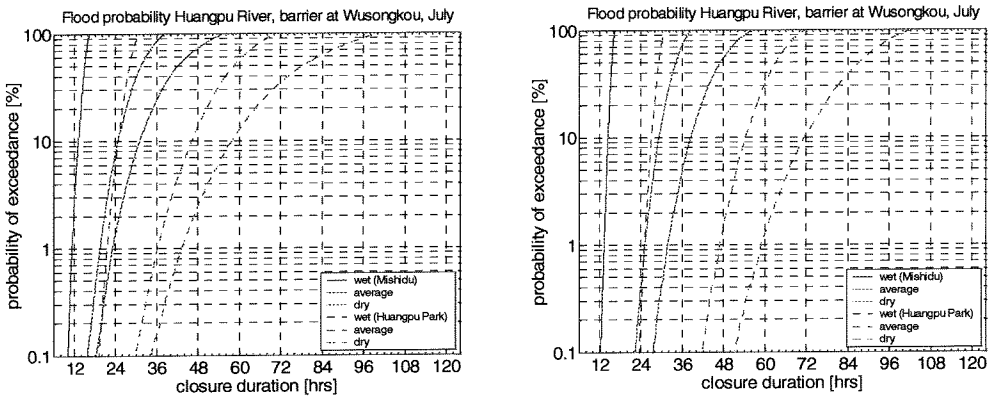

Figure 5-4 Flood probability of the Huangpu River given barrier closure, month and type of hydrological year in July with barrier at Wusongkou. Figure on the left is for 1 rain day whereas figure on the right is for 3 rain days.

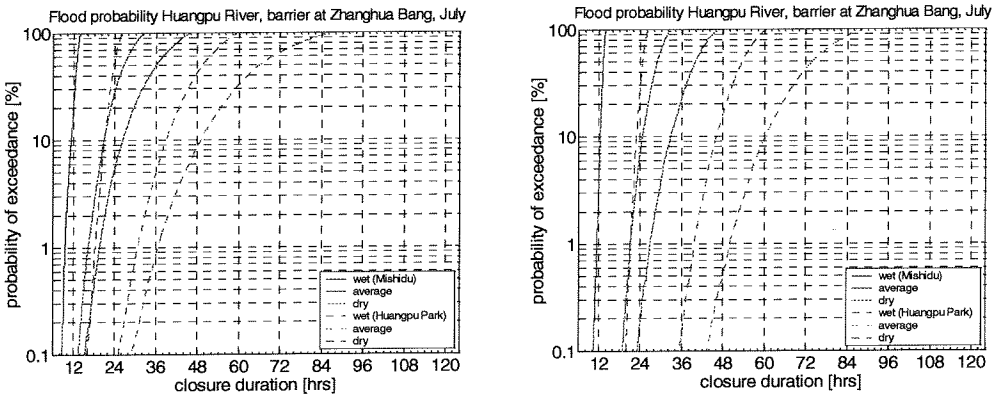

Figure 5-5 Flood probability of the Huangpu River given barrier closure, month and type of hydrological year in July with barrier at Zhanghua Bang. Figure on the left is for 1 rain day whereas figure on the right is for 3 rain days.

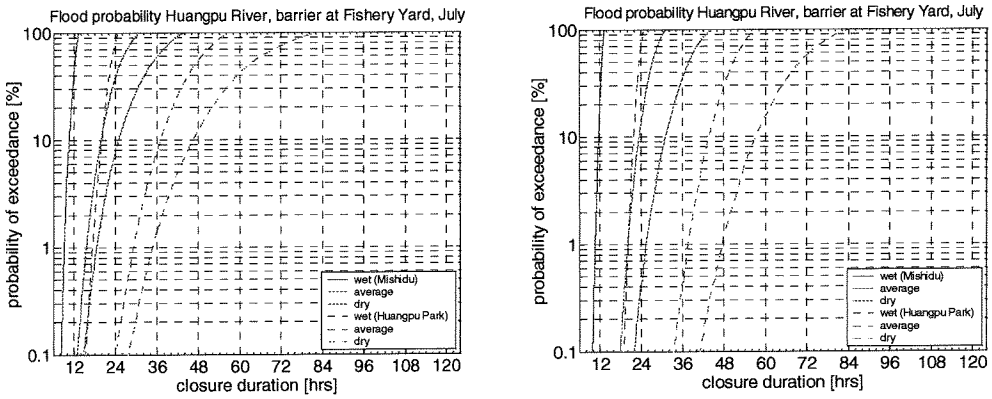

Figure 5-6 Flood probability of the Huangpu River given barrier closure, month and type of hydrological year in July with barrier at Fishery Yard. Figure on the left is for 1 rain day whereas figure on the right is for 3 rain days.

Given a wet year, a 1 day torrential rainfall and a representative 24 hours barrier closure, it appears that flooding at Mishidu is a sure event from June to September for all barrier locations, except a barrier at Wusongkou in September which still has a significant flood probability of 66%. In contrary, the flood probability at Huangpu Park in a 24 hours closure ranges from 6% annually with a barrier at Wusongkou to a significant 84% with a barrier at Fishery Yard. Furthermore, it seems that the flood probability for Huangpu Park with a barrier at Wusongkou in the typhoon season is about 10 times smaller compared with a barrier at Zhanghua Bang. Moreover, the flood probability for Huangpu Park with a barrier at Fishery Yard seems to be twice the flood probability with a barrier at Zhanghua Bang. This is probably caused by the linear relation between the storage capacities of the Huangpu River for the three barrier locations.

Month		June	July	August	September	October
Mishidu	P[%]	100	100	100	66	3.8
Huangpu Park	P[%]	0.18	6	0.3	0.06	0.003

Table 5-4: Flood probability given a wet year for a 24 hours barrier closure with a barrier at Wusongkou

Month		June	July	August	September	October
Mishidu	P[%]	100	100	100	100	15
Huangpu Park	P[%]	2.4	56	4	0.6	0.03

Table 5-5: Flood probability given a wet year for a 24 hours barrier closure with a barrier at Zhanghua Bang

Month		June	July	August	September	October
Mishidu	P[%]	100	100	100	100	21
Huangpu Park	P[%]	4.7	84	7.5	1.2	0.06

Table 5-6: Flood probability given a wet year for a 24 hours barrier closure with a barrier at Fishery Yard

5.3.3 Flood probability given month

Previously, we computed the flood probability of the Huangpu River for a given month and hydrological year. We are now interested in the flood probability given only the month of barrier closure, since eventually we wish to investigate the annual flood probability.

Recall the expression (5-3) for the flood probability of Huangpu River given barrier closure, month and corresponding hydrological year

$$P(Z < 0 \mid month, type\_year) = P(Q_{torrential} > Q_r) \tag{5.4}$$

The probability that one of the three given hydrological years is prevailing during barrier closure can be noted as

$$P(type\_year) = P(type\_year \mid month) \tag{5.5}$$

These probabilities are given in table 5-1. After normalizing these probabilities, since their sum exceeds 1, we can derive the flood probability taken into account the probability of the type of hydrological year for a given month only. The flood probability given a month only is now obtained by the sum of the products of the monthly flood probabilities and the normalized probabilities of the corresponding hydrological years. The expression for the flood probability then reads

$$P(Z < 0 \mid month) = \sum_{type\_year}^{3} P(type\_year) P(Q_{torrential} > Q_r) \tag{5.6}$$

Figure 5-7 depicts the expression (5.6). Note that the flood probabilities shown for a wet, dry and average June are already factorized with the corresponding hydrological year. The pink curve is the eventual flood probability given the month June.

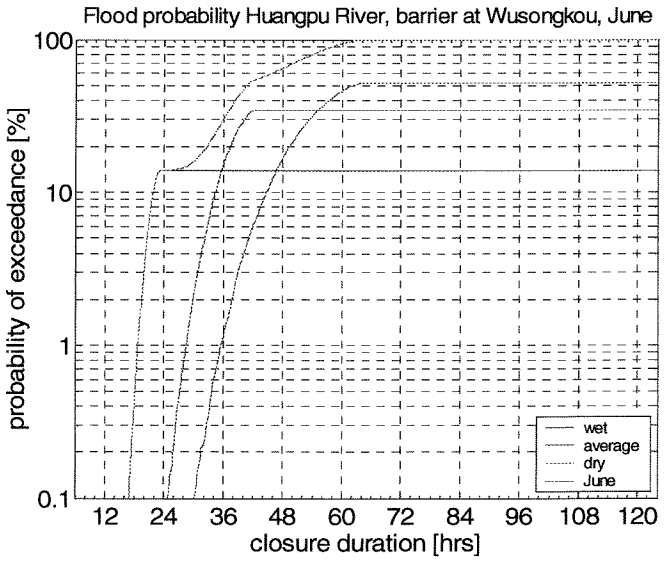

Figure 5-7: Sum of the factorized discrete flood probabilities for each hydrological year for a corresponding month results in the flood probability for the month

The flood probability given the month only is computed for each month in the typhoon season. The results for 1 rain day for the critical months July and August per barrier location are shown in the figures below. The figures for the remaining months and the flood probabilities for a 3 days rainfall are enclosed in appendix H to M

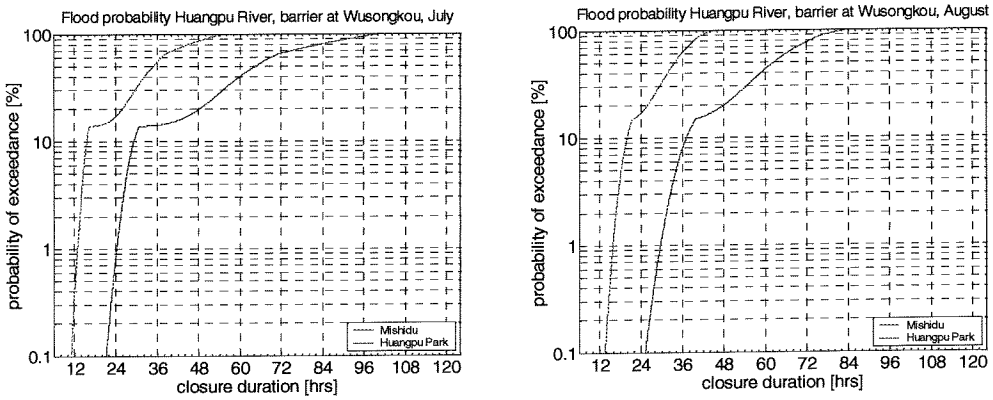

Figure 5-8: Flood probability of the Huangpu River given the critical months July and August for 1 rain day of torrential rainfall with barrier at Wusongkou

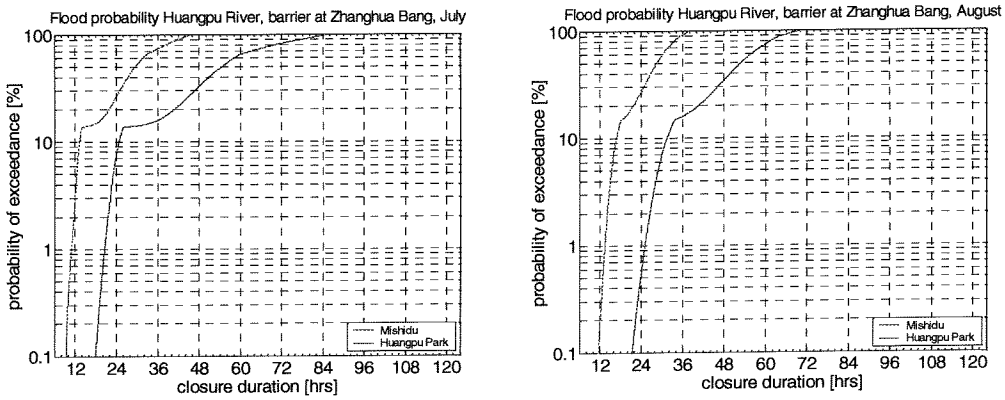

Figure 5-9: Flood probability of the Huangpu River given the critical months July and August for 1 rain day of torrential rainfall with barrier at Zhanghua Bang

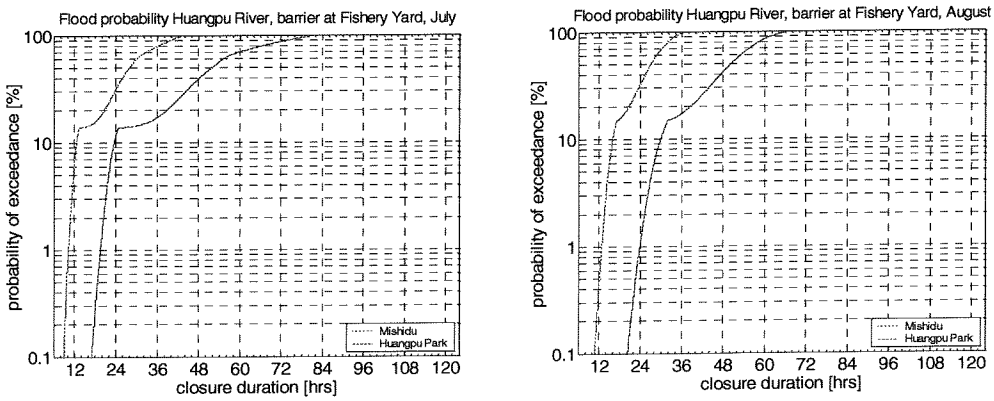

Figure 5-10: Flood probability of the Huangpu River given the critical months July and August for 1 rain day of torrential rainfall with barrier at Fishery Yard

The effects of the discrete probabilities used are clearly visible in the figures above. Because of the higher torrential rainfall probabilities required to cause flooding of the river, the effects of the discrete discharges are even stronger for the flood probability with 3 days of torrential rainfall. As a consequence, the flood probabilities shown are therefore only indicative.

The monthly maximum closure duration for each month equals the corresponding closure duration in a dry year. This is a straight forward consequence of the superposition of the factorized monthly flood probabilities given the hydrological year.

For comparison, we summarize the flood probabilities for the representative 24 hours closure duration per barrier location per month for 1 rain day in the tables 5-2 to 5-4. The flood probability during a 24 hours closure is highest at Mishidu in August and at Huangpu Park in July. The flood probability at Mishidu is higher as a result of the difference in warning water level with Huangpu Park. The flood probability at Huangpu Park is highest when the barrier is set at Zhanghua Bang and Fishery Yard.

	June	July	August	September	October
Mishidu P(Z<0) [%]	16	17	17.2	11	3
Huangpu Park P(Z<0) [%]	0.02	0.8	0.04	0.01	$>1{\cdot}10^{-4}$

Table 5-7: Monthly flood probabilities given barrier closure for a 24 hours closure with barrier at Wusongkou for 1 day of torrential rainfall

	June	July	August	September	October
Mishidu P(Z<0) [%]	22	26	27	21	10
Huangpu Park P(Z<0) [%]	0.3	8	0.6	0.1	0.02

Table 5-8: Monthly flood probabilities given barrier closure for a 24 hours closure with barrier at Zhanghua Bang for 1 day of torrential rainfall

	June	July	August	September	October
Mishidu P(Z<0) [%]	26	31	33	24	15
Huangpu Park P(Z<0) [%]	0.7	12	1	0.2	0.04

Table 5-9: Monthly flood probabilities given barrier closure for a 24 hours closure with barrier at Fishery Yard for 1 day of torrential rainfall

In the next section we incorporate the monthly variation in barrier closure frequency into the flood probability of the Huangpu River.

5.4 Flood frequency

5.4.1 Introduction

In subsection 4.2.5 we discovered that the probability of exceedance of the assumed barrier closure water level is underestimated in comparison with the actual data. It appears that this water level, which equals the present warning water level at Wusongkou, is annually exceeded 4.15 times. With random combination of tide and surge levels a probability of exceedance of 16% annually is found instead. As the aim of this section is to investigate the overall flood probability of the Huangpu River during barrier closure in the typhoon season, it is consequently not realistic to use the probability of exceedance found for this purpose.

Therefore, we carry on the analysis using the given frequency of exceedance of the warning water level at Wusongkou. Nevertheless, we assume that the mean surge level given this barrier closure level used in the analysis of the conditional torrential rainfall is representative. The results obtained in this section will be in terms of flood frequency instead of flood probability which is a consequence of using closure frequency instead of closure probability.

5.4.2 Flood frequency per month

The aim of this section is to analyse the flood frequency of the Huangpu River during barrier closure for a given month in the typhoon season. The first step in the analysis is to compute the distribution of the given frequency of exceedance of the presumed closure water level over the months in the typhoon season.

The present warning water level of 4.80m WD at Wusongkou is assumed to be the future barrier closure water level. From Shanghai Water Authority (2000) it seems that in the past 20 years, the frequency of exceedance of this water level is 4.15 times. Moreover, it appears that this water level is only exceeded during the typhoon season, which is logical since tropical cyclones are the only cause for storm tides in the Huangpu River. The frequency of exceedance is defined as the annual frequency of exceedance of a certain threshold. Hence, the distribution of the exceedance frequency can be found with the monthly probability of occurrence of tropical cyclones in the typhoon season of Shanghai. Naturally, not every tropical cyclone in the Northwest Pacific will cause barrier closure; this is however already taken into account in the frequency of exceedance of the warning water level. The probability of occurrence of tropical cyclones in the region is previously treated in section 2.3. We present in the next table the normalized probabilities of occurrence of tropical cyclones in the typhoon season of Shanghai.

	June	July	August	September	October
P [%]	8	20	28	25	9

Table 5-10: Normalized probability of occurrence of tropical cyclones in the typhoon season of Shanghai

When we combine the monthly distribution of tropical cyclones in the region with the barrier closure frequency we obtain the monthly distribution of the barrier closure frequency. The results are shown in the table below. As expected, the barrier closure frequency is highest in August during the peak of the typhoon season.

Month	June	July	August	September	October
Frequency [-]	0.33	0.83	1.16	1.04	0.79

Table 5-11: Monthly barrier closure frequency distribution in the typhoon season

With use of expression (5.9) for the flood probability for a given month, we derive the monthly frequency of exceedance of the storage capacity during barrier closure in the Huangpu River as

$$f_{month}(Z<0) = f_{closure} P(Z<0 \mid month) \tag{5.7}$$

Figure 5-11 to 5-13 presents the flood frequency of the Huangpu River during barrier closure for the critical months July and August per barrier location for 1 rain day of torrential rainfall. The figures for the remaining months and the flood frequencies for a 3 day torrential rainfall are enclosed in appendix N to S

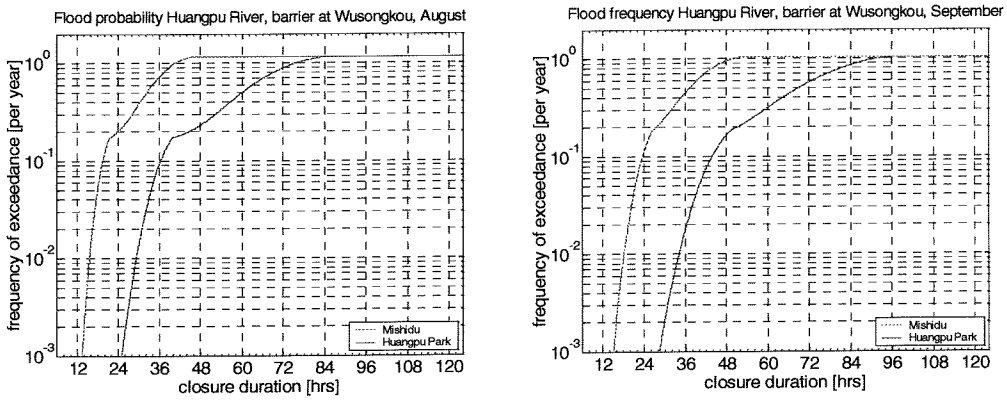

Figure 5-11: Flood frequency of exceedance of the Huangpu River during barrier closure with a barrier at Wusongkou.

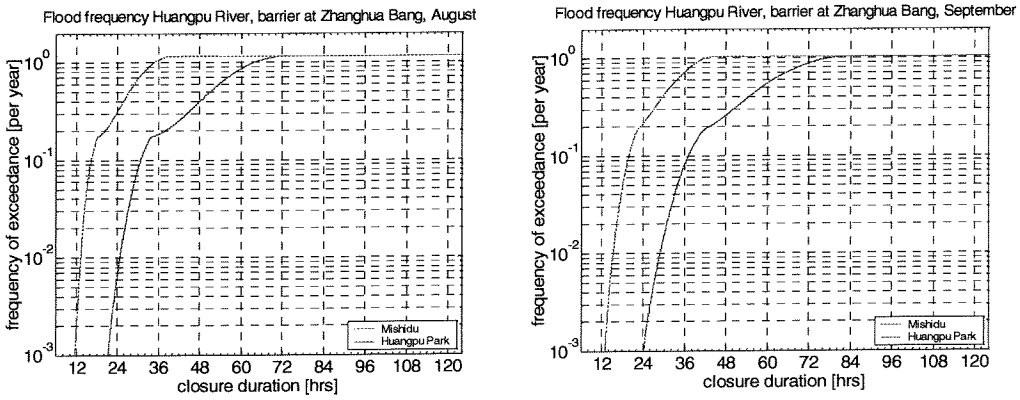

Figure 5-12: Flood frequency of exceedance of the Huangpu River during barrier closure with a barrier at Zhanghua Bang.

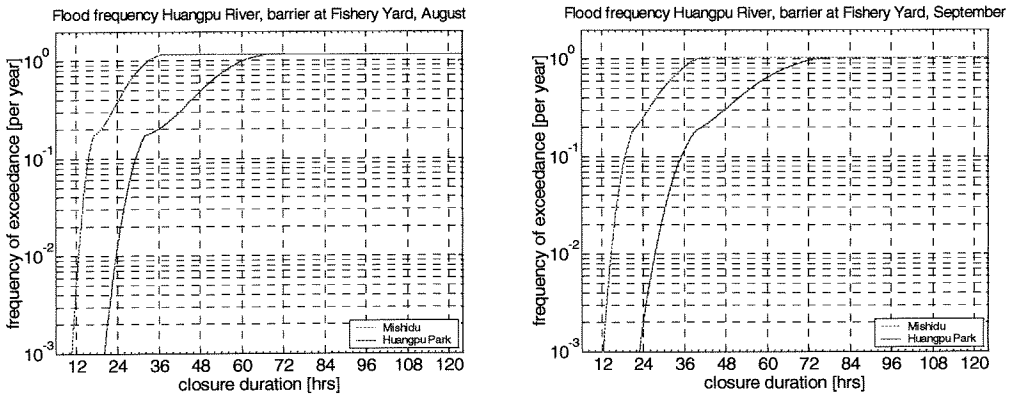

Figure 5-13: Flood frequency of exceedance of the Huangpu River during barrier closure with a barrier at Fishery Yard.

Again we compare the performance of each of the barrier locations with the representative closure duration of 24 hours. From the results, summarized in the tables below, we see that the flood frequency during barrier closure for both Mishidu and Huangpu Park is highest in the month July. Particularly, when the barrier is set at Fishery Yard, the flood frequency is alarming with a return period of 4 and 10 years respectively. The flood frequency for Mishidu is relative high for all barrier locations for all months in the typhoon season, whereas the flood frequency for Huangpu Park varies much more. This is the result of the higher warning water level at Huangpu Park. We assumed that flooding occurs when the warning water level in the river is exceeded.

The computed flood frequencies show that for a 24 hours closure with regard to the allowed flood frequency of the downtown area of Shanghai City, flooding of the Huangpu River during barrier closure is a real threat. The barrier location, off course, has a large influence in this. When the barrier is located at Wusongkou, the flood frequency is lower but in July it is still 1:7 and 1:143 years for Mishidu and Huangpu Park respectively.

Month		June	July	August	September	October
Mishidu	f(Z<0) [years]	19	7	5	9	48
Huangpu Park	f(Z<0) [years]	>1000	143	>1000	>1000	>1000

Table 5-12: Monthly flood frequencies during a 24 hours closure with barrier at Wusongkou for 1 day of torrential rainfall

Month		June	July	August	September	October
Mishidu	f(Z<0) [years]	14	5	3	4.5	12
Huangpu Park	f(Z<0) [years]	909	16	154	>1000	>1000

Table 5-13: Monthly flood frequencies during a 24 hours closure with barrier at Zhanghua Bang for 1 day of torrential rainfall

Month		June	July	August	September	October
Mishidu	f(Z<0) [years]	11	4	3	4	8
Huangpu Park	f(Z<0) [years]	500	10	77	500	>1000

Table 5-14: Monthly flood frequencies during a 24 hours closure with barrier at Fishery Yard for 1 day of torrential rainfall

5.4.3 Flood frequency in the typhoon season

Finally, we compute the overall flood frequency of the Huangpu River during barrier closure for each barrier location with reference to Mishidu and Huangpu Park. The flood frequency in the typhoon season during barrier closure is simply the sum of the monthly flood frequencies, which can be expressed as

$$f(Z<0) = \sum_{month}^{5} f_{month}(Z<0) \tag{5.8}$$

The results are shown in the figures below. The flood frequencies as a result of 3 days torrential rainfall are enclosed in appendix T. The effects of the discrete base discharges are still clearly visible in the frequency curves in figure. Again, it should be noted that the results are indicative as a result of the limited data used. The flood frequencies for the representative 24 hours barrier closure for each barrier location for a 1 day torrential rainfall are summarized in the table below.

		Wusongkou	Zhanghua Bang	Fishery Yard
Mishidu	f(Z<0) [years]	1.88	1.14	0.93
Huangpu Park	f(Z<0) [years]	135	14.30	7.70

Table 5-15: Flood frequency of the Huangpu River during a 24 hours closure for the three barrier locations with 1 day of torrential rainfall

The return periods of the flood frequency for all barrier locations for both Mishidu and Huangpu Park are significant. A low return period indicates a high frequency of exceedance. Remind that this does not mean that the threshold will be exceeded every year. As expected, the most upstream barrier location at Fishery has the highest flood frequency. However, even with a barrier at Wusongkou, the flood frequency is higher than 1:1000 years set for Shanghai City. To meet this return period, the barrier may not close for longer than 8 hours and 16 hours with regard to the warning water levels at Mishidu and Huangpu Park respectively.

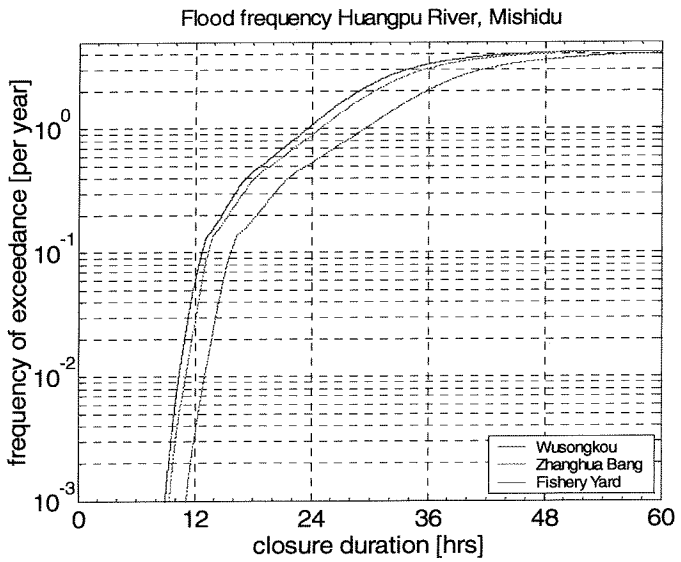

Figure 5-14: Flood frequency of the Huangpu River during barrier closure with reference to Mishidu with a warning water level of 3.50 m WD for the three barrier locations with 1 day of torrential rainfall

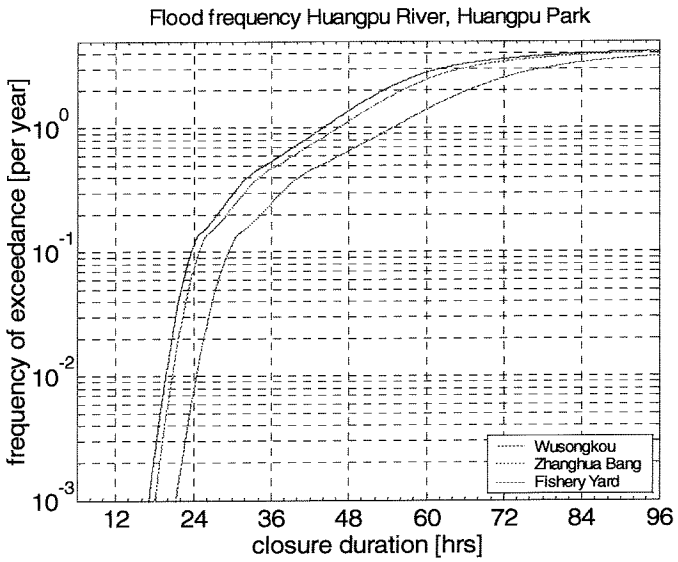

Figure 5-15: Flood frequency of the Huangpu River with reference to Huangpu Park during barrier closure with a warning water level of 4.55 m WD for the three barrier locations with 1 day of torrential rainfall

To prevent flooding of the Huangpu River during barrier closure the upstream discharge volume has to be either reduced or released. The first measure can be implemented simply with the existing control gate at the Taipu River. During barrier closure, the Huangpu River can be relieved from the stored water volume when hatches are facilitated in the barrier doors. During low tide, the river can discharge the stored water volume into the Yangtze River estuary through the hatches. The barrier itself remains closed, ready to protect Shanghai City against the next storm.

5.5 Conclusions

In this chapter, the flood probability of the Huangpu River is investigated. First we investigated the *flood probability* given barrier closure and month in the typhoon season and the type of hydrological year. This is done because of the format of the base discharge records available. Subsequently, we compute the flood probability given barrier closure and month only, taken into account the probability of the type of hydrological year. Subsequently, with these results we computed the *flood frequency* of the Huangpu River during barrier closure with the historical frequency of exceedance of the barrier closure water level, which is the warning water level at Wusongkou. Flooding of the Huangpu River is assumed as soon as the warning water level in the river is exceeded with respect to the warning water levels at Mishidu and Huangpu Park.

The flood probability caused by 3 days of torrential rainfall is lower as a result of the uniform assumed rainfall intensity in time, the conclusion are therefore based on a 1 day torrential rainfall.

The main conclusions of this chapter are summarized as follows:

- Flooding of the Huangpu River during barrier closure is a real threat even though limited base discharge records and conservative torrential rainfall runoff configurations are used in this study. The design flood frequency of 1:1000 years for Shanghai City is exceeded for barrier closure durations over 8 and 16 hours at Mishidu and Huangpu Park respectively.

The flood frequency in the typhoon season during a representative closure of 24 hours at Mishidu ranges from 1:0.93 to 1:1.88 years, whereas the flood frequency at Huangpu Park ranges from 1:7.7 to 1:135 years for a barrier at Fishery Yard and Wusongkou respectively.

- When the barrier is closed and both month and hydrological year are known, we may conclude that for a representative 24 hours barrier closure flooding at Mishidu is a sure event from June to September for all barrier locations in a wet year. Except a barrier at Wusongkou in September which still has a significant flood probability of 66%. The flood probability at Huangpu Park in that case ranges from 6% annually with a barrier at Wusongkou to a significant 84% with a barrier at Fishery Yard.

- For a given month in the typhoon season, the flood probability of exceedance at Huangpu Park ranges form 0.8% with a barrier at Wusongkou to 12% with a barrier at Fishery Yard in August. In contrary, the flood probability at Mishidu in July ranges from 17.2% to 33% respectively in July.

- The flood frequency during barrier closure for both Mishidu and Huangpu Park is highest in the month July. Particularly, when the barrier is set at Fishery Yard, the flood frequency is alarming with a return period of 4 and 10 years respectively. The flood frequency for Mishidu is relative high for all barrier locations for all months in the typhoon season, whereas the flood frequency for Huangpu Park varies much more.

- The flood frequency as well as the flood probability is lowest when the barrier is set at Wusongkou and highest when the barrier is set at Fishery Yard. Moreover, the difference between the location Fishery Yard and Zhanghua Bang are small.

- Flooding of the Huangpu River during barrier closure can be prevented by either reducing the upstream discharge with the control gate at the Taipu River or facilitate the barrier doors with hatches so that discharge during low tide is possible without opening up of the barrier itself.

- Despite of the higher probability of occurrence of tropical cyclones in August, the flood probability for a given month and in turn the flood frequency is highest in the month July because of the higher discharge then.

- The maximum closure duration of the Huangpu River during barrier closure is determined by the maximum closure duration in a dry year.

6 Conclusions and recommendations

6.1 Conclusions

The flood probability of the Huangpu River during barrier closure is investigated in this study. Flooding of the Huangpu River during barrier closure is defined as the exceedance of the warning water level in the river. This assumption is made in view with the uncertainty of the eventual top elevation of the floodwalls along the entire course of the river. Two stations along the river are used as reference for the flood probability. The Huangpu Park station is the most important station in the river as it is located in the city centre. The warning water level at this location is higher than that of the second station more upstream of the river at Mishidu. The difference in the warning water level is caused by the tidal dominance on the water levels in the river. During closure, flooding or exceedance of the warning water level in the river will first occur at Mishidu and subsequently at Huangpu Park station. The flood probability is analysed in this order. The water level which by exceedance is considered as flooding of the river is an essential parameter in the flood probability of the Huangpu River.

The main conclusions can be summarized as follows:

- In view of the assumptions on the storage capacity of the Huangpu River, flooding of the Huangpu River during barrier closure is a real threat. The design flood frequency of 1:1000 years for Shanghai City is exceeded for barrier closure durations over 8 and 16 hours at Mishidu and Huangpu Park respectively. The flood frequency in the typhoon season during a representative closure of 24 hours at Mishidu ranges from 1:0.93 to 1:1.88 years, whereas the flood frequency at Huangpu Park ranges from 1:7.7 to 1:135 years for a barrier at Fishery Yard and Wusongkou respectively. Furthermore, for a given month in the typhoon season, the flood probability of exceedance at Huangpu Park ranges from 0.8% with a barrier at Wusongkou to 12% with a barrier at Fishery Yard in August. In contrary, the flood probability at Mishidu in July ranges from 17.2% to 33% respectively in July.

- The location of the storm surge barrier is of high importance to the flood probability of the Huangpu River during barrier closure. When the barrier is located at Fishery Yard, the flood probability is significant higher in comparison with a barrier set at Wusongkou and little higher than for a barrier set at Zhanghua Bang.

- The flood probability of the Huangpu River depends largely on the base discharge of the river. The base discharge determines the maximum closure duration of the storm surge barrier. Consequently, the flood probability is highest in the month July because of the higher base discharge despite of the higher probability of occurrence of tropical cyclones in the month August.

- The present floodwall alongside the Huangpu River is of great importance to flooding of the river during barrier closure. After barrier completion, this floodwall is the first line of defence against flooding of the river during barrier closure. Even more, when the ground level subsidence of the downtown area is persisted as a result of the economic development of Shanghai.

Furthermore, we conclude that the storm tide levels cannot be computed correctly with random combination tide and storm surge levels only. The storm tide levels with lower probabilities are underestimated. Probably, other effects during complex meteorological conditions of a tropical cyclone like wind field and swells cannot be neglected. Also, the Huangpu River can be modelled correctly with SOBEK-RIVER. However, for barrier closure simulations, the upstream connections of the river have to be modelled correctly with regard to the storage capacity of the river. Finally, we conclude that copulas are very useful for flood probability studies. Copulas are very useful for modelling dependence between variables, especially when data required for analyses are limited of size.

6.2 Recommendations

This study is carried out with limited and sometimes conflicting data. Although the assumptions in this study are made with great care, they might be not reflecting the real situation as a result. Consequently, the final results in terms of the flood probability analysis are influenced by these assumptions directly. From this study, it seems that flood probability of the Huangpu River is significant. This result is a strong indication that accurate data and precise knowledge on the study area is vital to analyse the exact flood probability because flooding of the Huangpu River concerns the loss of property and even human lives. The methodology developed in this study, including the concept of copulas, is suitable for further analysis of the flood probability and we suggest the following work to be carried out:

- The discharge of the Huangpu River needs to be studied as this is the most important variable in the flood probability of the river during barrier closure. Continuous data on the upstream discharge into the river during the passage of tropical cyclones is essential. This also means that the runoff characteristics of torrential rainfall in Tai Lake Basin into the Huangpu River need to be studied.

- With regard to the storage capacity of the Huangpu River, the upstream connections of the Huangpu River are of great importance to the flood probability. Namely, in the situation that one of the tributaries is connected with open water, flood probability of the river during barrier closure is not an issue anymore.

- The eventual dimension of the floodwalls along the Huangpu River should be taken into account in the study.

- The flood probability during barrier closure is largely dependent on the closure duration. Therefore, the probability distribution of the closure duration should be investigated. This can be done by analysis on the probability distribution of the storm lengths in Shanghai

- Flooding of the Huangpu River during barrier closure can be prevented by either reducing the upstream discharge with the control gate at the Taipu River or facilitate the barrier doors with hatches so that discharge during low tide is possible without opening up of the barrier itself.

- An initial water level of the Huangpu River right after barrier closure of 2.5m WD is used in this study. In reality the initial water level should be regarded as a stochastic variable. The enhanced SOBEK-RIVER model of the Huangpu River is ready for this purpose.

A Required torrential rainfall runoff

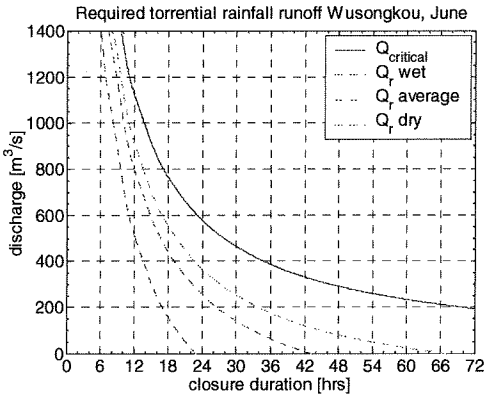

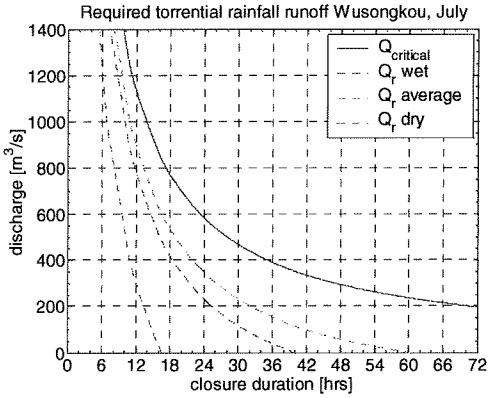

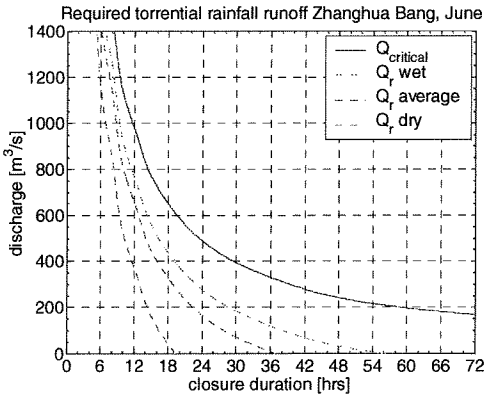

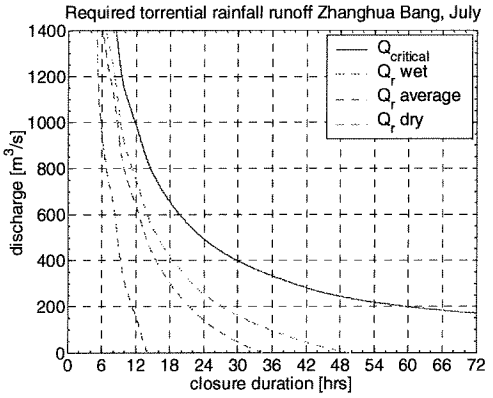

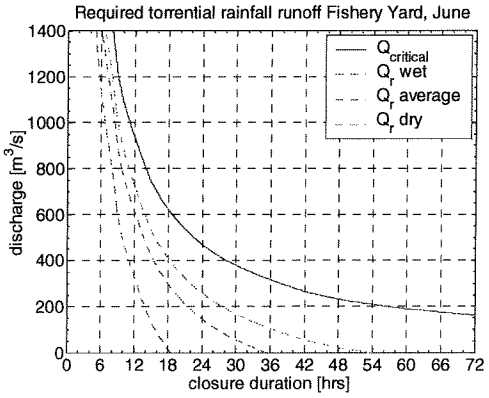

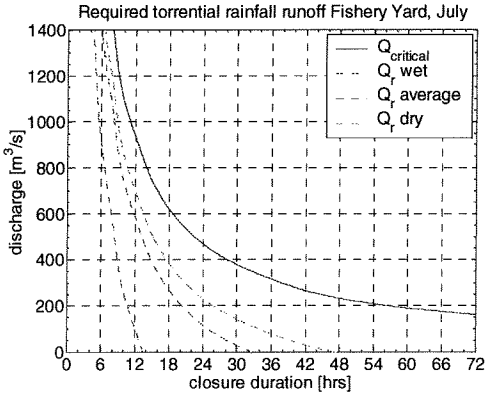

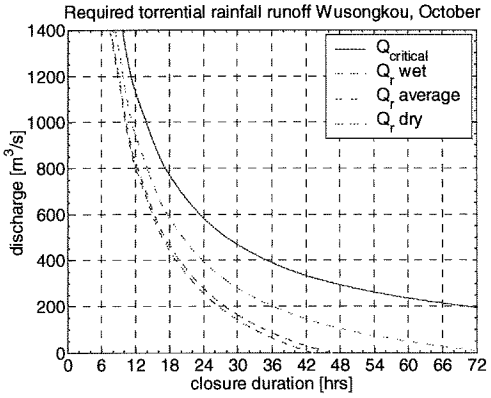
Required torrential rainfall runoff Wusongkou, October
discharge [m3/s]
closure duration [hrs]
Qcritical
Qr wet
Qr average
Qr dry

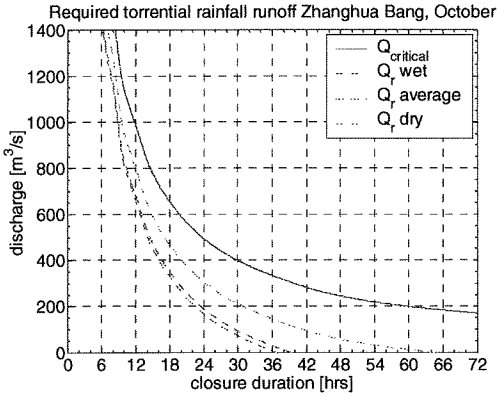
Required torrential rainfall runoff Zhanghua Bang, October
discharge [m3/s]
closure duration [hrs]
Qcritical
Qr wet
Qr average
Qr dry

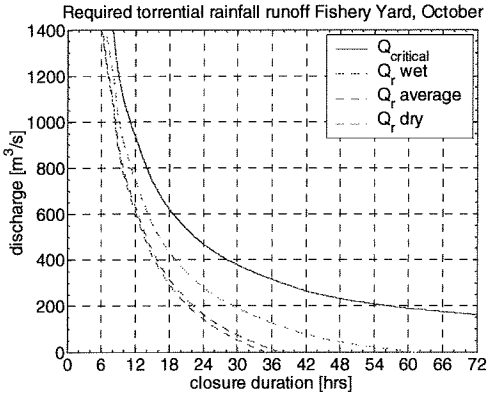
Required torrential rainfall runoff Fishery Yard, October
discharge [m3/s]
closure duration [hrs]
Qcritical
Qr wet
Qr average
Qr dry

B Flood probability given month and type year I rain day barrier at Wusongkou

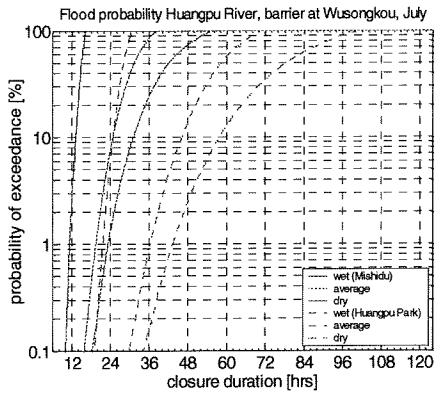

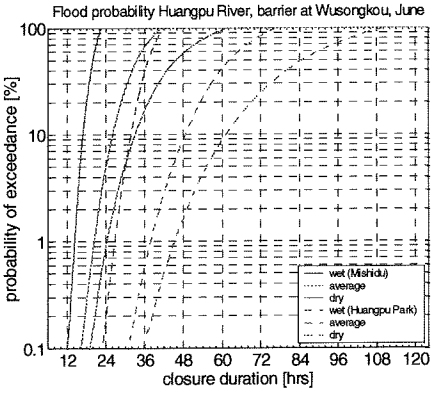

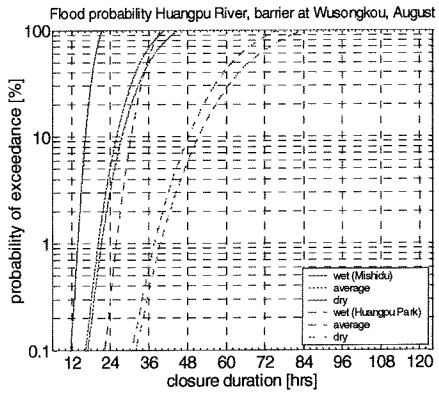

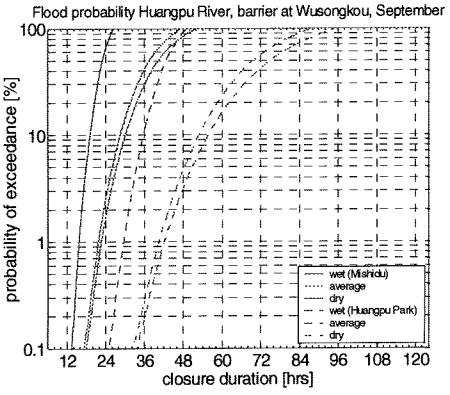

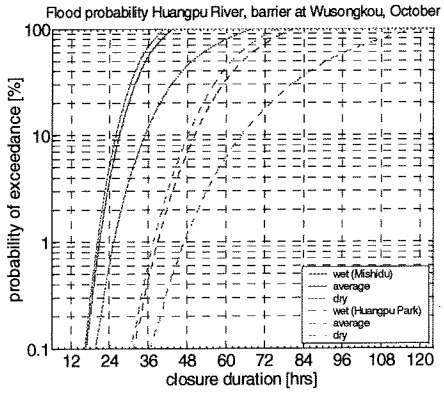

C Flood probability given month and type year I rain day barrier at Zhanghua Bang

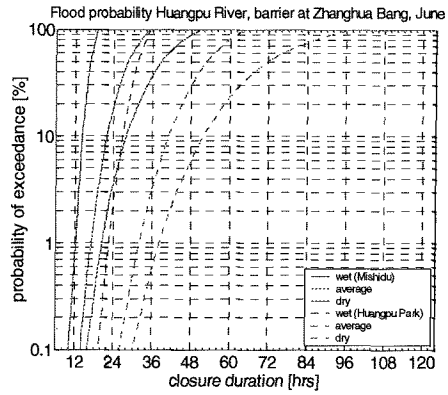

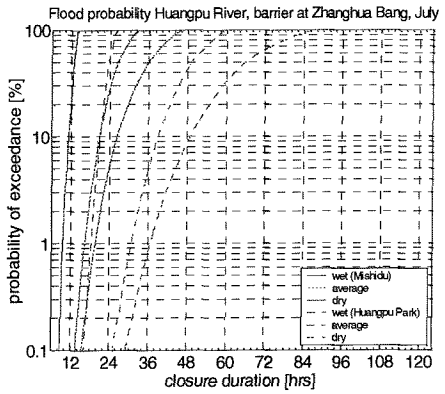

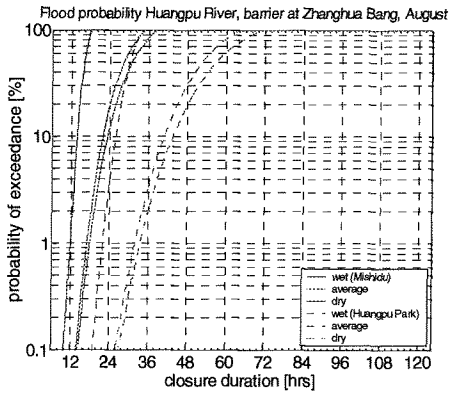

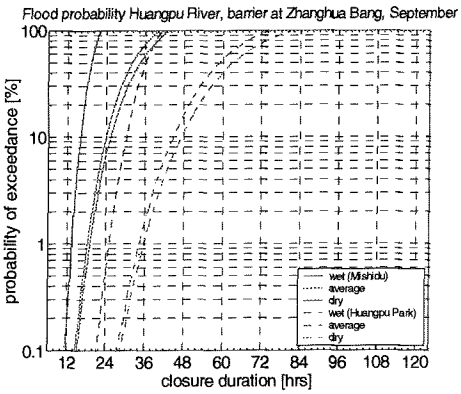

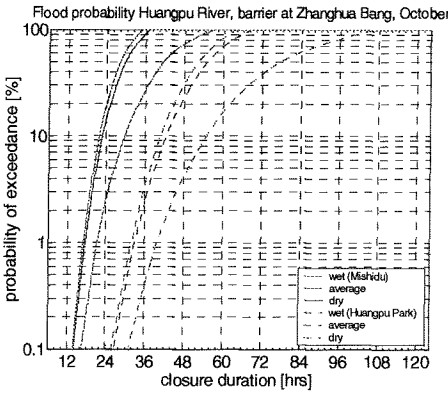

D Flood probability given month and type year I rain day barrier at Fishery Yard

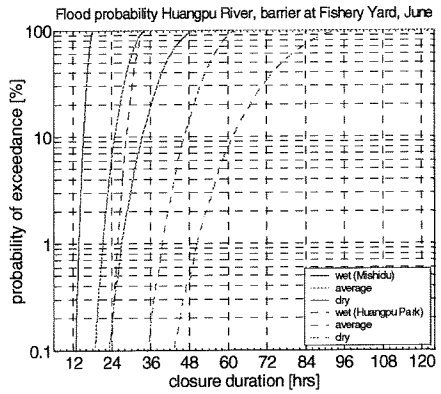

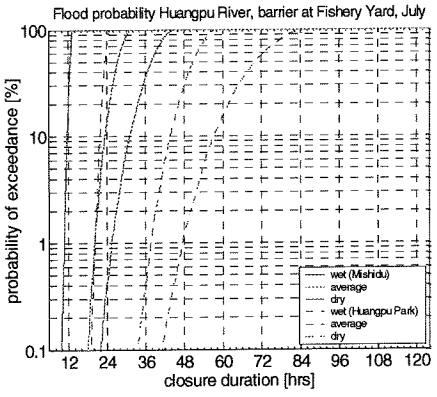

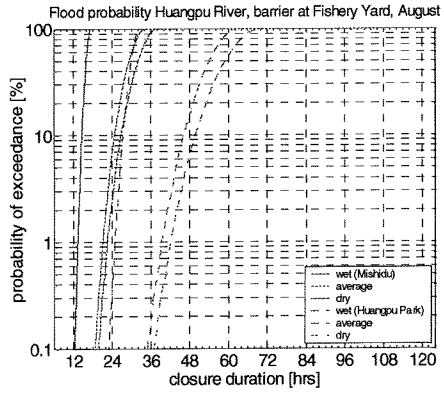

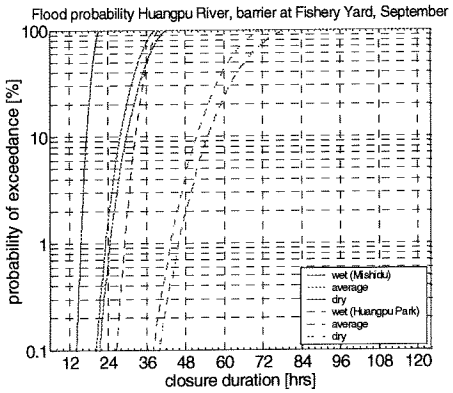

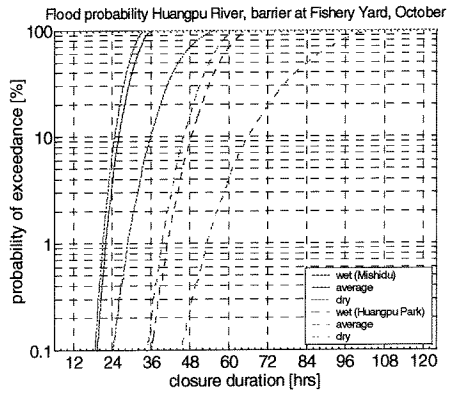

E Flood probability given month and type year 3 rain days barrier at Wusongkou

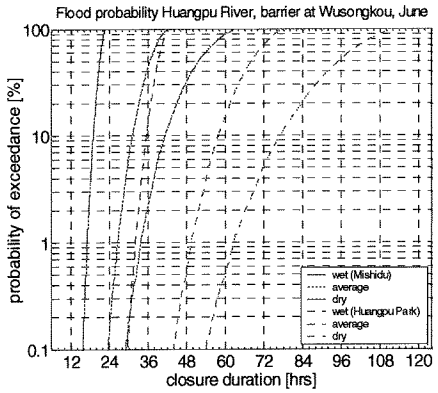

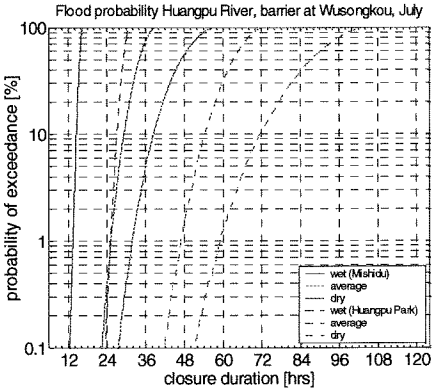

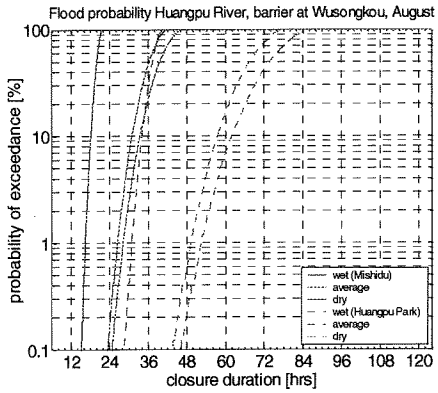

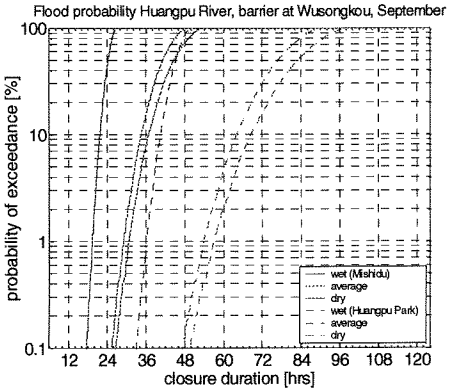

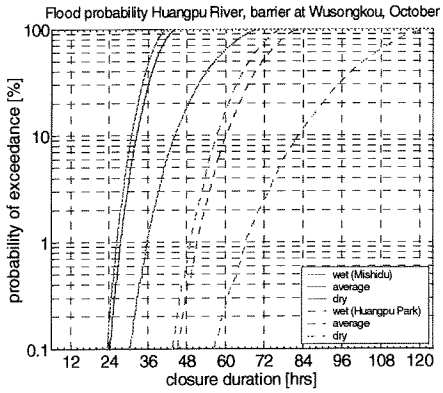

F Flood probability given month and type year 3 rain days barrier at Zhanghua Bang

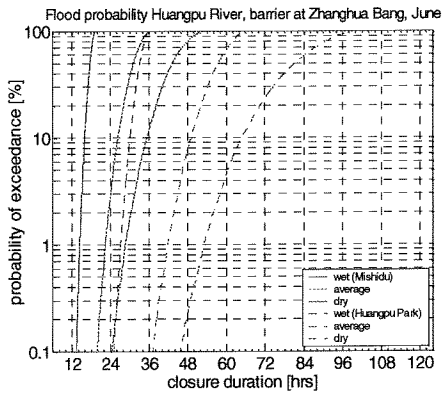

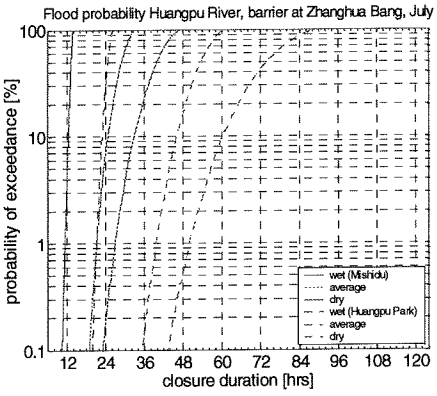

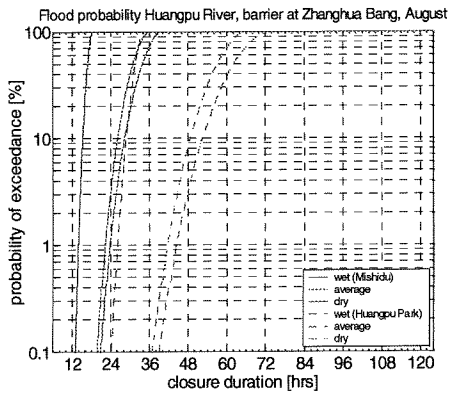

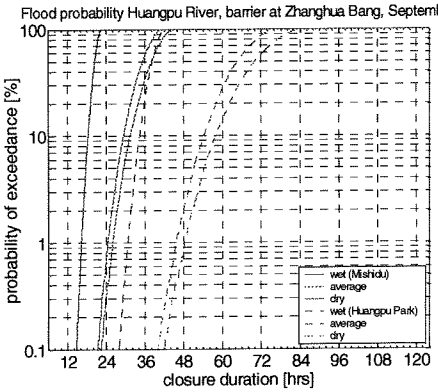

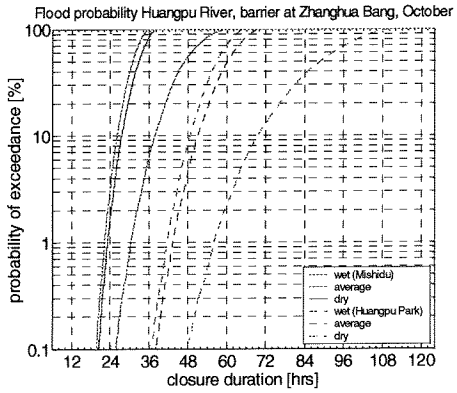

G Flood probability given month and type year 3 rain days barrier at Fishery Yard

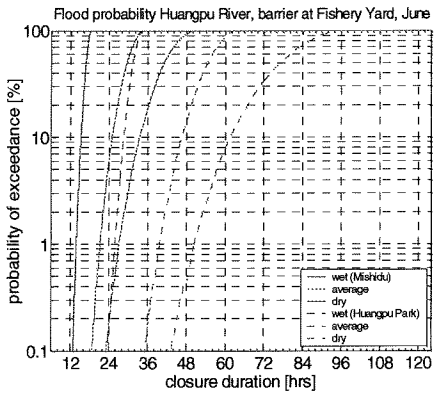

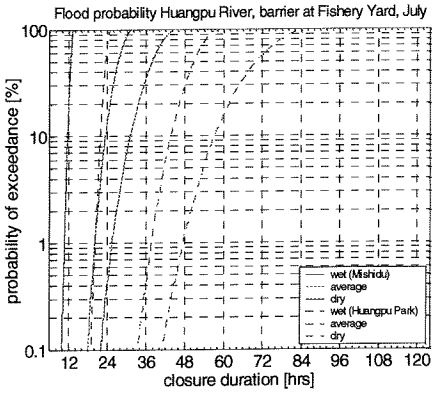

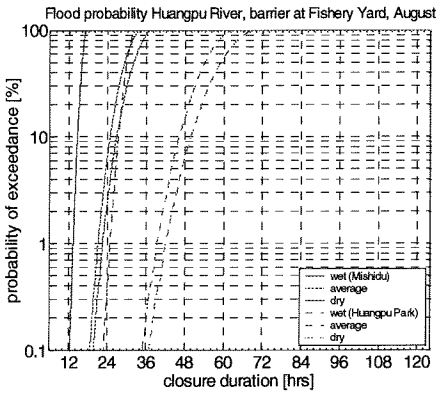

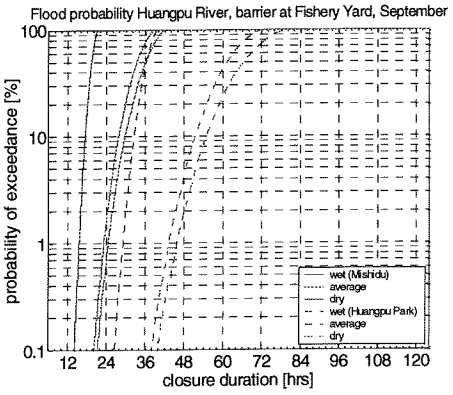

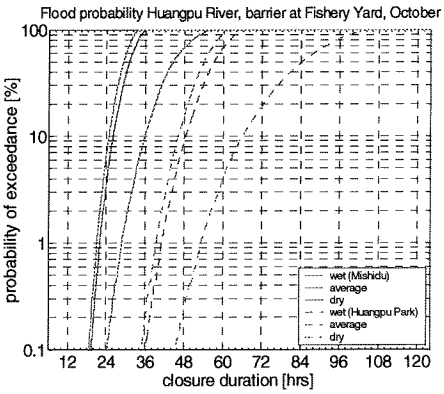

H Flood probability given month I rain day barrier at Wusongkou

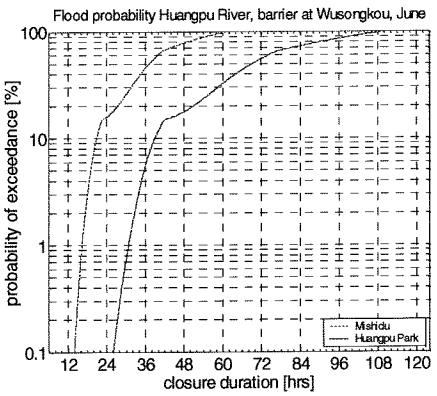

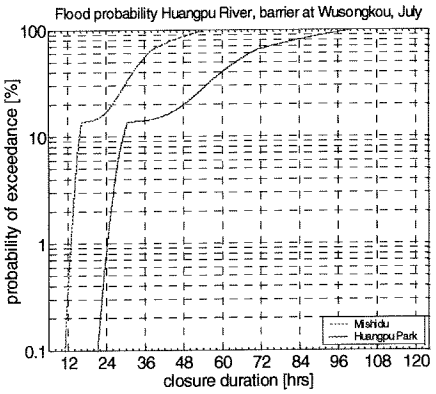

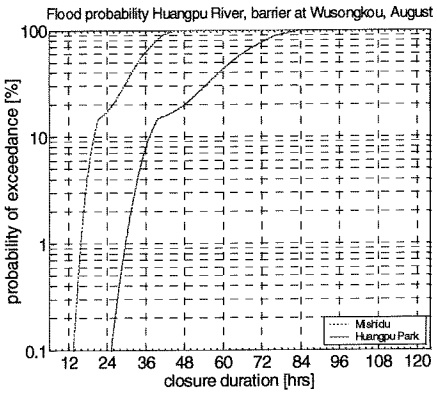

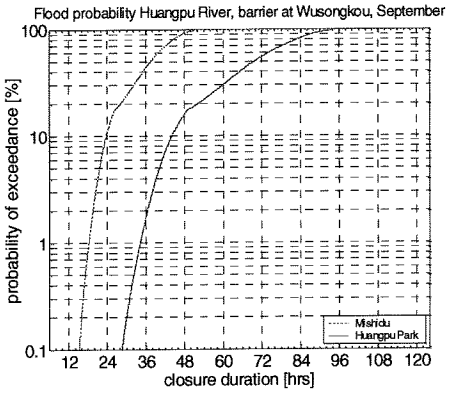

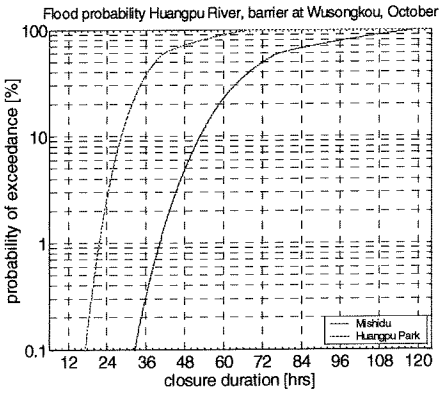

1 Flood probability given month 1 rain day barrier at Zhanghua Bang

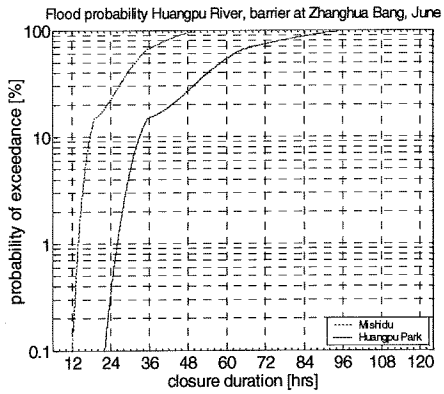

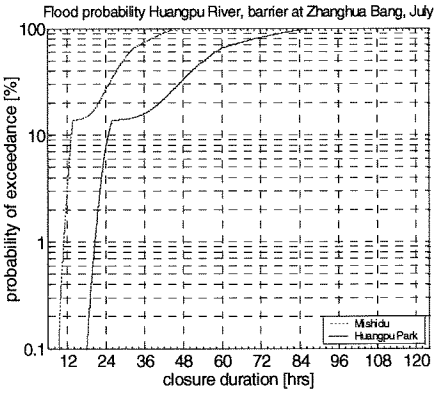

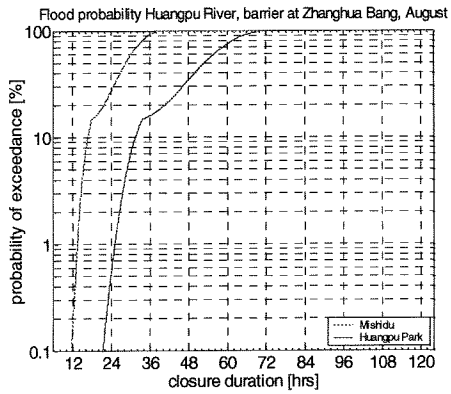

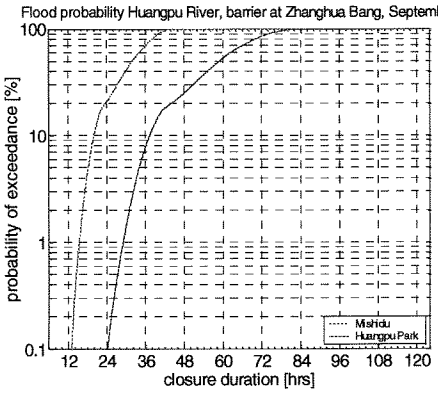

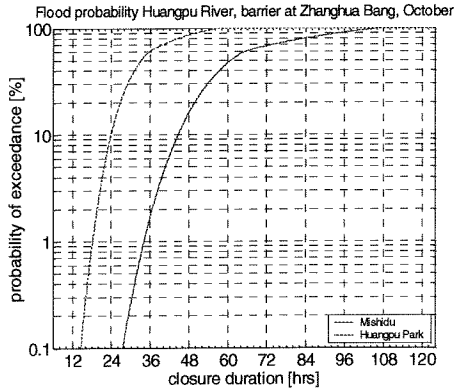

J Flood probability given month 1 rain day barrier at Fishery Yard

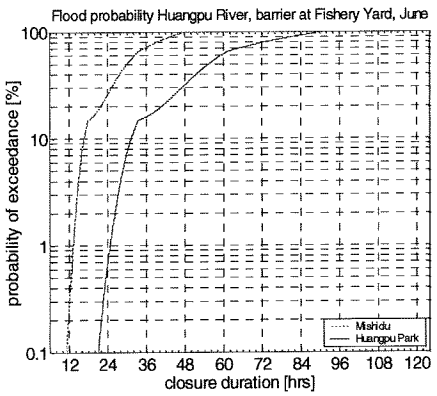

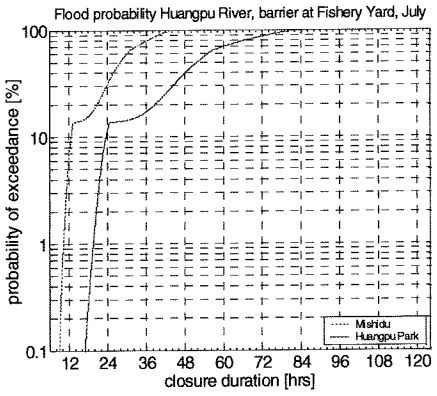

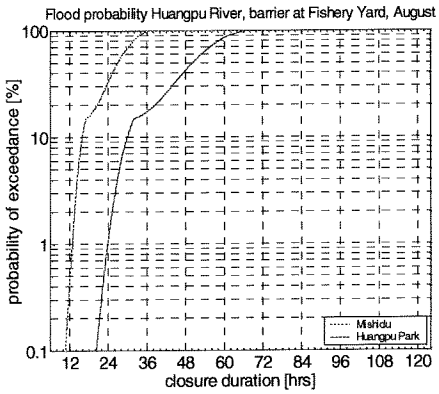

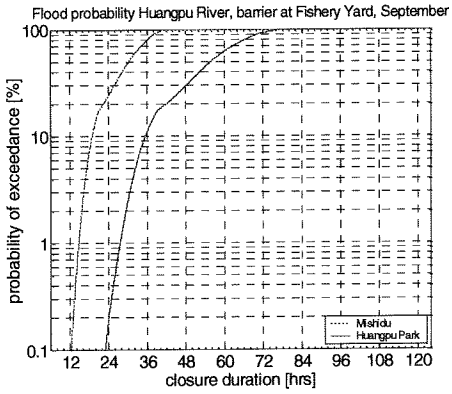

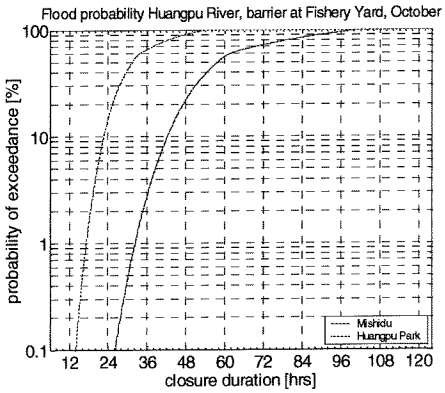

K Flood probability given month 3 rain days barrier at Wusongkou

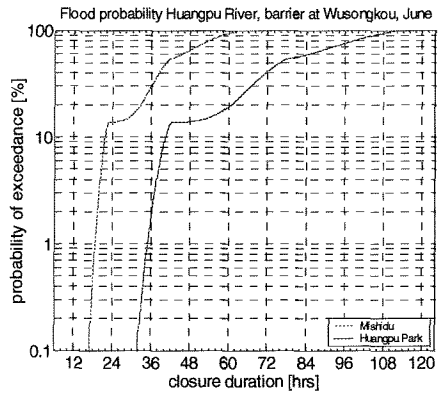

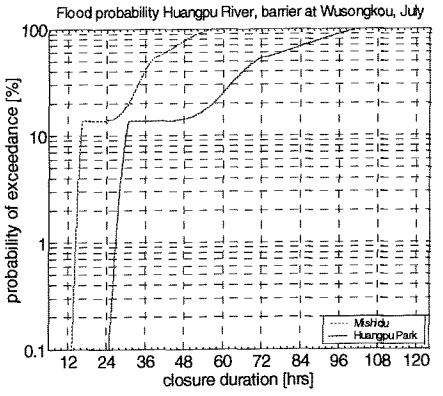

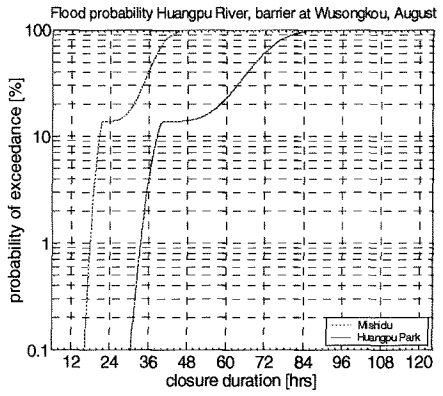

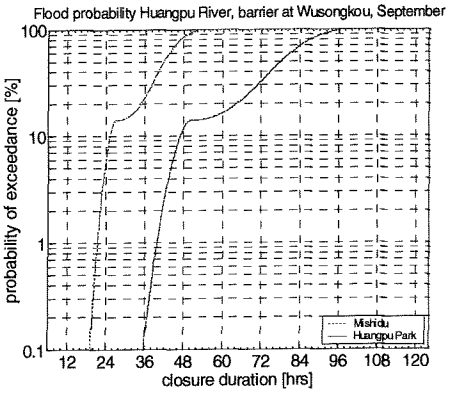

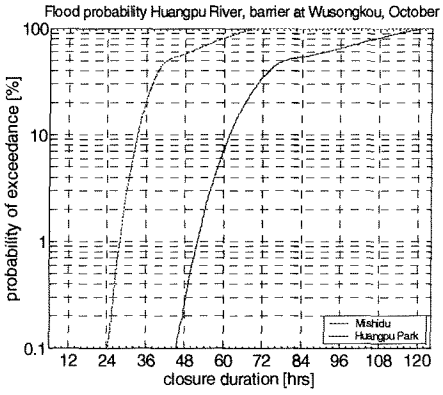

L Flood probability given month 3 rain days barrier at Zhanghua Bang

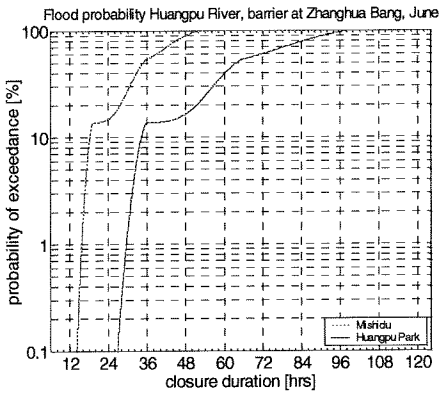

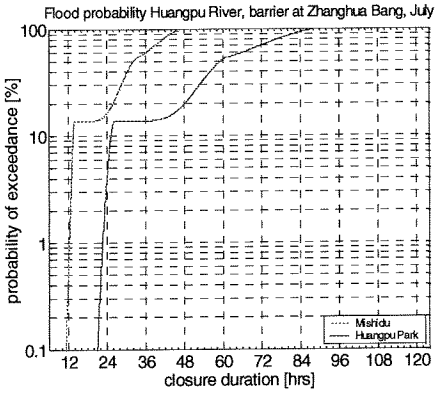

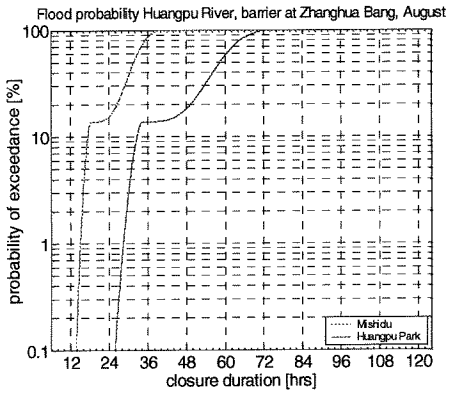

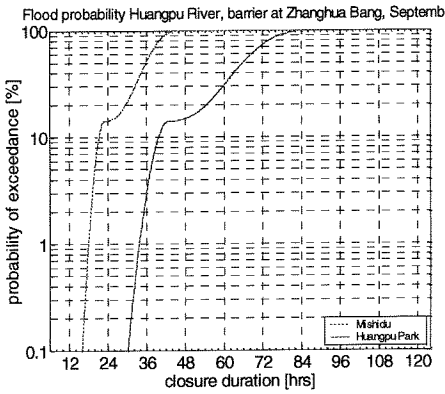

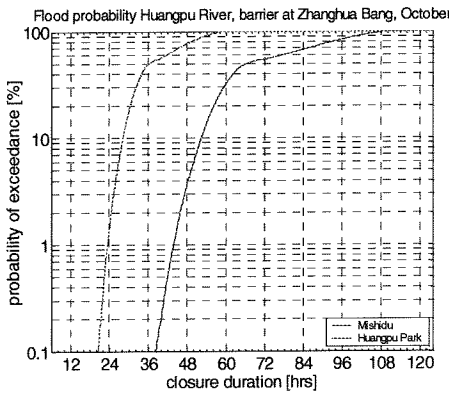

M Flood probability given month 3 rain days barrier at Fishery Yard

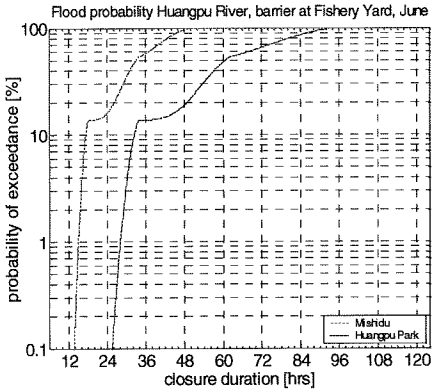

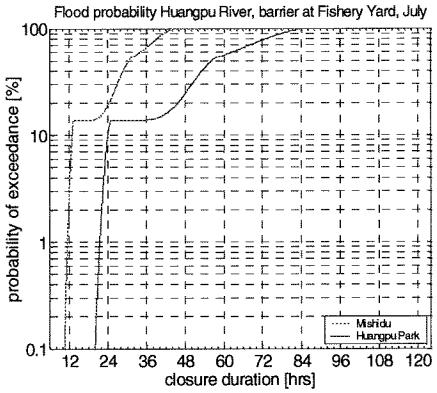

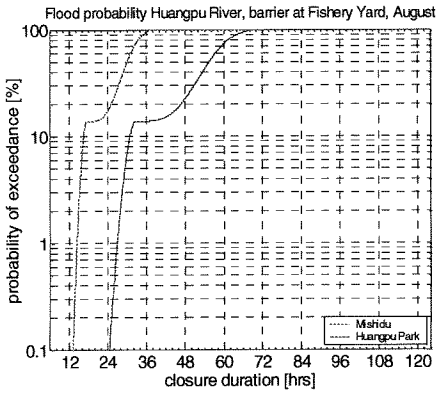

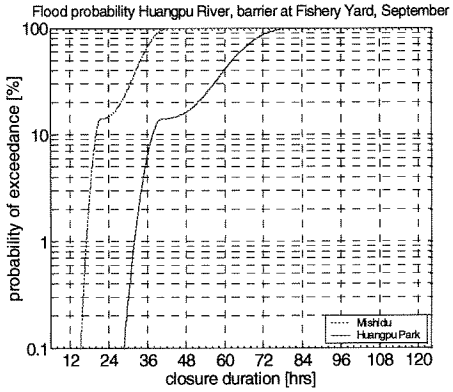

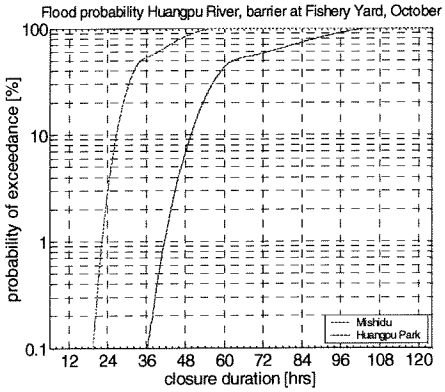

N Flood frequency given month I rain days barrier at Wusongkou

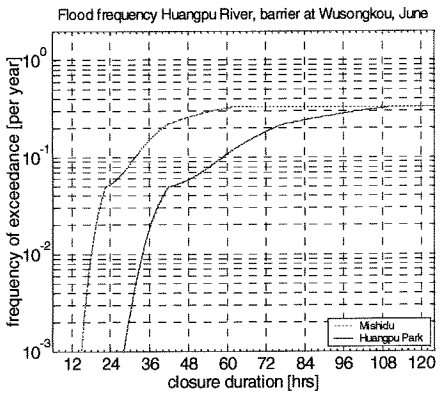

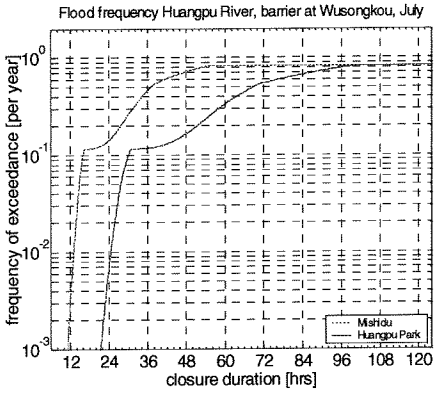

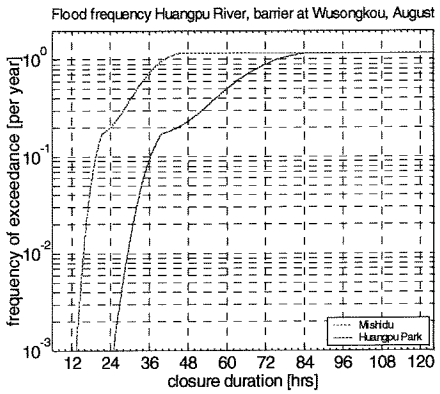

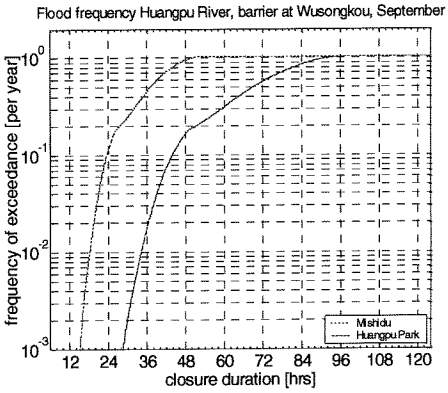

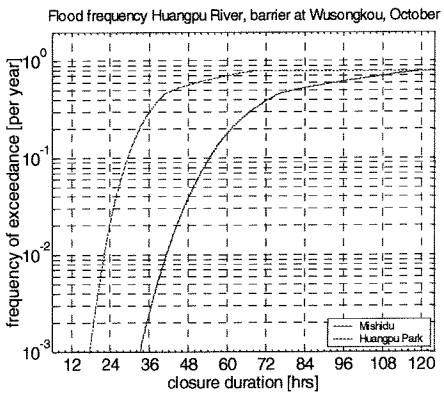

O Flood frequency given month I rain day barrier at Zhanghua Bang

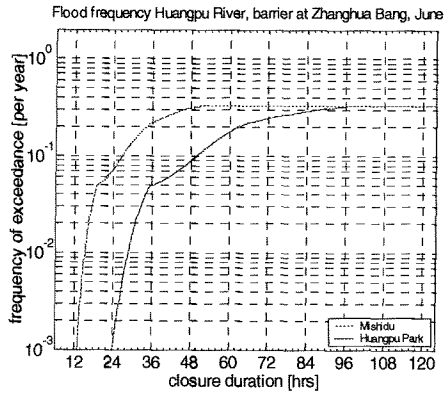

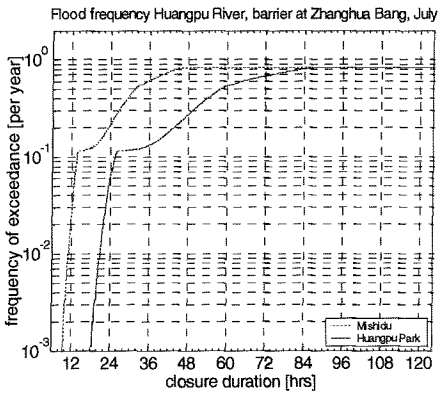

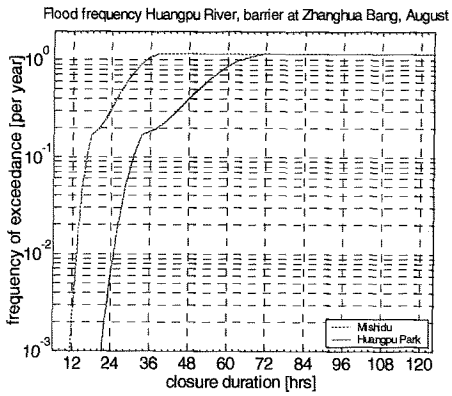

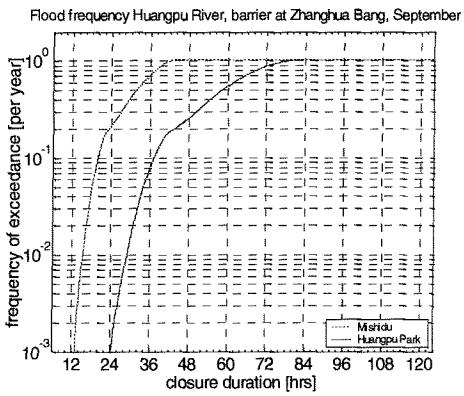

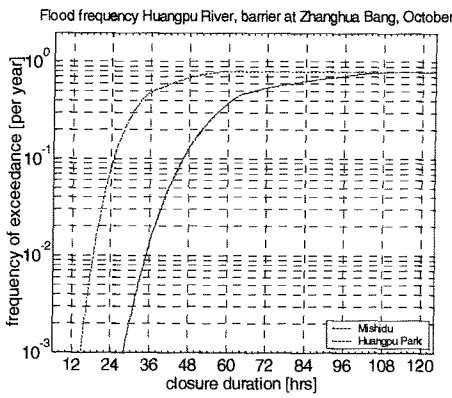

P Flood frequency given month 1 rain day barrier at Fishery Yard

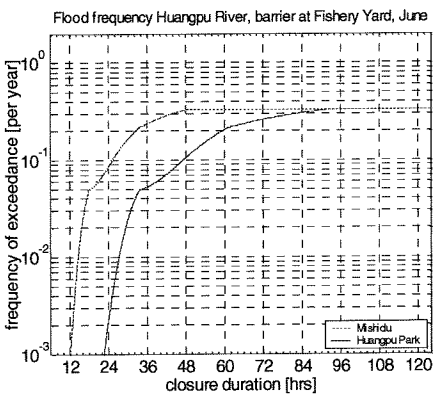

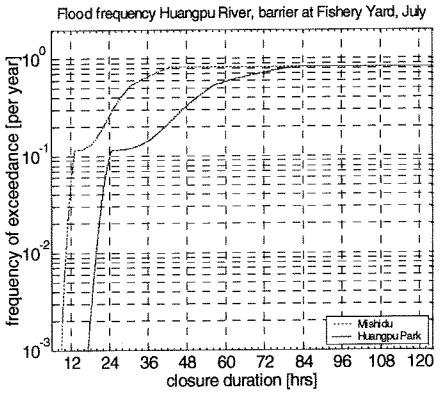

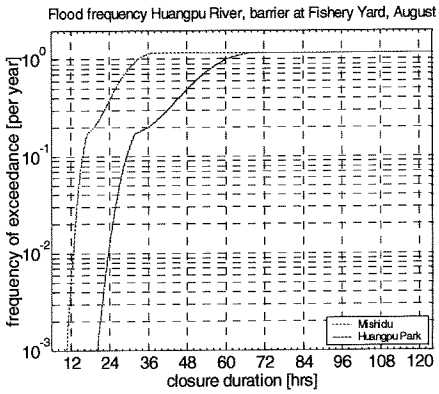

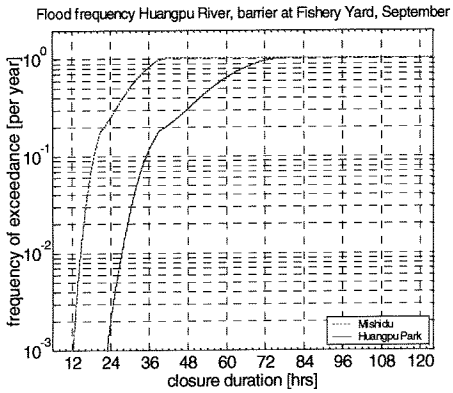

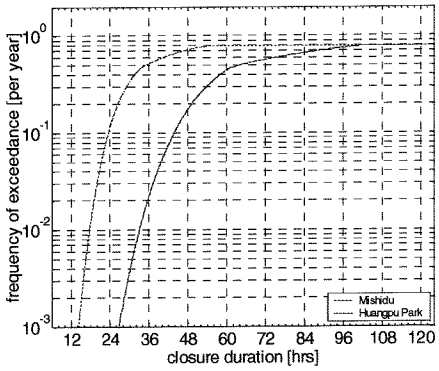

Q Flood frequency given month 3 rain days barrier at Wusongkou

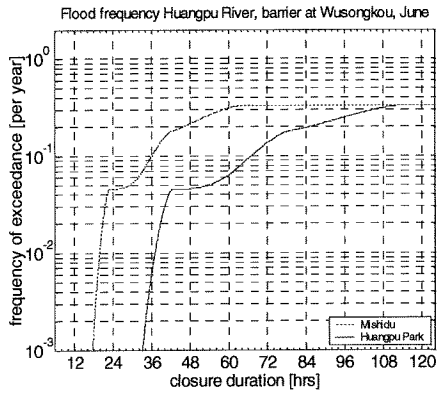

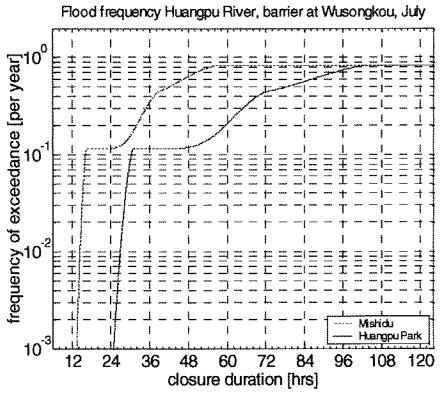

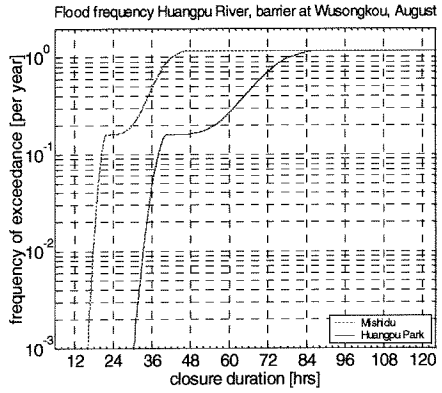

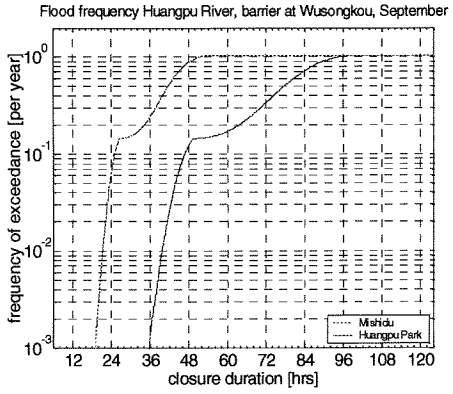

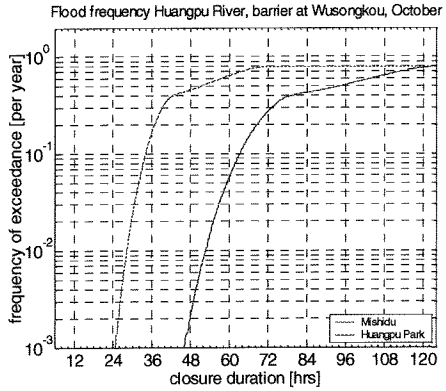

R Flood frequency given month 3 rain days barrier at Zhanghua Bang

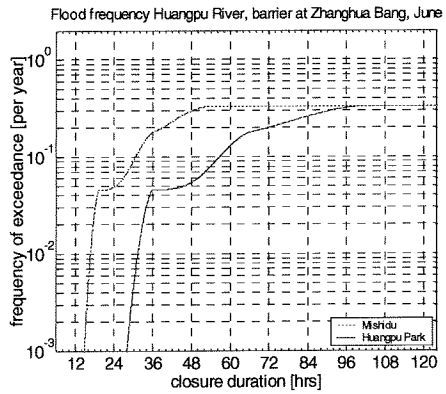

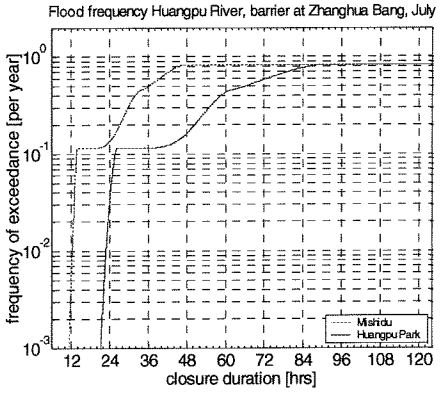

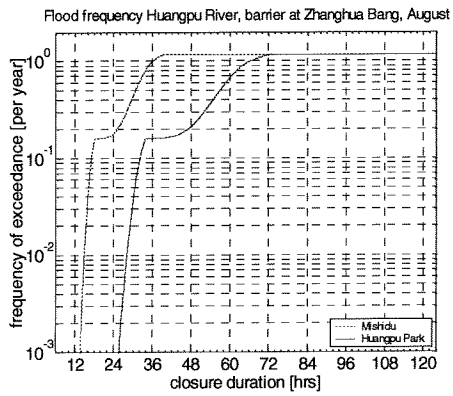

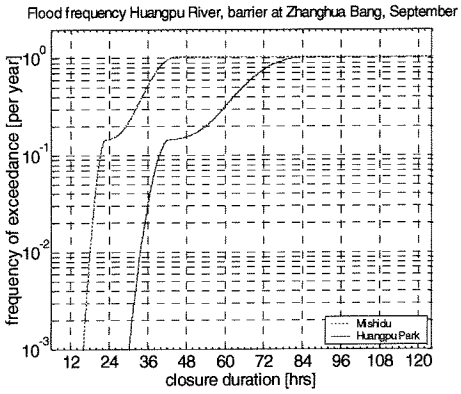

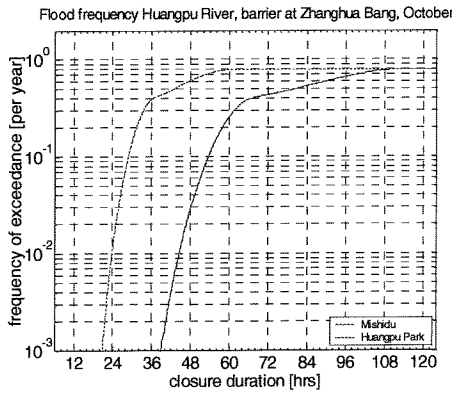

S Flood frequency given month 3 rain days barrier at Fishery Yard

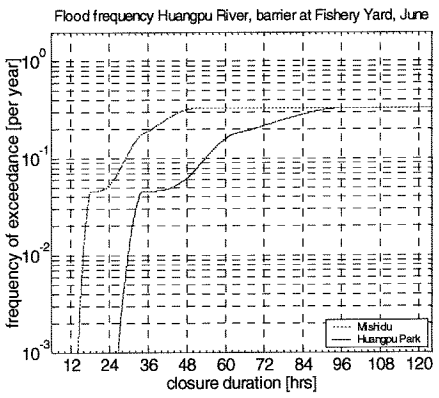

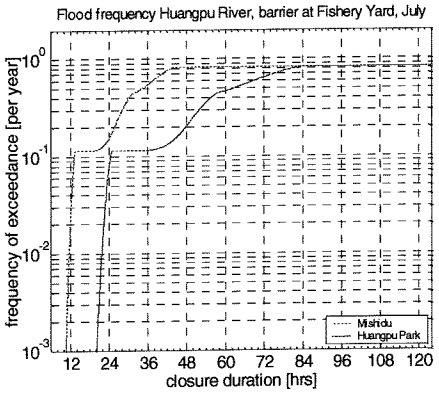

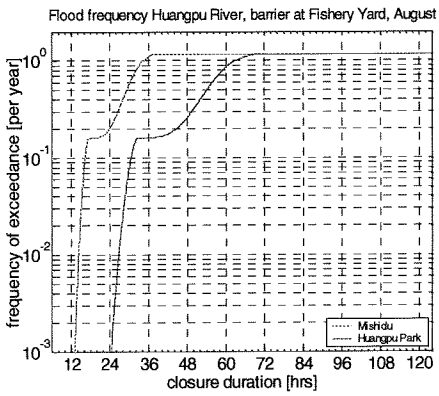

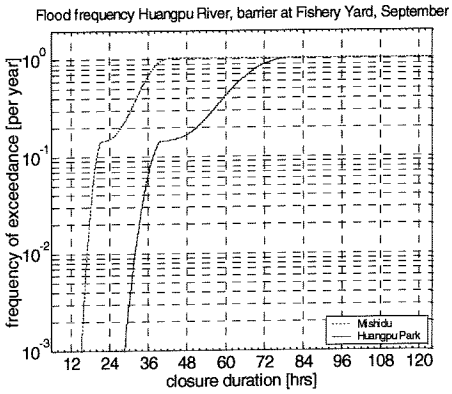

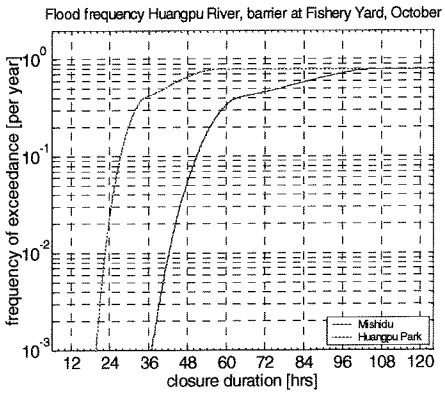

T Flood frequency in the typhoon season 1 and 3 rain days

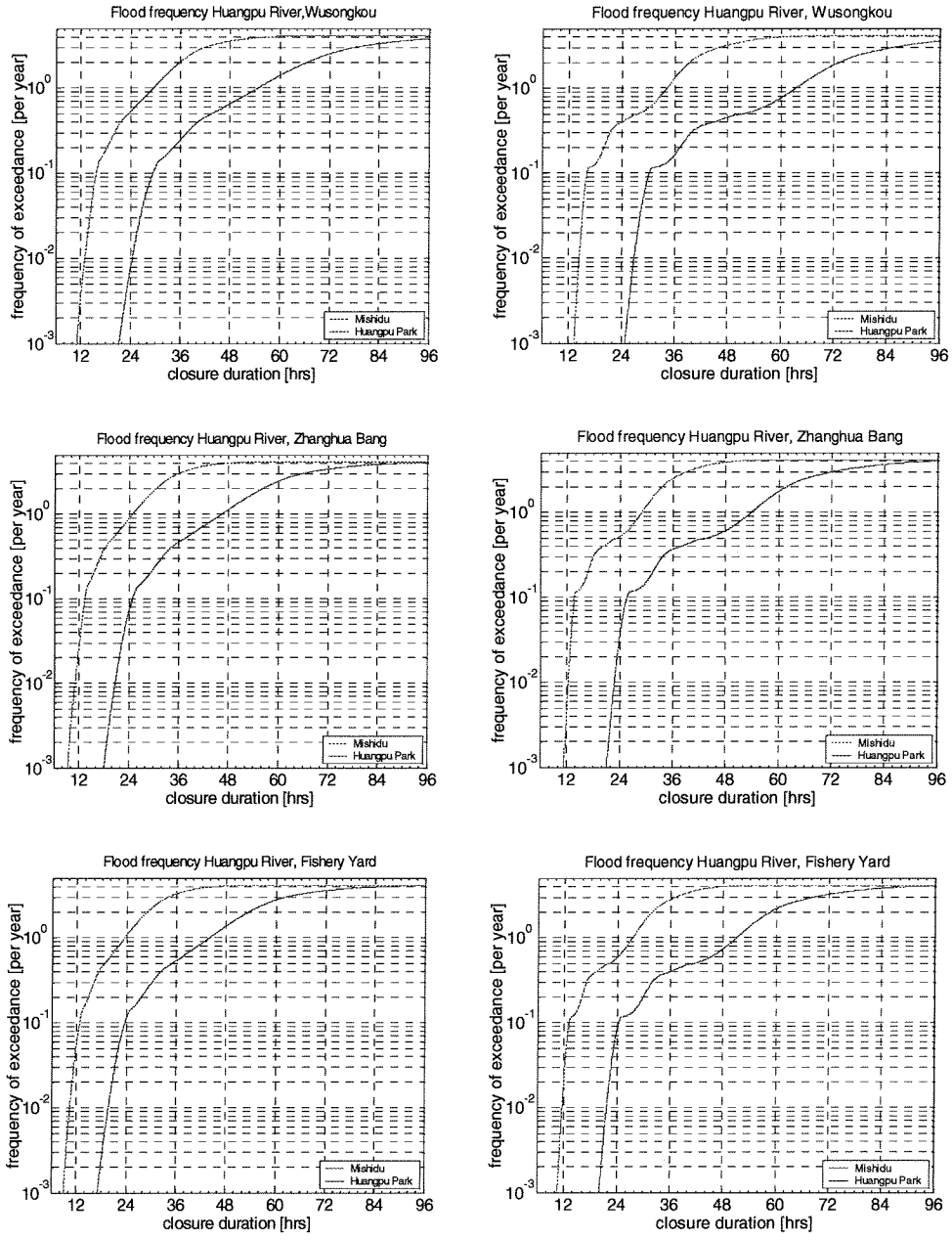

Figures in the left panel represent the flood frequency for 1 rain day, whereas the figures in the right panel represent the flood frequency for 3 rain days

U Constituents tidal prediction

Shanghai
\+ Wusongkou
\+ TIDAL PREDICTION

Mean water level
A0=2.0311 meters

Name constituent:	h [m]	g[deg]
J1	0,009	301,7
K1	0,235	212,3
K2	0,1336	58,5
L2	0,0599	328,6
M1	0,014	212
M2	1,0614	13,6
M3	0,0043	86,9
M4	0	0
M6	0	0
M8	0	0
N2	0,1857	359,8
2N2	0,0069	15,4
O1	0,1472	160,6
OO1	0,0091	323,6
P1	0,0652	218,6
Q1	0,0215	151,8
2Q1	0,0036	206,4
R2	0,0318	86,6
S1	0	0
S2	0,4638	63,3
S4	0	0
S6	0	0
T2	0,0315	103,7
LAMBDA2	0,026	359,6
MU2	0,0559	72,4
NU2	0,0304	324
RHO1	0,0084	78,6
MK3	0,0264	134
2MK3	0	0
MN4	0,0598	301,4
MS4	0	0
2SM2	0,0321	265,9
MF	0	0
MSF	0,0775	43,9
MM	0,0241	31,2
SA	0,2406	131,3
SSA	0,0519	1,9

not used but given:

Sa3	0,0619	147
Sa4	0,0165	225,4

Sa5	0,0214	9,2
Sa6	0,0194	254,1
Sa7	0,0183	61,8
Sa8	0,0164	11,8
M4Sam	0,0209	64,7
M3Ssm	0,0159	23,2
M2Ssm	0,029	304,7
MSsm	0,0054	198,7
SsMm	0,0181	187,6
2SsMm	0,0044	253,2
3SsMm	0,0142	99,5
4SsMm	0,0084	199,2
5SsMm	0,034	236,4
6SsMm	0,0267	234,8
7SsMm	0,017	268,4
MS3Ssf	0,0064	215,4
MS2Saf	0,0381	309,8
MSSaf	0,0117	27,7
SaMSf	0,0145	198,8
SaMf	0,0122	325,3
2SaMf	0,0328	301
3SaMf	0,0101	18,1
4SaMf	0,0074	178,1
5SaMf	0,0118	89
6SaMf	0,0121	56,1
7SaMf	0,0221	208,5
MT5Saf	0,0226	82,8
MT4Saf	0,0112	70,7
MT3Saf	0,0087	163,6
MT2Saf	0,0196	238,1
MTSaf	0,0143	270,8
MTM	0,0155	326
SaMTF	0,0125	9,2
SM7Saf	0,0038	159,5
SM6Saf	0,0202	89,2
SM5Saf	0,0056	263,9
SM4Saf	0,0133	177,8
SM3Saf	0,0068	107,3
SM2Saf	0,0261	188,9
SMSaf2	0,0108	120,9
SMf2	0,0096	5,3
SASMf2	0,0054	106,3
2SaSMf	0,0342	86,5
3SaSMf	0,0222	24
4SaSMf	0,0297	311,9
5SaSMf	0,0101	183,7
6SaSMf	0,0223	206,1
7SaSMf	0,0106	277,2
sigma1	0,019	244,2
Qa1-	0,0054	322,1
QA1	0,0064	205,1
04SA1	0,0031	358
03SA1	0,0037	61,6
0SA1	0,0113	254,9
SA01	0,0203	321

MP1	0,0325	298,9
3SA01	0,0058	247,5
4SA01	0,0069	294,2
7SA01	0,0031	162,6
X1	0,004	200,7
K7SA1	0,0036	65,2
K6SA1	0,004	96,9
K5SA1	0,0038	11,2
2PK1	0,0042	333,3
PI1	0,0016	249,1
S1	0,0327	131,7
PSI1	0,0163	19,2
PHI1	0,0034	245,1
3SAK1	0,0035	75
4SAK1	0,0038	60,6
THETA1	0,0088	225,3
2P01-	0,0037	352,1
S01-	0,0239	31,2
SQ1-	0,0068	17,2
2NS2	0,0081	282,5
2NK2S2	0,0074	236,4
MNS2-	0,0108	71,7
2MS2K2	0,0051	130,3
N7SA2	0,0054	260,1
N6SA2	0,0034	41,1
N5SA2	0,0054	130,1
N4SA2	0,0044	100,4
N3SA2	0,0048	129,1
NA2-	0,0115	188,2
NA2	0,014	34
3SAN2	0,0062	259,1
2KN2S2	0,0049	283,8
5SA2N2	0,0049	251,3
M7SA2	0,0141	186,9
M5SA2	0,0156	215,5
M4SA2	0,0082	119,5
MSK2	0,0072	212
MA2-	0,0463	189,2
MA2	0,0398	96,4
MKS2	0,0141	175,6
M2KS2)	0,0082	187,4
5SAM2	0,0047	307,3
6SAM2	0,0072	190,5
2SNMK)	0,0085	2,1
S6SA2	0,0036	107,3
S5SA2	0,0098	299,2
S4SA2	0,0065	196
S2SA2	0,013	38,4
3SAS2	0,0097	188,5
6SAS2	0,0059	336,8
7SAS2	0,0045	110,5
MSN2-	0,0111	250,9
KJ2	0,0064	300,3
SKM2	0,015	262,7
2SN2-	0,0034	294,6

N03	0,0035	37,9
M03	0,0169	43,5
2MP3	0,0054	191,9
S03	0,0162	125,4
2MQ3	0,0056	264,8
SP3	0,0072	228
SK3	0,0182	213,3
K3	0,0055	29,1
2MNS4	0,0084	21,7
N4	0,0086	275,3
3MS4-	0,0201	13,8
MNSA4	0,0045	17,5
SAMN4	0,0074	24,1
MNKS4	0,0077	343,5
M5SA4	0,0037	116,1
2MSK4	0,0034	114

V Example equal level curves

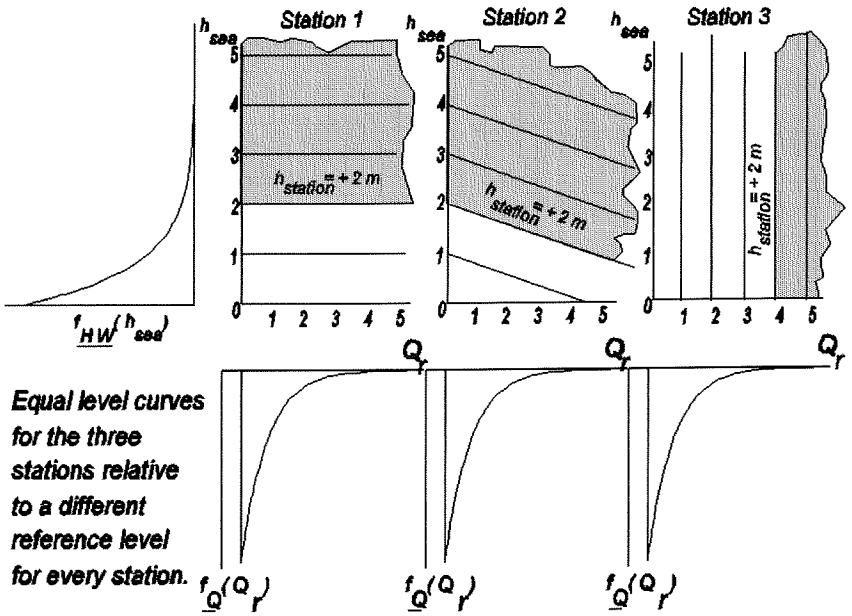

Equal level curves for the three stations relative to a different reference level for every station.

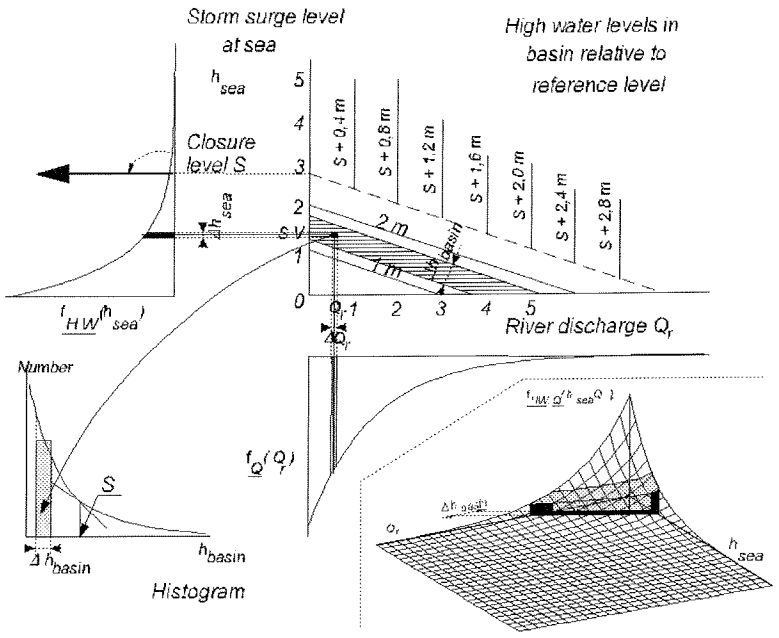

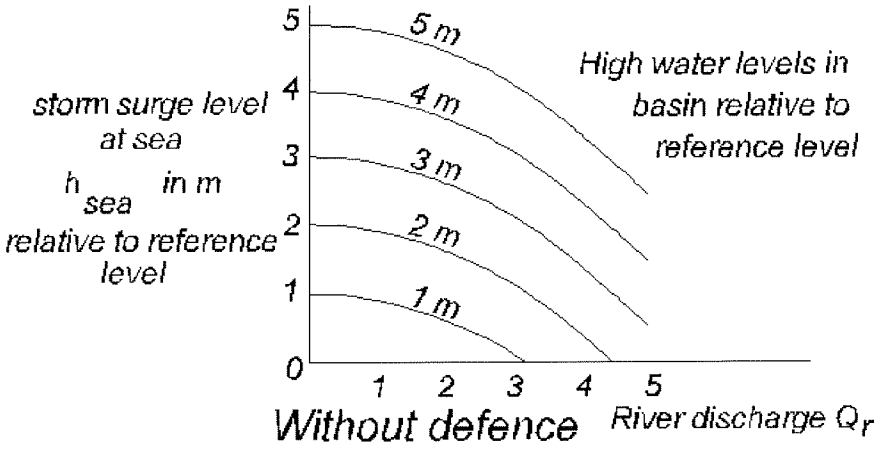
storm surge level at sea
h sea in m
relative to reference level
5 m
4 m
3 m
2 m
1 m
High water levels in basin relative to reference level
River discharge Q r
Without defence

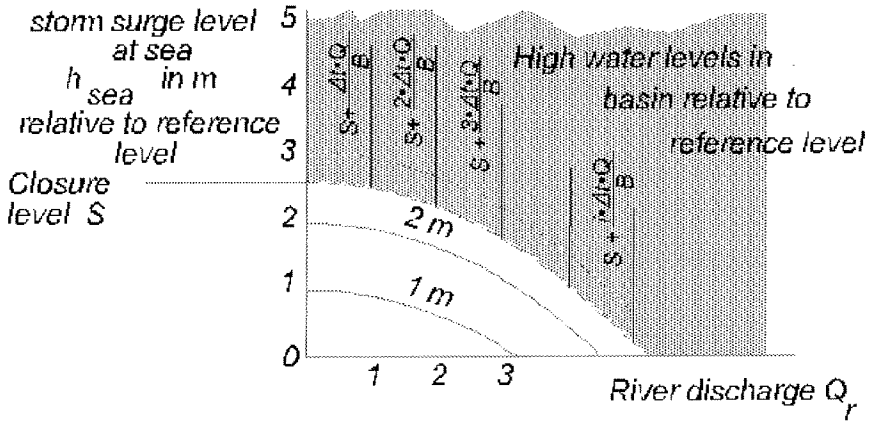
storm surge level at sea
h sea in m
relative to reference level
Closure level S
High water levels in basin relative to reference level
River discharge Q r
With defence

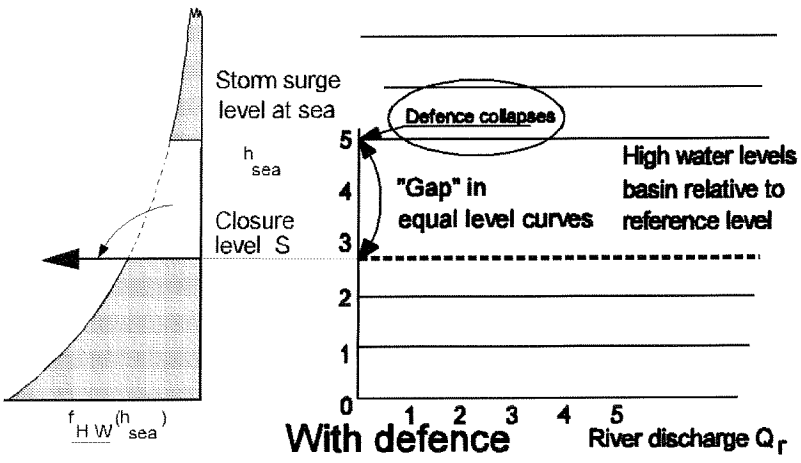
Storm surge level at sea
h sea
Closure level S
Defence collapses
"Gap" in equal level curves
High water levels basin relative to reference level
River discharge Q r
With defence

W Matlab source codes

The computations in this study are carried out with specially written scripts or programs in the Matlab language version 6.1. The scripts can be found in the CD-ROM enclosed with this thesis; the main scripts and their listing are treated hereafter. The flow charts below explain the steps carried out in the computations. Each step is in fact a separate script and the results of each step are used in the subsequent script, therefore the results of each step have to be saved and loaded in the next step. It is possible to link the subsequent scripts as procedures with each other. This is however experienced as not convenient. Furthermore, there are some separate scripts written for the output (plots) named outputrunoff.m and output conditional.m. The scripts for the simulation of Archimedean copulas are in fact universal. When a different copula is used, only the script with the copula generator has to be changed. Examples with other copulas are enclosed in the CD-ROM as well. A complete listing of Archimedean copulas can be found in Nelson (1999) and De Matteis (2001)

Computation joint storm surge and tide distribution:

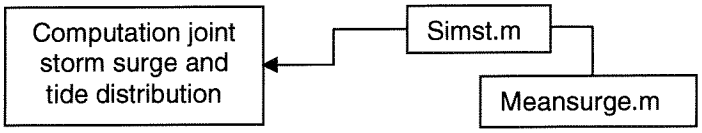

Computation flood probability with copula:

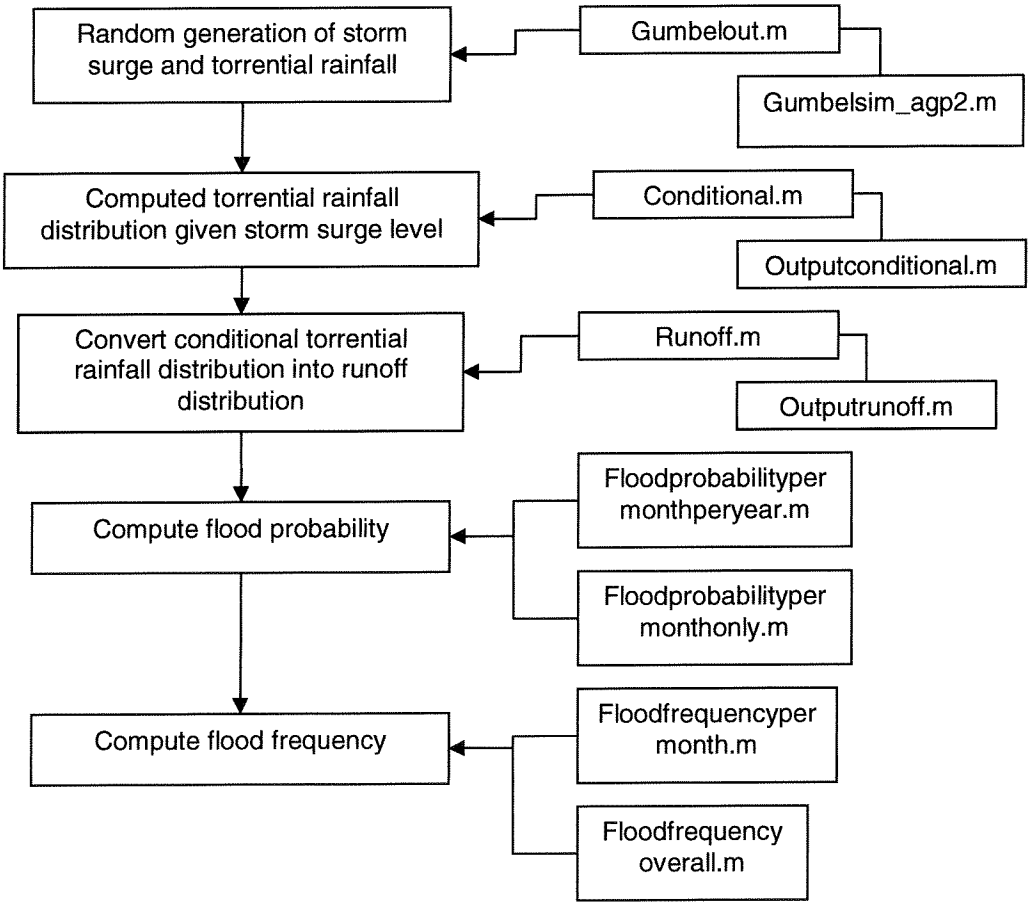

Joint storm surge and tide distribution:

Simst.m:

```
%Script for joint distribution of storm surge and tide
%=====================================================

N=1000; %number of realizations
h=zeros(N,6);
d=zeros(N,3);

%x=zeros(N,1); %
x1=zeros(N,1);
%parameters inverse PIII distribution
a=7.0302663;
b=0.0616619;
k=zeros(N,1); %
x2=zeros(N,1);
%probability matrix
PW=zeros(N,1);
PP=zeros(N,1);

   %backmapping tide
   x1=rand(N,1);
   %beta generalized
   x=betgenpdf2(x1);
   %weibull
   %x=(-alfa.*(log(1-x1)).^1./beta)+204,96;
   %backmapping surge
   %pearson III
   x2=rand(N,1);
   k=p3inv(x2,a,b);

%probabilities
u=1-x1;
p=1-x2;
x3=u.*p;
%x4=x1.*x2;
%h=x+k;
%result matrix
h(:,1)=x; %tide
h(:,2)=u; %probability tide
h(:,3)=k; %surge
h(:,4)=p; %probability surge
h(:,5)=x+k; %storm tide
h(:,6)=x3; %probability storm tide

%=============================================
%output
%=============================================
%subplot(2,2,1);
%plot(x,x1, '.');
%grid on;
```

```
%subplot(2,2,2);
%plot(k,x2, '.');
%grid on;
%subplot(2,2,3);

%i=find(h(:,6)==0.001);
%waarde=h(i,:);
save output7.out h -ASCII


%xi=interp1(h(:,5),q(:,6),p);
%plot(h(:,1),h(:,3),'.'); %onderschrijdingskans !! %getij - surge
plot(u,p, '.')
%hold on;
grid on;

%z=h(:,6);
%x=h(:,1);
%y=h(:,3);

%[xx,yy]=meshgrid(260:10:440,0:10:300);
%zz=griddata(x,y,z,xx,yy);
%[c,w]=contour(xx,yy,zz,0:0.1:1);
%clabel(c,w);

%hold on;
%plot3(x,k,x3, '.'); %3dimensionaal
%plot(x+k,x4, '.');

set(gca,'fontsize',19);
%xlabel('high tide level h_t  [m] WD');
%ylabel('storm surge level h_s  [m]');

%xlabel('P(h_t)');
%ylabel('P(h_s)')
%title('Joint probability surge and tide level');
xlabel('x');
ylabel('y');

grid on;
%tabulate(round(h));
```

Meansurge.m:

```
%Computation mean surge level for given storm tide levels
%-------------------------------------------------------------------------
clear;

load matrixhvier.mat;

%
h=480;
%
ht=x;
pht=u;
hs=k;
phs=p;
hst=x+k;
phst=x3;

data=[hst ht hs];

datas=sortrows(data);
   aq=find(datas(:,1)>h);
   data2=datas(min(aq):end,:); %matrix met hst vanaf gegeven hst

b=1000;
a=1:b;
   a=a';
   rt=zeros(b,6);
rt(:,1)=a;

for i=1:b;
   %map frequency to vector
rt(i,2)=length(find(datas(:,1)>=rt(i,1))); %map hst
rt(i,3)=length(find(data2(:,2)>=rt(i,1))); %map ht | hst >= h
rt(i,4)=length(find(data2(:,3)>=rt(i,1))); %map hs | hst >= h
rt(i,5)=length(find(datas(:,2)>=rt(i,1))); %map ht
rt(i,6)=length(find(datas(:,3)>=rt(i,1))); %map hs
end
%kans bepalen:
rt(:,2)=rt(:,2)./length(datas);     %p(hst)
rt(:,3)=(rt(:,3)./length(data2));   %p(ht|hst >= h)
rt(:,4)=(rt(:,4)./length(data2));   %p(hs|hst >= h)
rt(:,5)=rt(:,5)./length(datas);
rt(:,6)=rt(:,6)./length(datas);

save simstoutput.mat rt data2 -mat;
```

Random generation of storm surge and torrential rainfall:

Gumbelout.m:

```
%%Script to draw samples from the gumbel copula with arbitrary margins
%   Margins used in this script are p3 distributions of stormsurge and torrential rainfall
%   These margins can be changed into arbitrary margins.
%=========================================================================
function q=p(r,i);
%%input variables form the commandwindow are gumbelout(r,i) with
```

```
%r = correlation according to kendall's tau
%i = number of rainduration 1= 1 rainday, 2= 3 raindays, 3= 7 raindays
%procedure linked with gumbelsim_agp2, which is the script with the gumbel copula
%=========================================================================
%%Sampling
%=========================================================================
%number of realizations n:
n=4000;
%function call
a=gumbelsim_agp2(r,n);
%correlated pair C(u,v);
u=a(:,1);
v=a(:,2);
%=========================================================================
%%Backmapping to individual distributions
%=========================================================================
%Any other univariate distribution can be instead:
   %rainfall distribution with i=raindays
   m=ptba(u,i);
      %surge level distribution
   alfa=7.0302663;
   beta=0.0616619;
   k=p3inv(v,alfa,beta);

   %%
   q=[k m]; %m=rainfall, k=surge
%=========================================================================
%%Save data for analysis
%=========================================================================
save gumbelout.mat q -mat;
%=========================================================================
%%Output scatter plots
%=========================================================================
%%figure 1 is scatter plot of probabilities
fg1=figure
ax1=...
   plot(u,v,'.','markersize',20);
   title('Random variables with Gumbel copula, \rho_\tau \approx 0.3','fontsize',17);
   set(gca,'fontsize',19);
   xlabel('u');
   ylabel('v');
   set(gca,'ytick',0:0.2:1,'xtick',0:0.2:1);
   grid on;
%%figure 2 is scatter plot of the corresponding values
fg2=figure
ax2=...
   plot(m,k,'.','markersize',20);
   title('Gumbel copula for storm surge and torrential rainfall','fontsize',17);
   set(gca,'fontsize',19);
   xlabel('1 day torrential rainfall [mm]');
   ylabel('storm surge level [cm]');
   set(gca,'xlim', [0 300], 'ylim', [0 300]);
   set(gca,'ytick',0:50:300,'xtick',0:50:300);
   grid on;
```

Gumbelsim_aqp2.m :

```
%Script for sampling of gumbel copula with universal algorithm
% of genest and mackay (1986)
%
%Script is linked with gumbelout.m !!
%
%================================================================
function c=gmb(rho,i)

%Random sampling of Gumbel copula via its generator
%rho is correlation according to kendall's t rho=[0,1]
%i is number of raindays i=[1,7]
%---------------------------
if nargin < 2
  error('Not enough input arguments.');
end
%correlation for gumbel copula:
a=1/(1-rho);


%computation phi en phi':
   %counter t:
   tt=0.000001:.0001:0.999999;
   %phi
   phi=((-log(tt)).^a);
      phimx= [phi;tt];
      phimx=phimx.';
   %phi'
   phiacnt=a.*(((-log10(tt)).^a)./(tt.*log10(tt)));
   phiacntmx= [phiacnt ;tt];
      phiacntmx=phiacntmx.';

 %Simulation
 %-----------------------------------------------------------
%Random generate [0,1]
 u=rand(i,1);
 t=rand(i,1);

%Step1:
 %computation phi'(u)
   phiacntu=a.*(((-log10(u)).^a)./(u.*log10(u)));
   %phi'(u)/t
   ab=phiacntu./t;


 %Step 2
 %computation phi'(w)=phi'(u)/t;
   I=~isnan(phiacntmx(:,1));   %Gebruik alleen de niet NAN waarden
   w=interp1(real(phiacntmx(I,1)),real(phiacntmx(I,2)),ab);
 %computation v:
   phiw=((-log(w)).^a);
```

```
%----------------------------------------
   % filter nan's
  rr(:,1)=phiw;
  rr(:,2)=u;
  rr(:,3)=t;
rr(any(isnan(rr)'),:) = [];
  u=rr(:,2);
  phiw=rr(:,1);
   %
   phiu=((-log(u)).^a);
   delta=phiw-phiu;
   %delt=~isnan(delta);
   delta=real(delta);
%l=~isnan(phimx(:,1));
v=interp1(real(phimx(:,1)),real(phimx(:,2)),delta);
%-----------------------------------------------------
%Step 3
%correlated pair of u,v:
c= [u,v];
save gumbelsim_agp2.out  c -mat;
```

Computed torrential rainfall distribution given storm surge level:

Conditional.m:

```
%%copula results analysis (computes joint probability surge and rainfall)
%%run this script to sort and compute (conditional) torrential rainfall probabilities of the
output of gumbelout.sim
%%this sorting takes a lot of time!!, remember to change save destination location to
prevent overwrite
%=========================================================================
function  rt=cond(hs);
%%input variable hs is given surge level (in centimeters) for torrential rainfall
   %hs = given surge level
   %rho= kendall's tau
   %rainday = rainday

   %%data = outputmatrix of gumbel copula sim with [surge raindepth];
   %%data(:,2) splits up into rt(:,2) and rt(:,3)
%rt=output matrix , colomn 1=raindepth, 2=P(marginal), 3=P(conditional);
%hs=100;
%=========================================================================
%Load results from copula sampling
%=========================================================================
   load gumbelresults.mat q -mat
   data=q;
%=========================================================================
%Sort datamatrix
%and look for row number with surge>hs, make new matrix:
%%=======================================================================
datas=sortrows(data); %data.mat is van copula sim      data = 1day, data2=3 days data3=4
days, rho=0.306
   dummy=find(datas(:,1)>hs);
```

```
   datas1=datas(min(dummy):end,:);
%construct column for rainfall
b=1000;
a=1:b;
   a=a';
   rt=zeros(b,3);
rt(:,1)=a;

for i=1:b;
rt(i,2)=length(find(datas(:,2)>rt(i,1))); %look up values for marginal probability
rt(i,3)=length(find(datas1(:,2)>rt(i,1))); %look up values for conditional probability
end
rt(:,2)=rt(:,2)./length(datas); %computation marginal probability from values
rt(:,3)=(rt(:,3)./length(datas1));%computation conditional probability from values
%%%delete zeros from data matrix
y=find(rt(:,3)>0);
rt=rt(1:max(y+1),:);
%%
%
p_hs=p3cdf(hs,7.0302663,0.0616619); %computes marginal prob of hsurge
jpdf=(rt(:,3).*p_hs);              %computes joint prob from marginale kans X conditionele kans
->jpdf matrix
%%computation of h surge
%p_surge=p_hs*100;
%%-------------------------------------------------------------------------
%%%computes mariginal probability of rainfall (check purpose), input y = raindepth:
%y=hs;
%dummyy=find(datas1(:,2)>y);
%p_margin_rainfall=(length(dummyy)/length(data)).*100        %marginal p
%computes condtional proob
%dummyc=find(datas1(:,2)>y);
%p_conditional_rainfall=(length(dummyc)/length(datas1)).*100    %conditional p,
%p_delta=100*(p_conditional_rainfall-p_margin_rainfall)/p_margin_rainfall
%-------------------------------------------------------------------------
%
%=========================================================================
%%Save data for further analysis
%=========================================================================
rt=[rt jpdf];
save gumbelcond.mat rt -mat;
```

Outputconditional.m:

```
%Script to plot graphs of the sample distributions computed with conditional.m
%=========================================================================
%Load data
%=========================================================================|
oad gumbelcond.mat rt -mat;
%=========================================================================
jpdf=rt(:,4);
%=========================================================================
```

```
%%output jpdf plots
%=========================================================================
plot( rt(:,1),100.*rt(:,3),'b');%conditional
hold on
plot( rt(:,1),100.*rt(:,2),'k');%marginal
hold on
plot( rt(:,1),100.*jpdf, 'r'); %joint
%
%plot( rt(:,1),100.*rt(:,2),'r');%marginal
%hold on
%plot( tr(:,1),100.*tr(:,2),'b');%marginal
%set(gca,'fontsize',16,'ytick',0:25:100,'xlim',[33 350]);
%legend('3 days', '1 day');
%xlabel('rainfall Tai Lake Basin, d_{Basin} [mm]');
%
%set(gca, 'xlim', [55 350], 'fontsize',19,'ytick',0:25:100);
grid on
set(gca, 'xlim', [50 350], 'fontsize',19);
title('Rainfall distribution with Gumbel copula, \rho_\tau = 0.3, h_s \geq
118.46cm','fontsize',16);
xlabel('3 days torrential rainfall in Tai Lake Basin, d_{Basin} [mm]','fontsize',19);
ylabel('probability [%] ');%of occurrence[%]
%legend('conditional rainfall probability: P(D >d  | H_s_u_r_g_e>0.97m)');
%matlab3.mat-->data-->rho=0.306, data4=rho=0.99, data2=rho=0 of data3=0.75
legend('conditional','marginal','joint');
%rho linear = 0.45 -->rho tau =0.3
```

Convert conditional torrential rainfall distribution into runoff distribution:

Runoff.m:

```
%Script to compute convert conditional torrential rainfall probabilities into runoff probabilities
%Data used comes from conditional.m file, these results must be loaded first.
%=========================================================================
%function uv=runoff(yu)
%runoff module
%conversion raindepth into discharge!
yu = 0.6; %increment lake level, arbitrary value, required for verification of runoff percentage
%=========================================================================
%% load data from runoff.m, this is a data matrix with column 1=raindepth, 2, marginal
%%  p, 3=conditional p.
%=========================================================================
load gumbelcond.mat;
%%=========================================================================
%%delete zeros from data matrix
%y=find(rt(:,3)>0);
%rt=rt(1:max(y+1),:);
rd=rt(:,1);
%=========================================================================
%Computations
%=========================================================================
runoff=0.18 ; % 18% of rainfall in basin (excl. tai lake) flows into lake, remaining is stored!!
rd2=rd.*0.001; % convert effective raindepth into meters*divert
```

```
%
%surface areas
a_basin=36900000000; % in square meters
a_lake=2338000000;
a_basin=a_basin-a_lake; %basin area excl. lake
%%
volume=runoff.*rd2.*a_basin;    %netto inflow volume
deltah=volume./a_lake;          %netto increment lake level
%deltahnetto=deltah+(rd./1000); %  0.44.*
deltah_lake=deltah+rd2; %increment lake level incl. rainfall over lake
%%
volume2=deltah_lake.*a_lake;   %total volume for runoff
%
%%=========================================================================
% the total water level increment in the lake is the 'dicharge height' for free flow
%%=========================================================================
%%free flow from tai lake 150 is width taipu river at tai lake
divert=0.8;  %from the runoff about 80% is taken by huangpu river
discharge=divert.*150.*deltah_lake.*((2.*9.81*deltah_lake).^(0.5));
%
%=========================================================================
%% check: input tai lake water level increment ,yu, and interpolates flow volume
%=========================================================================
%
h_inflow=yu
matrix=[volume2 deltah];
inflow=interp1(matrix(:,2),matrix(:,1),yu)  %interp inflow
%%
matrix2=[rd volume2];
raindepth=interp1(matrix2(:,2),matrix2(:,1),inflow) %interp raindepth
%%
matrix3=[discharge rd];
discharge_out=interp1(matrix3(:,2),matrix3(:,1),raindepth)  %interp discharge
%%
p=rt(:,3); %conditional p
matrix4=[p discharge];
prob=interp1(matrix4(:,2), matrix4(:,1), discharge_out)
%
p=100-100.*p;
%%=========================================================================
%%     output
%%=========================================================================
%=======================================
%  P( discharge )
%=======================================
subplot (2,2,1);
set(gca,'fontsize',14);
plot(discharge, p,'b');%runoff
title('discharge');
ylabel('probability [%]');
xlabel('discharge [m3/s]');
grid on
axis tight
set(gca,'xlim', [0 700]);
```

```
%%
%=======================================
% p (delta h)
%=======================================
subplot(2,2,2);
set(gca,'fontsize',14);
plot( deltah,p,'b');%runoff
title('lake water level');
xlabel('delta h_{basin} [m]');
ylabel('p(delta h_{basin} [%]');
grid on
axis tight
%set(gca,'xlim', [0 0.76]);
%%
%=======================================
% p(raindepth)
%=======================================
subplot(2,2,3);
set(gca,'fontsize',14);
title('raindepth');
plot( rt(:,1),p,'b');%conditional
xlabel('raindepth [mm]');
ylabel('probability [%]');
grid on
axis tight
%set(gca,'xlim', [0 300],'xtick',[0:20:300]);
%%
%=========================================
% raindepth <-> delta h_lake
%=========================================
subplot(2,2,4);
set(gca,'fontsize',14);
%title('volume/delta h');
plot(rd,deltah);
%xlabel('volume [m^3]');
xlabel('rainfall');
ylabel('delta h_{basin} [m]');
grid on
axis tight
%set(gca,'xtick',[0:50:500],'ytick',[0:0.2:2.5],'xlim',[0 500]);
%
%set(gca,'xtick', [0:0.5e9:6e9]);
%
%=====================================================================
%%save output
%=====================================================================
ux=[rd p volume2 discharge deltah_lake deltah];
%save runoffdatagraphsgumbel1mean.mat ux -mat
%
```

Outputrunoff.m:

```
%Script to plot runoff and runoff depths from sorted data of runoff.m
```

```
%=========================================================================
%% to plot multiple curves with different runoff percentages, you must first
%% compute these data with runoff.m with different runoff
%% percentages and save them under different names. In this file,
%% runoff percentage 13% is named uz, 18% is named ux and 23% is named uv
%=========================================================================
%Load runoff percentages:
%=========================================================================
load runoffdatagraphsgumbel1mean.mat
load runoffdatagraphsgumbel1meanm5.mat
load runoffdatagraphsgumbel1meanp5.mat
%=========================================================================
%
%
rd=ux(:,1);
p=ux(:,2);
volume=ux(:,3);
discharge=ux(:,4)./3; %bij 3 days delen door 3
deltah_lake=ux(:,5)./3;
deltah=ux(:,6);
%
rd5=uv(:,1);
p5=uv(:,2);
volume5=uv(:,3);
discharge5=uv(:,4)./3;
deltah_lake5=uv(:,5)./3;
deltah5=uv(:,6);
%
rd1=uz(:,1);
p1=uz(:,2);
volume1=uz(:,3);
discharge1=uz(:,4)./3;
deltah_lake1=uz(:,5)./3;
deltah1=uz(:,6);
%
%
%=========================================================================
%%plot runoff probabilities
%=========================================================================
%
plot(discharge1, rd1,'m');
hold on
plot(discharge, rd,'r');
hold on
plot(discharge5,rd5, 'b');
%=========================================================================
%%plot runoff depth probabilities
%=========================================================================
%
%plot(deltah_lake1, rd1,'m');
%hold on
%plot(deltah_lake, rd,'r');
%hold on
%plot(deltah_lake5, rd5,'b');
```

```
%=========================================================================
%%labels
%=========================================================================
xlabel('surface runoff [m^3/s]','fontsize',19);
%xlabel('runoff depth [m]','fontsize',19);
%set(gca,'yscale','log');
ylabel('torrential rainfall [mm]','fontsize',19);
   set(gca,'position',[0.13 0.11 0.7 0.815])
set(gca,'ylim',[0 420],'fontsize',19,'ytick',0:60:420);%
%set(gca,'ylim',[0 360],'fontsize',19,'ytick',0:60:360);%
%
set(gca,'xlim',[0 500],'xtick',0:100:500);
%
%set(gca,'xlim',[0 1.75],'xtick',[0:.25:1.75],'fontsize',19);
%set(gca,'xlim',[0 0.75],'xtick',[0:.15:.75]);

grid on;
legend('runoff -5%','runoff (18%)','runoff +5%',4);
title('Runoff 3 days torrential rainfall, Gumbel \rho_\tau = 0.3','fontsize',17);
%title('Runoff depth 3 days torrential rainfall, Gumbel \rho_\tau = 0.3','fontsize', 17);
%
      ax2=axes('yaxislocation','right','xtick',[],'color','none','ylim',[0
420],'ytick',0:60:420,'fontsize',19);
   set(gca,'position',[0.13 0.11 0.7 0.815])
%    ylabel('probability of exceedance  Q_{required}  [years]');%

%% voor 3 raindays::
%pQ=interp1([0;rd;420],[0;p;100], 0:60:420);
%set(ax2,'ytickl',((100-pQ))) % uitrekenen ... of voordefinieren:
set(ax2,'ytickl',{'100','97' ,'63','26','7','1.2','0.13','0'});
%%
%%voor 1 rainday::
%pQ=interp1([0;rd;360],[0;p;100], 0:60:360);
%set(ax2,'ytickl',((100-pQ))) % uitrekenen ... of voordefinieren:
%set(ax2,'ytickl',{'100','76','25','3.8','0.35','0.04','0'});

ylabel('probability of occurrence [%]');
%pQ=interp1([0;matrix4(:,2);1400],[1;matrix4(:,1);0], 0:200:800);
```

Compute flood probability:

Al scripts for flood probability and frequency computations are based on the this script:

Floodprobabilityopermonthperyear.m:

```
%Script to compute flood probability for given month and year
%with reference to Huangpu Park and Mishidu
%computations done for each barrier location by simply loading the
%corresponding storage capacity
%=========================================================================
```

```
%%Load data acquired with runoff.m
%=========================================================================
load runoffdatagraphsgumbel1mean.mat;          %runoffdatagrapsb=3 dagen rho=03 and
hs=97cm; runoffdatagraphs.mat=1 dag rho=03 hs=97
%=========================================================================
%Load typhoon occurrence probability data
%=========================================================================
load landfall.mat;
%=========================================================================
%load storage capacity data
%=========================================================================
%load storageatwusong2.mat;
%load storageatzh2.mat;
load storageatfishery2.mat;
%
%=========================================================================
%Computations
%=========================================================================
rd=ux(:,1);
p=(ux(:,2)./100); %p tussen 0 en 1;
volume=ux(:,3);
discharge=ux(:,4);
deltah_lake=ux(:,5);
deltah=ux(:,6);
%
%Base discharges:
wet    = [607 833 639 517 305];
av     = [323 352 326 279 327];
dry    = [211 237 293 253 188];
%

%Computation required discharges
for i=1:1:5
   qrmwet(:,i)    =  q-wet(1,i);
   qrmav(:,i )    =  q-av(1,i);
   qrmdry(:,i)    =  q-dry(1,i);
end
%Find probabilities of the required discharges
matrix4=[1-p discharge];
   probwet=interp1(matrix4(:,2), matrix4(:,1), qrmwet);   %compute prob required qtr
   probav=interp1(matrix4(:,2), matrix4(:,1), qrmav);
   probdry=interp1(matrix4(:,2), matrix4(:,1), qrmdry);
   %
%probwet(isnan(probwet)) = 1;
%probav(isnan(probav)) = 1;
%probdry(isnan(probdry)) = 1;
   %
fldmwet    =probwet;
fldmav     =probav;
fldmdry    =probdry;
%
%monthly typhoon occurrence
pmonth=total';
pmonth(:,1:5)=[];
```

```
pmonth(:,6:7)=[];
pmonth=pmonth./100;

%%
fldmwet2     =fldmwet;%.*pmonth(:,i)     ;   %%met p(hst>=4.8) & p(typoon)
fldmav2      =fldmav;%.*pmonth(:,i)      ;
fldmdry2     =fldmdry;%.*pmonth(:,i)     ;

%closure durations with reference to mishidu and huangpu park
cnu=tms2(:,1);   %mishidu present
c2010=tms2(:,2); %mishidu 2010
c2030=tms2(:,3);
c2050=tms2(:,4);

chnu=thp2(:,1);   %huangpu park present
ch2010=thp2(:,2); %hp 2010
ch2030=thp2(:,3);
ch2050=thp2(:,4);
%
%
m1=[fldmwet2(:,1) fldmav2(:,1) fldmdry2(:,1)]; %june
m2=[fldmwet2(:,2) fldmav2(:,2) fldmdry2(:,2)]; %july
m3=[fldmwet2(:,3) fldmav2(:,3) fldmdry2(:,3)]; %august
m4=[fldmwet2(:,4) fldmav2(:,4) fldmdry2(:,4)]; %sept
m5=[fldmwet2(:,5) fldmav2(:,5) fldmdry2(:,5)]; %oct
%
%m1=sum(m1,2);
%m2=sum(m2,2);
%m3=sum(m3,2);
%m4=sum(m4,2);
%m5=sum(m5,2);


for i=1:3;
a=find(m1(:,i)<2e-5);
m1(min(a):end,i)=1e-7;
%
b=find(m2(:,i)<2e-5);
m2(min(b):end,i)=1e-7;
%
c=find(m3(:,i)<2.5e-5);
m3(min(c):end,i)=1e-7;
%
d=find(m4(:,i)<2e-5);
m4(min(d):end,i)=1e-7;
%
e=find(m5(:,i)<2e-5);
m5(min(e):end,i)=1e-7;
end
m1(isnan(m1)) = 1;
m2(isnan(m2)) = 1;
m3(isnan(m3)) = 1;
m4(isnan(m4)) = 1;
m5(isnan(m5)) = 1;
```

```
m1=100.*m1;
m2=100.*m2;
m3=100.*m3;
m4=100.*m4;
m5=100.*m5;
%============================================================
%Interpo1ate for results 24 hours flood prob.
%Change title with find and replace for each barrier location
%============================================================
d=[cnu m5];
ms24w=interp1(d(:,1),d(:,2),24)
%ms24a=interp1(d(:,1),(d:,3),24);
%ms24d=interp1(d(:,1),(d:,4),24);
g=[chnu m5];
hp24w=interp1(g(:,1),g(:,2),24)
%look up max closure duration
for i=1:3
a(i)=max(find(m1(:,i)>=100));
b(i)=max(find(m2(:,i)>=100));
c(i)=max(find(m3(:,i)>=100));
dd(i)=max(find(m4(:,i)>=100))
e(i)=max(find(m5(:,i)>=100));
end
dd=dd'
for i=1:3
   ms1(i)=cnu(a(i),:);
   ms2(i)=cnu(b(i),:);
   ms3(i)=cnu(c(i),:);
   ms4(i)=cnu(dd(i),:);
   ms5(i)=cnu(e(i),:);

   hp1(i)=chnu(a(i),:);
   hp2(i)=chnu(b(i),:);
   hp3(i)=chnu(c(i),:);
   hp4(i)=chnu(dd(i),:);
   hp5(i)=chnu(e(i),:);
end
ms1
ms2
ms3
ms4
ms5
%
hp1
hp2
hp3
hp4
hp5

%return
%====================================================================
%Output flood probability plots for given month and type of year
%====================================================================
```

```
%-----------------------------------------------------------------------
Fg1=figure;
Ax11=...
plot(cnu, m1);
hold on
plot(chnu, m1,':' );
hold on
set(gca,'yscale','log');
set(gca,'ylim',[0.1  100] ,'yticklabel', {'0.1','1','10','100'},'yminortick','on');
set(gca,'xtick',[0:12:124]);
%set(gca,'xlim',[18 72],'fontsize',19,'XMinorTick','on');
set(gca,'xlim',[6 124],'fontsize',19,'XMinorTick','on');
AX=...
legend('wet (Mishidu)','average','dry','wet (Huangpu Park)','average','dry',4);
LEG = findobj(AX,'type','text');
set(LEG,'FontSize',12)
ylabel('probability of exceedance [%]');
xlabel('closure duration [hrs]');
   grid on
% set(gca,'position',[0.13 0.11 0.775 0.78])
%ax2=axes('xaxislocation','top','ytick',[],'color','none','xlim',[6
124],'xtick',0:12:124,'fontsize',19);
title('Flood probability Huangpu River, barrier at Fishery Yard, June','fontsize',17);
%set(gca,'position',[0.13 0.11 0.775 0.78])
%return
%-----------------------------------------------------------------------
%
Fg2=figure;
Ax21=...
plot(cnu, m2);
hold on
plot(chnu,  m2,':' );
set(gca,'yscale','log');
set(gca,'ylim',[0.1  100] ,'yticklabel', {'0.1','1','10','100'},'yminortick','on');
set(gca,'xtick',[0:12:124]);
%set(gca,'xlim',[18 72],'fontsize',19,'XMinorTick','on');
set(gca,'xlim',[6 124],'fontsize',19,'XMinorTick','on');
AX=...
legend('wet (Mishidu)','average','dry','wet (Huangpu Park)','average','dry',4);
LEG = findobj(AX,'type','text');
set(LEG,'FontSize',12)

ylabel('probability of exceedance [%]');
xlabel('closure duration [hrs]');
   grid on
  %set(gca,'position',[0.13 0.11 0.775 0.78])
%ax2=axes('xaxislocation','top','ytick',[],'color','none','xlim',[6
124],'xtick',0:12:124,'fontsize',19);
 title('Flood probability Huangpu River, barrier at Fishery Yard, July','fontsize',17);
%set(gca,'position',[0.13 0.11 0.775 0.78])
%
%return
%-----------------------------------------------------------------------
%
```

```
Fg3=figure;
Ax31=...
plot(cnu, m3);
hold on
plot(chnu,  m3,':' );
set(gca,'yscale','log');
set(gca,'ylim',[0.1  100] ,'yticklabel', {'0.1','1','10','100'},'yminortick','on');
set(gca,'xtick',[0:12:124]);
%set(gca,'xlim',[18 72],'fontsize',19,'XMinorTick','on');
set(gca,'xlim',[6 124],'fontsize',19,'XMinorTick','on');
AX=...
legend('wet (Mishidu)','average','dry','wet (Huangpu Park)','average','dry',4);
LEG = findobj(AX,'type','text');
set(LEG,'FontSize',12)
ylabel('probability of exceedance [%]');
xlabel('closure duration [hrs]');
   grid on
 % set(gca,'position',[0.13 0.11 0.775 0.78])
%ax2=axes('xaxislocation','top','ytick',[],'color','none','xlim',[6
124],'xtick',0:12:124,'fontsize',19);
 title('Flood probability Huangpu River, barrier at Fishery Yard, August','fontsize',17);
%set(gca,'position',[0.13 0.11 0.775 0.78])
%------------------------------------------------------------------------
%
Fg4=figure;
Ax41=...
plot(cnu, m4);
hold on
plot(chnu,  m4,':' );
set(gca,'yscale','log');
set(gca,'ylim',[0.1  100] ,'yticklabel', {'0.1','1','10','100'},'yminortick','on');
set(gca,'xtick',[0:12:124]);
%set(gca,'xlim',[18 72],'fontsize',19,'XMinorTick','on');
set(gca,'xlim',[6 124],'fontsize',19,'XMinorTick','on');
AX=...
legend('wet (Mishidu)','average','dry','wet (Huangpu Park)','average','dry',4);
LEG = findobj(AX,'type','text');
set(LEG,'FontSize',12)
ylabel('probability of exceedance [%]');
xlabel('closure duration [hrs]');
   grid on
  %set(gca,'position',[0.13 0.11 0.775 0.78])
%ax2=axes('xaxislocation','top','ytick',[],'color','none','xlim',[6
124],'xtick',0:12:124,'fontsize',19);
 title('Flood probability Huangpu River, barrier at Fishery Yard, September','fontsize',17);
%set(gca,'position',[0.13 0.11 0.775 0.78])
%------------------------------------------------------------------------
%
Fg5=figure;
Ax51=...
plot(cnu, m5);
hold on
plot(chnu,  m5,':' );
set(gca,'yscale','log');
```

```
set(gca,'ylim',[0.1  100] ,'yticklabel', {'0.1','1','10','100'},'yminortick','on');
set(gca,'xtick',[0:12:124]);
%set(gca,'xlim',[18 72],'fontsize',19,'XMinorTick','on');
set(gca,'xlim',[6 124],'fontsize',19,'XMinorTick','on');
AX=...
legend('wet (Mishidu)','average','dry','wet (Huangpu Park)','average','dry',4);
LEG = findobj(AX,'type','text');
set(LEG,'FontSize',12)
ylabel('probability of exceedance [%]');
xlabel('closure duration [hrs]');
   grid on
%  set(gca,'position',[0.13 0.11 0.775 0.78])
%ax2=axes('xaxislocation','top','ytick',[],'color','none','xlim',[6
124],'xtick',0:12:124,'fontsize',19);
title('Flood probability Huangpu River, barrier at Fishery Yard, October','fontsize',17);
%set(gca,'position',[0.13 0.11 0.775 0.78])
```

Floodprobabilitypermonthonly:

```
%Script to compute FLOOD PROBAILITY for given MONTH ONLY
%with reference to Huangpu Park and Mishidu
%computations done for each barrier location by simply loading the
%corresponding storage capacity
%
%Script is based on floodprobabilitypermonthperyear.m !!!!
%
%=========================================================================
%Load data from runoff.m = torrential rainfall runoff distribution
%=========================================================================
load runoffdatagraphsgumbel1mean.mat;              %runoffdatagrapsb=3 dagen rho=03 and
hs=97cm; runoffdatagraphs.mat=1 dag rho=03 hs=97
%=========================================================================
%%Load typhoon occurrence probability data
%=========================================================================
load landfall.mat;
%=========================================================================
%load storage capacity data
%=========================================================================
load storageatwusong2.mat;    %storage capacity wusongkou
%load storageatzh2.mat;        %Zhanghua bang
%load storageatfishery2.mat;    %fishery yard
%
%=========================================================================
%Computations
%=========================================================================
rd=ux(:,1);
p=(ux(:,2)./100); %p tussen 0 en 1;
volume=ux(:,3);
discharge=ux(:,4);
deltah_lake=ux(:,5);
deltah=ux(:,6);
%Base discharges:
wet    = [607 833 639 517 305];
```

```
av     = [323 352 326 279 327];
dry    = [211 237 293 253 188];
%
%Required discharges:
for i=1:1:5
   qrmwet(:,i)    =  q-wet(1,i);
   qrmav(:,i )    =  q-av(1,i);
   qrmdry(:,i)    =  q-dry(1,i);
end
%
%Lookup probabilities required discharges
matrix4=[1-p discharge];
   probwet=interp1(matrix4(:,2), matrix4(:,1), qrmwet);   %compute prob required qtr
   probav=interp1(matrix4(:,2), matrix4(:,1), qrmav);
   probdry=interp1(matrix4(:,2), matrix4(:,1), qrmdry);
   %

   probwet(isnan(probwet)) = 1;
probav(isnan(probav)) = 1;
probdry(isnan(probdry)) = 1;
%
%%voor optellen maanden
fldmwet2     =0.138.*probwet;%.*pmonth(:,i)     ;   %%met p(hst>=4.8) & p(typoon)
fldmav2      =0.345.*probav;%.*pmonth(:,i)      ;
fldmdry2     =0.517.*probdry;%.*pmonth(:,i)      ;

%closure duration
cnu=tms2(:,1);   %Mishidu
c2010=tms2(:,2);  %ms 2010
c2030=tms2(:,3);
c2050=tms2(:,4);
%
chnu=thp2(:,1);   %huangpu park
ch2010=thp2(:,2);  %hp 2010
ch2030=thp2(:,3);
ch2050=thp2(:,4);
%
m1=[fldmwet2(:,1) fldmav2(:,1) fldmdry2(:,1)]; %june, etc
m2=[fldmwet2(:,2) fldmav2(:,2) fldmdry2(:,2)];
m3=[fldmwet2(:,3) fldmav2(:,3) fldmdry2(:,3)];
m4=[fldmwet2(:,4) fldmav2(:,4) fldmdry2(:,4)];
m5=[fldmwet2(:,5) fldmav2(:,5) fldmdry2(:,5)];
%
for i=1:3;
a=find(m1(:,i)<2e-5);
m1(min(a):end,i)=1e-7;
%
b=find(m2(:,i)<2e-5);
m2(min(b):end,i)=1e-7;
%
c=find(m3(:,i)<2.5e-5);
m3(min(c):end,i)=1e-7;
%
d=find(m4(:,i)<2e-5);
```

```
m4(min(d):end,i)=1e-7;
%
e=find(m5(:,i)<2e-5);
m5(min(e):end,i)=1e-7;
end
%
mm1=sum(m1,2);
mm2=sum(m2,2);
mm3=sum(m3,2);
mm4=sum(m4,2);
mm5=sum(m5,2);

mm1=100.*mm1;
mm2=100.*mm2;
mm3=100.*mm3;
mm4=100.*mm4;
mm5=100.*mm5;
%
t=[mm1 mm2 mm3 mm4 mm5];
r=[cnu mm1];
rr=[chnu mm1];
ms24=interp1(r(:,1),r(:,2),24)
hp24=interp1(rr(:,1),rr(:,2),24)
%return
%=============================================================
%Interpo1ate for results 24 hours flood prob.
%Change title with find and replace for each barrier location
%=============================================================
Fg1=figure;
Ax11=...
plot(cnu,mm1,'r');
hold on
plot(chnu, mm1,'b');
hold on
set(gca,'yscale','log');
set(gca,'ylim',[0.1  100] ,'yticklabel', {'0.1','1','10','100'},'yminortick','on');
set(gca,'xtick',[0:12:124]);
%%set(gca,'xlim',[18 72],'fontsize',19,'XMinorTick','on');
set(gca,'xlim',[6 124],'fontsize',19,'XMinorTick','on');%
AX=...
   legend('Mishidu','Huangpu Park',4);
%legend('wet','average','dry','June',4);
LEG = findobj(AX,'type','text');
set(LEG,'FontSize',12)
ylabel('probability of exceedance [%]');
xlabel('closure duration [hrs]');
   grid on
% set(gca,'position',[0.13 0.11 0.775 0.78])
%ax2=axes('xaxislocation','top','ytick',[],'color','none','xlim',[6
124],'xtick',0:12:124,'fontsize',19);
title('Flood probability Huangpu River, barrier at Wusongkou, June','fontsize',17);
%set(gca,'position',[0.13 0.11 0.775 0.78])
%return
%return
```

```
%-----------------------------------------------------------------------
%
Fg2=figure;
Ax21=...
plot(cnu, mm2,'r');
hold on
plot(chnu,  mm2,'b' );
set(gca,'yscale','log');
set(gca,'ylim',[0.1  100] ,'yticklabel', {'0.1','1','10','100'},'yminortick','on');
set(gca,'xtick',[0:12:124]);
%set(gca,'xlim',[18 72],'fontsize',19,'XMinorTick','on');
set(gca,'xlim',[6 124],'fontsize',19,'XMinorTick','on');
AX=...
legend('Mishidu','Huangpu Park',4);
LEG = findobj(AX,'type','text');
set(LEG,'FontSize',12)
ylabel('probability of exceedance [%]');
xlabel('closure duration [hrs]');
   grid on
  %set(gca,'position',[0.13 0.11 0.775 0.78])
%ax2=axes('xaxislocation','top','ytick',[],'color','none','xlim',[6
124],'xtick',0:12:124,'fontsize',19);
 title('Flood probability Huangpu River, barrier at Wusongkou, July','fontsize',17);
%set(gca,'position',[0.13 0.11 0.775 0.78])
%
%return

%-----------------------------------------------------------------------
%
Fg3=figure;
Ax31=...
plot(cnu, mm3,'r');
hold on
plot(chnu,  mm3,'b' );
set(gca,'yscale','log');
set(gca,'ylim',[0.1  100] ,'yticklabel', {'0.1','1','10','100'},'yminortick','on');
set(gca,'xtick',[0:12:124]);
%set(gca,'xlim',[18 72],'fontsize',19,'XMinorTick','on');
set(gca,'xlim',[6 124],'fontsize',19,'XMinorTick','on');
AX=...
legend('Mishidu','Huangpu Park',4);
LEG = findobj(AX,'type','text');
set(LEG,'FontSize',12)
ylabel('probability of exceedance [%]');
xlabel('closure duration [hrs]');
   grid on
 % set(gca,'position',[0.13 0.11 0.775 0.78])
%ax2=axes('xaxislocation','top','ytick',[],'color','none','xlim',[6
124],'xtick',0:12:124,'fontsize',19);
 title('Flood probability Huangpu River, barrier at Wusongkou, August','fontsize',17);
%set(gca,'position',[0.13 0.11 0.775 0.78])
%-----------------------------------------------------------------------
%
Fg4=figure;
```

```
Ax41=...
plot(cnu, mm4,'r');
hold on
plot(chnu,  mm4,'b' );
set(gca,'yscale','log');
set(gca,'ylim',[0.1  100] ,'yticklabel', {'0.1','1','10','100'},'yminortick','on');
set(gca,'xtick',[0:12:124]);
%set(gca,'xlim',[18 72],'fontsize',19,'XMinorTick','on');
set(gca,'xlim',[6 124],'fontsize',19,'XMinorTick','on');
AX=...
legend('Mishidu','Huangpu Park',4);
LEG = findobj(AX,'type','text');
set(LEG,'FontSize',12)
ylabel('probability of exceedance [%]');
xlabel('closure duration [hrs]');
   grid on
%  set(gca,'position',[0.13 0.11 0.775 0.78])
%ax2=axes('xaxislocation','top','ytick',[],'color','none','xlim',[6
124],'xtick',0:12:124,'fontsize',19);
 title('Flood probability Huangpu River, barrier at Wusongkou, September','fontsize',17);
%set(gca,'position',[0.13 0.11 0.775 0.78])
%-------------------------------------------------------------------------
%
Fg5=figure;
Ax51=...
plot(cnu, mm5,'r');
hold on
plot(chnu,  mm5,'b' );
set(gca,'yscale','log');
set(gca,'ylim',[0.1  100] ,'yticklabel', {'0.1','1','10','100'},'yminortick','on');
set(gca,'xtick',[0:12:124]);
%set(gca,'xlim',[18 72],'fontsize',19,'XMinorTick','on');
set(gca,'xlim',[6 124],'fontsize',19,'XMinorTick','on');
AX=...
legend('Mishidu','Huangpu Park',4);
LEG = findobj(AX,'type','text');
set(LEG,'FontSize',12)
ylabel('probability of exceedance [%]');
xlabel('closure duration [hrs]');
   grid on
  %set(gca,'position',[0.13 0.11 0.775 0.78])
%ax2=axes('xaxislocation','top','ytick',[],'color','none','xlim',[6
124],'xtick',0:12:124,'fontsize',19);
 title('Flood probability Huangpu River, barrier at Wusongkou, October','fontsize',17);
%set(gca,'position',[0.13 0.11 0.775 0.78])
%
%
```

Computation flood frequency:

Floodfrequencypermonth:

%Script to compute FLOOD FREQUENCY for given MONTH

```
%with reference to Huangpu Park and Mishidu
%computations done for each barrier location by simply loading the
%corresponding storage capacity
%
%Script is based on floodprobabilitypermonthperyear.m !!!!
%
%=========================================================================
%Load data from runoff.m = torrential rainfall runoff distribution
%=========================================================================
load runoffdatagraphsgumbel1mean.mat;              %runoffdatagrapsb=3 dagen rho=03 and
hs=97cm; runoffdatagraphs.mat=1 dag rho=03 hs=97
%=========================================================================
%%Load typhoon occurrence probability data
%=========================================================================
load landfall.mat;
%=========================================================================
%load storage capacity data
%=========================================================================
load storageatwusong2.mat;
%load storageatzh2.mat;
%load storageatfishery2.mat;
%
%=========================================================================
%Computations
%=========================================================================
rd=ux(:,1);
p=(ux(:,2)./100); %p tussen 0 en 1;
volume=ux(:,3);
discharge=ux(:,4);
deltah_lake=ux(:,5);
deltah=ux(:,6);
%Base discharges
wet    = [607 833 639 517 305];
av     = [323 352 326 279 327];
dry    = [211 237 293 253 188];
%Required discharges
for i=1:1:5
   qrmwet(:,i)    =  q-wet(1,i);
   qrmav(:,i )    =  q-av(1,i);
   qrmdry(:,i)    =  q-dry(1,i);
end
%
%Look up probabilities required discharges
matrix4=[1-p discharge];
   probwet=interp1(matrix4(:,2), matrix4(:,1), qrmwet);   %compute prob required qtr
   probav=interp1(matrix4(:,2), matrix4(:,1), qrmav);
   probdry=interp1(matrix4(:,2), matrix4(:,1), qrmdry);
   %

   probwet(isnan(probwet)) = 1;
probav(isnan(probav)) = 1;
probdry(isnan(probdry)) = 1;
%
%%voor optellen maanden
```

```
fldmwet2     =0.138.*probwet;%.*pmonth(:,i)     ;   %%met p(hst>=4.8) & p(typoon)
fldmav2      =0.345.*probav;%.*pmonth(:,i)      ;
fldmdry2     =0.517.*probdry;%.*pmonth(:,i)     ;

%
cnu=tms2(:,1);
c2010=tms2(:,2);  %ms 2010
c2030=tms2(:,3);
c2050=tms2(:,4);
%
chnu=thp2(:,1);   %hp present
ch2010=thp2(:,2);  %hp 2010
ch2030=thp2(:,3);
ch2050=thp2(:,4);
%
m1=[fldmwet2(:,1) fldmav2(:,1) fldmdry2(:,1)]; %june, etc
m2=[fldmwet2(:,2) fldmav2(:,2) fldmdry2(:,2)];
m3=[fldmwet2(:,3) fldmav2(:,3) fldmdry2(:,3)];
m4=[fldmwet2(:,4) fldmav2(:,4) fldmdry2(:,4)];
m5=[fldmwet2(:,5) fldmav2(:,5) fldmdry2(:,5)];
%
for i=1:3;
a=find(m1(:,i)<2e-5);
m1(min(a):end,i)=1e-7;
%
b=find(m2(:,i)<2e-5);
m2(min(b):end,i)=1e-7;
%
c=find(m3(:,i)<2.5e-5);
m3(min(c):end,i)=1e-7;
%
d=find(m4(:,i)<2e-5);
m4(min(d):end,i)=1e-7;
%
e=find(m5(:,i)<2e-5);
m5(min(e):end,i)=1e-7;
end
%
mm1=sum(m1,2);
mm2=sum(m2,2);
mm3=sum(m3,2);
mm4=sum(m4,2);
mm5=sum(m5,2);

%frequency per month:
mm1=0.33.*mm1;
mm2=0.83.*mm2;
mm3=1.16.*mm3;
mm4=1.04.*mm4;
mm5=0.79.*mm5;

%lookup closure duration for 24 hours closure
t1=[cnu chnu mm1];%3 kolommen
t2=[cnu chnu mm2];
```

```
t3=[cnu chnu mm3];
t4=[cnu chnu mm4];
t5=[cnu chnu mm5];
%
ms1=interp1(t1(:,1),t1(:,3),24) %results for mishidu per month
ms2=interp1(t2(:,1),t2(:,3),24)
ms3=interp1(t3(:,1),t3(:,3),24)
ms4=interp1(t4(:,1),t4(:,3),24)
ms5=interp1(t5(:,1),t5(:,3),24)
%
hp1=interp1(t1(:,2),t1(:,3),24) %results for huangpu park per month
hp2=interp1(t2(:,2),t2(:,3),24)
hp3=interp1(t3(:,2),t3(:,3),24)
hp4=interp1(t4(:,2),t4(:,3),24)
hp5=interp1(t5(:,2),t5(:,3),24)
%return
%================================================================
%Interpo1ate for results 24 hours flood prob.
%Change title with find and replace for each barrier location
%================================================================
%
Fg1=figure;
Ax11=...
plot(cnu, mm1,'r');
hold on
plot(chnu,mm1,'b' );
hold on
set(gca,'yscale','log');
set(gca,'ylim',[1e-3 2] );
set(gca,'xtick',[0:12:124]);
%set(gca,'xlim',[18 72],'fontsize',19,'XMinorTick','on');
set(gca,'xlim',[6 124],'fontsize',19,'XMinorTick','on');
AX=...
legend('Mishidu','Huangpu Park',4);
LEG = findobj(AX,'type','text');
set(LEG,'FontSize',12)
ylabel('frequency of exceedance [per year]');
xlabel('closure duration [hrs]');
   grid on
%  set(gca,'position',[0.13 0.11 0.775 0.78])
%ax2=axes('xaxislocation','top','ytick',[],'color','none','xlim',[6
124],'xtick',0:12:124,'fontsize',19);
title('Flood frequency Huangpu River, barrier at Fishery Yard, June','fontsize',17);
%set(gca,'position',[0.13 0.11 0.775 0.78])
%return

%-----------------------------------------------------------------
%
Fg2=figure;
Ax21=...
plot(cnu, mm2,'r');
hold on
plot(chnu,  mm2,'b' );
set(gca,'yscale','log');
```

```
set(gca,'ylim',[1e-3 2] );
set(gca,'xtick',[0:12:124]);
%set(gca,'xlim',[18 72],'fontsize',19,'XMinorTick','on');
set(gca,'xlim',[6 124],'fontsize',19,'XMinorTick','on');
AX=...
legend('Mishidu','Huangpu Park',4);
LEG = findobj(AX,'type','text');
set(LEG,'FontSize',12)
ylabel('frequency of exceedance [per year]');
xlabel('closure duration [hrs]');
   grid on
%  set(gca,'position',[0.13 0.11 0.775 0.78])
%ax2=axes('xaxislocation','top','ytick',[],'color','none','xlim',[6
124],'xtick',0:12:124,'fontsize',19);
 title('Flood frequency Huangpu River, barrier at Fishery Yard, July','fontsize',17);
%set(gca,'position',[0.13 0.11 0.775 0.78])
%
return
%------------------------------------------------------------------------
%
Fg3=figure;
Ax31=...
plot(cnu, mm3,'r');
hold on
plot(chnu,  mm3,'b' );
set(gca,'yscale','log');
set(gca,'ylim',[1e-3 2] );
set(gca,'xtick',[0:12:124]);
%set(gca,'xlim',[18 72],'fontsize',19,'XMinorTick','on');
set(gca,'xlim',[6 124],'fontsize',19,'XMinorTick','on');
AX=...
legend('Mishidu','Huangpu Park',4);
LEG = findobj(AX,'type','text');
set(LEG,'FontSize',12)
ylabel('frequency of exceedance [per year]');
xlabel('closure duration [hrs]');
   grid on
%  set(gca,'position',[0.13 0.11 0.775 0.78])
%ax2=axes('xaxislocation','top','ytick',[],'color','none','xlim',[6
124],'xtick',0:12:124,'fontsize',19);
 title('Flood frequency Huangpu River, barrier at Fishery Yard, August','fontsize',17);
%set(gca,'position',[0.13 0.11 0.775 0.78])
%------------------------------------------------------------------------
%
Fg4=figure;
Ax41=...
plot(cnu, mm4,'r');
hold on
plot(chnu,  mm4,'b' );
set(gca,'yscale','log');
set(gca,'ylim',[1e-3 2] );
set(gca,'xtick',[0:12:124]);
%set(gca,'xlim',[18 72],'fontsize',19,'XMinorTick','on');
set(gca,'xlim',[6 124],'fontsize',19,'XMinorTick','on');
```

```
AX=...
legend('Mishidu','Huangpu Park',4);
LEG = findobj(AX,'type','text');
set(LEG,'FontSize',12)
ylabel('frequency of exceedance [per year]');
xlabel('closure duration [hrs]');
   grid on
%  set(gca,'position',[0.13 0.11 0.775 0.78])
%ax2=axes('xaxislocation','top','ytick',[],'color','none','xlim',[6
124],'xtick',0:12:124,'fontsize',19);
title('Flood frequency Huangpu River, barrier at Fishery Yard, September','fontsize',17);
%set(gca,'position',[0.13 0.11 0.775 0.78])
%------------------------------------------------------------------------
%
Fg5=figure;
Ax51=...
plot(cnu, mm5,'r');
hold on
plot(chnu,  mm5,'b' );
set(gca,'yscale','log');
set(gca,'ylim',[1e-3 2] );
set(gca,'xtick',[0:12:124]);
%set(gca,'xlim',[18 72],'fontsize',19,'XMinorTick','on');
set(gca,'xlim',[6 124],'fontsize',19,'XMinorTick','on');
AX=...
legend('Mishidu','Huangpu Park',4);
LEG = findobj(AX,'type','text');
set(LEG,'FontSize',12)
ylabel('frequency of exceedance [per year]');
xlabel('closure duration [hrs]');
   grid on
%  set(gca,'position',[0.13 0.11 0.775 0.78])
%ax2=axes('xaxislocation','top','ytick',[],'color','none','xlim',[6
124],'xtick',0:12:124,'fontsize',19);
 title('Flood frequency Huangpu River, barrier at Fishery Yard, October','fontsize',17);
%set(gca,'position',[0.13 0.11 0.775 0.78])
%
%
```

Floodfrequencyoverall.m:

```
%Script to compute FLOOD FREQUENCY
%with reference to Huangpu Park and Mishidu
%computations done for each barrier location by simply loading the
%corresponding storage capacity
%
%Script is based on floodprobabilitypermonthperyear.m !!!!
%=========================================================================
%Load data from runoff.m = torrential rainfall runoff distribution
%=========================================================================
load runoffdatagraphsgumbel1mean.mat;          %runoffdatagrapsb=3 dagen rho=03 and
hs=97cm; runoffdatagraphs.mat=1 dag rho=03 hs=97
```

```
%=========================================================================
%%Load typhoon occurrence probability data
%=========================================================================
load landfall.mat;
%=========================================================================
%load storage capacity data
%=========================================================================
load storageatwusong2.mat;
%load storageatzh2.mat;
%load storageatfishery2.mat;
%
%=========================================================================
%Computations
%=========================================================================
rd=ux(:,1);
p=(ux(:,2)./100); %p tussen 0 en 1;
volume=ux(:,3);
discharge=ux(:,4);
deltah_lake=ux(:,5);
deltah=ux(:,6);
%Base discharges
wet    = [607 833 639 517 305];
av     = [323 352 326 279 327];
dry    = [211 237 293 253 188];
%Required discharges
for i=1:1:5
   qrmwet(:,i)    =  q-wet(1,i);
   qrmav(:,i )    =  q-av(1,i);
   qrmdry(:,i)    =  q-dry(1,i);
end
%
%Look up probabilities required discharges
matrix4=[1-p discharge];
   probwet=interp1(matrix4(:,2), matrix4(:,1), qrmwet);   %compute prob required qtr
   probav=interp1(matrix4(:,2), matrix4(:,1), qrmav);
   probdry=interp1(matrix4(:,2), matrix4(:,1), qrmdry);
   %

   probwet(isnan(probwet)) = 1;
probav(isnan(probav)) = 1;
probdry(isnan(probdry)) = 1;
%
%%voor optellen maanden
fldmwet2     =0.138.*probwet;%.*pmonth(:,i)    ;   %%met p(hst>=4.8) & p(typoon)
fldmav2      =0.345.*probav;%.*pmonth(:,i)     ;
fldmdry2     =0.517.*probdry;%.*pmonth(:,i)     ;

%
cnu=tms2(:,1);
c2010=tms2(:,2);  %ms 2010
c2030=tms2(:,3);
c2050=tms2(:,4);
%
chnu=thp2(:,1);   %hp present
```

```
ch2010=thp2(:,2);  %hp 2010
ch2030=thp2(:,3);
ch2050=thp2(:,4);
%
m1=[fldmwet2(:,1) fldmav2(:,1) fldmdry2(:,1)]; %june, etc
m2=[fldmwet2(:,2) fldmav2(:,2) fldmdry2(:,2)];
m3=[fldmwet2(:,3) fldmav2(:,3) fldmdry2(:,3)];
m4=[fldmwet2(:,4) fldmav2(:,4) fldmdry2(:,4)];
m5=[fldmwet2(:,5) fldmav2(:,5) fldmdry2(:,5)];
%
for i=1:3;
a=find(m1(:,i)<2e-5);
m1(min(a):end,i)=1e-7;
%
b=find(m2(:,i)<2e-5);
m2(min(b):end,i)=1e-7;
%
c=find(m3(:,i)<2.5e-5);
m3(min(c):end,i)=1e-7;
%
d=find(m4(:,i)<2e-5);
m4(min(d):end,i)=1e-7;
%
e=find(m5(:,i)<2e-5);
m5(min(e):end,i)=1e-7;
end
%
mm1=sum(m1,2);
mm2=sum(m2,2);
mm3=sum(m3,2);
mm4=sum(m4,2);
mm5=sum(m5,2);

%frequency per month
f1=0.33.*mm1;
f2=0.83.*mm2;
f3=1.16.*mm3;
f4=1.04.*mm4;
f5=0.79.*mm5;

%frequency overall
total=[mm1 mm2 mm3 mm4 mm5];
%total=[f1 f2 f3 f4 f5];
total2=4.15.*sum(total,2)./5;

u=[cnu total2];
v=[chnu total2];
%flood frequency for 24 hours closure
ms=interp1(u(:,1),u(:,2),24)
hp=interp1(v(:,1),v(:,2),24)
%return
%============================================================
%Interpo1ate for results 24 hours flood prob.
%Change title with find and replace for each barrier location
```

```
%=============================================================
%Fg1=figure;
%Ax11=...
plot(cnu, total2,'r');
hold on
plot(chnu,total2 ,'b');
hold on
%plot(cnu, mm1,'m' );
hold on
set(gca,'yscale','log');
set(gca,'ylim',[1e-3 5] );%'ytick', [0:200:1000],'yminortick','on'
set(gca,'xtick',[0:12:124]);
%set(gca,'xlim',[18 72],'fontsize',19,'XMinorTick','on');
set(gca,'xlim',[6 96],'fontsize',19,'XMinorTick','on');
AX=...
legend('Mishidu','Huangpu    Park',4);%,'Huangpu    Park'%legend('Wusongkou','Zhanghua
Bang','Fishery Yard',4);%,'Huangpu Park'
LEG = findobj(AX,'type','text');
set(LEG,'FontSize',12)
ylabel('frequency of exceedance [per year]');
xlabel('closure duration [hrs]');
   grid on
 %set(gca,'position',[0.13 0.11 0.775 0.78])
%ax2=axes('xaxislocation','top','ytick',[],'color','none','xlim',[6
124],'xtick',0:12:124,'fontsize',19);
title('Flood frequency Huangpu River, Wusongkou','fontsize',17);
%set(gca,'position',[0.13 0.11 0.775 0.78])
return
```

X CD-ROM

The enclosed CD-ROM contains the digital version of this thesis in PDF-format and the Matlab scripts used for computations. Also, the enhanced model of the Huangpu River in SOBEK-RIVER is enclosed.

References

Buishand T.A. and C.A. Velds, 1980. "Klimaat van Nederland 1: Neerslag en Verdamping", Koninklijke Meteorologisch Instituut (in Dutch), de Bilt.

BMK Bouwcombinatie Maeslantkering, Minsiterie van V&W and Directoraat Generaal Rijkswaterstaat, 1997. "Sluitstuk van de Deltawerken Stormvloedkering Nieuwe Waterweg", Ministerie van V&W (in Dutch), the Hague.

Chan J.C.L. and J. Shi, 1996. "Long Term Trends and Interannual Variability in Tropical Cyclone Activity over the western North Pacific" Geo. Res. Letters 23, pp.2765-2767.

Chen, X. and Y. Zong, 1999. "Typhoon hazards in the Shanghai area", Disasters, 1999, 23(1):66-88, Blackwell Publishers, Oxford.

Chen, X., 2002. Personal communications, Professor, Institute of Estuarine and Coastal Research, State Key Laboratory of Estuarine and Coastal Research, East China Normal University, Shanghai.

Chen Lianshou, 2000. "Tropical cyclone impacts in China" in: Pielke Jr., R. and R. Pielke Sr. (Eds), 2000. "Storms. Vol. I / ed. by Roger Pielke Jr. and Roger Pielke Sr.", Routeledge Hazards and Disasters Series, Routeledge, London.

Chu, A, 2002. "Extreme hydraulic conditions in the Yangtze River estuary", M.Sc. thesis ,Unesco-IHE Institute for Water Education, Delft

Clemen, Robert T. and Terence Reilly, 1999. "Correlations and copulas for decision and risk analysis", Management Science/Vol. 45, No 2

©CUR-publikatie 190, 1997. "Kansen in de civiele techniek, deel 1: probabilistisch ontwerpen in theorie", Stichting CUR (in Dutch), Gouda.

De Michelle C. and G. Salvadori, 2003. "A generalized Pareto intensity-duration model of storm rainfall exploiting 2-copulas", Journal of Geophysics Research Vol.108 (D2).

De Matteis, R., 2001. "Fitting copulas to data", Diploma thesis, Institute of Mathematics, University of Zurich.

Devroye, L., 1986. "Non-Uniform Random Variate Generation", Springer-Verlag, New York.

Dall'Aglio G., S. Kotz and G. Salinetti (Eds.), 1991. "Advances in probability distributions with given marginals, beyond copulas", Kluwer Academic Publishers, Dordrecht.

Dorst, M. Neal, 2003. Personal communications, Hurricane Research Division, Atlantic Oceanographic and Meteorological Laboratory, National Oceanographic and Atmospheric Administration, USA.

Fink, Andreas F. and Peter Speth, 1998. "Tropical Cyclones", Naturwissenshaften 85, 482-492,

Springer-Verlag, Heidelberg.

Frees, Edward W. and Emilio A. Valdez, 1997. "Understanding relationships using copulas", conference paper, 32nd Actuarial Research Conference, Calgary.

Genest, C. and J. Mackay, 1986. "Copules archimédiennes et familles de lois bidimensionnelles dont les marges sont données", Canadian Journal of Statistics. 14, 145-159.

Harris, D. L., 1963. "Characteristics of the Hurricane Storm Surge", U. S. Weather Bureau, Technical Data Report No. 48, U. S. Department of Commerce, Washington DC.

Henderson-Sellers, A., H. Zhang, G. Berz, K. Emanuel, W. Gray, C. Landsea, G. Holland, J. Lighthill, S-L. Shieh, P. Webster, K. McGuffie, 1998. "Tropical cyclones and global climate change: A post-IPCC assessment" Bull. Amer. Meteo. Soc. 79, pp.19-38.

Hohai University, 1999. "Storm tide, flood, urban torrential rainfall joint occurrence analysis", Huangpu River storm surge barrier study volume 1.3 (in Chinese), Shanghai Water Authority, Shanghai.

Hohai University, 2000. "Final Report: Huangpu River storm tide levels analysis", Huangpu River storm surge barrier study, Shanghai Water Authority (in Chinese), Shanghai.

Hohai University, 2001. "Shanghai City Huangpu River final flood protection and water level analysis report", Huangpu River storm surge barrier study volume 1(in Chinese),, Shanghai Water Authority, Shanghai.

Holland, G.J. 1997. "The maximum potential intensity of tropical cyclones", Journal of Atmospheric Science, 54, pp.2519-2541.

Holland, G.J. (Ed.), 1993. "Global Guide to Tropical Cyclone Forecasting", report WMO/TD-No. 560, Report No. TCP-31, World Meteorological Organization, Geneva.

Houghton, J. T., G. J. Jenkins and J. J. Ephramus (Eds.), 1990. "Climate Change: The IPCC Scientific Assessment", Cambridge University Press, New York.

Houghton, J. T., B. A. Callander and S. K. Varney (Eds.), 1992. "Climate Change 1992. "The Supplementary Report to the IPCC Scientific Assessment. Cambridge University Press, New York.

Houghton, J. T., L.G. Meria Filho, B.A. Callander, N. Harris, A. Kattenberg, and K. Maskell, (Eds.), 1996. "Climate Change 1995: The Science of Climate Change, Contribution of WGI to the Second Assessment Report of the Intergovernmental Panel on Climate Change", Cambridge University Press, New York.

Jäckel, Peter, 2002. "Monte Carlo Methods in Finance", John Wiley & Sons, New York

Marine Jorigny, Ferdinand Diermanse, Randa Hassan, Pieter van Gelder, "Correlation analysis of water levels along dike areas", pp.1677-1684, Volume 2, Proceedings of the XIVth International Conference on Computational Methods in Water Resources, June 23-28, 2002, Delft, The Netherlands. Edited by S. Majid Hassanizadeh, Ruud J. Schotting,

William G. Gray, and George F. Pinder. 2002, Elsevier Science, Developments in Water Science, 47.

Nelson, Roger B., 1999. "An introduction to copulas, Lecture notes in statistics", Springer-Verlag, New York.

Pore, N. A. and C. S. Barrientos, 1976. "Storm Surge", Marine EcoSystems Analysis (MESA) Program, MESA New York Bight Project, New York Sea Grant Institute, New York.

Sklar, A., 1959 "Fonctions de répartition à *n* dimensions et leurs marges", Publ. Inst. Statist. Univ. Paris 8, 229-231

Shanghai Flood Risk Information Centre, 1999. "Study on the historical and future water levels in the Huangpu River", report prepared for the Shanghai Water Authority, Shanghai Flood Risk Information Centre (in Chinese), Shanghai.

Shanghai Flood Control Administration, 1994. "Shanghai Flood Control Manual", Shanghai Scientific & Technical Publishers (in Chinese), Shanghai

Schureman, P., 1988. "Manual of harmonic analysis and prediction of tides", U.S. Department of Commerce, Coast and Geodetic Survey, Washington.

Tai Lake Basin Authority, 2000. "Tai Lake basin torrential rainfall design probabilities", Tai Lake Basin Authority (in Chinese), Shanghai.

Shanghai Water Authority, 2002. "Main project of research on planning for the tide gate project at estuary of the Huangpu River", briefing report, Shanghai Water Authority, Shanghai.

UNESCAP, Integrating Environmental Considerations into the Economic Decision-Making Process, Volume IV: Modalities for environmental assessments ST/ESCAP/2003.

Vrijling, J. K., 1999. "Probabilistisch ontwerpen in de waterbouwkunde, voorlopige uitgave", lecture notes ctwa5310 (in Dutch), Department of Civil Engineering, Delft University of Technology, Delft.

Vriend, H. J. de, 2002. "Rivierwaterbouwkunde", lecture notes CT3340 (in Dutch), Department of Civil Engingeering, Delft University of Technology.

Wang Songlin and Ruan Renliang, 2001. "General report on the water resources of Shanghai City", Shanghai Scientific & Technical Publishers (in Chinese), Shanghai.

WL | Delft Hydraulics/ AEA Technology/ Hohai University, 1998. "Water quality management planning for Suzhou Creek Project", main report R3096, WL | Delft Hydraulics, Delft.

WL | Delft Hydraulics and Nedeco, 2002. "Huangpu River Barrier, Shanghai: pre-feasibility/review study", report Q2786 WL | Delft Hydraulics, Delft.

The World Bank, 1993. "Staff appraisal report: China, Tai Lake Basin Flood Control Project", Report No. 11308-CHA, Agriculture Operations Division China/Mongolia Department, East Asia & Pacific Regional Office, The World Bank.

Ye Shouren, Zhu Yueming and Yao Xing, 2002. "Water management practice of the Tai Lake

Basin", Conference paper, Tai Lake Basin Authority, and Ministry of Water Resources, International Conference of Basin Organisations 2002.

Yuan Zhilun, 1999. "Flood and drought disasters in Shanghai", Hohai University Press (in Chinese), Nanjing

Zhang Jiyao, 1999. "Flood control project construction since last year", Press conference Vice Minister of Water Resources on the development of water conservancy projects, Information Office of the State Council, Beijing.

Zhu Wei, 2002. Personal communications. Tai Lake Basin Water Authority, Shanghai.

Websites

[1] http://hurricane.weathercenter.com/
Hurricane Centre
[2] http://www.prh.noaa.gov/hnl/cphc/pages/names.html
Names of tropical cyclones
[3] http://www.math.unizh.ch/
Papers on copulas
[4] http://www.eorc.nasda.go.jp/TRMM/typhoon/index_e.htm
TRMM tropical cyclones database
[5] http://www.edu.cn/20020701/3060473.shtml
Articles on flood defences of Shanghai
[6] http://trmm.gsfc.nasa.gov/
Satellite images of tropical cyclones
[7] http://www.weather.unisys.com
Satellite images of tropical cyclones
[8] http://www.aoml.noaa.gov/hrd/weather_sub/faq.html
General information of tropical cyclones
[9] http://www.unescap.org/drpad/publication/integra/modalities/china/4ch000ct.htm
UNESCAP site on Shanghai
[10] http://www.chinadaily.com.cn
Online newspaper with data clippings on the flooding of the Huangpu River
[11] http://www.visibleearth.nasa.gov
Satellite images of China
[12] http://www.kilroytravels.com
Images of China